Quantum Computing, Quantum Games and Geometric Algebra

James M. Chappell

The School of Chemistry and Physics,
University of Adelaide,
Australia

October 29, 2011

Contents

Abstract

Early researchers attempting to simulate complex quantum mechanical interactions on digital computers discovered that they very quickly consumed the computers' available memory resources, because the state space of a quantum system typically grows exponentially with problem size. Consequently, Richard Feynman proposed in 1982 that perhaps the only way to simulate complex quantum mechanical situations was by simulating them on some quantum mechanical system. Quantum computers attempt to exploit this idea incorporating the special properties of quantum mechanics, such as the superposition of states and entanglement, into a computing device. Two key algorithms have been discovered which would run on this new type of computer, Shor's factorization algorithm discovered in 1994, which provides an exponential speedup over classical algorithms and Grover's search algorithm in 1996, which provides a quadratic speedup. Following this in 1999 Meyer initiated the field of quantum game theory by introducing quantum mechanical states into the framework of classical game theory.

In this thesis, we firstly investigate the phase estimation procedure, due to its importance as the basis for Shor's factorization algorithm, for which a new error formula is found using an improved symmetrical definition of the error. Unlike other existing error formulas which require approximations in their derivation, our result is obtained analytically. The work on the phase estimation procedure then motivates the development of computer software written in the Java programming language, which can simulate the common algorithms and visually display their behavior on a circuit board type layout. The software is found useful in verifying the new error formula described above and to test ideas for new algorithms. Being written in Java, it is envisaged that it could be placed online and used as a learning tool for new students to the field.

We then investigate the second key algorithm of quantum computing, the Grover search algorithm. It is already known that the Grover search is an SU(2) rotation but the idea is extended by deriving the three generators in terms of the two non-orthogonal basis vectors, representing the solution and initial states. We then demonstrate that the Grover search is equivalent to the precession of the polarization axis of a spin-$\frac{1}{2}$ particle in a magnetic field.

At this point we introduce geometric algebra (GA), because of its efficient implementation of rotations and its associated visual representation, and hence ideal to describe the Grover search process. It was found to provide a simple algebraic solution to the exact Grover search problem as well providing a simple visual picture describing the general solution to Meyer's quantum penny flip game, which is a simple two-player quantum game based on the manipulation of a single qubit and hence closely analogous to the Grover search process.

We then extend the work on quantum games developing two-player, three-player and N-player quantum games in the context of an EPR type experiment, which has the advantage of providing a sound physical basis to quantum games avoiding the common criticism of other quantum game frameworks regarding the proper embedding of the classical game. Using the algebraic approach of GA, we solve the general N player game, without requiring the use of matrices which become unworkable for large N. Games based on non-factorisable joint probabilities were then also developed which provided a more general framework for both classical and quantum games, and allows the field of quantum games to be accessible to non-physicists, as it does not employ Dirac's bra-ket notation.

In summary, several new results in the field of Quantum computing were produced, including an improved error formula for phase estimation [JMCL11b], a general solution to Meyer's quantum penny flip game [CILVS09] and a paper producing quantum games from non-factorisable joint probabilities [CIA10], as well as an EPR framework for quantum games [JMCL11a], refer attached papers.

Statement of Originality

This work contains no material which has been accepted for the award of any other degree or diploma in any university or other tertiary institution to James Chappell and, to the best of my knowledge and belief, contains no material previously published or written by another person, except where due reference has been made in the text.

I give consent to this copy of my thesis, when deposited in the University Library, being made available for loan and photocopying, subject to the provisions of the Copyright Act 1968.

The author acknowledges that copyright of published works contained within this thesis (as listed below), resides with the copyright holders of those works.

I also give permission for the digital version of my thesis to be made available on the web, via the University's digital research repository, the Library catalogue, the Australasian Digital Theses Program (ADTP) and also through web search engines, unless permission has been granted by the university to restrict access for a period of time.

Published Articles:

1. An Analysis of the Quantum Penny Flip Game Using Geometric Algebra, J. M. Chappell(Adelaide University), A. Iqbal(Adelaide University), M. A. Lohe(Adelaide University) and Lorenz von Smekal(Adelaide University), *Journal of the Physical Society of Japan*, 78(5), 2009.

2. Constructing quantum games from symmetric non-factorisable joint probabilities, J. M. Chappell(Adelaide University), A. Iqbal(Adelaide University) and D. Abbott(Adelaide University), *Physics Letters A*, 374, 2010.

3. A Precise Error Bound for Quantum Phase Estimation, J. M. Chappell(Adelaide University), M. A. Lohe(Adelaide University), Lorenz von Smekal(Adelaide University), A. Iqbal(Adelaide University) and D. Abbott(Adelaide University), *PLoS ONE*, 6(5), 2011.

4. Analyzing three-player quantum games in an EPR type setup, J. M. Chappell(Adelaide University), A. Iqbal(Adelaide University) and D. Abbott(Adelaide University), *PLoS ONE*, 6(7), 2011.

Supervisors:

Dr Max Lohe, Prof. Tony Williams and Dr Lorenz von Smekal

Acknowledgments

I am grateful to my principal supervisor Dr Max Lohe for his patience, advice and encouragement, as well as the early guidance of Prof. Tony Williams and the many helpful technical discussions with Dr Lorenz von Smekal and thanks to the School of Chemistry of Physics for supporting me with a scholarship and their computing facilities during my Ph.D.

Special thanks also to my other co-authors Dr Azhar Iqbal and Prof. Derek Abbott for consultations in the field of quantum game theory, and to the School of Electrical and Electronic engineering for their ongoing support. Thanks also to Ian Fuss, Rodney Crewther, Sundance Bilson-Thompson, Langford White, Andrew Allison, Peter Cooke, Pinaki Ray, Faisal Shah Khan and Nicolangelo Iannella for many helpful discussions.

Thanks also to Marius and Johanna for proofreading the manuscript, to Antonio and my other fellow PhD students who gave me helpful advice and also to all my other colleagues who attend the weekly get-together at the university staff club for their motivation and encouragement. Thanks also to the many others in the global community working in the field of quantum computing and quantum game theory which I have had an opportunity to interact with, and who generously provided advice and guidance.

Thanks also to my parents and brothers for their encouragement, support and tolerance.

1

Introduction

The field of quantum computing was initiated in 1982 by Richard Feynman, when he proposed that perhaps the only way to solve complex quantum mechanical problems was by simulating them on some quantum mechanical system [Fey82], [Fey86], [RHA96]. This led to the idea by Deutsch of expanding the classical model of the Turing machine [Tur36] to a quantum Turing machine [Deu85] which could utilize the special properties of quantum mechanics during processing. Classical computers use binary states represented by a 0 and 1 as their basis, whereas quantum computers are typically based on two orthogonal states represented by $|0\rangle$ and $|1\rangle$. This allows non-classical quantum mechanical interactions to become part of this new processing paradigm. Following this, two key quantum algorithms were discovered that could run on this new quantum Turing machine and which appeared to conclusively demonstrate the inherent superiority of a quantum computer over a classical machine, Shor's algorithm for factorizing large numbers in 1994 [Sho94], which provided an exponential speedup over the best known classical algorithms and Grover's search algorithm in 1996 [Gro98a], which provided a quadratic speedup over classical search algorithms. From the initial Grover search algorithm, partial search algorithms were also developed [GR05], [KX07], [KL06], [KG06], which allowed an approximate solution to the search problem, as well as attempts at more general search algorithms [Gro98b], [LL01], [BBB$^+$00], [LLHL02], [LLZN99], [Joz99], [LLH05], [Pat98]. Since these early developments, a variety of other quantum algorithms have been developed [CvD10]. Other approaches to harnessing the quantum nature of particles, in a computational sense have also been developed, such as quantum walks, which incorporate quantum effects into classical random walks [FG98b] and the process of adiabatic evolution of quantum systems [FGGS00]. It should also be mentioned however, that the use of quantum qubits in place of classical bits does introduce some new difficulties into a computational device, such as the inability to copy quantum registers (the no-cloning theorem [WZ82]) and the extreme care required to shield qubits from any disturbances from the environment (decoherence) [Joh01], [YS99]. On the positive side, quantum computers appear to be a genuine superset of classical computers and so do indeed represent a genuine enhanced computing paradigm [LSP98], [Gru99], [BJ]. There is a large amount of experimental effort [VSS$^+$00], [VSB$^+$01] in the field, due to the formidable technical challenges in building a full scale working quantum computer and simple algorithms have been verified, with a few qubits implemented with several different quantum systems, such as cavity QED [THL$^+$95], [HMN$^+$97], ion traps [CZ95, MHT05] and nuclear magnetic resonance [VSB$^+$01], as well as the implementation of simple quantum games [DLX$^+$02a]. Even though quantum systems with only a small number of qubits have been successfully implemented, the development of quantum error correction [Sho95], [Ste96] and fault tolerant quantum computation may indicate that reliable quantum computing is indeed possible [BBBV97] [Sho].

In 1999, Meyer extended classical game theory with the inclusion of quantum mechanical interactions [Mey99]. Quantum game theory has been found useful in developing quantum-mechanical protocols against eavesdropping [GH97], as well as an alternate way to formulate quantum algorithms, as games between classical and quantum players [Mey02], and can also be used to investigate fundamental questions about quantum mechanics through games against nature [Mil51]. We introduce the mathematical formalism of Geometric algebra into quantum games [CILVS09,JMCL11a] which allows a visual description of the general solution to Meyer's penny flip game, as well as the solution of N-player games. Several different game frameworks have been proposed [EWL99, ITC08, Iqb05], but we use the approach based on an EPR ex-

periment [EPR35,Iqb05], which properly embeds the underlying classical game, thus avoiding a common criticism of quantum games, as being simply different classical games [vEP02]. Many useful applications for quantum game theory have been proposed, such as the development of new quantum algorithms, quantum communication protocols, as well as strategic interactions in the fields of economics and biology. We also describe Grover's search algorithm using GA, as well as some simple quantum gates, indicating that GA is a suitable formalism for the field of quantum computing. Geometric algebra(GA) was first developed by William Clifford [Cli78] in the nineteenth century, but largely sidelined by other mathematical systems until popularized in modern times by David Hestenes [Hes99].

1.1 Overview of thesis

We begin by introducing the theoretical underpinnings of the field of quantum computing, such as qubits and associated operations, followed by a description of the mathematical formalism of geometric algebra (GA), which we show can replace the more conventional formalism of Dirac bra-ket notation and matrices. GA is particularly efficient at representing rotations in any number of dimensions and so naturally implements quantum unitary rotations on qubits and we find, as expected, to be a very efficient formalism with which to describe the Grover search algorithm which can be described by rotation in an abstract space, as developed in Chapters 3 and 4.

In order to develop quantum algorithms, the circuit model of quantum computing is employed, which seeks to model a quantum computer, by extending the classical circuit model approach. This may appear somewhat restrictive, however, it has been shown that this approach is actually equivalent to other approaches to quantum computing, such as a Hamiltonian based approach. Basic circuit elements are therefore firstly introduced, the one qubit and two qubit gates, along with some simple circuits as shown in Chapters 1 and 2. Their representation in GA is also described, thus demonstrating the suitability of GA for the basic building blocks of quantum computing.

A key algorithm of quantum computing, the quantum Fourier transform in Chapter 2, is then presented, which leads to a new result for the error formula used in phase estimation [JMCL11b]. One significance of this result is that errors obtained during simulation of the phase estimation procedure can now be compared with precise bounds as opposed to approximate values. The Java circuit model program was extended to model the phase estimation procedure, and by observing the maximum errors from a series of simulations, close convergence to the bound predicted by the new error formula was observed, whereas the previous error formulas showed large discrepancies.

We then investigate the Grover search algorithm, the second main class of quantum algorithms, firstly by developing an approach using SU(2) generators (Chapter 3) and then by using GA (Chapter 4). This was the first use of geometric algebra in analyzing the Grover search algorithm and we were able to demonstrate that it is a suitable formalism for this key algorithm.

The research then naturally extended to quantum games, with Meyer's penny flip game, because this game is also based on the manipulation of a single qubit like the Grover search and we were able to generate the most general solution using GA [CILVS09] (attached). The work on this quantum game was then naturally extended to two-player (Chapter 6), three-player (Chapter 7) [JMCL11a] (attached), and N-player games (Chapter 8) using GA. The quantum game setting used, is based on a general EPR (Einstein-Podolsky-Rosen) type experiment, and has the advantage that we regain the classical game at zero entanglement, which demonstrates that the quantum game is a true generalization of the corresponding classical game. The N-player game is intractable with matrices but we find that it becomes tractable and solvable in GA. We then cast quantum games as a table of non-factorisable joint probabilities [CIA10]

(attached), which allows the presentation of quantum games inside a general framework using the language of classical probabilities, without reference to quantum mechanics, which thus allows quantum game theory to become more accessible to non-physicists. This completed the body of research and the results were then summarized in a final conclusion in Chapter 9.

Along with the above theoretical developments, a Java application was also developed to simulate the action of all the common gates and circuits, and in the text there is reference to the relevant Java simulation to demonstrate the theoretical concept. A basic Pentium workstation with 3 Gigabytes of RAM allowed simulations to handle up to 19 qubits.

1.2 Basic principles of quantum computers

Classical computers operate on the principle of manipulating two state physical devices represented by the logical bits 0 and 1, using logic gates such as NOT, OR, AND, NOR, XOR, NAND etc. The quantum computing circuit representation which we are using proceeds similarly, except that the classical bits become two-state quantum bits or qubits.

The Stern-Gerlach experiment [Mac83] demonstrates that the property of spin has the right properties to represent a two state quantum bit. A measurement always returns an up or a down spin represented by $|0\rangle$ (parallel to the field) and $|1\rangle$ (anti-parallel), where we call the up and down orientations our basis states. We also know, however, that before measurement the dipole exists in a superposition of these states. If we have the ground state represented as $|0\rangle$ and the excited state as $|1\rangle$, then we can write the wave function of the qubit as

$$|\psi\rangle = \alpha\,|0\rangle + \beta\,|1\rangle\,, \tag{1.1}$$

where $\alpha, \beta \in \mathbb{C}$, the complex numbers, with the normalization condition

$$|\alpha|^2 + |\beta|^2 = 1. \tag{1.2}$$

Operations on qubits can now become general unitary transformations.

Definition 1.2.1 *A quantum bit is a two-level quantum system, represented by the two-dimensional Hilbert space $\mathcal{H}_2$. Space $\mathcal{H}_2$ is equipped with a fixed basis $B = \{|0\rangle, |1\rangle\}$, a so-called computational basis. States $|0\rangle$ and $|1\rangle$ are called basis states.*

The basis B is an orthonormal basis such that $\langle 0|0\rangle = \langle 1|1\rangle = 1$ and $\langle 0|1\rangle = \langle 1|0\rangle = 0$.

A key issue in quantum computing, is, extracting information from quantum states, because even though there is theoretically an infinite amount of information held in α and β, after measurement this information is lost and we can only obtain a $|0\rangle$ and $|1\rangle$ quantum state measured with probability $|\alpha|^2$ and $|\beta|^2$, respectively. After measurement α and β are reset to either 0 or 1. This behavior is, in fact, one of five key properties that distinguish quantum computing from classical computing:

1. Superposition:
   A quantum system unlike a classical system can be in a superposition of $|0\rangle$ and $|1\rangle$ basis states, see Eq. (1.1).

2. Entanglement [B$^+$64]:
   Given two qubits in the state $|\psi\rangle = |0\rangle|0\rangle + |1\rangle|1\rangle$, there is no way this can be written in the form $|\phi\rangle|\chi\rangle$, so the two states are intimately entangled.

3. Reversible unitary evolution:
   Schrödinger's equation tells us $\hat{H}|\psi\rangle = \mathrm{i}\hbar\,\partial|\psi\rangle/\partial t$. Formally, this can be integrated to give $|\psi(t)\rangle = \hat{U}(t)|\psi(0)\rangle$, where $\hat{U}(t)$ is a unitary operator given by
   $\hat{U}(t) = \hat{P}\,\exp[(\mathrm{i}/\hbar)\int_0^t dt'\hat{H}(t')]$, where $\hat{P}$ is the path ordering operator. Clearly such an evolution can be reversed by and application of $\hat{U}^\dagger$.

4. Irreversibility, measurement and decoherence [PZ93]:
   All interactions with the environment are irreversible whether they be measurements or the system coming to thermal equilibrium with its environment. These interactions disturb the quantum system, a process called decoherence and destroy the quantum properties of the system.

5. No-cloning:
   The irreversibility of measurement also leads us to our inability to copy a state without disturbing it in some way and, in fact, it can be proven that any general copying routine is impossible.

The last two properties are certainly restrictive and create operational and manufacturing limitations for quantum computers, but these are simply the difficulties that must be overcome, in order to harness the computational power of quantum states.

1.2.1 Tensor product notation

If we allow N qubits to interact, the state generated has a possible 2^N basis states. We form a combined Hilbert space, with the tensor product $\mathcal{H}_N = \mathcal{H}_2 \otimes \mathcal{H}_2 \otimes ... \otimes \mathcal{H}_2$, where the order of each term is important. The following notations are all equivalent for the given state

$$|0\rangle_1 \otimes |1\rangle_2 \otimes |0\rangle_3 \otimes ...|0\rangle_N \equiv |0\rangle_1|1\rangle_2|0\rangle_3...|0\rangle_N \equiv |\overset{1}{0}, \overset{2}{1}, \overset{3}{0}, ..., \overset{N}{0}\rangle \equiv |010...0\rangle, \tag{1.3}$$

where $|010...0\rangle$ means qubit '1' is in state $|0\rangle$, qubit '2' is in state$|1\rangle$ and qubit '3' is in state $|0\rangle$ etc.

We will choose the ordering of the N-qubit basis states $|x\rangle$ where $x \in \{0,1\}^N$ representing a string of 0 and 1's of length N, such that when x is viewed as a binary number, this number orders the basis. For example, a system of two quantum bits is a four-dimensional Hilbert space $\mathcal{H}_4 = \mathcal{H}_2 \otimes \mathcal{H}_2$, having an orthonormal basis $\{|00\rangle, |01\rangle, |10\rangle, |11\rangle\}$.

1.3 Geometric algebra (GA)

In 1843, Sir William Hamilton, inspired by the usefulness of complex numbers in describing the geometry of the two dimensional plane, sought a generalized system for the physical three dimensions of space. He found correctly that trying to expand the two dimensional complex numbers to a three dimensional structure was not possible, but by jumping to four dimensions, discovered the quaternions defined by

$$q = a + bi + cj + dk, \tag{1.4}$$

where each of i, j, k now square to minus one, with $ij = k$ and $a, b, c, d \in \Re$. He succeeded in successfully duplicating the role of complex numbers for three dimensions, however, in doing so, he had to sacrifice commutivity, requiring $ij = -ji$. To understand Hamilton's generalization we can write a quaternion as

$$q = f + \vec{r}g, \tag{1.5}$$

where $\vec{r}^2 = \vec{r}.\vec{r} = -1$ and $f, g \in \Re$. Viewed in this way, we see that effectively Hamilton replaced the single complex plane, with an infinity of complex planes, oriented in 3-space according to the unit vector $\vec{r}$, which thus allows us to do rotations in the full three dimensions of space. It is conventional to call Im(H) the vector quaternions and we find that as a vector space Im(H) is isomorphic to $\mathbb{R}^3$. This led Hamilton to postulate, many years ahead of his time, that the quaternion provided a natural unification of time and the three dimensions of space.

To produce proper three dimensional rotations using the vector quaternions, however, Hamilton also found that he had to proceed slightly differently than for the complex plane, in that the quaternion i, for example, must now act by conjugation(a bi-linear transformation), that is to rotate a vector $u \in \mathrm{Im(H)}$, we use

$$u^{'} = iui^{-1}, \tag{1.6}$$

which now completes a proper 3-dimensional rotation about a plane perpendicular to i, although, now by π, rather than $\frac{\pi}{2}$. In fact, for a rotation of θ about a plane perpendicular to i, we require

$$u^{'} = \mathrm{e}^{\frac{i\theta}{2}} u \mathrm{e}^{\frac{-i\theta}{2}}. \tag{1.7}$$

1.3.1 The vector cross product and quaternions

Working in the subspace of the vector quaternions with $u, v \in \mathrm{Im(H)}$, we have

$$uv = -u.v + u \times v, \tag{1.8}$$

where $u \times v$ is the conventional cross product of two vectors and we also have

$$vu = -u.v - u \times v. \tag{1.9}$$

Adding and subtracting these equations we find

$$u.v = -\frac{1}{2}(uv + vu) \tag{1.10}$$

$$u \times v = \frac{1}{2}(uv - vu), \tag{1.11}$$

$$\tag{1.12}$$

which shows that the vector algebra of $\mathbb{R}^3$ can be interpreted in terms of quaternions.

Gibbs popularized a form of vector algebra based on the dot and cross product in the 1880s, which sidelined quaternions, due to their perceived unusual approach to rotations and their anti-commutivity [AR10], [Sze04].

1.3.2 Generalizations beyond quaternions

We might naturally expect higher dimensional generalizations beyond quaternions, however, Frobenius proved in 1878 that a finite dimensional associative division algebra over $\mathbb{R}$, must be isomorphic to $\mathbb{R}, \mathbb{C}$ or $\mathbb{H}$. This shows the important position held by the quaternions, which also are associative, so we can always represent this algebra with matrices. If we are willing to sacrifice associativity, then we can go one more step to the eight dimensional octonions.

1.3.3 Clifford's geometric algebra

William Clifford, just a few years after Hamilton, incorporated the quaternions into a unified framework he called geometric algebra (GA). Clifford found that by using a wedge product (developed earlier by Grassman), as opposed to the vector cross product, he was able to produce an algebraic structure, which automatically incorporated the properties of both complex numbers and quaternions. Clifford defined the geometric product for two vectors a, b [DL03], as

$$ab = a \cdot b + a \wedge b, \tag{1.13}$$

where $a.b$ is the conventional dot or inner product and $a \wedge b$ is the wedge or outer product, which represents a signed area in the plane of the two vectors. In three dimensions, we have

the simple relationship with the conventional vector product of $a \wedge b = \iota a \times b$, where ι will be defined shortly, with properties identical to the unit imaginary number $\mathrm{i} = \sqrt{-1}$. The outer product inherits the anti-symmetric nature of the cross product, so we see that the geometric product splits naturally into symmetric and anti-symmetric components.

The big advantage of the outer product is that it represents a directed area (spinning clockwise or anti-clockwise) in the plane of the two vectors a and b, whereas the vector cross product produces a vector perpendicular to the plane of a and b. In four dimensions, for example, a plane has an infinity of perpendicular vectors, so is ambiguously defined, whereas the outer product stays within the defined plane and therefore more easily generalizes to higher dimensions. For researchers unfamiliar with GA, the Cambridge University hosts an educational website at http://www.mrao.cam.ac.uk.

1.3.4 Geometric algebra (GA) in 3 dimensions

If we define a right-handed set of orthonormal basis vectors $\sigma_1, \sigma_2, \sigma_3$, that is

$$\sigma_i . \sigma_j = \delta_{ij}, \tag{1.14}$$

then expanding the geometric product for distinct basis vectors, we have

$$\sigma_i \sigma_j = \sigma_i . \sigma_j + \sigma_i \wedge \sigma_j = \sigma_i \wedge \sigma_j = -\sigma_j \wedge \sigma_i = -\sigma_j \sigma_i. \tag{1.15}$$

This can be summarized by

$$\sigma_i \sigma_j = \sigma_i . \sigma_j + \sigma_i \wedge \sigma_j = \delta_{ij} + \iota \epsilon_{ijk} \sigma_k. \tag{1.16}$$

Thus, we have an isomorphism between the basis vectors $\sigma_1, \sigma_2, \sigma_3$ and the Pauli matrices through the use of the geometric product, which justifies using the same symbols for both, where we have defined the trivector

$$\iota = \sigma_1 \sigma_2 \sigma_3, \tag{1.17}$$

which represents a signed unit volume. We find that

$$\iota^2 = \sigma_1 \sigma_2 \sigma_3 \sigma_1 \sigma_2 \sigma_3 = -1 \tag{1.18}$$

and we find that ι commutes with all other elements of the algebra and so acts equivalently to the complex number i. We could replace ι with i in our case with three dimensions, however, in even dimensions, ι is actually anti-commuting, so it is preferable to define a different symbol. The bivectors also square to -1, that is

$$(\sigma_i \sigma_j)^2 = (\sigma_i \sigma_j)(\sigma_i \sigma_j) = -\sigma_i \sigma_j \sigma_j \sigma_i = -1 \tag{1.19}$$

and we use these to define the isomorphism with quaternions identifying i, j, k with $\sigma_2 \sigma_3 = \iota \sigma_1, \sigma_1 \sigma_3 = -\iota \sigma_2, \sigma_1 \sigma_2 = \iota \sigma_3$ respectively, and hence the Pauli algebra $\mathrm{i}\sigma_1, -\mathrm{i}\sigma_2, \mathrm{i}\sigma_3$.

Summary of Clifford's algebra in 3 dimensions

Thus, we have at our disposal in 3-space:

a	$\{\sigma_1, \sigma_2, \sigma_3\}$	$\{\sigma_1\sigma_2, \sigma_2\sigma_3, \sigma_3\sigma_1\}$	$\sigma_1\sigma_2\sigma_3$
1 scalar	3 vectors	3 bivectors area elements	1 trivector volume element

We will use the vectors $\sigma_1, \sigma_2, \sigma_3$, to define a coordinate system equivalent to a typical real Cartesian co-ordinate system, the bivectors will be used to represent spinors or rotations in this space and the trivector takes the place of the complex number i.

A general multivector can be written

$$M = a + \vec{v} + \iota\vec{w} + \iota b, \tag{1.20}$$

which shows in sequence, scalar, vector, bivector and trivector terms, where a vector would be represented $\vec{v} = v_1\sigma_1 + v_2\sigma_2 + v_3\sigma_3$, where v_i are scalars. This multivector, can be used to represent many mathematical objects, such as scalars (a), complex numbers ($a + \iota b$), quaternions ($a + \iota\vec{w}$), vectors (polar) ($\vec{v}$), four-vectors ($a + \vec{v}$), pseudovectors ($\iota\vec{w}$), pseudoscalars (ιb), the electromagnetic anti-symmetric tensor ($\vec{v} + \iota\vec{w}$) and spinors ($a + \iota\vec{w}$), with the four complex component Dirac spinor represented by the full multivector M. This illustrates how GA can replace a diverse range of mathematical formalisms. The spinor mapping defined in Eq. (1.24), for example, employed in chapters 4 to 8 in order to represent qubit spinors and their associated rotations. GA is the largest possible associative algebra that integrates all these algebraic systems into a coherent mathematical framework. It has been claimed that GA, in fact, provides a unified language to physics and engineering and can be used to develop all branches of theoretical physics [DL03], [HS84], [Hes99], [Hes03], [DL03], [HD02a] bringing geometrical meaning to all operations and physical interpretation to mathematical elements [DSD07] . Clifford algebra variables have also been proposed as a solution to the EPR paradox [EPR35], [Chr07].

1.3.5 Rotations in 3-space with GA

To rotate an arbitrary vector by an angle $|\vec{v}|$ about an axis given by the vector $\vec{v}$, we define a Rotor which acts by conjugation similar to quaternions

$$R = \mathrm{e}^{-\iota\vec{v}/2} = \cos(|\vec{v}|/2) - \iota\frac{\vec{v}}{|\vec{v}|}\sin(|\vec{v}|/2), \tag{1.21}$$

which can also be written in terms of Euler angles

$$\mathrm{e}^{-\iota\sigma_3\phi/2}\mathrm{e}^{-\iota\sigma_2\theta/2}\mathrm{e}^{-\iota\sigma_3\chi/2}, \tag{1.22}$$

so that, we have

$$\vec{v}' = R\vec{v}R^{\dagger}. \tag{1.23}$$

The † is also called the Reversion operation, which acts the same as the conventional conjugate operation for complex numbers, flipping the order of the terms and the sign of ι.

The bilinear transformation needed to calculate rotations does appear a little more complicated than the left sided action of rotation matrices, however, the formula does apply completely generally, being able to rotate not only vectors but also any component of the algebra, such as bivectors and trivectors and in any number of dimensions besides three.

1.3.6 Representing quantum states in GA

Spinors can be identified with the scalars and bivectors of 3-dimensional GA and we find a simple 1 : 1 mapping to GA as follows [DL03, DSD07, PD01]

$$|\psi\rangle = \alpha|0\rangle + \beta|1\rangle = \begin{bmatrix} a_0 + \mathrm{i}a_3 \\ -a_2 + \mathrm{i}a_1 \end{bmatrix} \leftrightarrow \psi = a_0 + a_1\iota\sigma_1 + a_2\iota\sigma_2 + a_3\iota\sigma_3. \tag{1.24}$$

Hence, we are mapping spinors to the even subalgebra, which is also closed under multiplication.

1.3.7 Measurement probabilities in GA

The overlap probability between two states ψ and ϕ in the N-particle case is given by Doran, [DL03]

$$P(\psi,\phi) = 2^{N-2}\langle\psi E\psi^\dagger\phi E\phi^\dagger\rangle_0 - 2^{N-2}\langle\psi J\psi^\dagger\phi J\phi^\dagger\rangle_0, \tag{1.25}$$

where the angle brackets $\langle\rangle_0$ mean to retain only the scalar part of the expression, that is, to disregard all vectors, bivectors and higher elements. We have the two observables $\psi J\psi^\dagger$ and $\psi E\psi^\dagger$, where

$$\begin{aligned} E &= \prod_{b=2}^{N}\frac{1}{2}(1-\iota\sigma_3^1\iota\sigma_3^b) \\ &= \frac{1}{2^{N-1}}\left(1+\sum_{n=1}^{\lceil\frac{N-1}{2}\rceil}(-)^n C_{2n}^N\left(\iota\sigma_3^i\right)\right) \end{aligned} \tag{1.26}$$

and where $C_r^N(\iota\sigma_3^i)$ represents all possible combinations of N items taken r at a time, acting on the objects inside its bracket. For example $C_2^3(\iota\sigma_3^i) = \iota\sigma_3^1\iota\sigma_3^2+\iota\sigma_3^1\iota\sigma_3^3+\iota\sigma_3^2\iota\sigma_3^3$. The number of terms given by the well known formula

$$C_r^N = \frac{N!}{r!(N-r)!}. \tag{1.27}$$

For the second observable, we have

$$J = E\iota\sigma_3^1 = \frac{1}{2^{N-1}}\sum_{n=1}^{\lfloor\frac{N+1}{2}\rfloor}(-)^{n+1}C_{2n-1}^N(\iota\sigma_3^i). \tag{1.28}$$

For the case $N=2$, for example, we find

$$\begin{aligned} J &= \frac{1}{2}\left(\iota\sigma_3^1+\iota\sigma_3^2\right) \\ E &= \frac{1}{2}\left(1-\iota\sigma_3^1\iota\sigma_3^2\right). \end{aligned} \tag{1.29}$$

In order to implement this formula on a given N-particle state ψ, we encode the measurement directions we intend to use into an auxiliary state ϕ, and then calculate the overlap probability according to Eq. (1.25).

1.4 Java software development

In order to develop an intuitive feel for the behavior of quantum circuits, a Java simulation program was developed. Initially, the program modeled basic gate elements, such as the Hadamard gate and the Controlled-Not gate, but then expanded to model simple circuits such as the circuit to create Bell states, Deutsch's algorithm and the Deutsch-Jozsa algorithm. It was then expanded further to allow construction of the Fourier transform and to allow the inclusion of black-box elements circuit elements, as used in the Grover search algorithm.

Following conventional programming practice, a user interface using a menu system to hold the available operations is provided, along with a drag and drop mouse driven interface, with the use of the right-click button as a property editor for the component being clicked on, or a way of adding new components depending on the context. A screen in the form of a grid is presented upon which quantum circuit elements can be placed. Additionally, the progress of the wave function is displayed underneath the circuit and for some circuits some technical

readout is also provided. The simulator can be run either as a standalone Java application or online embedded in a web page.

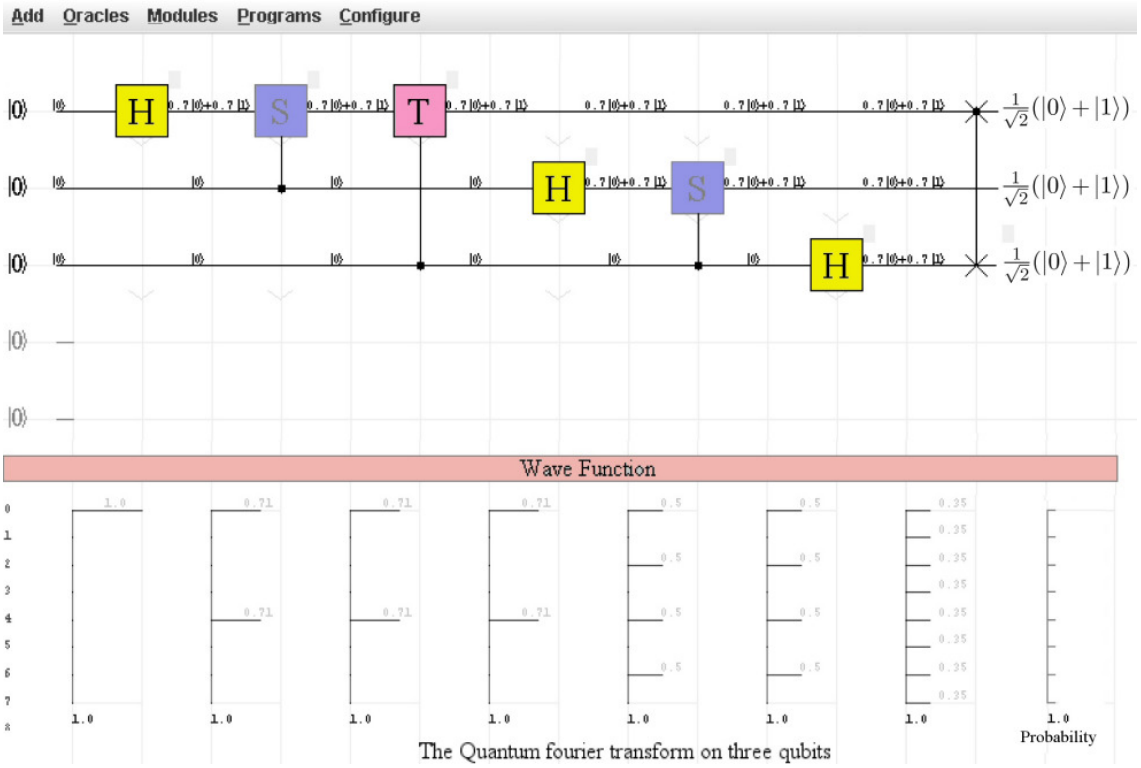

The Quantum fourier transform on three qubits

In the circuit above, we see the use of the single qubit Hadamard gates(H) and the two-qubit Ctrl-S and Ctrl-T gates, where the control line is the filled in black circle, followed at the end by swap gate. The gates with a Ctrl- line means that the associated gate is activated only if the control line is set to 1, otherwise an identity operation is performed. The action of these gates is further described in the next section. The circuits are read left to right, where the lines do not necessarily represent a physical wire but can represent the movement of a particle such as a photon through space, or alternatively to the passage of time.

In the example above, the first three qubits on the canvas are activated and the progress of these three qubits is shown written at each step of the circuit. Underneath the circuit, we also see visually the progress of the wave function, shown for each basis state $0 \ldots 7$, starting from $|0\rangle \otimes |0\rangle \otimes |0\rangle$, which is the first basis vector. Underneath each wave function reads the number 1.0, which shows that each wave function is normalized correctly and on each probability amplitude the actual numerical values are displayed in gray. After the last wave function, the wave function in black indicates actual probabilities. We can see that the circuit has correctly created a uniform superposition wave function. Some of the modifications we can easily now implement on the circuit include: clicking on the small gray square to the top right of the box representing each gate in order to raise the gate to higher and higher powers, or we can right-click on a gate to select a different gate or modify the gate in some way from a pull down list, or alternatively we can select a completely different circuit from the main menu provided. We can also toggle the starting qubits between the $|0\rangle$ and $|1\rangle$ states by clicking on them.

The circuit model of quantum computing implements the unitary transformation describing a particular circuit. An alternative approach is to directly implement the Hamiltonian for some required unitary evolution. This approach has also been modeled in a Java simulator, allowing various Hamiltonian operators to visually evolve a starting wave function. A variant of the Hamiltonian approach, adiabatic computing, is also modeled in this program, which involves adiabatically evolving a Hamiltonian, from some simple starting Hamiltonian to a solution Hamiltonian.

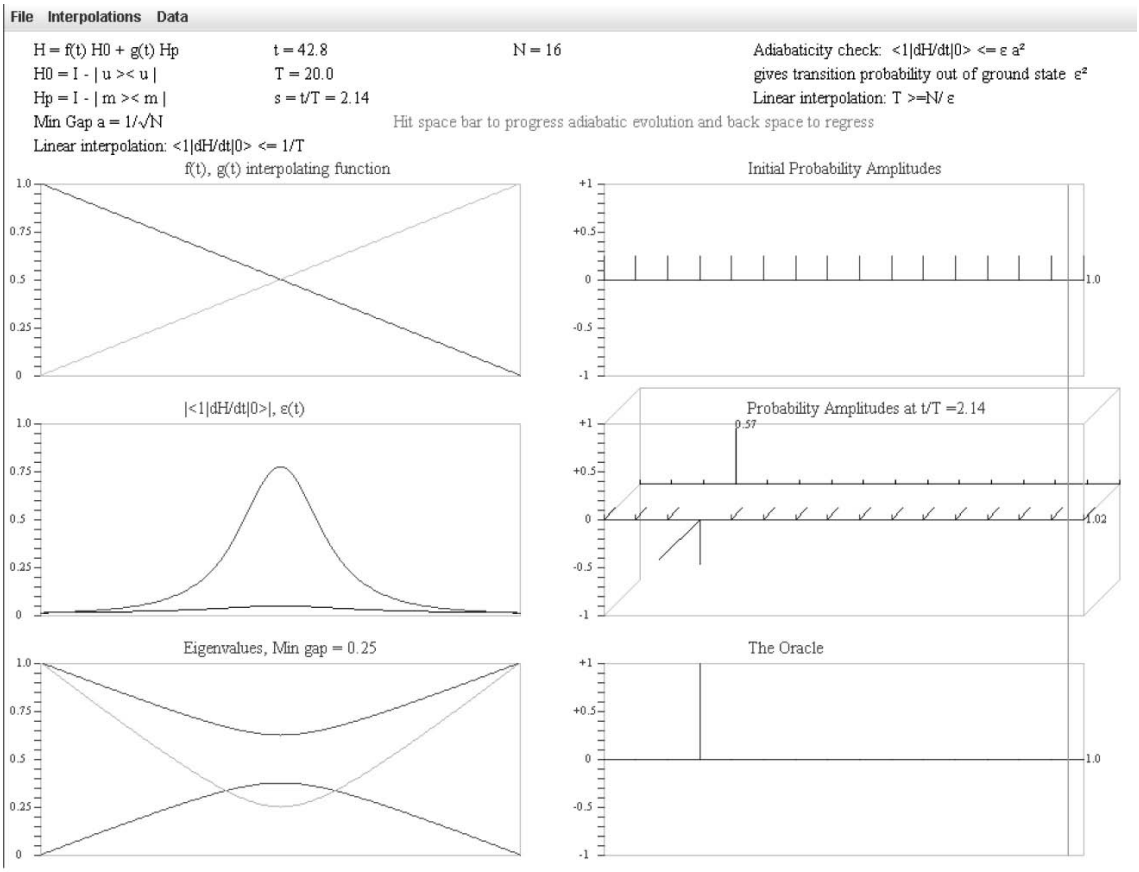

Adiabatic quantum search algorithm

The adiabatic search program is shown, searching for a single target item out of 16 elements. The left hand screens show the interpolating functions from the starting Hamiltonian to the solution Hamiltonian, followed by the adiabicity of the evolution process shown by the graph of $\langle 0|dH/dt|1\rangle$ and, finally, a readout on the eigenvalues of the Hamiltonian and their separation distance. The three right hand screens show the initial wave function, followed by the current wave function, showing the dominance of the target probability amplitudes after time $t/T = 2.14$, and the final screen shows the location of the target item in the database. So, the probability amplitude is 0.57 showing the evolution is succeeding in amplifying the probability amplitude of the solution.

1.5 Quantum Gates

Following the circuit model approach to quantum computing, we create a quantum analog of classical circuit design, constructed from a set of elementary gates. As mentioned, this may appear overly restrictive because, in general, for a set of n qubits we have a 2^n dimensional Hamiltonian evolving a set of quantum states, however, it has been shown that the Hamiltonian and circuit models are equivalent to each other. With N qubits, we also need to apply an $2^N \times 2^N$ unitary transformation matrix acting on the N qubits, however, it has been proven that any general unitary transformation on N qubits can be decomposed into just one type of two qubit gate (the controlled-NOT) and single qubit gates [NC02]. So, without loss of generality, we can investigate quantum algorithms based on a quantum circuit using primitive quantum circuit components. The only N-qubit gate we use is a black box oracle which returns a 0 or 1, depending on the input state, as used in the Grover search algorithm.

While looking at single qubit and two qubit gates it is helpful to keep the following points in mind:

1. Gates must be unitary, if a gate is not unitary, then the probability is not conserved through the gate. Unitary gates also immediately imply reversibility because the inverse of a unitary transformation is also unitary from the unitary condition: $U^\dagger U = I$. In fact any unitary operation is a valid gate.

2. We can characterize an arbitrary quantum gate by specifying its action on the basis states, since superposition holds, that is $|\psi\rangle = \sum_{i=1}^{N} c_i |\psi_i\rangle$. This means, for example, for single qubit gates, we only need to define their effect on the $|0\rangle$ and $|1\rangle$ basis states to completely define the gate.

For quantum circuits, which have a classical digital electronic analog, the circuit connects basis states to basis states. However, many quantum gates do not have a classical analogue because, while they input a set of basis states, they output superposition states intermediate between 0 and 1, and so have no classical analogue.

1.5.1 Single qubit gates

Any unitary matrix acting on a single qubit is a valid quantum operation, so we have the following definition:

Definition 1.5.1 *An operation on a qubit, called a unary quantum gate, is a unitary mapping $U : \mathcal{H}_2 \to \mathcal{H}_2$, where $\mathcal{H}_2$ represents a two-dimensional Hilbert space.* [Hir01]

Note: A unary quantum gate acts on a single qubit, as opposed to a binary quantum gate acting on two qubits.

A single qubit may appear to be a fairly elementary component, however a single qubit is sufficient to model the Grover search algorithm (Chapters 3 and 4), and also Meyers' penny flip game (Chapter 5).

The Bloch sphere

Because any single qubit can be represented by (ignoring the global phase):

$$|\psi\rangle = \cos\frac{\theta}{2}|0\rangle + e^{i\phi}\sin\frac{\theta}{2}|1\rangle\,, \tag{1.30}$$

we have an isomorphism between single qubit operations and solid body rotations, that is we have the isomorphism $SO3 \approx SU2$. Thus, the Bloch sphere is a useful visual representation for a qubit.

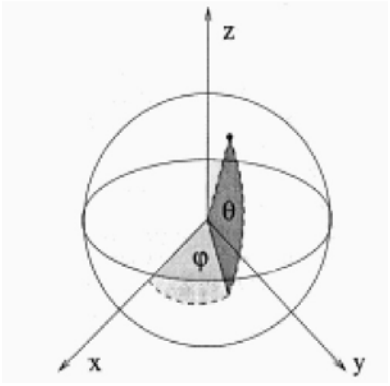

Figure 1.1: The Bloch sphere.

The Pauli gates

The three Pauli operators $\sigma_1, \sigma_2, \sigma_3$ are useful as single qubit gates, and for ease of depiction on circuit diagrams are represented by the symbols X, Y, Z, respectively.

The X gate

The X gate or NOT gate, is given by the action of the Pauli σ_1 matrix, that is $X = \begin{bmatrix} 0 & 1 \\ 1 & 0 \end{bmatrix}$.
Looking at the actions on the basis states:

$|0\rangle$ —— $\boxed{X}$ —— $|1\rangle$

$|1\rangle$ —— $\boxed{X}$ —— $|0\rangle$

This shows that the quantum NOT gate is akin to the classical NOT gate, switching the value of a bit from 0 to 1. We can also write the NOT gate as a unitary operator $\hat{U}_{NOT} = |1\rangle\langle 0| + |0\rangle\langle 1|$.

The Y gate

In matrix form, $Y = \begin{bmatrix} 0 & -\mathrm{i} \\ \mathrm{i} & 0 \end{bmatrix}$, and as a unitary operator we have $\hat{U}_Y = \mathrm{i}|1\rangle\langle 0| - \mathrm{i}|0\rangle\langle 1|$.

The Z gate

In matrix form, $Z = \begin{bmatrix} 1 & 0 \\ 0 & -1 \end{bmatrix}$, and as a unitary operator we have $\hat{U}_Z = |0\rangle\langle 0| - |1\rangle\langle 1|$.

1.5.2 Single qubit gates in geometric algebra

The three basis vectors $\sigma_1, \sigma_2, \sigma_3$, used in GA are isomorphic with the Pauli matrices. So that, for example, the action of the NOT gate in GA is simply $\mathrm{e}^{\iota\pi\sigma_1/2} = \iota\sigma_1$, which acts on a general vector $\vec{v}$ through conjugation, such that

$$\vec{v}' = \mathrm{i}\sigma_1\vec{v}(-\mathrm{i}\sigma_1) = v_1\sigma_1 - v_2\sigma_2 - v_3\sigma_3, \tag{1.31}$$

which is the correct action of the NOT gate if represented on the Bloch sphere. For the Hadamard gate we have $H = \frac{1}{\sqrt{2}}\begin{bmatrix} 1 & 1 \\ 1 & -1 \end{bmatrix} = \frac{1}{\sqrt{2}}(X + Z)$ then we can see in GA the gate is

simply $\frac{\iota}{\sqrt{2}}(\sigma_1 + \sigma_3)$. The T or $\frac{\pi}{8}$ gate can be written as

$$T = \begin{bmatrix} 1 & 0 \\ 0 & e^{\mathrm{i}\pi/4} \end{bmatrix} \equiv \mathrm{e}^{-\iota\pi\sigma_3/8}, \tag{1.32}$$

which in this case is more obvious than the matrix form which has a $\frac{\pi}{4}$ coefficient. Thus, GA gives a simple and efficient representation for single qubit gates.

Java simulator

Single qubit gates - Hadamard gate

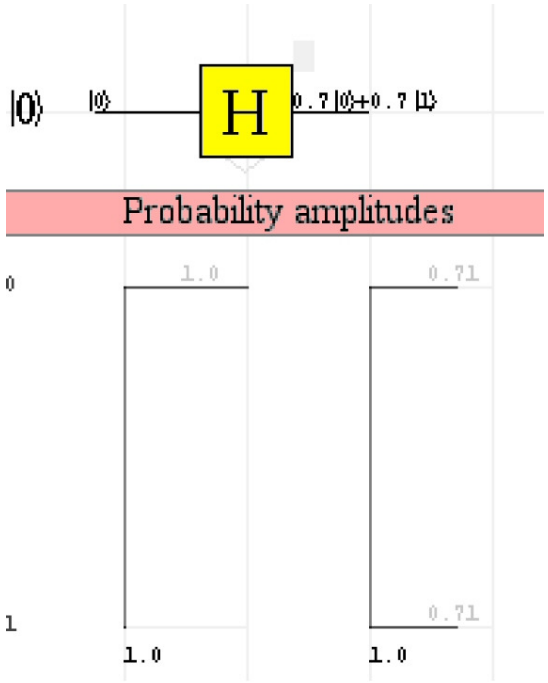

Simulation of Hadamard gate.

The action of the Hadamard gate is demonstrated in the Java simulator. We can now see written alongside the gate a calculation of how it transforms the $|0\rangle$ state into the $\frac{1}{\sqrt{2}}(|0\rangle + |1\rangle)$ state. At the bottom of the screen, we also see the behavior of the probability amplitudes of the wave function before and after the action of the Hadamard gate.

1.5.3 Two qubit gates

A system of two quantum bits is a four-dimensional Hilbert space $\mathcal{H}_4 = \mathcal{H}_2 \otimes \mathcal{H}_2$, having an orthonormal basis $\{|00\rangle, |01\rangle, |10\rangle, |11\rangle\}$. For a two qubit state we can then write

$$|\psi\rangle = \alpha_{00}\,|00\rangle + \alpha_{01}\,|01\rangle + \alpha_{10}\,|10\rangle + \alpha_{11}\,|11\rangle\,, \tag{1.33}$$

with the normalization condition

$$\sum_{x\in\{0,1\}^2} |\alpha_x|^2 = 1, \tag{1.34}$$

where $\{0,1\}^2$ represents a string of 0's and 1's of length 2.

Definition 1.5.1 *A binary quantum gate is a unitary mapping $\mathcal{H}_4 \to \mathcal{H}_4$.*

The Controlled-NOT or CNOT gate

A two qubit version of the NOT gate is the Controlled-NOT or CNOT gate and is represented in circuits by:

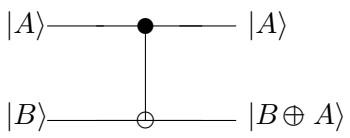

The top line of the circuit is the control line for the gate, represented by the filled in circle. The open circle indicates the qubit that will be flipped if the control line is set to one. The $|A\rangle$ line on the control line continues through the CNOT gate unchanged, however, a phase can be 'kicked back' from the other line. The $|B\rangle$ line is the data qubit line, which combines with the first qubit and produces the target qubit. The notation $|B \oplus A\rangle$ represents addition modulo 2 or the XOR gate. This is meaningfully defined here because the input states are assumed to be basis states represented as 0 or 1 in this case. The XOR operation is 1, if one of the input bits is 1 and the other one is 0, otherwise the XOR operation gives zero.

Similarly to single qubits, two qubit gates can be represented by transformation matrices, see definition (1.5.1), specifically for the CNOT gate:

$$U_{CN} = \begin{bmatrix} 1 & 0 & 0 & 0 \\ 0 & 1 & 0 & 0 \\ 0 & 0 & 0 & 1 \\ 0 & 0 & 1 & 0 \end{bmatrix}. \tag{1.35}$$

Thus,

$$\psi' = U_{CN}\psi = \begin{bmatrix} 1 & 0 & 0 & 0 \\ 0 & 1 & 0 & 0 \\ 0 & 0 & 0 & 1 \\ 0 & 0 & 1 & 0 \end{bmatrix} \begin{bmatrix} \alpha_{00} \\ \alpha_{01} \\ \alpha_{10} \\ \alpha_{11} \end{bmatrix} = \begin{bmatrix} \alpha_{00} \\ \alpha_{01} \\ \alpha_{11} \\ \alpha_{10} \end{bmatrix}.$$

This can also be written as a unitary operator $|00\rangle\langle 00| + |01\rangle\langle 01| + |11\rangle\langle 10| + |10\rangle\langle 11|$. For example, if $|\psi\rangle = |10\rangle$ the CNOT produces the state $|\psi\rangle = |11\rangle$.

Universality

We have now reached an important point in the development of quantum gates, because it can be shown that any multiple qubit gate can be composed from just controlled-NOT and single qubit gates [NC02]. It is found that any k-qubit unitary operation can be simulated with $O(4^k k)$ such gates. Of course, the set of possible single qubit gates is infinite, because this is the set of all possible unitary transformations. Other combinations of gates can be found as a basis if we only require it to be universal in an approximate sense, for example the controlled-NOT, along with the Hadamard gate and the $\pi/8$ gate, can be considered a universal set of gates in an approximate sense.

So, with these two types of gates (CNOT and single qubit), we now have all the gates we need to develop any quantum algorithm. This theorem is the quantum equivalent of the universality of the NAND gate in classical computing.

Other useful two qubit gates

The swap gate is used to swap the position of two qubits given by the matrix $\begin{bmatrix} 1 & 0 & 0 & 0 \\ 0 & 0 & 1 & 0 \\ 0 & 1 & 0 & 0 \\ 0 & 0 & 0 & 1 \end{bmatrix}$.

The Ctrl-Phase gate gate applies the phase gate operation if the control line is set, $\text{Ctrl} - \text{phase} = \begin{bmatrix} 1 & 0 & 0 & 0 \\ 0 & 1 & 0 & 0 \\ 0 & 0 & 1 & 0 \\ 0 & 0 & 0 & \mathrm{e}^{\mathrm{i}\phi} \end{bmatrix}$. If we set $\phi = \pi$ then we form the $\text{Ctrl} - \text{Z}$ gate.

1.5.4 Three qubit gates

Three qubit gates are not required to develop a universal quantum computer but they are of theoretical interest. For example, the three qubit Toffoli gate can implement a reversible NAND gate and the universality of the NAND gate in classical computing means we can therefore duplicate any classical algorithm on a quantum computer.

The other property of classical computers is Fanout, which can also be implemented with this gate, though only on basis states. Another process of classical computers is random number generation and, because the Hadamard gate creates an equal superposition of two states, upon measurement it gives a random choice of basis states, and so can be used to introduce indeterminism into a quantum computer.

1.5.5 Measurements

Even though measurement is not a unitary transformation it can be useful in circuits, because it creates the operation of collapsing the quantum state to one of the basis values.
Given a state $|\psi\rangle = \alpha\,|0\rangle + \beta\,|1\rangle$ a measurement is represented by:

where M represents the classical bits 0,1. Or for a 2 qubit state, given by (1.33), if we measure the first qubit to be 0, we know we are left with the state: $|\psi\rangle = \frac{\alpha_{00}|00\rangle + \alpha_{01}|01\rangle}{\sqrt{|\alpha_{00}|^2 + |\alpha_{01}|^2}}$.

1.6 General quantum circuits

The rows and columns of the unitary transforms are labeled from left to right and top to bottom as 00...0,00...1, to 11...1, with the bottom-most wire being the least significant bit. A wire carrying n qubits is represented by:

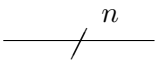

Quantum circuits must satisfy:

1. No loops: a loop or some sort of feedback would make the circuit non-reversible and so is not permitted. Also, the circuit would become non-linear.
2. No fan-in: in a classical circuit this is achieved by joining two wires together to form a single wire (a bitwise or) but this operation is not reversible and therefore not unitary and so not allowed.
3. No fan-out: it can be shown that quantum mechanics does not allow qubits to be copied, thus making general fan-out impossible. This result is also known as the no-cloning theorem.

1.6.1 Copying circuit

The no-cloning theorem states that we cannot create a circuit to duplicate a general quantum state, so it might appear that any form of copying is impossible, however we demonstrate that we can copy orthogonal states using the CNOT gate as shown below. The data qubit is passed straight through, and the target qubit holds the result of the gate operation. If we set the input target qubit to $|0\rangle$, then we can copy the set of orthogonal states $|0\rangle$ and $|1\rangle$ as shown.

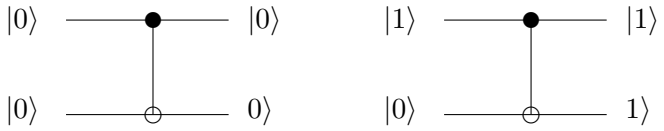

So, in the two cases above, the data bit is copied.
We can prove this algebraically, with a general basis state $|\psi_{xy}\rangle = |x, 0\rangle$, where $x \in \{0, 1\}$ and $y = 0$, we have for the final state

$$\psi' = [CNOT] \left[\begin{bmatrix} 1-x \\ x \end{bmatrix} \otimes \begin{bmatrix} 1 \\ 0 \end{bmatrix} \right].$$

If we expand the tensor product and act with the CNOT gate we find

$$\psi' = \begin{bmatrix} 1 & 0 & 0 & 0 \\ 0 & 1 & 0 & 0 \\ 0 & 0 & 0 & 1 \\ 0 & 0 & 1 & 0 \end{bmatrix} \begin{bmatrix} 1-x \\ 0 \\ x \\ 0 \end{bmatrix} = \begin{bmatrix} 1-x \\ 0 \\ 0 \\ x \end{bmatrix} = (1-x) \begin{bmatrix} 1 \\ 0 \\ 0 \\ 0 \end{bmatrix} + x \begin{bmatrix} 0 \\ 0 \\ 0 \\ 1 \end{bmatrix},$$

which can be written conveniently in Dirac notation as

$$|\psi'\rangle = (1-x)|0, 0\rangle + x|1, 1\rangle).$$

We notice this can be combined into a single term $|\psi'\rangle = |x, x\rangle$, which implies we have the mapping $|x, 0\rangle \rightarrow |x, x\rangle$, thus showing that we are successfully copying the input basis state $|x\rangle$, where $x \in \{0, 1\}$.

1.6.2 Creating a Bell state or an EPR pair

The Bell state is a maximally entangled two qubit state, and is useful in modeling two-player games, see Chapter 6. Consider the following circuit with 2 qubits:

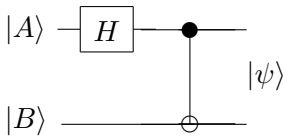

Assuming $|A\rangle$ and $|B\rangle$ are basis states, we have an initial state $|\psi_{xy}\rangle = |x, y\rangle$ where $\{x, y\} \in \{0, 1\}$. We can construct the final state

$$\psi' = [CNOT]\left[[H]\begin{bmatrix}1-x\\ x\end{bmatrix} \otimes \begin{bmatrix}1-y\\ y\end{bmatrix}\right].$$

Expanding the Hadamard gate and the tensor product:

$$\psi' = [CNOT]\left[\tfrac{1}{\sqrt{2}}\begin{bmatrix}1\\ 1-2x\end{bmatrix} \otimes \begin{bmatrix}1-y\\ y\end{bmatrix}\right] = [CNOT]\tfrac{1}{\sqrt{2}}\begin{bmatrix}1-y\\ y\\ (1-2x)(1-y)\\ (1-2x)y\end{bmatrix}.$$

Allowing the CNOT gate to act we obtain the final state

$$\psi' = \frac{1}{\sqrt{2}}\begin{bmatrix}1&0&0&0\\0&1&0&0\\0&0&0&1\\0&0&1&0\end{bmatrix}\begin{bmatrix}1-y\\ y\\ (1-2x)(1-y)\\ (1-2x)y\end{bmatrix} = \frac{1}{\sqrt{2}}\begin{bmatrix}1-y\\ y\\ (1-2x)y\\ (1-2x)(1-y)\end{bmatrix}$$

and writing as a sum of basis vectors

$$\psi' = \frac{1-y}{\sqrt{2}}\begin{bmatrix}1\\0\\0\\0\end{bmatrix} + \frac{y}{\sqrt{2}}\begin{bmatrix}0\\1\\0\\0\end{bmatrix} + \frac{(1-2x)y}{\sqrt{2}}\begin{bmatrix}0\\0\\1\\0\end{bmatrix} + \frac{(1-2x)(1-y)}{\sqrt{2}}\begin{bmatrix}0\\0\\0\\1\end{bmatrix}.$$

This can be written conveniently as states: $|\psi'\rangle = \frac{1}{\sqrt{2}}(|0, y\rangle + (-1)^x|1, 1-y\rangle)$.
So, can we find a single unitary matrix applied to the input state in $\mathcal{H}_4$, such that

$$U_{bell}\begin{bmatrix}(1-x)(1-y)\\ (1-x)y\\ x(1-y)\\ xy\end{bmatrix} = \frac{1}{\sqrt{2}}\begin{bmatrix}1-y\\ y\\ (1-2x)y\\ (1-2x)(1-y)\end{bmatrix}?$$

With some simple algebra, looking at the four possible input states, we find

$$U_{bell} = \frac{1}{\sqrt{2}}\begin{bmatrix}1&0&1&0\\0&1&0&1\\0&1&0&-1\\1&0&-1&0\end{bmatrix},$$

where we can fairly easily see that U_{bell} is unitary.
So, we can find $\psi' = U_{bell}\psi$, which can be used to switch to the Bell basis.

Entanglement

Definition 1.6.1 *A state $z \in \mathcal{H}_4$ of a two-qubit system is decomposable if z can be written as a product of states in $\mathcal{H}_2, z = x \otimes y$. A state that is not decomposable is entangled.*

So, for the Bell state, we require

$$\frac{|00\rangle + |11\rangle}{\sqrt{2}} = (a_0|0\rangle + a_1|1\rangle)(b_0|0\rangle + b_1|1\rangle) = a_0b_0|00\rangle + a_0b_1|01\rangle + a_1b_0|10\rangle + a_1b_1|11\rangle \quad (1.36)$$

for some complex numbers $a_0, a_1, b_0, b_1 \in \mathbb{C}$. However $a_0b_0 = \frac{1}{\sqrt{2}}$, $a_0b_1 = 0$, $a_1b_0 = 0$ and $a_1b_1 = \frac{1}{\sqrt{2}}$, which is impossible, and so the state is entangled. It has been shown that correlations as strong as entanglement cannot exist in classical physics, and it is one of the resources available to quantum computers unavailable on classical machines.

Given a general two qubit state

$$|\psi\rangle = a|00\rangle + b|01\rangle + c|10\rangle + d|11\rangle,$$

if it is not entangled, then we can split the state into two qubits, that is $|\psi\rangle = |\phi\rangle|\chi\rangle$. If all four terms are present, then to be able to factorize the state we must have $b/a = d/c$ or $ad - bc = 0$. Hence, $ad - bc = 0$ implies no entanglement.

1.6.3 Quantum parallelism

Because of the property of the superposition of states, a quantum computer can be constructed to be massively parallel, for example, a quantum computer can evaluate a function $f(x)$ for many different values of x simultaneously. Suppose we have a function from a binary state to a binary state $f(x) : 0, 1 \to 0, 1$. This can be conveniently computed with a 2 qubit quantum computer using the unitary transformation

$$|x, y\rangle \xrightarrow{U_f} |x, y \oplus f(x)\rangle\,.$$

We know that given, say, a classical circuit for computing $f(x)$, we can always mimic it with a quantum circuit of comparable efficiency. So, we will call this black box circuit U_f.

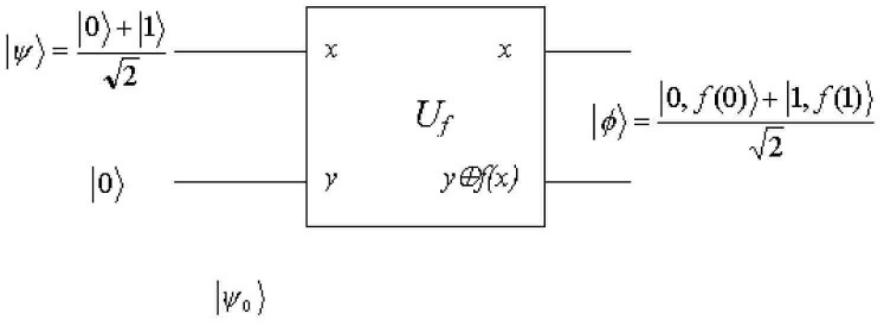

This can be also represented as a unitary matrix:

$$U_f = \begin{bmatrix} 1-f(0) & f(0) & 0 & 0 \\ f(0) & 1-f(0) & 0 & 0 \\ 0 & 0 & 1-f(1) & f(1) \\ 0 & 0 & f(1) & 1-f(1) \end{bmatrix}. \quad (1.37)$$

The initial state $|\psi\rangle$ can be obtained by passing $|0\rangle$ through a Hadamard gate. Now, we can see from the final state that a measurement on $|\phi\rangle$ gives either $|0, f(0)\rangle$ or $|1, f(1)\rangle$. So, if the first qubit measures the state $|0\rangle$, then the second qubit will be $|f(0)\rangle$, if the first qubit

measures $|1\rangle$ then the second qubit will be $|f(1)\rangle$. So, the final quantum state appears to have evaluated the function $f(x)$ for two different values of x simultaneously.

If we now had two data bits x_1 and x_2 instead of just x, and each initially passing through Hadamard gates, we would create an input state:

$$|\psi_0\rangle = \frac{|0\rangle + |1\rangle}{\sqrt{2}} . \frac{|0\rangle + |1\rangle}{\sqrt{2}} |0\rangle = \frac{|00\rangle + |01\rangle + |10\rangle + |11\rangle}{2} |0\rangle . \tag{1.38}$$

We can write $H^{\otimes 2}$ to denote the action of two Hadamard gates on two qubits. Similarly for n Hadamard gates acting on n qubits we can write $H^{\otimes n}$. For $H^{\otimes n}$ acting on n $|0\rangle$ state qubits we will obtain:

$$\frac{1}{\sqrt{2^n}} \sum_{x \in \{0,1\}^n} |x\rangle , \tag{1.39}$$

which produces an equal superposition of all basis states. This equal superposition of the basis states is in fact a convenient starting state for many algorithms.

We can now extend the concept to quantum parallel evaluation of a function with an n bit input x and 1 bit out, $f(x)$, which can be performed in the following manner:

1. $|0\rangle^{\otimes n} |0\rangle$: prepare an $n+1$ qubit state
2. $\xrightarrow{H^{\otimes n}} \frac{1}{\sqrt{2^n}} \sum_{x \in \{0,1\}^n} |x\rangle |0\rangle$: apply Hadamard transformation
3. $\xrightarrow{U_f} \frac{1}{\sqrt{2^n}} \sum_{x \in \{0,1\}^n} |x\rangle |f(x)\rangle$: apply U_f
4. $\xrightarrow{M} (x, f(x))$: measure the state.

So, all possible values of f are available even though we only evaluated the algorithm once. However, measurement of the final state only gives $f(x)$ for a single value of x at a time. We could fairly straightforwardly extend the function $f(x)$ to output several bits, that is $f(x) : \{0,1\}^n \to \{0,1\}^m$ where $m, n \in \mathbb{Z}^+$.

Even though the function has been evaluated at several values of x simultaneously and is held in the quantum qubits, we have no way of accessing this information, because after a single measurement the wave function collapses and we lose all other amplitudes. We need some way to extract the extra information, in order to take full advantage of quantum parallelism. This is implemented in Grover's algorithm where a black box oracle is used and the results of many parallel operations are interfered with each other to allow a measurement to return the solution state.

1.7 Summary of quantum algorithms

Currently, two main classes of problems are known, where it appears a quantum computer will outperform a classical one. Firstly, Shor's quantum algorithm which factorizes large numbers exponentially faster than a classical computer and which is based on the quantum Fourier transform. Classically, the Fourier transform takes roughly $N \log(N) = n2^n$ steps to transform $N = 2^n$ numbers, whereas a quantum computer takes about $\log^2(N) = n^2$ steps, an exponential saving. The second main class of quantum algorithms, allowing a speedup over classical computers although not an exponential speedup, is the quantum search algorithms. Given a search space of size N, and no prior knowledge of its structure, we want to find an element satisfying a known property. Classically, this problem requires N operations, but the quantum search algorithm allows it to be solved in $\sqrt{N}$ operations. Combining these two algorithms, we find the quantum counting algorithm which can count the number

of solutions in a database (without actually finding their identities). The main classes of quantum algorithms are illustrated in Fig. 1.2.

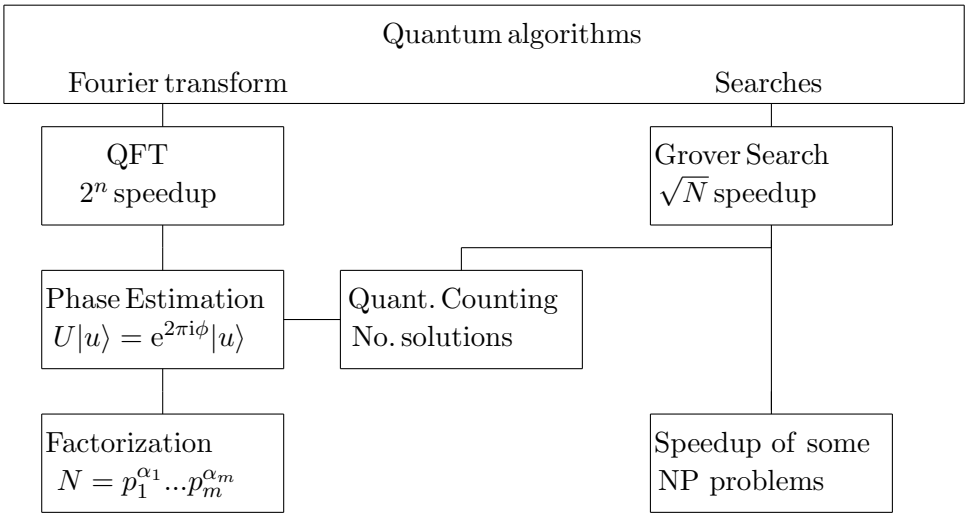

Figure 1.2: The main quantum algorithms.

2

The Fourier Transform and the Phase Estimation Algorithm

Initially, we describe the quantum Fourier transform (QFT) followed by a review of the phase estimation algorithm which is based on the QFT. This algorithm is important because it forms the basis for Shor's factorization algorithm which provides an exponential speedup over equivalent classical algorithms. This investigation firstly produces a new result of an exact error formula for the phase estimation algorithm and secondly we develop, in the following chapter, an alternative approach to the Grover search process using the phase estimation procedure.

2.1 Quantum Fourier transform (QFT)

2.1.1 Definition of the Fourier transform

The discrete Fourier transform (DFT), takes as input a vector of N complex numbers, $x_0, \ldots, x_{N-1}$ and outputs the transformed data as a vector of complex numbers $y_0, \ldots, y_{N-1}$ defined by

$$y_k = \frac{1}{\sqrt{N}} \sum_{j=0}^{N-1} x_j \mathrm{e}^{2\pi \mathrm{i} jk/N}. \tag{2.1}$$

The quantum Fourier transform acting on a set of basis states $|0\rangle, \ldots, |N-1\rangle$ is defined to be a linear operator with the following action on an arbitrary state:

$$\sum_{j=0}^{N-1} x_j |j\rangle \rightarrow \sum_{k=0}^{N-1} y_k |k\rangle. \tag{2.2}$$

We, of course, can presume that the initial state is normalized to one, that is:

$$\sum_{j=0}^{N-1} x_j^* x_j = \sum_{j=0}^{N-1} |x_j|^2 = 1.$$

So, for the transformed state we have:

$$\sum_{k=0}^{N-1} |y_k|^2 = \sum_{k=0}^{N-1} \frac{1}{N} \sum_{j=0}^{N-1} x_j^* \mathrm{e}^{-2\pi \mathrm{i} jk/N} x_j \mathrm{e}^{2\pi \mathrm{i} jk/N} = \sum_{k=0}^{N-1} \frac{1}{N} = \frac{N}{N} = 1.$$

So, we can see that the Fourier transform acting on a general state is unitary, and thus can be implemented as the dynamics for a quantum computer.

2.1.2 Definition of binary expansion

In the following analysis we take $N = 2^n$, where n is some integer and the basis $|0\rangle, \ldots, |2^n - 1\rangle$ is the computational basis for an n qubit quantum computer. We will also represent the state $|j\rangle_n$ or $|j\rangle^{\otimes n}$ using a binary expansion written as $j = j_1 j_2 \ldots j_n$, where

$$j = j_1 2^{n-1} + j_2 2^{n-2} + \ldots + j_n 2^0. \tag{2.3}$$

We will also use the notation $0.j_\ell j_{\ell+1}\dots j_n$ to represent a related binary fraction. That is, if we divide Eq. (2.3) by 2^k and we find the fractional part

$$\text{frac}\left(\frac{j}{2^k}\right) = j_\ell/2 + j_{\ell+1}/2^2 + ... + j_n/2^k = 0.j_\ell j_{\ell+1}\dots j_n = \sum_{i=\ell}^{n} j_i/2^i, \tag{2.4}$$

where $\ell = n+1-k$, then we will find typically that we can drop the integer part of many expressions because when we find terms such $\mathrm{e}^{\mathrm{i}2\pi j}$, obviously any integer part will contribute an extra 2π, and so will not affect its numerical value.

2.1.3 Rearranging the Fourier transform formula

It can be shown that the Fourier transform can now be written in the form

$$|j\rangle \to \frac{1}{2^{n/2}}\left[\left(|0\rangle + \mathrm{e}^{2\pi\mathrm{i}0.j_n}|1\rangle\right)\left(|0\rangle + \mathrm{e}^{2\pi\mathrm{i}0.j_{n-1}j_n}|1\rangle\right)\dots\left(|0\rangle + \mathrm{e}^{2\pi\mathrm{i}0.j_1 j_2\dots j_n}|1\rangle\right)\right]. \tag{2.5}$$

This product representation makes it easy to derive an efficient circuit for the quantum Fourier transform. The final swap operations to invert the order of the bits and the normalization is omitted from the right hand side of the diagram below for clarity.

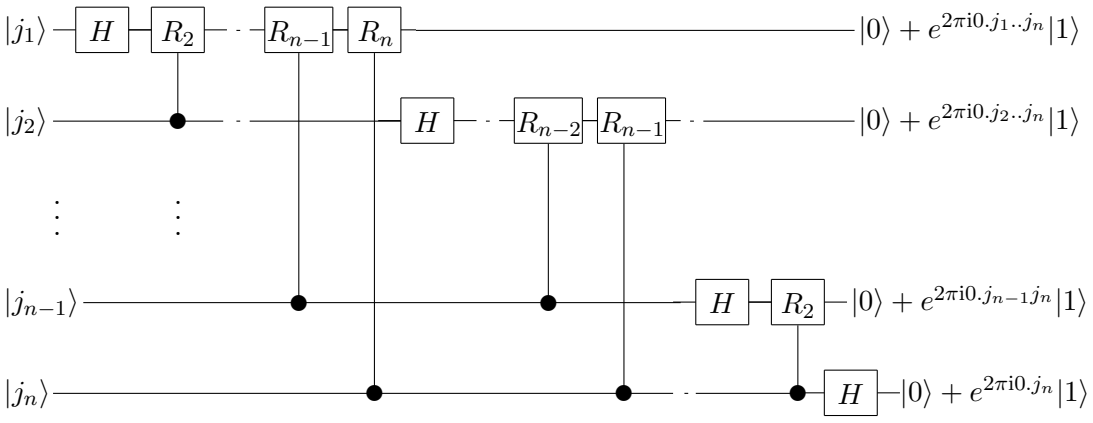

Figure 2.1: Fourier transform.

The gate R_k is defined as: $R_k = \begin{bmatrix} 1 & 0 \\ 0 & e^{2\pi i/2^k} \end{bmatrix}$. So the control-$R_k$ on a pair of qubits will be

$$\begin{bmatrix} I_2 & 0_2 \\ 0_2 & [R_k] \end{bmatrix} = \begin{bmatrix} 1 & 0 & 0 & 0 \\ 0 & 1 & 0 & 0 \\ 0 & 0 & 1 & 0 \\ 0 & 0 & 0 & e^{2\pi i/2^k} \end{bmatrix}.$$

The Fourier transform in geometric algebra

The Fourier transform was represented in a product representation Eq. (2.5), so knowing the mapping to geometric algebra for a single qubit Eq. (1.24), we can write down the same expression in GA as

$$|j\rangle \to \frac{1}{2^{n/2}}\left(1 - \mathrm{e}^{-2\pi 0.j_n \iota\sigma_3}\iota\sigma_2\right)\left(1 - \mathrm{e}^{-2\pi 0.j_{n-1}j_n\iota\sigma_3}\iota\sigma_2\right)\dots\left(1 - \mathrm{e}^{-2\pi 0.j_1 j_2\dots j_n\iota\sigma_3}\iota\sigma_2\right). \tag{2.6}$$

2.2 Phase estimation

The Fourier transform is the key to the phase estimation algorithm, which is the eigenvalue determination of a unitary matrix. That is we have:

$$U|u\rangle = \mathrm{e}^{2\pi \mathrm{i}\phi}|u\rangle. \tag{2.7}$$

Suppose a unitary operator U has an eigenvector $|u\rangle$ with eigenvalue $\mathrm{e}^{2\pi \mathrm{i}\phi}$, where the value of $\phi \in \Re$ is unknown. The goal of the phase estimation algorithm is to estimate ϕ. To perform the estimation, we assume that we have available *black boxes*, sometimes known as oracles, capable of performing the controlled-U^{2^j} operation, for selected non-negative integers j.

$$U^{2^j}|u\rangle = \underbrace{U \ldots U}_{2^j \, terms}|u\rangle = \mathrm{e}^{2\pi \mathrm{i}(2^j\phi)}|u\rangle \tag{2.8}$$

The algorithm uses two registers. The first register contains t qubits initially in the state $|0\rangle$. How we choose t depends on two things, the number of digits of accuracy we wish to have in our estimate of ϕ, and with what probability we wish the phase estimation procedure to be successful. The second register begins in the state $|u\rangle$ and contains as many qubits as necessary to store $|u\rangle$. Phase estimation is performed in two stages. The first stage is shown below, where we have omitted the normalization for simplicity.

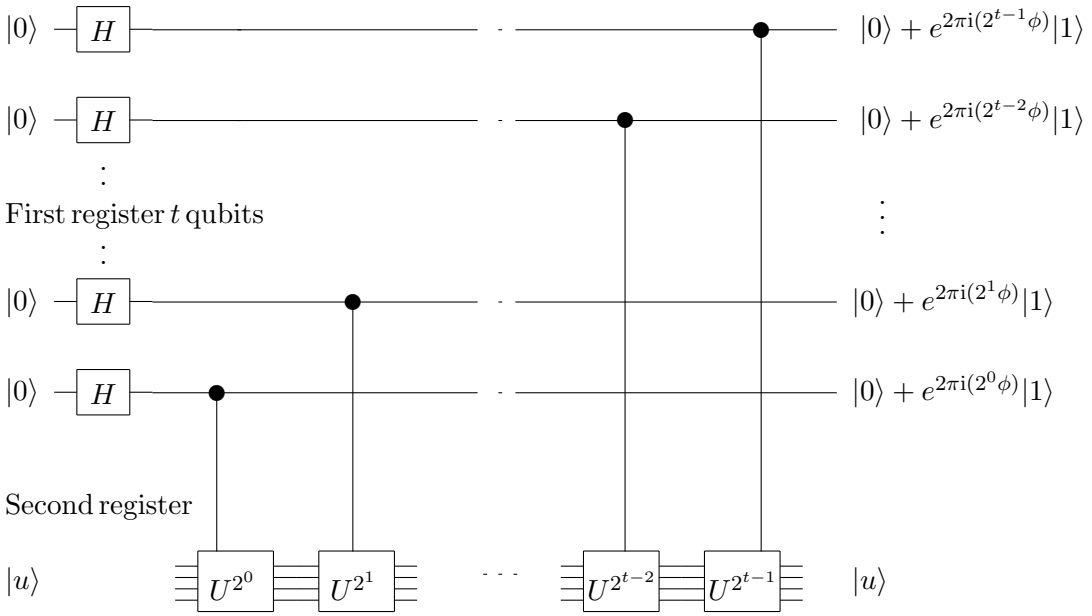

Figure 2.2: Phase Estimation.

This circuit begins by applying a Hadamard transform to the first register, followed by application of controlled-U operations on the second register, with U raised to successive powers of two. The final stage of the first register is seen to be therefore

$$\frac{1}{2^{t/2}}\left(|0\rangle + \mathrm{e}^{2\pi \mathrm{i}2^{t-1}\phi}|1\rangle\right)\left(|0\rangle + \mathrm{e}^{2\pi \mathrm{i}2^{t-2}\phi}|1\rangle\right)\ldots\left(|0\rangle + \mathrm{e}^{2\pi \mathrm{i}2^{0}\phi}|1\rangle\right) \tag{2.9}$$

and by multiplying out the brackets, this can be seen to equal

$$\frac{1}{2^{t/2}}\sum_{k=0}^{2^t-1} \mathrm{e}^{2\pi \mathrm{i}\phi k}|k\rangle. \tag{2.10}$$

We omit a description of the second register because it stays in the state $|u\rangle$ throughout the computation. We can describe the transformation by:

$$\left(I_f \otimes U^j\right)\left(|t\rangle \otimes |u\rangle\right) = |t\rangle \otimes U^j|u\rangle = \mathrm{e}^{2\pi \mathrm{i} j\phi}|t\rangle|u\rangle. \tag{2.11}$$

Suppose now that ϕ can be expressed exactly in t bits, as $\phi = 0.\phi_1\phi_2\ldots\phi_t$, then the first register can be written:

$$\frac{1}{2^{n/2}}\left(|0\rangle + \mathrm{e}^{2\pi \mathrm{i} 0.\phi_n}|1\rangle\right)\left(|0\rangle + \mathrm{e}^{2\pi \mathrm{i} 0.\phi_{n-1}\phi_n}|1\rangle\right)\ldots\left(|0\rangle + \mathrm{e}^{2\pi \mathrm{i} 0.\phi_1\phi_2\ldots\phi_n}|1\rangle\right). \tag{2.12}$$

Comparing with (2.5), we see this is exactly the QFT of the state $|\phi_1\phi_2\ldots\phi_n\rangle$. So, applying the inverse quantum Fourier transform to the first register will give us ϕ. That is

$$\frac{1}{2^{t/2}}\sum_{j=0}^{2^t-1}\mathrm{e}^{2\pi \mathrm{i}\phi j}|j\rangle|u\rangle \stackrel{\mathcal{F}^\dagger}{\Longrightarrow} |\phi\rangle|u\rangle. \tag{2.13}$$

So, a measurement on the first register in the computational basis gives us ϕ exactly (assuming it can be exactly represented in the available t qubits).

2.3 Reliability of Estimate

Generally speaking, the phase ϕ may not be representable in a fraction containing n terms and so only an approximation will typically be obtained. However, if we choose $t \geq n$ qubits in the first register, we obtain ϕ accurate to n qubits with probability of success $= 1 - \epsilon$. Currently, only approximate formulas are known for this relationship, such as the one given by Nielsen and Chuang:

$$t - n \leq \left\lceil \log_2\left(\frac{1}{2\epsilon} + \frac{1}{2}\right)\right\rceil. \tag{2.14}$$

However, this approximate formula was found to lack usefulness when actual simulations were carried out because it was desired to compare actual errors obtained with a reliable estimate, so that convergence to an exact answer could be observed. Because of this, we now derive an exact formula for the maximum roundoff error from first principles.

If the phase ϕ, used in phase estimation, cannot be expressed exactly in t bits, then the algorithm will only form an estimate for the value of ϕ. However, to calculate ϕ accurate to n bits with probability of success $1 - \epsilon$, we need to find a $t = t(n, \epsilon)$. An exact formula was obtained using $p = t - n$ as:

$$\epsilon_{max} = \frac{2}{\pi^2}\psi'\left(\frac{1 + 2^p}{2}\right), \tag{2.15}$$

where $\psi'(z) = \frac{d\psi}{dz}$ is the trigamma function, $\psi(z) = \frac{\Gamma'(z)}{\Gamma(z)}$ is the digamma function and $\Gamma(z) = \int_0^\infty t^{z-1}\mathrm{e}^{-t}dt$ is the standard gamma function.

We have written ϵ_{max}, because for a complete range of possible ϕ angles, this will be the worst possible error. So, if we run the phase estimation procedure many times with random values of ϕ, the worst error will converge to ϵ_{max}.

Expressions are also developed in the limit as the number of qubits $t \to \infty$ and in the limit as the added qubits $p \to \infty$. The exact formula is useful in confirming classical programs simulating quantum phase estimation.

2.3.1 Introduction

Phase estimation is an integral part of Shor's algorithm [Sho97], so an exact expression for the maximum probability of error is valuable in order to precisely achieve a predetermined accuracy.

Given the eigenvalue equation $U|u\rangle = \mathrm{e}^{2\pi\mathrm{i}\phi}|u\rangle$ for a unitary operator U, we can find an approximation to the phase $\phi \in [0, 1)$ using the quantum phase estimation procedure [Mos99]. The first stage in phase estimation produces, in the measurement register with a t qubit basis $\{|k\rangle\}$, the state [NC02]

$$|\tilde{\phi}\rangle_{\text{Stage1}} = \frac{1}{2^{t/2}} \sum_{k=0}^{2^t-1} \mathrm{e}^{2\pi\mathrm{i}\phi k} \, |k\rangle. \tag{2.16}$$

If $\phi = b/2^t$ for some integer $b = 0, 1, \ldots 2^t - 1$, then

$$|\tilde{\phi}\rangle_{\text{Stage1}} = \sum_{k=0}^{2^t-1} y_k |k\rangle \ , \quad \text{with} \quad y_k = \frac{\mathrm{e}^{2\pi\mathrm{i}bk/2^t}}{2^{t/2}} \tag{2.17}$$

is the discrete Fourier transform of the basis state $|b\rangle$, that is, the state with amplitudes $x_k = \delta_{kb}$. We then read off the exact phase $\phi = b/2^t$, from the inverse Fourier transform, as $|b\rangle = \mathcal{F}^\dagger|\tilde{\phi}\rangle$.

In general, however, when ϕ cannot be written in an exact t bit binary expansion, the inverse Fourier transform, in the final stage of the phase estimation procedure, yields a state

$$|\phi\rangle \equiv \mathcal{F}^\dagger|\tilde{\phi}\rangle_{\text{Stage1}} \ , \tag{2.18}$$

from which we only obtain an estimate for ϕ. That is, the coefficients x_k of the state $|\phi\rangle$ in the t qubit basis $\{|k\rangle\}$, will yield probabilities which peak at the values of k closest to ϕ.

Given a desired accuracy s with an associated probability of success $1-\epsilon$, however, we can determine the number of extra qubits p necessary to be added to the register for ϕ. Previously, Cleve, Ekert, Macchiavello and Mosca [CEMM98] determined the following upper bound:

$$p \leq p_{\text{CEM}} = \left\lceil \log_2 \left(\frac{1}{2\epsilon} + \frac{1}{2} \right) \right\rceil . \tag{2.19}$$

A similar derivation is given in Nielsen and Chuang [NC02] using similar approximations (for example the derivation of equation 5.28). More recently in [IB02] another upper bound was developed which also still used approximations.

Our goal now is to derive an upper bound which avoids the approximations used in the above formulas and, hence, obtain a precise result.

2.3.2 Accuracy formula

Initially we follow the procedure given in [CEMM98]. Let b be the integer in the range 0 to $2^t - 1$ such that $b/2^t = 0.b_1 \ldots b_t$ is the best t bit approximation to ϕ, which is less than ϕ, then we define

$$\delta = \phi - b/2^t,$$

which is the difference between ϕ and $b/2^t$ and where clearly $0 \leq \delta < 2^{-t}$. The first stage of the phase estimation procedure produces the state given by Eq. (2.16). Applying the inverse quantum Fourier transform to this state produces

$$|\phi\rangle = \sum_{k=0}^{2^t-1} x_k \, |k\rangle \ , \tag{2.20}$$

where

$$x_k = \frac{1}{2^t} \sum_{\ell=0}^{2^t-1} \mathrm{e}^{2\pi\mathrm{i}(\phi - k/2^t)\ell} = \frac{1}{2^t} \, \frac{1 - \mathrm{e}^{2\pi\mathrm{i}\, 2^t\delta}}{1 - \mathrm{e}^{2\pi\mathrm{i}(\delta - \frac{k-b}{2^t})}} \ . \tag{2.21}$$

Assuming the outcome of the final measurement is m, we can bound the probability of obtaining a value of m such that $|m - b| \leq e$, where e is a positive integer characterizing our desired

tolerance to error and where m and b are integers such that $0 \leq m < 2^t$ and $0 \leq b < 2^t$. The probability of observing such an m is given by

$$p(|m-b| \leq e) = \sum_{\ell=-e}^{e} |x_{b+\ell}|^2 \tag{2.22}$$

which is simply the sum of the probabilities of the states within e of b, where

$$x_{b+\ell} = \frac{1}{2^t} \frac{1 - \mathrm{e}^{2\pi \mathrm{i}\, 2^t \delta}}{1 - \mathrm{e}^{2\pi \mathrm{i}(\delta - \ell/2^t)}}, \tag{2.23}$$

which is the standard result obtained from Eq. (2.21), (in particular see equation 5.26 in [NC02]). Typically, at this point approximations are now made to simplify x_ℓ, however, we proceed without approximations. We have

$$|x_{b+\ell}|^2 = \frac{1}{2^{2t}} \frac{1 - \cos(2\pi 2^t \delta)}{1 - \cos(2\pi(\delta - \ell/2^t))} \,. \tag{2.24}$$

If we wish to approximate ϕ to an accuracy of 2^{-s}, we choose $e = 2^{t-s-1} = 2^{p-1}$ [1], using $t = s + p$, and if we denote the probability of failure

$$\epsilon = p(|m-b| > e), \tag{2.25}$$

then we have

$$\epsilon = 1 - \frac{1 - \cos 2\pi 2^t \delta}{2^{2t}} \sum_{\ell=-2^{p-1}}^{2^{p-1}} \frac{1}{1 - \cos 2\pi(\delta - \ell/2^t)}. \tag{2.26}$$

This formula assumes that for a measurement m, we have a successful result if we measure a state either side of b within a distance of e, which is the conventional assumption.

This definition of error, however, is asymmetric because there will be unequal numbers of states summed about the phase angle ϕ in order to give the probability of a successful result, because an odd number of states is being summed. We now present a definition of the error which is symmetric about ϕ.

Modified definition of error

Given an actual angle ϕ that we are seeking to approximate in the phase estimation procedure, a measurement is called successful if it lies within a certain tolerance e of the true value ϕ. That is, for a measurement of state m out of a possible 2^t states, the probability of failure will be

$$\epsilon = p\left(\left|2\pi\frac{m}{2^t} - \phi\right| > \frac{1}{2}\frac{2\pi}{2^s}\right). \tag{2.27}$$

Thus, we consider the angle to be successfully measured accurate to s bits, if the estimated ϕ lies in the range $\phi \pm \frac{1}{2}\frac{2\pi}{2^s}$. Considering our previous definition Eq. (2.25), due to the fact that b is defined to be always less than ϕ, then compared to the previous definition of ϵ, we lose the outermost state at the lower end of the summation in Eq. (2.26) as shown in Fig. (2.3). For example, for $p = 1$, the upper bracket in Fig. (2.3) (representing the error bound) can only cover two states instead of three, and so the sum in Eq. (2.26) will now sum from 0 to 1, instead of -1 to 1, for this case.

[1] Nielsen and Chuang [NC02] in the preliminary to Eq. 5.35, appear to have written incorrectly $2^p - 1$ instead of 2^{p-1}.

An optimal bound

Based on this new definition then for all cases we need to add 1 to the lower end of the summation giving

$$\epsilon = 1 - \frac{1-\cos 2\pi 2^t\delta}{2^{2t}} \sum_{\ell=-2^{p-1}+1}^{2^{p-1}} \frac{1}{1-\cos 2\pi(\delta-\ell/2^t)} \tag{2.28}$$

and if we define $a = 2^t\delta$ and rearrange the cosine term in the summation, we find

$$\epsilon = 1 - \frac{1-\cos 2\pi a}{2^{2t+1}} \sum_{\ell=-2^{p-1}+1}^{2^{p-1}} \csc^2\frac{\pi}{2^t}(a-\ell). \tag{2.29}$$

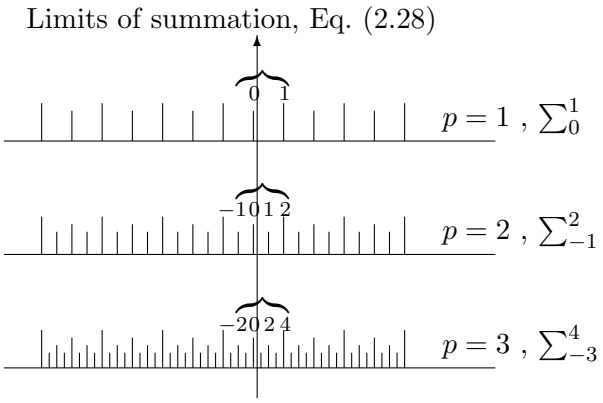

Figure 2.3: Analysis of phase estimation accuracy.

Next, we demonstrate that the right hand side of Eq. (2.29) takes its maximum value at $a = \frac{1}{2}$. Since we know $0 \le a < 1$, and since we expect the maximum value of $\epsilon = \epsilon(a,t,p)$ to lie about midway between the two nearest states to generate the largest error, that is at $a = 1/2$, we will substitute $a = \frac{1}{2} + \Delta$, where $\Delta \ll \frac{1}{2}$. To maximize ϵ we need to minimize

$$\cos 2\pi\left(\frac{1}{2}+\Delta\right) \sum_{\ell=-2^{p-1}+1}^{2^{p-1}} \csc^2\frac{\pi}{2^t}\left(\frac{1}{2}-\ell+\Delta\right), \tag{2.30}$$

as a function of Δ. Expanding to quadratic order with a Taylor series, we seek to minimize

$$\left(1-\pi^2\Delta^2+O(\Delta^4)\right)\left(c_0+c_1\Delta+c_2\Delta^2+c_3\Delta^3+O(\Delta^4)\right), \tag{2.31}$$

where c_i are the coefficients of the Taylor expansion of cosecant^2 in Δ. We find by the odd symmetry of the cotangent about $\ell = \frac{1}{2}$ that

$$c_1 = \frac{2\pi}{2^t} \sum_{\ell=-2^{p-1}+1}^{2^{p-1}} \cot\frac{\pi}{2^t}(\tfrac{1}{2}-\ell)\csc^2\frac{\pi}{2^t}(\tfrac{1}{2}-\ell) = 0, \tag{2.32}$$

and so we just need to minimize

$$c_0 + (c_2 - c_0\pi^2)\Delta^2 + O(\Delta^3). \tag{2.33}$$

Differentiating, we see we have an extremum at $\Delta = 0$ and, therefore, $\epsilon(a,t,p)$ has a maximum at $a = 1/2$. Substituting $a = \frac{1}{2}$ we obtain

$$\epsilon \le 1 - \frac{2}{2^{2t}} \sum_{\ell=-2^{p-1}+1}^{2^{p-1}} \frac{1}{1-\cos\frac{2\pi}{2^t}(\frac{1}{2}-\ell)}. \tag{2.34}$$

We note that the summation is symmetrical about $\ell = 1/2$, and substituting $t = p + s$, we obtain for our final result

$$\epsilon(s,p) = 1 - \frac{1}{2^{2(p+s)-2}} \sum_{\ell=1}^{2^{p-1}} \frac{1}{1-\cos\frac{\pi(2\ell-1)}{2^{(p+s)}}}. \tag{2.35}$$

That is, given a desired accuracy of s bits, then if we add p more bits, we have a probability of success given by $1-\epsilon$, of obtaining a measurement to at least s bits of accuracy. Thus, we have succeeded in deriving a best possible bound for the failure rate $\epsilon = \epsilon(s,p)$.

2.3.3 Special cases

Numerical calculations show that $\epsilon(t,p)$ quickly approaches its asymptotic value as $t \to \infty$, and this limit gives a fairly accurate upper bound for ϵ, for t greater than about 10 qubits. Using $\cos x \geq 1 - \frac{x^2}{2}$ which is valid for all x, and is accurate for $x = O(1/2^t)$ as $t \to \infty$

$$\begin{aligned} \epsilon &\leq 1 - \frac{4}{2^{2t}} \sum_{\ell=1}^{2^{p-1}} \frac{1}{1-(1-\frac{1}{2}(\frac{\pi}{2^t}(2\ell-1))^2)} \\ &= 1 - \frac{8}{\pi^2} \sum_{\ell=1}^{2^{p-1}} \frac{1}{(2\ell-1)^2}. \end{aligned} \tag{2.36}$$

An exact form for this can be found in terms of the trigamma function, being a special case of the polygamma function as shown in Abramowitz and Stegun [AS64], Eq. 6.4.5

$$\epsilon \leq \frac{2}{\pi^2} \psi'\left(\frac{1+2^p}{2}\right), \tag{2.37}$$

where $\psi'(z) = \frac{d\psi}{dz}$ is the trigamma function, $\psi(z) = \frac{\Gamma'(z)}{\Gamma(z)}$ is the digamma function and $\Gamma(z) = \int_0^\infty t^{z-1}\mathrm{e}^{-t}dt$ is the standard gamma function.

Now, considering the $p \to \infty$ limit, which also includes the $t \to \infty$ limit because $t = p + s$, we can find an asymptotic form in the limit of large p also from [AS64], see Eq 6.4.12, namely

$$\epsilon = \frac{4}{\pi^2} 2^{-p}, \tag{2.38}$$

which shows that the error rate drops off exponentially with the extra qubits p. It is found numerically that the $p = \infty$ limit is approached closely for small p, namely $p \approx 5$. The formula Eq. (2.38) can be re-arranged to give

$$p_\infty = \left\lceil \log_2 \frac{2\sqrt{2}}{\pi^2 \epsilon} \right\rceil, \tag{2.39}$$

which compares with the previous approximate formula shown in Eq. (2.19).

We have confirmed these formulas through a simulation by running the phase estimation algorithm on the 2-dimensional rotation matrix, and undertaking a numerical search for the rotation angle which maximizes the error ϵ. For the case $p = 1$ at the limit of large t using Eq. (2.36), we can calculate the maximum expected error to $\epsilon = 1 - \frac{8}{\pi^2} = 18.9430531\%$.

We can see from Table I, that even for a relatively small number of qubits such as $t = s + p = 15$, the upper bound formula at $t \to \infty$ is accurate to seven decimal places.

s	simulation	$\epsilon(\infty,1)=1-\frac{8}{\pi^2}$	$\epsilon(s,1)$, Eq. (2.35)
1	14.013022	18.9430531	14.644661
2	17.86115	18.9430531	17.893305
3	18.680222	18.9430531	18.682134
4	18.877800	18.9430531	18.877918
5	18.926767	18.9430531	18.9267751
6	18.9389835	18.9430531	18.9389840
7	18.9420358	18.9430531	18.9420358
8	18.9427988	18.9430531	18.9427988
9	18.9429895	18.9430531	18.9429895
10	18.9430373	18.9430531	18.9430372
11	18.9430491	18.9430531	18.9430491
12	18.9430521	18.9430531	18.9430521
13	18.9430526	18.9430531	18.9430528
14	18.943052	18.9430531	18.9430530

Table 2.1: Simulation results, $p = 1$

ϵ %	$p_{\text{Eq.[2.37]}}$	p_{CEM}	p_∞
100.00	0	0	-1
18.943	1	2	1
9.937	2	3	2
5.040	3	4	3
2.530	4	5	4
1.266	5	6	5
0.632	6	7	6
0.3166	7	8	7
0.1583	8	9	8
0.07916	9	10	9
0.03958	10	11	10
0.019789	11	12	11
0.0098946	12	13	12
0.0049473	13	14	13
0.0024737	14	15	14
0.0012368	15	16	15
0.0006184	16	17	16
0.0003092	17	18	17
0.00015460	18	19	18
0.00007730	19	20	19
0.000038651	20	21	20

Table 2.2: Comparison of the $t \to \infty$ bounds formulas.

2.3.4 Summary

To calculate ϕ accurate to a specified s bits with a given probability of success $1-\epsilon$ we add p extra qubits, where p is given by Eq. (2.35). If we have a large number of qubits, then we can use the formula Eq. (2.37) valid at the $t \to \infty$ limit. In the $p \to \infty$ limit the asymptote is found as a simple exponential form Eq. (2.38). We see that the previous upper bound formula p_{CEM} overshoots by 1 for each choice of ϵ in Table II, so the newly derived formulas are a significant improvement. We have found this formula to be useful in confirming the operation of classical algorithms, since it enables us to equate simulation outputs with exact numbers

from Eq. (2.35).

The improved error formula in Eq. (2.35) was published in Public Library of Science, Volume 6(5). [JMCL11b] (attached).

Authors: J. M. Chappell(Adelaide University), M. A. Lohe(Adelaide University), Lorenz von Smekal(Adelaide University), A. Iqbal(Adelaide University) and D. Abbott(Adelaide University).

Statement of contributions: J. Chappell modified the conventional error formula by increasing its symmetry to allow an exact solution. J. Chappell, M. A. Lohe, Lorenz von Smekal and A. Iqbal prepared the paper for publication, with checking by D. Abbott, M. A. Lohe and Lorenz von Smekal.

Signed:

J. M. Chappell Dr M.A. Lohe Dr L. von Smekal Dr A. Iqbal

Prof. D.Abbott

3

Grover's Algorithm

Grover's search algorithm [Gro98a] is a general search routine to retrieve a set of required items from an unstructured data set. Given an unsorted database of size N, we would classically expect that it will take $N/2$ queries, on average, to find a specific entry, Grover's quantum algorithm, on the other hand, allows a specific entry to be found in just $O(\sqrt{N})$ queries. The speedup that this algorithm provides is a result of quantum parallelism. The database is effectively put into a uniform superposition of all possible search outcomes and then the results interfered with each other to produce a probability distribution concentrated at the solutions. In this section, after reviewing the Grover search procedure, we look at ways to speedup the search and we find a different type of search based on the phase estimation procedure, developed from the previous chapter (Chapter 2). We then proceed to model the search as the precession of a spin-$\frac{1}{2}$ particle. Generalizing the Hamiltonian based search, we find SU(2) generators for the Grover search space, which can be modeled as the precession of a single spin-$\frac{1}{2}$ particle. In the following chapter, because GA is known to be a very efficient formalism for handling rotations and hence precession, we extend this analysis using GA, which shows the efficiency of the formalism and also confirms the optimality of the standard Grover search [BBB$^+$00], [Høy00].

3.1 Grover's search algorithm

Suppose we have a search space of N elements, indexed by a number in the range 0 to $N-1$. For convenience we assume $N = 2^n$, so that the index can be stored in n bits. We assume we have M solutions to the search query, with $1 \leq M \leq N$. A particular instance of the solution set can be flagged by a function f, which takes as input an integer x in the range 0 to $N-1$. We define $f(x) = 1$ if x is a solution to the search problem, and $f(x) = 0$ otherwise. We assume we have an oracle which can recognize solutions to the search problem, defined as a unitary operator

$$|x\rangle|q\rangle \xrightarrow{O} |x\rangle|q \oplus f(x)\rangle, \tag{3.1}$$

where $|\, x\rangle$ is the index register, $\oplus$ denotes addition modulo 2 and an extra bit called the oracle qubit $|q\rangle$ is a single qubit which is flipped if $f(x) = 1$, and is unchanged otherwise. For example we can check to see if x is a solution by preparing the state $|x\rangle|0\rangle$, applying the oracle, and checking to see if the oracle qubit has been flipped to $|1\rangle$. However, in practice, it is preferable to initialize the oracle qubit to $(|0\rangle - |1\rangle)/\sqrt{(}2)$, so that in this case the action of the oracle will simply be to the flip the sign of the qubit, that is

$$|x\rangle\frac{|0\rangle - |1\rangle}{\sqrt{2}} \xrightarrow{O} (-1)^{f(x)}|x\rangle\frac{|0\rangle - |1\rangle}{\sqrt{2}}. \tag{3.2}$$

However, we notice in this case that the state of oracle qubit is not changed and so can be omitted from further analysis, hence the action of the oracle can now be written

$$|x\rangle \xrightarrow{O} (-1)^{f(x)}|x\rangle. \tag{3.3}$$

We say that the oracle marks the solution to the search problem by shifting the phase of the solution.

The oracle makes use of n qubits along with extra work bits. Initially, the algorithm begins with a Hadamard transform to put the computer in an equal superposition state

$$|\psi\rangle = \frac{1}{N^{1/2}} \sum_{x=0}^{N-1} |x\rangle. \tag{3.4}$$

The main algorithm then consists of repeated applications of the Grover iteration G, which will be shown to only be needed to be called $O(\sqrt{N})$ times. The two main components of a Grover iteration are the oracle and a phase shift operation.
The phase shift operation, in which all states except $|0\rangle^{\otimes n}$ receive a phase shift of -1, can be written:

$$|x\rangle \longrightarrow -(-1)^{\delta_{x0}}|x\rangle. \tag{3.5}$$

Clearly, this could also be written as $2|0\rangle\langle 0| - I_{N\times N}$. That is

$$\begin{bmatrix} 1 & 0 & 0 & \dots & 0 \\ 0 & -1 & 0 & \dots & 0 \\ \vdots & & & & \\ 0 & 0 & 0 & \dots & -1 \end{bmatrix} = 2 \begin{bmatrix} 1 & 0 \dots 0 \\ 0 & 0 \dots 0 \\ \vdots & \\ 0 & 0 \dots 0 \end{bmatrix} - \begin{bmatrix} 1 & 0 \dots 0 \\ 0 & 1 \dots 0 \\ \vdots & \\ 0 & 0 \dots 1 \end{bmatrix} = 2|0\rangle\langle 0| - I_{N\times N}. \tag{3.6}$$

Combining steps 2, 3 and 4 gives

$$H^{\otimes n}(2|0\rangle\langle 0| - I)H^{\otimes n} = 2H^{\otimes n}|0\rangle\langle 0|H^{\otimes n} - H^{\otimes n}H^{\otimes n} = 2|\psi\rangle\langle\psi| - I, \tag{3.7}$$

where ψ is the equal superposition of states defined in Eq. (3.4) and we know $H^2 = I$. Thus, the full Grover iteration may be written:

$$G = (2|\psi\rangle\langle\psi| - I)\, O. \tag{3.8}$$

We will now show that the Grover iteration can be regarded as a rotation in the the two-dimensional space spanned by the starting vector $|\psi\rangle$ and the state consisting of a uniform superposition of solutions to the search problem. To demonstrate this we define $\sum_x{}'$ to indicate a sum over all x which are solutions to the search problem and $\sum_x{}''$ to indicate a sum

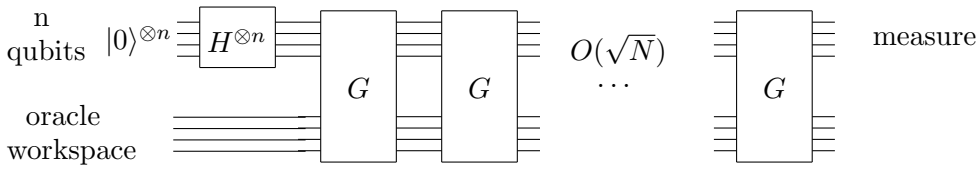

Figure 3.1: The search algorithm.

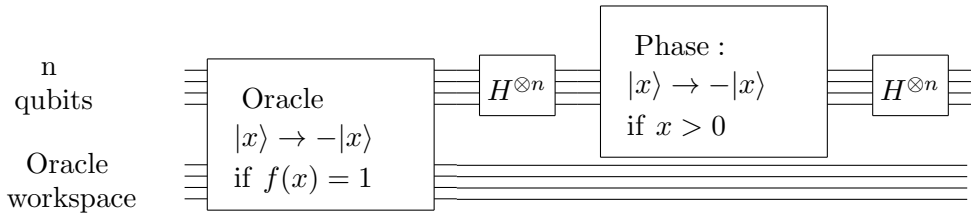

Figure 3.2: One Grover iteration.

over all x which are not solutions to the search problem. We can then define the normalized states

$$\begin{aligned} |m^{\perp}\rangle &\equiv \frac{1}{\sqrt{N-M}}\sum_{x}{}'' |x\rangle \\ |m\rangle &\equiv \frac{1}{\sqrt{M}}\sum_{x}{}' |x\rangle. \end{aligned} \tag{3.9}$$

It is then easy to see that

$$|\psi\rangle = \sqrt{\frac{N-M}{N}}|m^{\perp}\rangle + \sqrt{\frac{M}{N}}|m\rangle, \tag{3.10}$$

and so the initial state $|\psi\rangle$ of the quantum computer is in the space spanned by $|m^{\perp}\rangle$ and $|m\rangle$. Now, the effect of G operating on the state $|\psi\rangle$ can be seen as simply a rotation in the plane of $|m^{\perp}\rangle$ and $|m\rangle$. Referring to the Grover iteration defined in Eq.(3.8), initially we apply the oracle O. We have in the general case $O(a|m^{\perp}\rangle + b|m\rangle) = a|m^{\perp}\rangle - b|m\rangle$, so O creates a reflection about the vector $|m^{\perp}\rangle$. Next, applying $2|\psi\rangle\langle\psi| - I$, we notice it also forms a reflection in the plane defined by $|m^{\perp}\rangle$ and $|m\rangle$, about the vector $|\psi\rangle$ and the product of two reflections is a rotation. Thus, $G^k|\psi\rangle$ remains in the space defined by $|m^{\perp}\rangle$ and $|m\rangle$ for all k. The angle of rotation is given by

$$\cos\theta/2 = \sqrt{(N-M)/N} \tag{3.11}$$

and clearly then also

$$\sin\theta/2 = \sqrt{M/N}. \tag{3.12}$$

Hence, we have $|\psi\rangle = \cos\frac{\theta}{2}|m^{\perp}\rangle + \sin\frac{\theta}{2}|m\rangle$. Looking at Fig. 3.3 we can say

$$G|\psi\rangle = \cos\frac{3\theta}{2}|m^{\perp}\rangle + \sin\frac{3\theta}{2}|m\rangle, \tag{3.13}$$

so this implies a rotation angle of θ.

Hence, it follows that the continued application of G takes the state to

$$G^k|\psi\rangle = \cos\frac{(2k+1)\theta}{2}|m^{\perp}\rangle + \sin\frac{(2k+1)\theta}{2}|m\rangle. \tag{3.14}$$

Repeated applications of Grover's iteration thus rotates the state vector by θ, closer and closer to $|m\rangle$. When this occurs, an observation in the computational basis produces with high probability one of the outcomes superposed in $|m\rangle$, which is a solution to the search problem. Clearly, therefore, we could also write the Grover iteration in $|m\rangle$, $|m^{\perp}\rangle$ space in matrix form as

$$G = \begin{bmatrix} \cos\theta & -\sin\theta \\ \sin\theta & \cos\theta \end{bmatrix}. \tag{3.15}$$

3.1.1 Performance

The initial state of the system is $|\psi\rangle = \sqrt{\frac{N-M}{N}}|m^{\perp}\rangle + \sqrt{\frac{M}{N}}|m\rangle$, so clearly rotating through $\arccos\sqrt{M/N}$ radians takes the system to $|m\rangle$. Then, repeating the Grover iteration

$$\begin{aligned} f &= \frac{\arccos\sqrt{M/N}}{\theta} \\ &= \frac{\pi/2 - \theta/2}{\theta} \\ &= \frac{\pi}{2\theta} - \frac{1}{2} \\ &= \frac{\pi}{4}\frac{1}{\sin^{-1}\sqrt{\frac{M}{N}}} - \frac{1}{2} \end{aligned} \tag{3.16}$$

times rotates $|\psi\rangle$ to within an angle $\theta/2$ of $|m\rangle$. We notice the number of iterations f may not turn out to be an integer which indicates that in this case that we cannot find the solution exactly. However, we will discover in the next section that we can modify the phases in the Grover iteration to adjust θ so that f is an integer and hence reduce this error to zero. Assuming that $M \leq N/2$, from Eq. (3.12) we have $\theta/2 \geq \sin\theta/2 = \sqrt{M/N}$, and for large N, we can approximate the number of iterations required to

$$f \approx \frac{\pi}{4}\sqrt{\frac{N}{M}} - \frac{1}{2}. \tag{3.17}$$

That is, $f = O(\sqrt{N/M})$ Grover iterations (and thus oracle calls) must be performed in order to obtain a solution to the search problem with high probability, a quadratic improvement over the $O(N/M)$ oracle calls required classically.

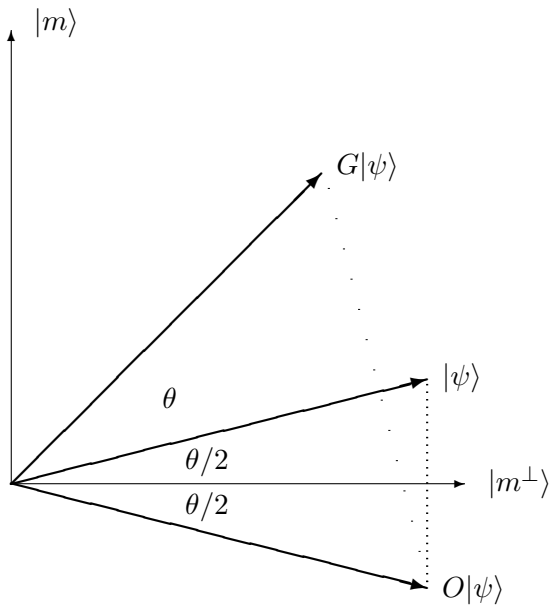

Figure 3.3: The Grover iteration as a rotation. The action of the oracle O is to flip the starting state about $|m^{\perp}\rangle$, followed by a reflection about the starting state $|\psi\rangle$, giving $G|\psi\rangle$ an anticlockwise rotation of the starting state by θ.

3.1.2 Quantum counting

It might appear from this result that any knowledge at all about the solution is going to require $O(\sqrt{N})$ queries of the oracle, for example, to find out if even a solution exists. However, there is a shortcut procedure called quantum counting, which applies the phase estimation procedure to the Grover iterate matrix directly, which in this case will return the eigenvalues of the Grover iterate matrix, from which we can calculate the number of solutions.

So, suppose $|a\rangle$ and $|b\rangle$ are the two eigenvectors of the Grover iteration in the space spanned by $|m\rangle$ and $|m^{\perp}\rangle$ and let θ be the rotation angle determined by the Grover iteration. In this space the corresponding eigenvalues are $\mathrm{e}^{\mathrm{i}\theta}$ and $\mathrm{e}^{\mathrm{i}(2\pi-\theta)}$, seen clearly by inspecting the Grover iteration in matrix form Eq.(3.15).

The function of the phase estimation circuit is to estimate θ to s bits of accuracy, with a probability of success at least $1-\epsilon$. The first register contains t qubits to give the desired accuracy, as per the phase estimation algorithm and the second register contains n qubits sufficient to represent the database and to run the Grover iteration. The state of the second register is initialized to an equal superposition of all possible inputs $\sum_x |x\rangle$ by a Hadamard transform, which can be shown to be an equal superposition of the the two eigenstates $|a\rangle$ and $|b\rangle$. So, phase estimation will give us an estimate of θ or $2\pi-\theta$ accurate to within $|\Delta\theta| \leq 2^{-s}$, with probability at least $1-\epsilon$. Quantum counting then uses the formula $\sin^2\theta = M/N($ Eq. (3.12)), and because we know N the size of the search space, we can calculate M, the number of solutions.

However, once we know the number of solutions, by running the quantum counting algorithm, we now have redundant information, because we can now calculate the number of iterations required either from quantum counting or from the Grover formula, found in Eq. (3.16). Writing out these two formulas we have

$$f_{grover} = \frac{\pi}{4}\frac{1}{\sin^{-1}(a)} - \frac{1}{2}, \tag{3.18}$$

where a is the overlap amplitude of the starting wave function with the solution states and from quantum counting after finding θ, we can also find the number of iterations as

$$f_{qc} = \frac{\pi}{2\theta} - \frac{1}{2}. \tag{3.19}$$

Therefore, if we equate these two equations, we find

$$\begin{aligned} \frac{\pi}{4}\frac{1}{\sin^{-1}(a)} - \frac{1}{2} &= \frac{\pi}{2\theta} - \frac{1}{2} \\ \frac{1}{2}\frac{1}{\sin^{-1}(a)} &= \frac{1}{\theta} \\ 2\sin^{-1}(a) &= \theta. \end{aligned}$$

From which we obtain the formula (which is related to Eq.(3.12))

$$a = \sin\frac{\theta}{2}. \tag{3.20}$$

Hence, we can calculate the starting probability overlap amplitude, with the solution state from the measured θ obtained from phase estimation. Using Hadamard gates to generate the starting probability distribution, this amplitude is fixed by the size of the search problem, if, however, we use a two-step starting probability distribution then, depending on which half of the search space the solution lies in, we will obtain two different values of θ from phase estimation.

For example using Hadamard gates to generate the initial probability distribution, we have $a = 1/\sqrt{N}$. So, if we take $N = 16$ we have $a = 1/4$, and so $f_{opt} = \frac{\pi}{4}\frac{1}{\sin^{-1}(1/4)} - \frac{1}{2} = 2.6083$. Using the phase estimation algorithm in the Java simulator with 7 qubits of accuracy we obtain $f_{qc} = 2.70 \pm 0.135$, which agrees within the uncertainty limits.

3.1.3 Two-step starting probability distributions

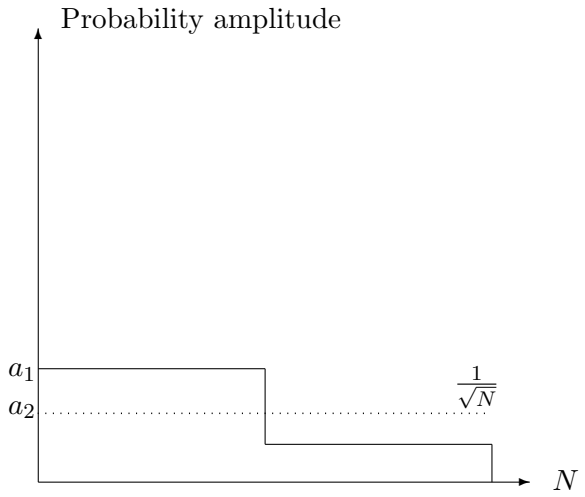

Figure 3.4: Starting probability distribution. The first part of the Grover operator flips the starting state $|\psi\rangle$ about the $|m^{\perp}\rangle$ axis given by $O|\psi\rangle$, followed by a reflection about the starting state axis $|\psi\rangle$, resulting in the state $G|\psi\rangle$, a rotation of the starting state by θ towards the solution $|m\rangle$.

So, if we assume we have a two step probability distribution as shown in Fig. (3.4), then looking again at our previous result:

$$a = \sin\frac{\theta}{2}, \tag{3.21}$$

we have $0 < \theta < \pi/2$, hence we have a 1:1 map between θ and a. For large databases, we have $a \sim \frac{1}{\sqrt{N}} \to 0$ hence $\theta \approx 2a$. That is, the rotation angle for each Grover iteration is approximately twice the probability amplitude at the solution state.

If the solution lies in the left half of the probability distribution, then the angle corresponding to this probability will be measured or $2\sin^{-1}(a_1)$, otherwise the angle θ based on the other probability amplitude $2\sin^{-1}(a_2)$ will be measured. Hence, by running the phase estimation procedure on the Grover matrix for the two level probability distribution, we can determine which half of the search space the solution lies in. However, we could then repeat this process on the half where the solution lies, partitioning this half into two parts, and then continuing the process until we are left with just one element in the search space, which must be the solution. So, if we have a search space of size $N = 2^n$, then after $n = \log N$ applications of the phase estimation procedure, we will be left with a single entry and we will have thus found the solution state. As an example a search space of size 64, will need to be split six times (32,16,8,4,2,1) to reduce to a single entry which equals $\log_2 64$. The phase estimation procedure requires $O(\log^3(N))$ operations, hence, overall, this search procedure will require $O(\log^4(N))$ operations and therefore apparently exponentially faster then Grover's algorithm of $O(\sqrt{N})$.

The only change we have made to the phase estimation procedure is to include a two-step probability amplitude, which reduces one half of the probability distribution to zero and increases the other half by the square root of two. So, in the phase estimation we will either measure zero or $\theta = 2\sin^{-1}(a)$. The two-step distribution is actually easily formed from a uniform superposition of Hadamard gates with the first qubit left at zero, that is $I \otimes H^{\otimes(n-1)}$, which will replace the conventional $H^{\otimes n}$ to form the uniform starting probability distribution. This means the first half of the probability distribution will have amplitude $\frac{\sqrt{2}}{\sqrt{N}}$ and the

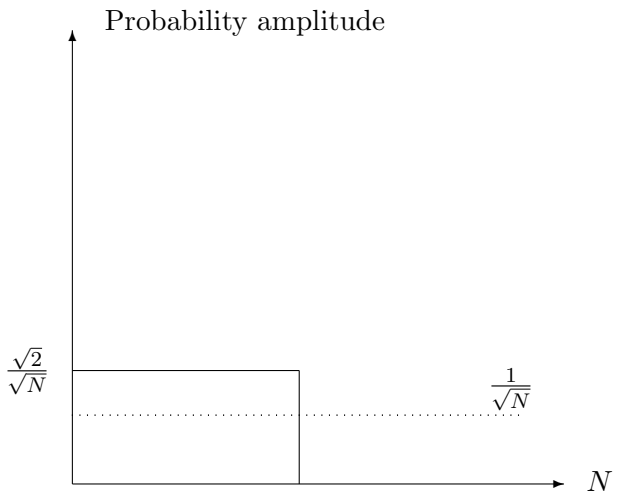

Figure 3.5: First pass.

second half will have probability amplitude zero and will actually simplify the Grover iterate somewhat. Instead of modifying the unitary transformation to form a narrower and narrower step, we could also just slide the first two step distribution across half a division. This will also enable the location of the solution state to be continually refined with a much smaller change to the unitary transformation, which will basically just require row swaps.

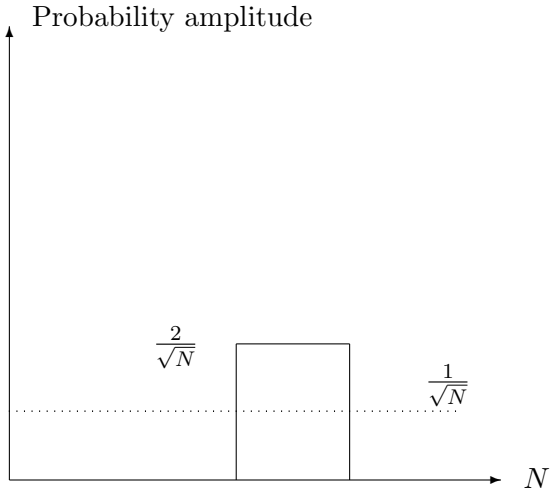

Figure 3.6: Second pass.

Incidentally, the two-step unitary matrix will be of the form

$$\begin{bmatrix} \frac{\sqrt{2}}{\sqrt{N}} \dots \frac{-\sqrt{2}}{\sqrt{N}} & 0 \dots 0 \\ \vdots & \vdots \\ \frac{\sqrt{2}}{\sqrt{N}} \dots \frac{\sqrt{2}}{\sqrt{N}} & 0 \dots 0 \\ 0 \dots 0 & 1 \dots 0 \\ \vdots & \vdots \\ 0 \dots 0 & 0 \dots 1 \end{bmatrix}.$$

The two-step probability distributions can be demonstrated in the Java simulator, in the *Distributions* option under the *Modules* menu. To see the change in θ depending on the

location of the solution in the search space select *Modules: Quantum Counting: Quantum Counting 32 two-Step.*

3.1.4 A single pass search using phase estimation

If we recall that we have a 1:1 correspondence between θ and a from Eq.(3.20), then if we can create a one to one correspondence between a and the solution state τ, then by measuring θ we can then immediately calculate τ, that is $\theta \rightarrow a \rightarrow \tau$. If this is possible, then this would enable us to solve the search problem with a single pass of the phase estimation procedure.

To do this we create a linear starting probability distribution, which simply requires us to derive an appropriate unitary transformation acting on $|0\rangle^{\otimes n}$ to generate this distribution, that is we require

$$\begin{bmatrix} U \end{bmatrix} \begin{bmatrix} 1 \\ 0 \\ \vdots \\ 0 \end{bmatrix} = \begin{bmatrix} a_1 \\ a_2 \\ \vdots \\ a_N \end{bmatrix}, \tag{3.22}$$

where $\sum |a_i|^2 = 1$, and therefore U must be of the form

$$\begin{bmatrix} a_1 & u_{12} \dots u_{1N} \\ a_2 & u_{22} \dots u_{2N} \\ \vdots & \\ a_N & u_{N2} \dots u_{NN} \end{bmatrix}. \tag{3.23}$$

That is, the first column must simply be the probability distribution we have selected and using the property of orthonormal matrices, the remaining columns must be all orthonormal, so we can easily obtain them using the Gramm-Schmidt procedure. For example, the next column can be obtained by creating an arbitrary column of N numbers y and then the next column obtained by $u_{j1} = (y_j - (y.a)a_j)/Z$, where Z is a normalization factor. The Gramm-Schmidt procedure is then continued for the remaining columns.

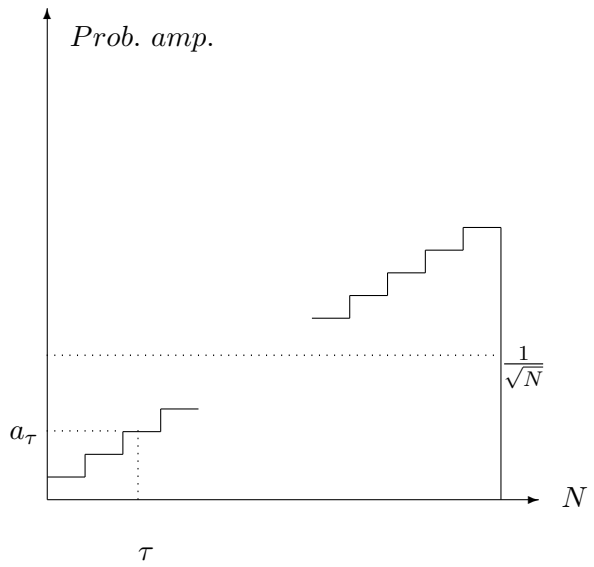

Figure 3.7: Linear starting probability amplitude.

A possible starting linear starting probability distribution would be of the form

$$a_j = \frac{j}{Z}, \tag{3.24}$$

where $j = 0...N-1$ and the normalization factor Z would need to be defined as $Z^2 = \frac{N^3}{3} - \frac{N^2}{2} + \frac{N}{6}$. We remember for large N that $\theta \approx 2a = \frac{2j}{Z}$, therefore the angular distance we need to be able to discriminate between successive states is

$$\delta\theta = \frac{2(j+1)}{Z} - \frac{2j}{Z} = \frac{2}{Z}. \tag{3.25}$$

So, the error in the θ measurement $\frac{1}{2^s}$ due to truncation of bits is $\frac{\delta\theta}{2\pi}$ and so using Eq. (3.25) we have

$$\frac{1}{2^s} < \frac{2/Z}{2\pi},$$

which we can simplify to

$$2^s > \pi Z \tag{3.26}$$

$$s > \log Z + \log \pi \tag{3.27}$$

but $\frac{N^3}{3} > \frac{N^3}{3} - \frac{N^2}{2} + \frac{N}{6}$, which approaches an equality for large N, so therefore we have

$$\log\sqrt{\frac{N^3}{3} - \frac{N^2}{2} + \frac{N}{6}} + \log\pi < \log\sqrt{\frac{N^3}{3}} + \log\pi = \frac{3}{2}\log N + \log\frac{\pi}{\sqrt{3}} < \frac{3}{2}\log N + 1$$

and $N = 2^n$, hence, conservatively, we require

$$s > \frac{3}{2}\log N + 1 = \frac{3}{2}n + 1. \tag{3.28}$$

Hence, for a search space of size 16, that is $n = 4$, we require $s = 7$ bits in accuracy to measure θ sufficiently accurately to distinguish between adjacent states. Importantly, though, the number of bits required only scales as $\log N$.

For the inverse Fourier transform we require $O(t^2)$ operations, however, we also require t ctrl-Grover operations and to raise matrices to a power requires $O(\log^2 N)$ operations, where N is the size of the search space. However, we need to repeat this procedure $t-1$ times, hence this gives us $O(\log^3 N)$ operations.

If we have have multiple solutions, then the linear probability distribution method will fail because the phase estimation will return the angle based on the root mean square of the contributing amplitudes, as discussed earlier, that is $a_{eff} = \sqrt{a_1^2 + a_2^2 + ... + a_m^2}$, and so the target solutions will be ambiguously defined. Fortunately, we can do a quantum counting procedure with the standard Grover to confirm that there is only a single solution.

The circuit to calculate the eigenvalues of the Grover matrix given by

$$G|u\rangle = \mathrm{e}^{2\pi\mathrm{i}\theta}|u\rangle, \tag{3.29}$$

where u is an eigenvector and we have t qubits required for measurement.

From the phase estimation procedure, we obtain θ and inverting Eq.(3.20) and Eq.(3.24), we find the final result which enables us to calculate the solution state from the measured θ, from phase estimation:

$$\tau = Z\sin\frac{\theta}{2}, \tag{3.30}$$

where $Z = \sqrt{\frac{N^3}{3} - \frac{N^2}{2} + \frac{N}{6}}$ and we round τ to the nearest integer, which will be the index of the solution state

$$\tau = \lceil Z\sin\frac{\theta}{2} - \frac{1}{2}\rceil. \tag{3.31}$$

Hence it appears possible to undertake a search process via an alternate process of using the phase estimation procedure on the Grover search matrix. This approach may have computational advantages, however it will only be successful if there is a single target item within the search space.

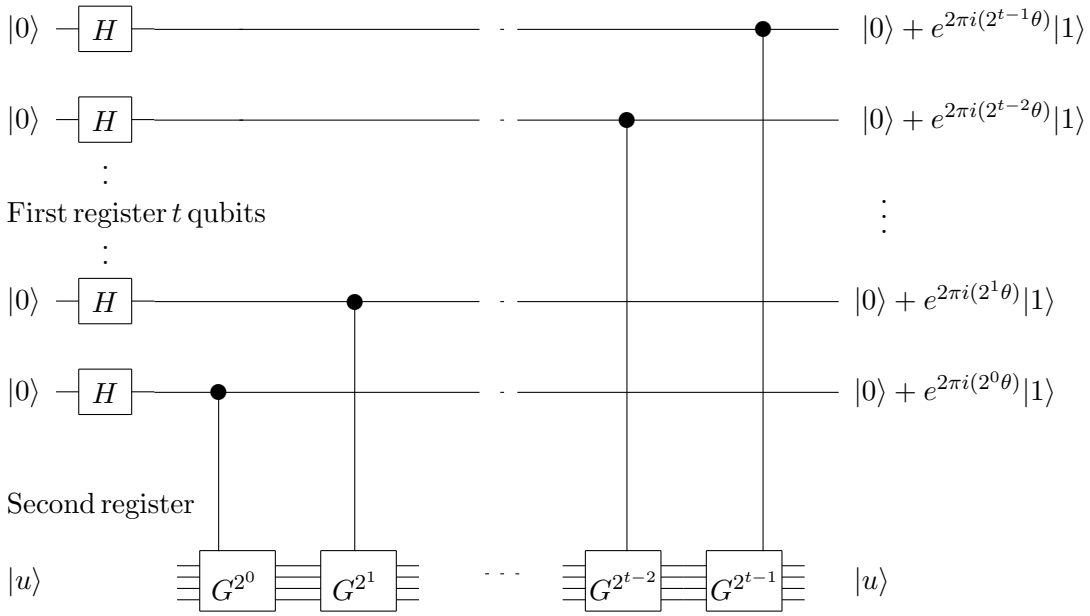

Figure 3.8: Phase estimation of the Grover matrix

Java simulation

We can simulate a search over a database of 16 elements with, say, seven bits of precision as shown in Table (3.1) by selecting *Modules: Quantum Counting: Quantum Counting-16 U=Linear*. We note that to achieve a result accurate to n qubits enabling us to calculate a solution with 81.1% reliability (18.9 % failure rate), we add one extra qubit. The matching first and last columns in Table (3.1) indicate 100 percent reliability in finding the solution, using phase estimation.

3.2 Quantum search using a Hamiltonian

Following the discovery of the Grover search algorithm, which is designed to run in the circuit model form of quantum computing, Fenner [Fen00] discovered the equivalent Hamiltonian, which is a continuous time version of the Grover search [BK02a], [RC08]. This showed the equivalence between the two approaches and we also use the Hamiltonian form of the search given here to find the SU(2) generators, as another alternative way to describe the Grover search. The Hamiltonian form can also be run adiabatically [VDMV01], [EF02], [FGGS00], [RC02].

This type of search involves finding a Hamiltonian, which evolves the starting state, $H|0\rangle$ onto the solution state $|m\rangle$. The Hamiltonian shown below achieves this and, in fact, can be shown to be equivalent to the standard Grover iteration G, if the Hamiltonian evolution is observed at some constant time increment t_0.

Assuming we have a search problem with exactly one solution, labeled m, we desire a Hamiltonian H which when evolving over time changes some initial state, say $|\psi_0\rangle$ into $|m\rangle$. As usual, we select our initial state $|\psi_0\rangle$ to be $|\sigma\rangle = H|0\rangle$. We use the Hamiltonian as shown in [Fen00]

$$H = \frac{2\mathrm{i}}{\sqrt{N}} \left(|m\rangle\langle\sigma| - |\sigma\rangle\langle m| \right), \tag{3.32}$$

which can be shown for the appropriate time step t_0, that $\mathrm{e}^{-\mathrm{i}Ht_0} = G$. We can, in fact, find $t_0 = \frac{N(\pi - 2\arccos\frac{1}{\sqrt{N}})}{2\sqrt{N-1}} \approx 1$. This shows that 1 time unit will equate to approximately 1 Grover

τ	a	$\theta = 2\sin^{-1} a$	7 bit	$\tau_{calc} = \frac{Z}{2}\sin\frac{\theta}{2} - \frac{1}{2}$	$\tau' = \lceil \tau_{calc} - \frac{1}{2} \rceil$
0	0.0135	1.55	0	-0.5	0
1	0.0406	4.66	5.6	1.3	1
2	0.0677	7.76	8.4	2.2	2
3	0.0948	10.9	11.2	3.1	3
4	0.1218	14.0	14.0	4.0	4
5	0.1489	17.1	16.8	4.89	5
6	0.1760	20.3	19.6	5.79	6
7	0.2031	23.4	22.5	6.7	7
8	0.2302	26.6	25.3,28.1	7.59,8.47	8
9	0.2572	29.8	30.9	9.3	9
10	0.2843	33.0	33.7	10.2	10
11	0.3114	36.3	36.5	11.1	11
12	0.3385	39.6	39.3	11.92	12
13	0.3655	42.9	42.1	12.8	13
14	0.3926	46.2	45.0,47.8	13.6,14.46	14
15	0.4197	49.6	50.6	15.28	15

Table 3.1: Phase estimation search simulation.

iteration in the circuit model. For analysis, we can restrict our analysis to the plane defined by $|m\rangle$ and $|\sigma\rangle$ as previously. Using $|\sigma\rangle = \alpha|m\rangle + \beta|y\rangle$, in Eq. (3.32), we have

$$\begin{aligned} H &= \frac{2\mathrm{i}}{\sqrt{N}}\left(|m\rangle\left(\alpha\langle m| + \beta\langle y|\right) - \left(\alpha|m\rangle + \beta|y\rangle\right)\langle m|\right) && (3.33)\\ &= \frac{2\mathrm{i}}{\sqrt{N}}\begin{bmatrix} 0 & \beta \\ -\beta & 0 \end{bmatrix} \\ &= \frac{2\mathrm{i}\beta}{\sqrt{N}} ZX. && (3.34) \end{aligned}$$

So,

$$\mathrm{e}^{-\mathrm{i}Ht} = \mathrm{e}^{-\mathrm{i}(\frac{2\mathrm{i}\beta}{\sqrt{N}}ZX)t} = \mathrm{e}^{\frac{2\beta t}{\sqrt{N}}ZX}.$$

We find

$$\mathrm{e}^{\frac{2\beta t}{\sqrt{N}}ZX} \equiv I + \frac{2\beta}{\sqrt{N}}ZXt + (\frac{2\beta}{\sqrt{N}}ZX)^2 t^2/2! + (\frac{2\beta}{\sqrt{N}}ZX)^3 t^3/3! + \ldots$$

but $(ZX)^2 = ZXZX = -ZXXZ = -I$ using $[X, Z]_+ = 0$, so we find

$$\mathrm{e}^{\frac{2\beta t}{\sqrt{N}}ZX} = I + \frac{2\beta}{\sqrt{N}}tZX - (\frac{2\beta}{\sqrt{N}})^2 t^2/2! - (\frac{2\beta}{\sqrt{N}})^3 t^3/3!ZX + \ldots$$

hence

$$\mathrm{e}^{\frac{2\beta t}{\sqrt{N}}ZX} = I\cos\frac{2\beta t}{\sqrt{N}} + ZX\sin\frac{2\beta t}{\sqrt{N}}$$

and so

$$\mathrm{e}^{-\mathrm{i}Ht}|\sigma\rangle = \cos\frac{2\beta t}{\sqrt{N}}|\sigma\rangle + \sin\frac{2\beta t}{\sqrt{N}}ZX|\sigma\rangle.$$

We note

$$ZX|\sigma\rangle = ZX(\alpha|m\rangle + \beta|y\rangle) = \beta|m\rangle - \alpha|y\rangle.$$

Hence, the state of the system after time t is

$$\begin{aligned} \mathrm{e}^{-\mathrm{i}Ht}|\sigma\rangle &= \cos\frac{2\beta t}{\sqrt{N}}|\sigma\rangle + \sin\frac{2\beta t}{\sqrt{N}}\left(\beta|m\rangle - \alpha|y\rangle\right) && (3.35)\\ &= \cos\frac{2\beta t}{\sqrt{N}}|\sigma\rangle + \sin\frac{2\beta t}{\sqrt{N}}\frac{\alpha}{\beta}\left(\frac{\beta^2}{\alpha}|m\rangle + \alpha|m\rangle - |\sigma\rangle\right) \\ &= \left(\cos\frac{2\beta t}{\sqrt{N}} - \frac{\alpha}{\beta}\sin\frac{2\beta t}{\sqrt{N}}\right)|\sigma\rangle + \sin\frac{2\beta t}{\sqrt{N}}\frac{\alpha}{\beta}\left(\frac{\beta^2}{\alpha} + \alpha\right)|m\rangle && (3.36)\\ &= \left(\cos\frac{2\beta t}{\sqrt{N}} - \frac{\alpha}{\beta}\sin\frac{2\beta t}{\sqrt{N}}\right)|\sigma\rangle + \frac{1}{\beta}\sin\frac{2\beta t}{\sqrt{N}}|m\rangle. && (3.37) \end{aligned}$$

So, we require $\sin\frac{2\beta t}{\sqrt{N}} = \beta$, or $t = \frac{\sqrt{N}}{2\beta}\arcsin\beta$, where clearly all coefficients are real. For the uniform superposition state $|\sigma\rangle$, we know $\alpha = \frac{1}{\sqrt{N}}$, hence an observation of the system at time

$$t = \frac{N}{2\sqrt{N-1}}\arcsin\sqrt{1-\frac{1}{N}} \approx \frac{\pi}{4}\sqrt{N} \tag{3.38}$$

yields the solution m with probability one. This agrees with the complexity of the Grover circuit search of $\frac{\pi\sqrt{N}}{4} - \frac{1}{2}$. (These two can be equated because $t_0 \approx 1$.) Hence, the state of the system at solution time T is

$$\mathrm{e}^{-\mathrm{i}HT}|\sigma\rangle = |m\rangle.$$

Hypothetically, if we could start with a Hamiltonian of higher energy E,

$$H = \frac{2E\mathrm{i}}{\sqrt{N}}\left(|m\rangle\langle\sigma| - |\sigma\rangle\langle m|\right), \tag{3.39}$$

then the state of the system after time t will be

$$\mathrm{e}^{-\mathrm{i}Ht}|\sigma\rangle = \left(\cos\frac{2E\beta t}{\sqrt{N}} - \frac{\alpha}{\beta}\sin\frac{2E\beta t}{\sqrt{N}}\right)|\sigma\rangle + \frac{1}{\beta}\sin\frac{2E\beta t}{\sqrt{N}}|m\rangle, \tag{3.40}$$

which gives us

$$t = \frac{N}{2E\sqrt{N-1}}\arcsin\sqrt{1-\frac{1}{N}}. \tag{3.41}$$

For $E = \frac{N}{\sqrt{N-1}}\arcsin\sqrt{1-\frac{1}{N}} \approx \sqrt{N}$, we have

$$T = \frac{1}{2} \tag{3.42}$$

searching in constant time and the state at this time will be

$$\mathrm{e}^{-\mathrm{i}HT}|\sigma\rangle = |m\rangle.$$

So if it is possible to increase the energy of the Hamiltonian within the abstract Grover search space, then this will allow a speedup of the search process.

3.3 The Grover Search using SU(2) rotations

The conventional Grover search algorithm [Gro97] involves evolving a wave function, from a uniform superposition starting state $|\psi\rangle = |\sigma\rangle$, onto the solution state $|\psi\rangle = |m\rangle$, where $|m\rangle$ is the set of all solutions and where, upon measurement, it will yield one element from this set. In order to analyze this evolution efficiently, typically an orthonormal basis $|m\rangle$ and $|m^{\perp}\rangle$ is

defined, as shown on Fig. (3.9). We now identify an improved basis for analyzing the search process, which allows a simple mapping to the Bloch sphere. From this, we are able to identify the Grover search evolution as equivalent to the precession of the polarization axis of spin-$\frac{1}{2}$ particle in a magnetic field, that is, precessing from the $|\sigma\rangle$ direction to the $|m\rangle$ direction.

In the field of adiabatic quantum computing [FG98a], it has been proposed that the Grover search time can be reduced to unity [WY04], by simply increasing the energy of the search Hamiltonian, thus reducing the time. Using the precession analogy, this would be equivalent to increasing the strength of the magnetic field, which would indeed reduce the precession time, thus appearing to speedup the search process. However, these ideas need to be reconciled with proofs that Grover's quantum search algorithm has been shown to be the optimal search strategy on a quantum computer [BBHT98], [Zal99], [SSB05], with complexity of $O(\sqrt{N})$. We will find that the answer to this dilemma lies in the oracle and, in fact, a circuit can indeed be constructed to search in unit time provided the Oracle is enhanced. However as stated in [CvD10], there are still unresolved issues regarding the Hamiltonian search.

To analyze the Grover search algorithm, an SU(2) approach has been used previously [HL02], which found the conditions to find a search solution with a probability of one, whereas with the conventional Grover operator, only an approximation to the solution state is ever found (except in the special case with just four states). An SO(3) picture has also been employed [LTL$^+$01] to plot the path of the state vector during each application of the Grover operator, which we will also find useful in plotting the path of the polarization axis in 3-space.

In this chapter, we will firstly define the three generators for the SU(2) search space. From these, we can derive a general rotation in this search space and the standard Grover search will then be identified as simply a special case of this. We will show that raising the energy of a search Hamiltonian in the adiabatic setting is equivalent to raising the Grover operator to a power in the circuit model representation and, as a by-product, we will give a formula for the Grover matrix raised to any non-integer power. The general search formula will also enable us to easily derive the phase matching condition for an exact search along with its matrix evolution. We will then use one of the generators to produce a quantum circuit for searching in unit time, but which will require, unfortunately, an enhanced oracle in order to succeed.

3.3.1 The Grover search space

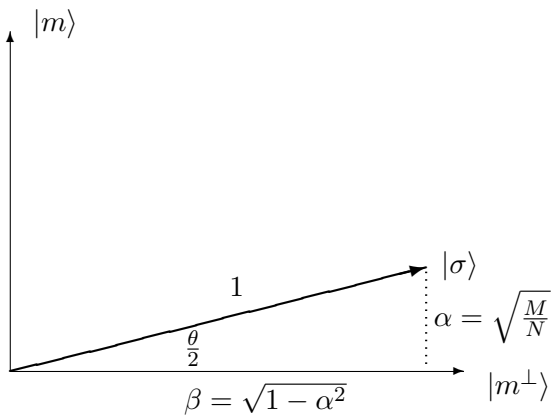

Figure 3.9: Geometry of starting state $|\sigma\rangle$. The starting state $|\sigma\rangle$ represented in the basis of $|m\rangle$ and $|m^\perp\rangle$, with M solution states in a space of size N.

Our goal in the search procedure is to rotate the starting vector $|\sigma\rangle$ in the space spanned by $|m\rangle$ and $|m^\perp\rangle$ onto the vector $|m\rangle$ so that, upon measurement, a solution to the search

problem will be achieved.

Grover's solution to this involves iteratively applying an operator G defined by

$$G = -\left(I - 2|\sigma\rangle\langle\sigma|\right)\left(I - 2|m\rangle\langle m|\right). \tag{3.43}$$

This operator applied to the $n = \log N$ qubits representing the search space, rotates the state vector an angle θ at each application, with the number of iterations given by

$$R \approx \frac{\pi}{4}\sqrt{\frac{N}{M}}. \tag{3.44}$$

3.3.2 SU(2) generators for the Grover search space

Working from the two-dimensional complex space shown in Fig. (3.9), and restricting ourselves to the well defined states $|m\rangle$ and $|\sigma\rangle$, we have four possible operators: $|m\rangle\langle\sigma|$, $|\sigma\rangle\langle m|$, $|m\rangle\langle m|$ and $|\sigma\rangle\langle\sigma|$. From these we define

$$\begin{aligned} K &= -\frac{\beta^2}{2}P \\ J_1 &= \frac{P - |\sigma\rangle\langle\sigma| - |m\rangle\langle m|}{2|\alpha|} \\ J_2 &= \frac{-\mathrm{i}\left(\alpha^*|m\rangle\langle\sigma| - \alpha|\sigma\rangle\langle m|\right)}{2|\alpha|\beta} \\ J_3 &= \frac{|\sigma\rangle\langle\sigma| - |m\rangle\langle m|}{2\beta}, \end{aligned} \tag{3.45}$$

where $\alpha = \langle\sigma|m\rangle$, in general, a complex number, and $\beta = \sqrt{1 - |\alpha|^2}$. With

$$P = \frac{\left(|\sigma\rangle\langle\sigma| - |m\rangle\langle m|\right)^2}{\beta^2}, \tag{3.46}$$

we find

$$\begin{aligned} [J_i, J_j] &= \mathrm{i}\epsilon_{ijk}J_k \\ [J_i, J_j]_+ &= \delta_{ij}\frac{P}{2} \\ [K, J_i] &= 0, \end{aligned} \tag{3.47}$$

confirming that we have an SU(2) algebra. Squaring the generators we find

$$J_1^2 = J_2^2 = J_3^2 = \frac{1}{4\beta^2}\left(|\sigma\rangle\langle\sigma| - |m\rangle\langle m|\right)^2 = \frac{1}{4}P. \tag{3.48}$$

We can easily check $P|\sigma\rangle = |\sigma\rangle$ and $P|m\rangle = |m\rangle$, with $P^2 = P$ and the Casimir invariant

$$C = J_1^2 + J_2^2 + J_3^2 = \frac{3}{4}P,$$

which corresponds to a spin $\frac{1}{2}$ system. We have raising and lowering operators

$$J_\pm = J_1 \pm \mathrm{i}J_2$$

and requiring

$$\begin{aligned} J_+|\uparrow\rangle &= 0 \\ J_-|\downarrow\rangle &= 0, \end{aligned} \tag{3.49}$$

we find the states of highest and lowest weight

$$|\uparrow\rangle = \sec\frac{\theta}{2}\left(\sin\frac{\theta}{4}|m\rangle - \mathrm{e}^{\mathrm{i}\delta}\cos\frac{\theta}{4}|\sigma\rangle\right)$$

$$|\downarrow\rangle = \sec\frac{\theta}{2}\left(\cos\frac{\theta}{4}|m\rangle - \mathrm{e}^{\mathrm{i}\delta}\sin\frac{\theta}{4}|\sigma\rangle\right),$$

which is a rotation of the $|m\rangle$ and $|m^{\perp}\rangle$ axes by $\frac{\theta}{4}$, where we have defined

$$\sin\frac{\theta}{2} = |\alpha| \tag{3.50}$$

and

$$\alpha = |\alpha|\mathrm{e}^{\mathrm{i}\delta}. \tag{3.51}$$

We can then find

$$\begin{aligned} J_3|\uparrow\rangle &= +\frac{1}{2}|\uparrow\rangle \\ J_3|\downarrow\rangle &= -\frac{1}{2}|\downarrow\rangle, \end{aligned} \tag{3.52}$$

as expected for a spin$-\frac{1}{2}$ system. Writing $|\sigma\rangle$ and $|m\rangle$ in this new basis, we obtain

$$|\sigma\rangle = \mathrm{e}^{-\mathrm{i}\delta}\left(-\cos\frac{\theta}{4}|\uparrow\rangle + \sin\frac{\theta}{4}|\downarrow\rangle\right) \tag{3.53}$$

and

$$|m\rangle = -\sin\frac{\theta}{4}|\uparrow\rangle + \cos\frac{\theta}{4}|\downarrow\rangle, \tag{3.54}$$

with

$$|m^{\perp}\rangle = \frac{1}{\beta}\left(|\sigma\rangle - \alpha^*|m\rangle\right) = \cos\frac{\theta}{4}|\uparrow\rangle + \sin\frac{\theta}{4}|\downarrow\rangle. \tag{3.55}$$

Using these results for $|\sigma\rangle$ and $|m\rangle$, and substituting into the Grover iteration Eq.(3.43), we find

$$G = -I + 2\cos^2\frac{\theta}{2}|\uparrow\rangle\langle\uparrow| + \sin\theta|\uparrow\rangle\langle\downarrow| - \sin\theta|\downarrow\rangle\langle\uparrow| + 2\cos^2\frac{\theta}{2}|\downarrow\rangle\langle\downarrow| \tag{3.56}$$

and because we have an orthonormal basis for G, we can find a matrix form for the standard Grover iteration as

$$G = \begin{bmatrix} \cos\theta & \sin\theta \\ -\sin\theta & \cos\theta \end{bmatrix}, \tag{3.57}$$

where the starting state is

$$|\sigma\rangle = \mathrm{e}^{-\mathrm{i}\delta}\begin{bmatrix} -\cos\frac{\theta}{4} \\ \sin\frac{\theta}{4} \end{bmatrix}. \tag{3.58}$$

This matrix form can be used to calculate the Grover iterations, which can then be transformed back to the $|\sigma\rangle$, $|m\rangle$ basis when required. The matrix form for the exact Grover search is developed in a later section.

General rotation

Applying a rotation $\vec{\phi} = (\phi_1, \phi_2, \phi_3)$, where each ϕ_1, ϕ_2, ϕ_3 apply to the generators J_1, J_2, J_3 respectively, so that we can define

$$\begin{aligned} Q &= \mathrm{e}^{2\mathrm{i}\vec{\phi}.\vec{J}} \\ &= I + 2\mathrm{i}\vec{\phi}.\vec{J} - \frac{|\phi|^2 P}{2!} - \frac{|\phi|^2 2\vec{\phi}.\vec{J}}{3!} + \frac{|\phi|^4 P}{4!} \dots \\ &= I + 2\mathrm{i}\frac{\vec{\phi}.\vec{J}}{|\phi|}\sin|\phi| - P(1-\cos|\phi|), \end{aligned} \tag{3.59}$$

where we have used

$$\left(2\vec{\phi}.\vec{J}\right)^2 = 4\left(\phi_1^2 J_1^2 + \phi_2^2 J_2^2 + \phi_3^2 J_3^2\right) = |\phi|^2 P. \tag{3.60}$$

Special case 1: $\vec{\phi} = \{0, \phi_2, 0\}$

In this case we are restricting ourselves to the generator, J_2, so we have

$$Q_2 = I + 2\mathrm{i}J_2 \sin\phi_2 - P\left(1 - \cos\phi_2\right)$$

and for $\phi_2 = \theta$ we find

$$Q_2|\psi\rangle = G|\psi\rangle, \tag{3.61}$$

that is, we have a direct relationship

$$\mathrm{e}^{2\mathrm{i}\theta J_2}|\psi\rangle = G|\psi\rangle. \tag{3.62}$$

Fenner [Fen00] found previously, as shown in section 5.2, that a Hamiltonian equivalent to J_2 up to a scale factor, can be equated to the standard Grover iteration, provided the wave function is measured at specified time intervals. This time step can simply be equated to θ and the conventional Grover operator G is, therefore, just rotating an angle 2θ with the generator J_2.

From this, we now investigate the possibility of raising G to any power, including non-integer powers.

Raising the Grover matrix to an arbitrary power

From the previous section, we can deduce the relationship

$$\begin{aligned} G^k|\psi\rangle &= \mathrm{e}^{2\mathrm{i}k\theta J_2}|\psi\rangle. \\ &= \left(I + 2\mathrm{i}J_2\sin(k\theta) - P\left(1-\cos(k\theta)\right)\right)|\psi\rangle. \end{aligned} \tag{3.63}$$

This formula which can be seen as a generalization of the Grover search iteration G^k for real k. We also see that raising the Grover operator to a power in this context is equivalent to increasing the energy of the Hamiltonian, $2J_2$, [DKK03]. We have included the state $|\psi\rangle$ because the equality applies to the effect of the operation on a particular state in the Grover subspace. To match the operators themselves, we would have

$$G^k = \mathrm{e}^{\mathrm{i}k\pi}\mathrm{e}^{-2k\mathrm{i}(\pi-\theta)J_2}. \tag{3.64}$$

Of course, we know that Grover rotates the starting vector $|\sigma\rangle$, an angle $\frac{\pi}{2} - \frac{\theta}{2}$ onto the solution state, as shown in Fig.(3.9). Hence, a completed Grover search in a single operation will be

$$\begin{aligned} Q_2 &= \mathrm{e}^{2\mathrm{i}\left(\frac{\pi}{2}-\frac{\theta}{2}\right)J_2} \\ &= I + 2\mathrm{i}J_2\sin\left(\frac{\pi}{2}-\frac{\theta}{2}\right) - 4J_2^2\left(1-\cos\left(\frac{\pi}{2}-\frac{\theta}{2}\right)\right) \\ &= I + 2\mathrm{i}J_2\cos\frac{\theta}{2} - P\left(1-\sin\frac{\theta}{2}\right). \end{aligned} \tag{3.65}$$

Incidentally, we can write this in terms of the Grover matrix as

$$Q_2 = \frac{1+2\alpha}{2(1+\alpha)} I + \frac{1}{4\alpha(1+\alpha)} G - \frac{1+2\alpha}{4\alpha(1+\alpha)} G^\dagger, \tag{3.66}$$

but the difficulty is to represent this as a circuit. To check this result, we multiply Q_2 by the starting state $|\sigma\rangle$, to find

$$Q_2|\sigma\rangle = \frac{\alpha^*}{|\alpha|}|m\rangle,$$

which is the solution as required up to a global phase.

Searching using J_1

We know we can complete a search using J_2, being equivalent to the standard Grover search, however, we can also complete a search using J_1. In terms of J_1, we have

$$Q_1 = I + 2\mathrm{i}J_1 \sin\phi - P\left(1 - \cos\phi\right). \tag{3.67}$$

We find that the generator J_1 rotates in the complex plane and so we need a rotation of $\phi = -\frac{\pi}{2}$ to complete the search, hence

$$\begin{aligned} Q_1 &= I - 2\mathrm{i}J_1 - P \\ &= I - P\left(1 + \frac{\mathrm{i}}{|\alpha|}\right) + \mathrm{i}\frac{|\sigma\rangle\langle\sigma| + |m\rangle\langle m|}{|\alpha|}. \end{aligned} \tag{3.68}$$

In this case we find

$$Q_1|\sigma\rangle = \mathrm{i}|m\rangle,$$

thus successfully completing the search. We notice that P commutes with the other operators so we can simplify the exponential, as follows:

$$\begin{aligned} \mathrm{e}^{2\mathrm{i}k\theta J_1} &= \mathrm{e}^{\mathrm{i}k\theta(P - |\sigma\rangle\langle\sigma| - |m\rangle\langle m|)/|\alpha|} \\ &= \mathrm{e}^{\frac{\mathrm{i}k\theta}{|\alpha|}} \mathrm{e}^{-\frac{\mathrm{i}k\theta}{|\alpha|}(|\sigma\rangle\langle\sigma| + |m\rangle\langle m|)}. \end{aligned} \tag{3.69}$$

However, this is precisely the form that can be used in quantum simulation [NC02], where to allow simulation, we alternatively apply each Hamiltonian, as follows

$$\mathrm{e}^{\mathrm{i}\Delta t} \mathrm{e}^{-\mathrm{i}|\sigma\rangle\langle\sigma|\Delta t} \mathrm{e}^{-\mathrm{i}|m\rangle\langle m|\Delta t} + O(\Delta t^2) \tag{3.70}$$

with a circuit shown in [NC02], with complexity $\mathrm{O}(\sqrt{N})$, to implement this. Hence, J_1 is more suitable to be used as a quantum simulation, whereas J_2 is more suitable for a quantum circuit.

3.3.3 Analogy to spin precession

We can view the rotation of the starting vector $|\sigma\rangle$ as an analogy to the precession of the quantization axis of a spin half particle in a magnetic field. The evolution of a magnetic dipole in a magnetic field $\vec{B}$ is given by

$$\mathrm{e}^{-\mathrm{i}\gamma\vec{B}.\vec{\sigma}/2}, \tag{3.71}$$

where γ is the gyromagnetic ratio. We have the Larmor frequency for a magnetic field $\vec{B} = B_0\hat{z}$

$$\omega = \gamma B_0. \tag{3.72}$$

Comparing this with the Grover search, and taking $\gamma = 2$, we can equate $\vec{\sigma} = \vec{H}$ and $B_0 = \phi = \theta \approx \frac{2\sqrt{M}}{\sqrt{N}}$. So, we have for one Grover iteration

$$\omega = \gamma B_0 \approx \frac{4\sqrt{M}}{\sqrt{N}}. \tag{3.73}$$

So, the time taken will be for a half period, which is the time for the maximum deviation of the precession axis

$$T = \frac{\pi}{\omega} = \frac{\pi}{4}\frac{\sqrt{N}}{\sqrt{M}}, \tag{3.74}$$

which agrees with the expected time taken for a Grover search Eq. (3.44). Viewing the search problem in this context, we could clearly reduce the time of the search to unity by scaling the magnetic field in the $\hat{z}$ direction, by $\sqrt{N}$.

Viewing the rotation of the $|\sigma\rangle$ vector onto the $|m\rangle$ vector as precession in a magnetic field, the case with the magnetic field in the z direction is shown.

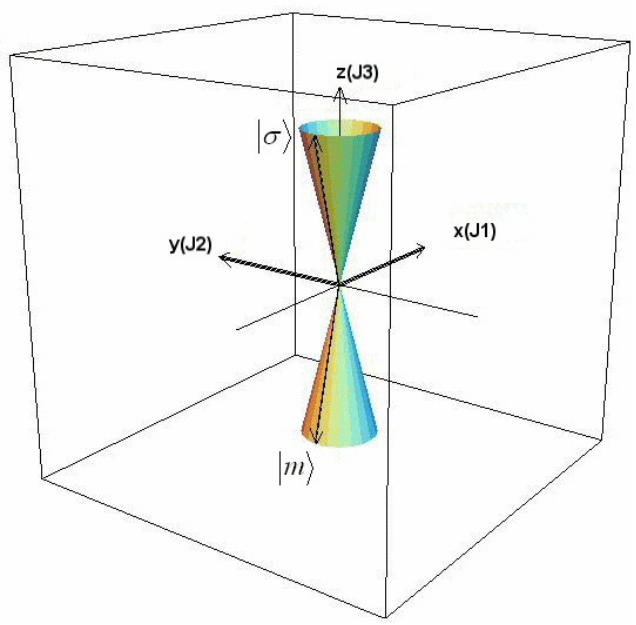

Figure 3.10: Grover search visualization. The starting state $|\sigma\rangle$ will lie on the upper cone, and with a precession axis chosen to lie approximately on the plane of x and y, with a rotation of approximately π, will rotate this vector onto the solution state vector $|m\rangle$.

The starting angle of $|\sigma\rangle$ and $|m\rangle$ with the z-axis is always exactly $\frac{\theta}{2}$. Each rotation of the starting vector $|\sigma\rangle$ is 2θ for the Grover iteration but slightly less for exact Grover searches. We can see from Fig. 3.10 that the Grover search, which is equivalent to using the generator J_2, will rotate the starting vector $|\sigma\rangle$ about the y axis, in the plane of x-z onto $|m\rangle$, clearly taking the shortest route. The other alternative would be to use the generator J_1, rotating about the x axis, in the plane of y-z, which we can see will also rotate $|\sigma\rangle$ onto $|m\rangle$. We can also see that J_3 will be ineffective and not be able to move $|\sigma\rangle$ any closer to $|m\rangle$. We can also clearly see from this diagram, that any variations in the complex phase in the starting state will be detrimental, because it will move the $|\sigma\rangle$ vector around the top of cone shown and further away from the solution state $|m\rangle$, which confirms visually the result in [BBB$^+$99a], [BK02b], [BBB$^+$99b], [CH01], that the performance of Grover's algorithm cannot be improved by varying the phases of the starting amplitudes. Modifying Grover to

complete an exact search involves simply rotating the precession axis, which sits along the y-axis for the conventional Grover, around in the plane of x-y towards the x-axis the appropriate amount, which can be easily calculated.

3.3.4 Exact search

To incorporate the conventional Grover oracle, we need to be able to factorize the search operator with a term

$$(I - \kappa|m\rangle\langle m|) \tag{3.75}$$

and the unitary condition requires $\kappa = 2\cos(\rho)\mathrm{e}^{\mathrm{i}\rho}$, where $\rho \in \Re$. Now, beginning from Eq.(3.59) and substituting in

$$a_i = \frac{\phi_i \sin|\phi|}{|\phi|} \tag{3.76}$$

and using

$$P = \frac{(|\sigma\rangle\langle\sigma| + |m\rangle\langle m| - \alpha|\sigma\rangle\langle m| - \alpha^*|m\rangle\langle\sigma|)}{\beta^2} \tag{3.77}$$

and Eq.(3.46), we have

$$\begin{aligned}
Q &= I + 2\mathrm{i}(a_1J_1 + a_2J_2 + a_3J_3) - P(1-\cos|\phi|) \qquad (3.78)\\
&= I + \frac{\mathrm{i}a_1}{|\alpha|}(P - |s\rangle\langle s| - |m\rangle\langle m|)\\
&+ \frac{a_2}{|\alpha|\beta}(\alpha^*|m\rangle\langle s| - \alpha|s\rangle\langle m|)\\
&+ \frac{\mathrm{i}a_3}{\beta}(|s\rangle\langle s| - |m\rangle\langle m|) - (1-\cos|\phi|)P\\
&= I + \left(\frac{\mathrm{i}a_3}{\beta} + \frac{\mathrm{i}a_1|\alpha|}{\beta^2} - \frac{1-\cos|\phi|}{\beta^2}\right)|s\rangle\langle s|\\
&+ \left(\frac{-\mathrm{i}a_3}{\beta} + \frac{\mathrm{i}a_1|\alpha|}{\beta^2} - \frac{1-\cos|\phi|}{\beta^2}\right)|m\rangle\langle m|\\
&+ \left(\frac{a_2\alpha^*}{|\alpha|\beta} - \frac{\mathrm{i}a_1\alpha^*}{|\alpha|\beta^2} + \frac{\alpha^*(1-\cos|\phi|)}{\beta^2}\right)|m\rangle\langle s|\\
&+ \left(\frac{-a_2\alpha}{\beta|\alpha|} - \frac{\mathrm{i}a_1\alpha}{|\alpha|\beta^2} + \frac{\alpha(1-\cos|\phi|)}{\beta^2}\right)|s\rangle\langle m|.
\end{aligned}$$

We require the $|m\rangle\langle s|$ term to vanish, so that we can factorize, hence we require

$$\alpha^*\left(\frac{a_2}{|\alpha|\beta} - \frac{\mathrm{i}a_1}{|\alpha|\beta^2} + \frac{(1-\cos|\phi|)}{\beta^2}\right) = 0. \tag{3.79}$$

Equating real and imaginary parts, we see that this implies $a_1 = 0$, which then implies

$$a_2 = -\frac{|\alpha|}{\beta}(1-\cos|\phi|). \tag{3.80}$$

Hence,

$$\begin{aligned}
Q &= I + \left(\frac{\mathrm{i}a_3}{\beta} - \frac{1-\cos|\phi|}{\beta^2}\right)|s\rangle\langle s| \qquad (3.81)\\
&+ \left(\frac{-\mathrm{i}a_3}{\beta} - \frac{1-\cos|\phi|}{\beta^2}\right)|m\rangle\langle m| + \frac{2\alpha(1-\cos|\phi|)}{\beta^2}|s\rangle\langle m|
\end{aligned}$$

and to mimic the Grover search we require this to factorize as

$$\begin{aligned} Q &= \left(I - \left(\frac{1-\cos|\phi|}{\beta^2} - \frac{\mathrm{i}a_3}{\beta}\right)|s\rangle\langle s|\right) \\ &\times \left(I - \left(\frac{1-\cos|\phi|}{\beta^2} + \frac{\mathrm{i}a_3}{\beta}\right)|m\rangle\langle m|\right). \end{aligned} \tag{3.82}$$

To avoid the cross term $|s\rangle\langle m|$, we require

$$a_3^2 + \frac{(1-\cos|\phi|)^2}{\beta^2} = 2(1-\cos|\phi|) \tag{3.83}$$

and rearranging, we find

$$a_3 = \pm\frac{2\sin\frac{\phi}{2}}{\beta}\sqrt{\cos^2\frac{|\phi|}{2} - |\alpha|^2}. \tag{3.84}$$

Substituting back into Eq. (3.82), we find

$$\begin{aligned} Q &= \left(I - \left(\frac{2\sin^2\frac{|\phi|}{2}}{\beta^2} \pm \frac{2\mathrm{i}\sin\frac{\phi}{2}}{\beta}\sqrt{1 - \frac{\sin^2\frac{|\phi|}{2}}{\beta^2}}\right)|s\rangle\langle s|\right) \\ &\times \left(I - \left(\frac{2\sin^2\frac{|\phi|}{2}}{\beta} \mp \frac{2\mathrm{i}\sin\frac{\phi}{2}}{\beta}\sqrt{1 - \frac{\sin^2\frac{|\phi|}{2}}{\beta^2}}\right)|m\rangle\langle m|\right), \end{aligned} \tag{3.85}$$

which can be written in the form

$$Q = (I - 2\cos(\rho)\mathrm{e}^{\pm\mathrm{i}\rho}|s\rangle\langle s|)(I - 2\cos(\rho)\mathrm{e}^{\mp\mathrm{i}\rho}|m\rangle\langle m|), \tag{3.86}$$

where

$$\cos\rho = \pm\sin\frac{\phi}{2}\sec\frac{\theta}{2}. \tag{3.87}$$

We notice that the signs in the exponentials inside the two brackets in Eq. (3.86) are of opposite sign, which seems to contradict the need for a phase matching condition in this form of the Grover operator [LXS01] and if we simulate this search process numerically, we find that this operator indeed rotates the starting vector $|s\rangle$ onto the non-solution vector $|m^\perp\rangle$. This, however, can be easily remedied by inverting the oracle to return $m^\perp$ instead of m, which implies the operator Q will now converge to the solution m instead of $m^\perp$. That is, we search with

$$Q = (I - 2\cos(\rho)\mathrm{e}^{\pm\mathrm{i}\rho}|s\rangle\langle s|)(I - 2\cos(\rho)\mathrm{e}^{\mp\mathrm{i}\rho}|m^\perp\rangle\langle m^\perp|). \tag{3.88}$$

This use of $|m^\perp\rangle$ in place of $|m\rangle$ in the Grover operator is consistent with Fig. 3.9, which involves a reflection of the state vector about $|m^\perp\rangle$. The oracle can be inverted by simply requiring the oracle to return a 1 for a non-solution and a 0 for a solution, as opposed to the conventional operation of returning a 1 for a solution, and a 0 for a non-solution. If, in fact, we make the substitution $|m^\perp\rangle$ for $|m\rangle$ into the generators, we find

$$\begin{aligned} J_1 &\rightarrow -J_3 \\ J_2 &\rightarrow -J_2 \\ J_3 &\rightarrow -J_1, \end{aligned} \tag{3.89}$$

which implies that we are now applying the rotation in reverse. The form of Eq.(3.86) can be related to the results of [LXS01], for exact Grover searches, giving us

$$\rho = \arccos\left(\frac{1}{|\alpha|}\sin\frac{\pi}{4\lceil k\rceil + 2}\right) \tag{3.90}$$

where we use the conventional grover expression for the number of iterations

$$k = \frac{\pi}{4 \arcsin |\alpha|} - \frac{1}{2} \tag{3.91}$$

and equating these two gives us finally

$$\sin \frac{|\phi|}{2} = \cot \frac{\theta}{2} \sin \frac{\pi}{4 \lceil k \rceil + 2}. \tag{3.92}$$

ϕ_2 and ϕ_3 can be calculated from

$$\phi_2 = -|\phi| \tan \frac{\theta}{2} \tan \frac{|\phi|}{2} \tag{3.93}$$

and using the theorem of Pythagoras

$$\phi_3 = \sqrt{|\phi|^2 - |\phi_2|^2}. \tag{3.94}$$

It is interesting to note that the exact search takes the same number of iterations as the standard Grover search, however, ρ can be decreased below its optimum value, thus allowing the Grover search to be slowed down to an arbitrary degree. Of course, to maintain an exact search, though slower because it involves more iterations, ρ will still have to satisfy Eq. (3.90).

Hence, the general rotation vector for an exact search is $\vec{\phi} = (0, \phi_2, \phi_3)$. If $k = \lceil k \rceil$, then $|\phi| = \pi - \theta$, as for a normal Grover iteration.

Writing in terms of the states of maximum and minimum weight, we find

$$G_{\text{exact}} = \begin{bmatrix} q(1 - \frac{q}{2} \sin^2(\frac{\theta}{2})) - 1 & q \sin(\frac{\theta}{2})(q \cos^2(\frac{\theta}{4}) - 1) \\ q \sin(\frac{\theta}{2})(q \sin^2(\frac{\theta}{4}) - 1) & q(1 - \frac{q}{2} \sin^2(\frac{\theta}{2})) - 1 \end{bmatrix}, \tag{3.95}$$

where

$$q = 2 \cos \rho e^{i\rho}. \tag{3.96}$$

After $\lceil k \rceil$ iterations, the final state will have a phase on the solution state

$$e^{i(\pi - \rho)} |m\rangle. \tag{3.97}$$

Simple search example

For a small database of 16 elements, we have $n = 16$ giving $\rho = 0.47327$, which gives us $|\phi| = 2.07769$, and $\phi_2 = -0.91151$ and $\phi_3 = 1.86707$ to five decimal places and which, thus, gives us 3 iterations exactly, with

$$G = (I - (1.584 + 0.811i)|s\rangle\langle s|)(I - (1.584 + 0.811i)|m\rangle\langle m|) \tag{3.98}$$

(three decimal places) and we find $G^3|s\rangle = e^{5i\rho}|m\rangle$, thus solving the search exactly, ignoring the global phase.

3.3.5 Application: developing a circuit

Looking at the search using the generator J_2, we found

$$Q_2 = e^{2i(\frac{\pi}{2} - \frac{\theta}{2})J_2}. \tag{3.99}$$

So, with a starting state of n qubits $|\sigma\rangle = H^{\otimes n}|0\rangle$, we are mapping from the real amplitudes to real amplitudes. Looking at J_2 Eq.(3.45) for real α, we have

$$\begin{aligned} J_2 &= \frac{-\mathrm{i}\left(\alpha|m\rangle\langle\sigma| - \alpha|\sigma\rangle\langle m|\right)}{2\alpha\beta} && (3.100)\\ &= \frac{-\mathrm{i}}{2\beta\sqrt{N}}\begin{bmatrix} f(0)\\ f(1)\\ \vdots\\ f(N)\end{bmatrix}\begin{bmatrix}1 & 1\ldots & 1\end{bmatrix} && (3.101)\\ &+ \frac{\mathrm{i}}{2\beta\sqrt{N}}\begin{bmatrix}1\\1\\\vdots\\1\end{bmatrix}\begin{bmatrix}f(0) & f(1)\ldots & f(N)\end{bmatrix} && (3.102)\\ &= \frac{-\mathrm{i}}{2\beta\sqrt{N}}\begin{bmatrix} 0 & f(0)-f(1) & \ldots & f(0)-f(N)\\ f(1)-f(0) & 0 & \ldots & \ldots\\ \ldots & \ldots & \ldots & \ldots\\ f(N)-f(0) & \ldots & \ldots & 0\end{bmatrix}, \end{aligned}$$

where $N = 2^n$. We can see that this matrix is anti-symmetric, hence we can write this in terms of anti-symmetric basis matrices. Defining E_{ij}, which consists of zeros except for a single 1 at the position (m, n)

$$(E_{ij})_{mn} = \delta_{mi}\delta_{nj}, \tag{3.103}$$

where $i, j \in 0 \ldots N-1$. Then, to make this matrix anti-symmetric, we add a -1 across the diagonal, to give

$$\begin{aligned}(J_{ij})_{mn} &= (E_{ij})_{mn} - (E_{ij})_{nm} && (3.104)\\ &= \delta_{mi}\delta_{nj} - \delta_{ni}\delta_{mj}.\end{aligned}$$

So, we can use J_{ij} as an anti-symmetric basis for J_2. Hence,

$$(J_2)_{mn} = \frac{-\mathrm{i}}{2\beta\sqrt{N}}\sum_{i=0}^{N-2}\sum_{j=i+1}^{N-1}\left(f(j)-f(i)\right)(J_{ij})_{mn}, \tag{3.105}$$

so that

$$Q_{J_2} = \mathrm{e}^{-2\mathrm{i}(\frac{\pi}{2}-\frac{\theta}{2})\frac{-\mathrm{i}}{2\beta\sqrt{N}}\sum_{i=0}^{N-2}\sum_{j=i+1}^{N-1}(f(j)-f(i))(J_{ij})_{mn}}. \tag{3.106}$$

Now J_{ij}, which consists of a sum of $\frac{N(N-1)}{2}$ terms, can be written in a Pauli basis. To form an antisymmetric matrix, we will need an odd number of occurrences of the σ_y gate. Switching to a Pauli basis $P_{ij} = \otimes_{j=1}^{n}\sigma_u$, where $u \in \{x, y, z\}$ and we only use an odd number of σ_y Pauli matrices in this tensor product. All possible permutations with an odd number of σ_y matrices will be $\binom{n}{1}3^{n-1} + \binom{n}{3}3^{n-3} + \binom{n}{5}3^{n-5} + \cdots = \frac{N(N-1)}{2}$, which is the same as for the J_{ij} basis, and so we can switch to this new basis

$$Q_{J_2} = \mathrm{e}^{\phi\sum_{k=1}^{N(N-1)/2}s_k P_{ij}}.$$

We find that writing this in a product form, we need n terms,

$$Q_{J_2} = \mathrm{e}^{\frac{q_1\mathrm{i}\pi}{4}\sigma_y\otimes I\otimes I\otimes\cdots\otimes I}\mathrm{e}^{\frac{q_2\mathrm{i}\pi}{4}I\otimes\sigma_y\otimes I\otimes\cdots\otimes I}\ldots.\mathrm{e}^{\frac{q_n\mathrm{i}\pi}{4}I\otimes I\otimes\cdots\otimes\sigma_y} \tag{3.107}$$

where q_n is $+1$ if the n^{th} qubit is zero, otherwise, -1. The 1^{st} qubit represents the most significant bit.

A circuit is already known for $U = \mathrm{e}^{-\mathrm{i}\sigma_z \Delta t}$ [NC02] and, because the Pauli matrix Z can be transformed into the other Pauli matrices with single qubit operations, we can modify this circuit to implement any Hamiltonian consisting of arbitrary tensor products of Pauli matrices. That is, in our case, we can use the relation

$$\sigma_y = H_i \sigma_z H_i^\dagger, \tag{3.108}$$

where $H_i = \frac{1}{\sqrt{2}} \begin{bmatrix} 1 & \mathrm{i} \\ \mathrm{i} & 1 \end{bmatrix}$. For our circuits, we see that $\Delta t = \frac{\pi}{4}$ and, hence

$$\mathrm{e}^{-\mathrm{i}\Delta t \sigma_z} = \begin{bmatrix} \mathrm{e}^{-\mathrm{i}\frac{\pi}{4}} & 0 \\ 0 & \mathrm{e}^{\mathrm{i}\frac{\pi}{4}} \end{bmatrix} = \mathrm{e}^{-\mathrm{i}\frac{\pi}{4}} \begin{bmatrix} 1 & 0 \\ 0 & \mathrm{i} \end{bmatrix} = \mathrm{e}^{-\mathrm{i}\frac{\pi}{4}} S. \tag{3.109}$$

Hence, for the first term for Q_2, we have

$$\begin{aligned} \mathrm{e}^{-\mathrm{i}\sigma_y \otimes \ldots I_2 \otimes I_2 \otimes I_2 \phi} &= (\cos\phi I_2 - \mathrm{i}\sin\phi\sigma_y) \otimes I_{N/2} \\ &= \left(H_i \left(\cos\phi I_2 - \mathrm{i}\sin\phi\sigma_z\right) H_i^\dagger \right) \otimes I_{N/2} \\ &= \mathrm{e}^{-\mathrm{i}\frac{\pi}{4}} \left(H_i S H_i^\dagger \right) \otimes I_{N/2}. \end{aligned} \tag{3.110}$$

To include the effect of the oracle, we need to add a ctrl−Y gate as follows:

$$U = -\mathrm{i}\mathrm{e}^{-\mathrm{i}\frac{\pi}{4}} \left(H_i S Y_q H_i^\dagger \right) \otimes I_{N/2},$$

where Y_q means a Y gate is activated, if the q-th qubit is not in the solution. Hence, inductively, we can now write down the full equation

$$Q_{J_2} = \mathrm{e}^{-\mathrm{i}\kappa} H_i S Y_{q_1} H_i^\dagger \otimes H_i S Y_{q_2} H_i^\dagger \otimes \cdots \otimes H_i S Y_{q_n} H_i^\dagger. \tag{3.111}$$

This can be simplified to

$$Q_{J_2} = X_{q_1} H \otimes X_{q_2} H \otimes \cdots \otimes X_{q_n} H \tag{3.112}$$

where X_q means the X gate is activated, if the q-th qubit is 1 in the solution state. Hence, we have clearly found a viable circuit derived from the generator approach and, being a search in unit time, we require the oracle to answer the query of whether the j-th qubit is in the solution, thus a search in unit time is indeed feasible provided a more powerful oracle is accepted.

3.4 Summary

After introducing the conventional Grover search process, we introduce an alternate approach based on the use of the phase estimation procedure. This approach is limited though, in that it can only search for single items in a database, but nevertheless provides an alternate search procedure and so may have advantages in some settings. We then introduce the search approach based on constructing an appropriate Hamiltonian for the search query. This approach was then recast in terms of three SU(2) generators for the search space.

The set of three generators (J_1, J_2, J_3), for the complex non-orthogonal space $|m\rangle$, $|\sigma\rangle$, allows us to follow the search process on the Bloch sphere in 3-space, analogous to the precession of a spin-$\frac{1}{2}$ particle in a magnetic field, giving us a good pedagogical tool to describe the Grover search. We found that the Grover operation G is generated solely by J_2, that is $G = \mathrm{e}^{2\mathrm{i}\theta J_2}$ Eq. (3.62). An alternative search can also be undertaken using J_1, rotating in the complex direction, but not J_3. Because J_1 cannot be factorized, it appears more suitable for simulation and adiabatic approaches. A general search was then investigated, using Eq.

(3.59), using a rotation in a general direction, which enabled us to simply derive an exact search Eq. (3.96) and the phase matching condition Eq. (3.86). The matrix $Q(k)$ could find the solution exactly, because k now does not need to be restricted to an integer, as it does when referring to the power of a Grover matrix. We saw how increasing the energy of the Grover search Hamiltonian in the adiabatic setting was equivalent to raising the Grover matrix to a power in the circuit model representation. We were able to construct a unit time Grover search circuit, however, this required an enhanced oracle, which was able to answer the query of whether a particular qubit was set at 0 or 1 in the solution state.

Hence in this chapter we have introduced several new approaches to the Grover search algorithm which provided new insights into the search process and which may have computational advantages in certain settings. We now complete our analysis of the Grover search algorithm in the following chapter using the mathematical formalism of geometric algebra.

4

The Grover Search using Geometric Algebra

We now extend the previous analysis of the Grover search algorithm using the mathematical formalism of GA. To demonstrate its value, we efficiently solve the exact search and easily represent more general search situations. The two strengths of GA are its method of handling rotations and its integral geometric representation, and we indeed find it to be an ideal formalism for the Grover search.

The Grover search algorithm [Gro97] seeks to evolve a wave function, from some starting state $|\sigma\rangle$, into the solution state $|m\rangle$, where $|m\rangle$ is the set of all solutions, which, upon measurement, will yield one element from this set. In order to analyze this evolution efficiently, typically an orthonormal basis $|m\rangle$ and $|m^\perp\rangle$ is defined, as shown on Fig (3.9), upon which the starting state is plotted. However, in this chapter, we once again use the alternative basis, the states of maximum and minimum weight identified in Section 3, as the basis for the Grover search space, which allows us to interpret the Grover search as the precession of a spin-$\frac{1}{2}$ particle, precessing from the $|\sigma\rangle$ direction to the $|m\rangle$ direction.

Representing the Grover basis states in GA

From the previous section 3.3, we have

$$|\sigma\rangle = \mathrm{e}^{-\mathrm{i}\delta}\left(-\cos\frac{\theta}{4}|\uparrow\rangle + \sin\frac{\theta}{4}|\downarrow\rangle\right), \tag{4.1}$$

where we can ignore the global phase, and

$$|m\rangle = -\sin\frac{\theta}{4}|\uparrow\rangle + \cos\frac{\theta}{4}|\downarrow\rangle. \tag{4.2}$$

Converting these spinors into GA, we find using Eq. (1.24)

$$\sigma_s = -\cos\frac{\theta}{4} - \sin\frac{\theta}{4}\iota\sigma_2 = -\mathrm{e}^{\iota\sigma_2\theta/4} \tag{4.3}$$

$$m_s = -\sin\frac{\theta}{4} - \cos\frac{\theta}{4}\iota\sigma_2 = -\mathrm{e}^{\iota\sigma_2(\pi/2-\theta/4)} = -\iota\sigma_2\mathrm{e}^{-\iota\sigma_2\theta/4} \tag{4.4}$$

$$m_s^\perp = \cos\frac{\theta}{4} - \sin\frac{\theta}{4}\iota\sigma_2 = \mathrm{e}^{-\iota\sigma_2\theta/4}. \tag{4.5}$$

This GA form of the spinors clearly indicates their fundamental nature as rotations, and so by acting on the σ_3 vector, we can find the Bloch sphere representation as

$$S = \psi\sigma_3\psi^\dagger, \tag{4.6}$$

which gives us in real space

$$\sigma = \mathrm{e}^{\iota\sigma_2\theta/4}\sigma_3\mathrm{e}^{-\iota\sigma_2\theta/4} = \mathrm{e}^{\iota\sigma_2\theta/2}\sigma_3 = -\sin\frac{\theta}{2}\sigma_1 + \cos\frac{\theta}{2}\sigma_3 \tag{4.7}$$

$$m = \mathrm{e}^{\iota\sigma_2(\pi/2-\theta/4)}\sigma_3\mathrm{e}^{-\iota\sigma_2(\pi/2-\theta/4)} = -\sigma_3\mathrm{e}^{\iota\sigma_2\theta/2} = \mathrm{e}^{\iota\sigma_2(\pi-\theta/2)}\sigma_3 = -\sin\frac{\theta}{2}\sigma_1 - \cos\frac{\theta}{2}\sigma_3$$

$$m^\perp = \mathrm{e}^{-\iota\sigma_2\theta/4}\sigma_3\mathrm{e}^{\iota\sigma_2\theta/4} = \sigma_3\mathrm{e}^{\iota\sigma_2\theta/2} = \sin\frac{\theta}{2}\sigma_1 + \cos\frac{\theta}{2}\sigma_3.$$

Recall that the bi-vectors $\iota\sigma_1, \iota\sigma_2, \iota\sigma_3$ are used to represent rotations, however, the unit vectors, $\sigma_1, \sigma_2, \sigma_3$ can be equated to a real 3-space co-ordinate system x, y, z, respectively. Hence $|\sigma\rangle$, $|m\rangle$ and $|m\rangle^\perp$ can now be plotted in real Cartesian space analogous to the Bloch vector representation of a single qubit, as shown in Fig (4.1). As can be seen, we use the σ_3 (z-axis) to measure the angle θ, with ϕ measured from σ_1 rotating in the perpendicular plane. It might appear this Bloch-sphere type representation contains less information than the Dirac bra-ket representation with complex phases, however, it can be shown that the polarization vector in fact contains all of the knowable information about the state of the particle. This is because the global phase term can be ignored in this case.

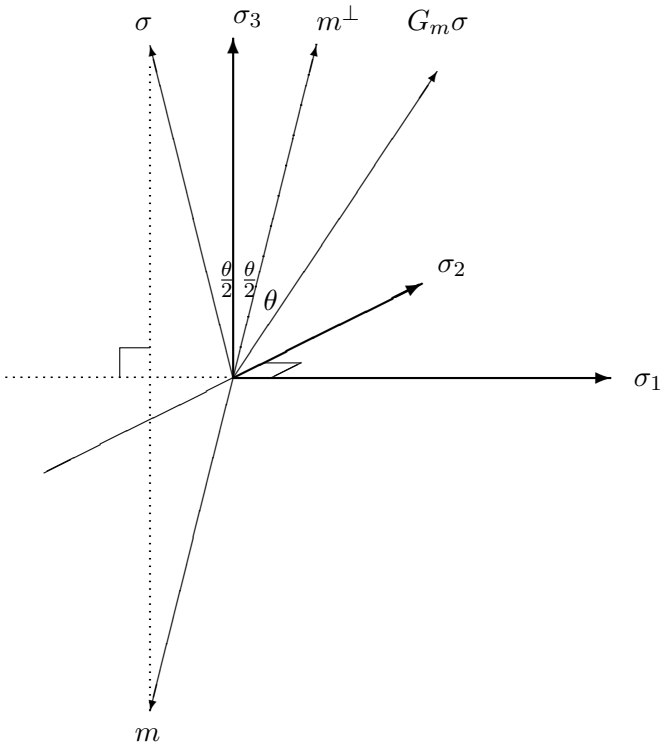

Figure 4.1: Geometric algebra of 3 dimensions. The starting state σ lies at an angle of $\theta/2$ from the vertical σ_3 axis. The action of the oracle shown as a reflection about the $m^\perp$ axis, creating a rotation by θ from $m^\perp$. Clearly a rotation by π about the σ_1 axis, or a rotation by $\pi - \theta$ about the σ_2 axis will solve the search problem through rotating the starting vector σ onto the solution vector m.

4.1 The Grover search operator in GA

The action of the Grover oracle on the state $|m\rangle$ is $(I - 2|m\rangle\langle m|)|m\rangle = -|m\rangle$, which is to flip the '$m$' coordinate about the $|m^\perp\rangle$ axis, as detailed in [NC02]. Reflections are easily handled in GA, through double sided multiplication of the vector representing the axis of reflection, the action of the Oracle being therefore

$$m^\perp \sigma m^\perp = m\sigma m. \tag{4.8}$$

Thus, we can say simply that

$$G_m = m, \tag{4.9}$$

where we assume that G_m acts by conjugation, that is

$$\text{Oracle}(\psi) = G_m \psi G_m.$$

Substituting Eq. (4.7), we find the action of the oracle on σ as

$$m\sigma m = \mathrm{e}^{-\iota\sigma_2\theta/2}\sigma_3\sigma_3\mathrm{e}^{-\iota\sigma_2\theta/4}\mathrm{e}^{-\iota\sigma_2\theta/2}\sigma_3 = \mathrm{e}^{-\iota\sigma_2 3\theta/2}\sigma_3 = \cos\frac{3\theta}{2}\sigma_3 + \sin\frac{3\theta}{2}\sigma_1, \tag{4.10}$$

which is the required vector, as shown in Fig. (4.1). The action of the other half of the Grover operator $I - 2|m\rangle\langle m|$, implies a reflection about the σ vector, so that

$$G_\sigma = \sigma. \tag{4.11}$$

Hence, the combined Grover operator is simply

$$G = -G_\sigma G_m = -\sigma m = \mathrm{e}^{\iota\sigma_2\theta/2}\sigma_3\sigma_3\mathrm{e}^{\iota\sigma_2\theta/2} = \mathrm{e}^{\iota\sigma_2\theta}, \tag{4.12}$$

which is a compact representation for the Grover operator if compared with the conventional form of Eq. (3.43) and clearly reveals that the Grover operation is fundamentally a rotation, specifically, a rotation by 2θ about the σ_2 axis. Now, in the language of geometric algebra, to solve the search problem after k iterations of the Grover operator acting onto the starting state σ, we require

$$m \;=\; G^k\sigma G^{\dagger k},$$

which is a three-vector equation indicating that the starting vector σ needs to be rotated onto the solution vector m, through the repeated action of G. Substituting for m, σ and G into Eq. (4.13), we find

$$\begin{aligned} \mathrm{e}^{\iota\sigma_2(\pi-\theta/2)}\sigma_3 &= \mathrm{e}^{\iota k\sigma_2\theta}\mathrm{e}^{\iota\sigma_2\theta/2}\sigma_3\mathrm{e}^{-\iota k\sigma_2\theta} \\ &= \mathrm{e}^{\iota\sigma_2(2k\theta+\theta/2)}\sigma_3, \end{aligned} \tag{4.13}$$

and equating exponentials, and ignoring rotations modulo 2π, we require

$$2k\theta + \frac{\theta}{2} = \pi - \frac{\theta}{2}, \tag{4.14}$$

or

$$k = \frac{\pi}{2\theta} - \frac{1}{2}. \tag{4.15}$$

Using $\theta = 2\arcsin\frac{\sqrt{M}}{\sqrt{N}}$ for a database with M solutions, we find

$$k = \frac{\pi}{4\arcsin\frac{\sqrt{M}}{\sqrt{N}}} - \frac{1}{2} \approx \frac{\pi\sqrt{N}}{4\sqrt{M}}, \tag{4.16}$$

agreeing with the well known result for the Grover search.

4.1.1 Exact Grover search

The Grover operator is typically generalized to

$$G = -\left(I - \left(1 - \mathrm{e}^{\mathrm{i}\phi_1}\right)|\sigma\rangle\langle\sigma|\right)\left(I - \left(1 - \mathrm{e}^{\mathrm{i}\phi_2}\right)|m\rangle\langle m|\right), \tag{4.17}$$

so that, when the Oracle identifies a solution, it applies a complex phase $\mathrm{e}^{\mathrm{i}\phi_2}$ to the wave function, not just the scalar -1.

A reflection can be viewed as a rotation by π in one higher dimension, so if we rotate by an angle ϕ_2 about the m axis, which will be clockwise as viewed from above the σ_3 axis, we obtain the oracle

$$G_m = \mathrm{e}^{\iota\frac{\phi_2}{2}(\sin(\theta/2)\sigma_1 + \cos(\theta/2)\sigma_3)}. \tag{4.18}$$

For $\phi_2 = \pi$, we find $G_m = \iota\left(\sin(\theta/2)\sigma_1 + \cos(\theta/2)\sigma_3\right) = \iota m$, so that the action of the oracle

$$G_m \sigma G_m^\dagger = \iota m \sigma(-\iota m) = m\sigma m, \tag{4.19}$$

which gives the same result as the standard Grover oracle found previously Eq. (4.8), similarly

$$G_\sigma = \mathrm{e}^{-\iota\frac{\phi_1}{2}(-\sin(\theta/2)\sigma_1 + \cos(\theta/2)\sigma_3)} \tag{4.20}$$

will be a rotation about the σ axis. Hence, for the exact search for the Grover operator we have

$$\begin{aligned} G &= -G_\sigma G_m \\ &= -\mathrm{e}^{-\iota\frac{\phi_1}{2}(-\sin(\theta/2)\sigma_1+\cos(\theta/2)\sigma_3)}\mathrm{e}^{\iota\frac{\phi_2}{2}(\sin(\theta/2)\sigma_1+\cos(\theta/2)\sigma_3)} \\ &= \cos\frac{\phi_1}{2}\cos\frac{\phi_2}{2} + \cos\theta\sin\frac{\phi_1}{2}\sin\frac{\phi_2}{2} + \sin\frac{\phi_1+\phi_2}{2}\sin\frac{\theta}{2}\iota\sigma_1 \\ &\quad + \sin\frac{\phi_1}{2}\sin\frac{\phi_2}{2}\sin\theta\iota\sigma_2 - \cos\frac{\theta}{2}\sin\frac{\phi_1-\phi_2}{2}\iota\sigma_3 \\ &= \mathrm{e}^{\iota\beta(\sin\gamma\sin\alpha\sigma_1+\sin\gamma\cos\alpha\sigma_2+\cos\gamma\sigma_3)}, \end{aligned} \tag{4.21}$$

for some real numbers α, β, γ, which represents a precession about a nearly arbitrary axis on the Bloch sphere.

Phase matching

We can see from Fig. (4.1), using the basis of $|\uparrow\rangle$ and $|\downarrow\rangle$, that σ and m lie in the plane of σ_1 and σ_3, and hence the Grover precession axis must lie in the plane of σ_1,σ_2. Hence, we need to remove the σ_3 component, and so we require the well known phase matching condition, $\phi_1 = \phi_2$, giving the exact search as

$$G = -\mathrm{e}^{\iota\beta(\sin\alpha\sigma_1+\cos\alpha\sigma_2)}, \tag{4.22}$$

where after some algebra, α and β are obtained from Eq. (4.21) we find

$$\begin{aligned} \sin\frac{\beta}{2} &= \sin\frac{\theta}{2}\sin\frac{\phi}{2} \\ \cot\alpha &= \cos\frac{\theta}{2}\tan\frac{\phi}{2}, \end{aligned} \tag{4.23}$$

which can be easily re-expressed assuming a normalization factor Z as

$$G = \mathrm{e}^{\iota\beta(\cos\frac{\phi}{2}\sigma_1+\cos\frac{\theta}{2}\sin\frac{\phi}{2}\sigma_2)/Z}, \tag{4.24}$$

which shows clearly the precession plane perpendicular to the vector $\cos\frac{\phi}{2}\sigma_1 + \cos\frac{\theta}{2}\sin\frac{\phi}{2}\sigma_2$.

To calculate ϕ for the exact search, we have the algebraic equation

$$G^k \sigma G^{\dagger k} = m. \tag{4.25}$$

Using Eq.(4.7), we have

$$\mathrm{e}^{\iota k\beta(\sin\alpha\sigma_1+\cos\alpha\sigma_2)}\mathrm{e}^{\iota\sigma_2\theta/2}\sigma_3\mathrm{e}^{-\iota k\beta(\sin\alpha\sigma_1+\cos\alpha\sigma_2)} = -\mathrm{e}^{-\iota\sigma_2\theta/2}\sigma_3, \tag{4.26}$$

which can be rearranged to

$$\mathrm{e}^{\iota k\beta(\sin\alpha\sigma_1+\cos\alpha\sigma_2)}\mathrm{e}^{\iota\sigma_2\theta/2}\mathrm{e}^{\iota k\beta(\sin\alpha\sigma_1+\cos\alpha\sigma_2)}\mathrm{e}^{\iota\sigma_2\theta/2} = -1 \tag{4.27}$$

or

$$(\mathrm{e}^{\iota k\beta(\sin\alpha\sigma_1+\cos\alpha\sigma_2)}\mathrm{e}^{\iota\sigma_2\theta/2})^2 = -1. \tag{4.28}$$

Now, because we can always replace two consecutive precessions with a single precession operation, we can write

$$e^{\iota k\beta(\sin\alpha\sigma_1+\cos\alpha\sigma_2)}e^{\iota\sigma_2\theta/2} = e^{\iota\kappa\vec{v}} = \cos\kappa + \iota\vec{v}\sin\kappa, \tag{4.29}$$

for some unit vector $\vec{v}$. Thus, we need to solve from Eq. (4.28)

$$(e^{\iota\kappa\hat{v}})^2 = e^{2\iota\kappa\hat{v}} = \cos 2\kappa + \iota\sin 2\kappa\hat{v} = -1, \tag{4.30}$$

giving $\kappa = \frac{\pi}{2}$. Thus the right hand side of Eq. (4.29) is equal to $\iota\vec{v}$ with the scalar part zero. Hence, expanding the left hand side of Eq. (4.29) and setting it equal to zero, we have

$$\begin{aligned}&\langle(\cos k\beta + \sin k\beta\iota(\sin\alpha\sigma_1 + \cos\alpha\sigma_2))\,(\cos\frac{\theta}{2} + \sin\frac{\theta}{2}\iota\sigma_2)\rangle_0\\ &= \cos k\beta\cos\frac{\theta}{2} - \sin k\beta\sin\frac{\theta}{2}\cos\alpha\\ &= 0.\end{aligned}$$

Re-arranging this equation, we find

$$\cot k\beta = \tan\frac{\theta}{2}\cos\alpha = \frac{\sin\frac{\theta}{2}}{\sqrt{\cos^2\frac{\theta}{2} + \cot^2\frac{\phi}{2}}}. \tag{4.31}$$

Isolating k, we find

$$k = \frac{\operatorname{arccot}\left(\frac{\sin\frac{\theta}{2}}{\sqrt{\cos^2\frac{\theta}{2}+\cot^2\frac{\phi}{2}}}\right)}{2\arcsin(\sin\frac{\theta}{2}\sin\frac{\phi}{2})}. \tag{4.32}$$

Graphing this in Fig. 4.2, we see a minimum corresponding to the $\sqrt{N}$ bound, showing that we cannot speed up the Grover search, however, we can slow the search slightly to find the exact solution. Using calculus we can find the minimum for k at $\phi = \pi$, as illustrated in Fig. 4.2 for a database of 16 elements, and substituting into Eq. (4.32), we find the k which corresponds to the fastest search

$$k = \frac{\pi}{2\theta} - \frac{1}{2}, \tag{4.33}$$

the same as found for the standard Grover search.
Hence, the minimum integer iterations will be

$$k_m = \left\lceil \frac{\pi}{2\theta} - \frac{1}{2} \right\rceil. \tag{4.34}$$

Seeking the ϕ to give an exact search, we substitute $k = k_m$ back into Eq. (4.32) and re-arranging, we find an expression for ϕ

$$2k_m \arcsin\left(\sin\frac{\theta}{2}\sin\frac{\phi}{2}\right) = \operatorname{arccot}\left(\frac{\sin\frac{\theta}{2}}{\sqrt{\cos^2\frac{\theta}{2} + \cot^2\frac{\phi}{2}}}\right), \tag{4.35}$$

which we can simplify to give explicitly

$$\sin\frac{\phi}{2} = \sin\frac{\pi}{4k_m + 2}\csc\frac{\theta}{2}. \tag{4.36}$$

We have ϕ now determined directly from the known θ and k_m defined in Eq. (3.50) and Eq. (4.34) respectively, thus solving the exact search using the Grover operator Eq.(4.22).

The polarization vector ψ, can now be calculated after k iterations

$$\begin{aligned}
\psi &= G^k \sigma G^{\dagger k} && (4.37)\\
&= \mathrm{e}^{\iota k\beta(\sin\alpha\sigma_1+\cos\alpha\sigma_2}\mathrm{e}^{\iota\sigma_2\theta/2}\sigma_3\mathrm{e}^{-\iota k\beta(\sin\alpha\sigma_1+\cos\alpha\sigma_2} && (4.38)\\
&= -(\sin^2\alpha\sin\frac{\theta}{2}+\sin\frac{\theta}{2}\cos^2\alpha\cos 2\beta k+\cos\alpha\cos\frac{\theta}{2}\sin 2\beta k)\sigma_1 && (4.39)\\
&+ (-\frac{1}{2}\sin\frac{\theta}{2}\sin 2\alpha+\frac{1}{2}\sin 2\alpha\sin\frac{\theta}{2}\cos 2\beta k+\cos\frac{\theta}{2}\sin\alpha\sin 2\beta k)\sigma_2\\
&+ (\cos\frac{\theta}{2}\cos 2\beta k-\cos\alpha\sin\frac{\theta}{2}\sin 2\beta k)\sigma_3,
\end{aligned}$$

where α and β, Eq. (4.23) are defined in terms of ϕ given by Eq. (4.36), which equals the solution vector m exactly after $k = k_m$ iterations, where k_m given by Eq.(4.34). This could be graphed in a 3-space, defined by the three vectors $\sigma_1, \sigma_2, \sigma_3$.

Example of an exact search using GA

For a database of 16 elements we have the condition on ϕ from Eq. (4.36), for an exact search, which gives us $\phi = 2.19506$ to five decimal places, from which we can now find α and β. This gives us the equation for the polarization vector after k iterations:

$$\begin{aligned}
\psi &= -(0.0546434+0.195357\cos 2\beta k+0.855913\sin 2\beta k)\sigma_1 && (4.40)\\
&+ (-0.10332+0.10332\cos 2\beta k+0.452673\sin 2\beta k)\sigma_2\\
&+ (0.968246\cos 2\beta k-0.220996\sin 2\beta k)\sigma_3.
\end{aligned}$$

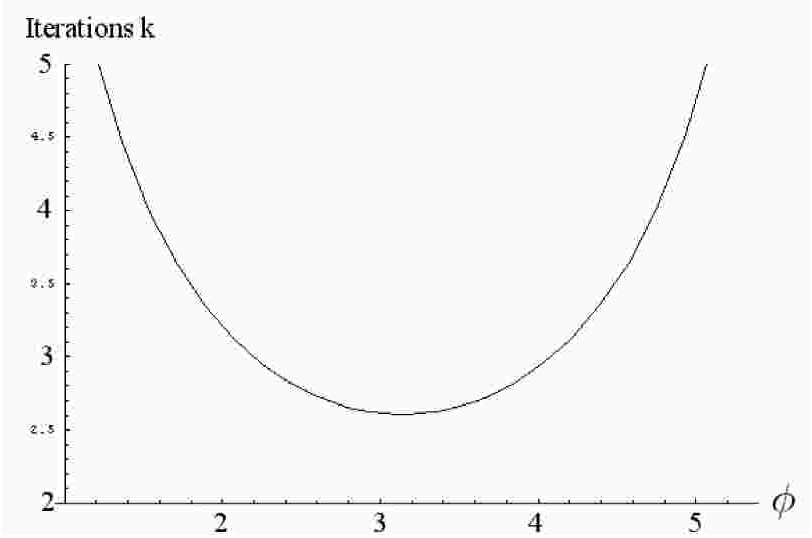

Figure 4.2: Minimum search iterations. The minimum lying at $\phi = \pi$, showing that the Grover search is optimal.

Substituting in for $k = 1, 2, 3$ iterations, we find

$$\begin{aligned} \psi &= (\sigma_1, \sigma_2, \sigma_3) \\ \sigma &= (-0.25, 0, 0.9682) \\ G\sigma &= (-0.8456, 0.315, 0.4309) \\ G^2\sigma &= (-0.8456, 0.315, -0.4309) \\ G^3\sigma &= (-0.25, 0, -0.9682), \end{aligned} \tag{4.41}$$

thus producing the exact solution m after $k_m = 3$ iterations, as required.

4.1.2 General exact Grover search

Most generally we can write the Grover operator as

$$G = -UI_\gamma U^{-1} G_m, \tag{4.42}$$

where

$$I_\gamma = I + (\mathrm{e}^{\mathrm{i}\phi_1} - 1)|\gamma\rangle\langle\gamma|, \tag{4.43}$$

where we normally choose $\gamma = |0\rangle = |0 \ldots 0\rangle$. For $U = H$, we have

$$G = -UI_\gamma U^{-1} G_m = -(I + (\mathrm{e}^{\mathrm{i}\phi_1} - 1)H|\gamma\rangle\langle\gamma|H = -(I + (\mathrm{e}^{\mathrm{i}\phi_1} - 1)|\sigma\rangle\langle\sigma| = -G_\sigma G_m. \tag{4.44}$$

So, with this modified operator, we effectively use a modified vector to σ, namely the vector $\gamma = U|0\rangle$. As this is a unit vector, we simply adapt G_σ to rotate about this new vector, that is, we have

$$G_\gamma = \mathrm{e}^{-\iota\gamma\phi_1/2} = \mathrm{e}^{-\iota\frac{\phi_1}{2}(-\sin(\theta_\gamma/2)\cos(\delta)\sigma_1 - \sin(\theta_\gamma/2)\sin(\delta)\sigma_2 + \cos(\theta_\gamma/2)\sigma_3)}, \tag{4.45}$$

where a and b describe a general unit vector in 3 space. Hence, for the general exact search, we have

$$G = -G_\gamma G_m = -\mathrm{e}^{-\iota\frac{\phi_1}{2}(-\sin(\theta_\gamma/2)\cos(\delta)\sigma_1 - \sin(\theta_\gamma/2)\sin(\delta)\sigma_2 + \cos(\theta_\gamma/2)\sigma_3)} \mathrm{e}^{\iota\phi_2/2(\sin(\theta/2)\sigma_1 + \cos(\theta/2)\sigma_3)}. \tag{4.46}$$

However, because we have two consecutive precession operations, we can replace this with a single precession operation

$$G = \mathrm{e}^{\iota\beta(\sin\gamma\sin\alpha\sigma_1 + \sin\gamma\cos\alpha\sigma_2 + \cos\gamma\sigma_3)}, \tag{4.47}$$

for some real numbers α, β, γ, where once again we require the coefficient of σ_3 to be zero.

We also have a general starting state adjusted, because by replacing H with U, we have changed the overlap on the starting state, so generally we have

$$|\gamma\rangle = -\mathrm{e}^{-\mathrm{i}\phi/2}\cos\frac{\theta_0}{4}|\uparrow\rangle + \mathrm{e}^{\mathrm{i}\phi/2}\sin\frac{\theta_0}{4}|\downarrow\rangle.$$

In GA we can write it as

$$\gamma_s = -\mathrm{e}^{-\iota\phi_0\sigma_3/2}\mathrm{e}^{\iota\theta_0\sigma_2/4} \tag{4.48}$$

and as a polarization vector

$$\begin{aligned} \gamma &= \gamma_s\sigma_3\gamma_s \\ &= \sin\frac{\theta_0}{2}\cos\phi_0\sigma_1 + \sin\frac{\theta_0}{2}\sin\phi_0\sigma_2 + \cos\frac{\theta_0}{2}\sigma_3 \\ &= \mathrm{e}^{\iota\frac{\theta_0}{2}(\sin\phi_0\sigma_1 - \cos\phi_0\sigma_2)}\sigma_3, \end{aligned} \tag{4.49}$$

so the full Grover search will give a polarization vector

$$\begin{aligned} \psi &= G^k \gamma_s \sigma_3 \gamma_s^\dagger {G^\dagger}^k \\ &= G^k \mathrm{e}^{\iota \frac{\theta_0}{2}(\sin\phi_0\sigma_1 - \cos\phi_0\sigma_2)} \sigma_3 {G^\dagger}^k \\ &= -\sigma_3 \mathrm{e}^{\iota\sigma_2\theta/2}. \end{aligned} \tag{4.50}$$

We can expand this expression using G defined above and equate this to the m vector to solve for the phases ϕ_1 and ϕ_2. We would expect $\theta_0 = \theta$, if no knowledge is given about the solution.

4.2 Summary

The Grover search algorithm is a central algorithm in the field of quantum computing, and hence it is important to represent it in the most efficient formalism possible. The two main strengths of geometric algebra are its method of handling rotations and its integral geometric representation, and hence its perfect suitability in describing the Grover search. We find Clifford's geometric algebra, provides a simplified representation for the Grover operator Eq. (4.12) and a clear geometric picture of the search process. Using the states of maximum and minimum weight, we find that we can interpret the search process as the precession of a spin-$\frac{1}{2}$ particle, thus providing a simple visual picture, as shown in Fig 4.1. This is not possible with the standard formalism as it requires two complex axes, forming a four-dimensional space, and hence difficult to visualize. We also find that the exact Grover search Eq. (4.22) has an efficient algebraic solution, as shown in Eq. (4.36). This agrees with the exact search analysis undertaken in the previous chapter 3, however as anticipated, GA provides a clearer and more efficient solution. We also wrote down the equation for a completely general Grover search in Eq. (4.42), which can now be visualized in terms of the Bloch sphere, in which the problem is to rotate a given starting vector onto a target vector through selection of the appropriate precession axis, as shown in Fig. 4.1 or Fig. 3.10. Improved intuition obtained via the use of Clifford's geometric algebra, may possibly enhance the search for new quantum algorithms.

5

Quantum Game Theory

"Games combining chance and skill give the best representation of human life, particularly of military affairs." Gottfried Wilhelm von Leibniz.

We now extend our research into the arena of quantum game theory, which is closely related to quantum computing in that they both involve the manipulation of qubits in order to achieve a desired outcome. For example, one of the first quantum games studied [Mey99], involved two players applying operations on a single qubit, but which can be extended to multiple qubit games.

Quantum game theory extends classical game theory [Ras07], [SÖMI04b], [CT06], [VE00] an established branch of mathematics that describes and analyzes the strategic interaction among a set of players, and which began fairly recently in 1999 with a seminal paper by David Meyer [Mey99], that described a penny-flip game involving a classical and a quantum player. By allowing the quantum player access to general unitary transformations performed on his qubit, whereas his opponent, the classical player, only had access to classical coin flips, Meyer showed that the quantum player achieved an overwhelming advantage, going from a 50:50 chance of winning, to a game where he had a foolproof winning strategy. Following this, further motivation soon came in [EWL99], with the proposal of a quantum mechanical version of the famous two player game of Prisoner dilemma which allowed new strategic solutions. Quantum games with decoherence was also investigated in [Joh01], [YSÖ$^+$05].

In the following, as stated in the literature [Mey99], [EWL99], [FNA02], [FA05b], [Fli05], [Iqb05], we list some of the key reasons for the significance of game-theoretic studies in the quantum regime:

1. Game theory uses the concepts and methods of probability theory, in order to analyze games. Playing quantum games provides an opportunity to generalize conventional probability into a quantum probability framework [Gud88].

2. Games of competition have an intimate connection with quantum communication concepts. For example, the quantum-mechanical protocols for eavesdropping [GH97], [Eke91], finance [PS02, PS08], optimal cloning [F.98], computer architectures [dSR08] and quantum teleportation [Pir05], can readily be formulated as games between players and have the potential to shed new light on fundamental questions in quantum computing and quantum mechanics [NC02]. For example, Frieden [Fri89], [FS95], [FB00] showed that physical laws can be derived by considering the information content of a physical quantity, implying that the process of making a measurement represents a game against nature. It turns out that the observer can never 'win', in the sense of obtaining complete information about a particular physical phenomenon.

3. It is possible [Mey99], [Mey02] to re-formulate certain quantum algorithms as games between classical and quantum players and hence it has been suggested that quantum games may shed new light on the working of quantum algorithms, possibly helping to find new ones.

4. Games can provide [Pie02] a useful set of tools in giving semantics to quantum logic and can be brought to bear on questions concerning the interpretation and the nature of the concept of uncertainty in the foundations of quantum theory.

5. Nanoscopic level interactions are dictated by quantum mechanics. Can Dawkins' dictum [Daw76] of the 'Selfish Gene' be thought of in terms of games of survival with quantum interactions?

Although recent years have seen a steady increase in the literature of quantum games [LJ02, PS03], several fundamental questions remain unanswered. For example, do quantum games offer a genuine extension of the classical game theory or are they only transformed classical games? Assuming the answer to this question is 'yes', then a reasonable domain, where quantum games have genuine potential to benefit game theory, is in the area of N-player games, where N can become infinite. It is precisely in this domain that only minimal investigations have been performed to date. It is because the standard mathematical formalism of quantum games uses density matrices, and those being complex matrices, the analysis of N-player games becomes nearly impossible. Also, with density matrices, constructing a geometric representation of the problem at hand is often hard and sometimes becomes an impossible task. Hence, one of the key components of this section is the implementation of GA for the analysis of quantum games. Generally speaking, with the density matrix formalism, we use Dirac's bra-ket formalism or density matrices and complex matrices for SU(2) rotations, whereas with GA, we use quaternion style rotations of vectors in a real 3-space, which thus naturally provides a convenient geometric picture. GA has also been applied to quantum information and computation [DL03] [HD02b], [DDL02]. As the area of quantum games is a part of this field, this provides a basis for a systematic investigation into quantum games using GA. It has also been noted [PS02] that research into quantum game theory should not be neglected, because current technological progress suggests that sooner or later someone will take full advantage of quantum theory and use quantum strategies to defeat us at some game, that is, an economic, diplomatic or perhaps military one.

A central concept in game theory, is the Nash equilibrium, which is the theoretically optimal response by each player, assuming rational self interest, based on the games payoff structure. The non-cooperative games we will consider assume that there is no communication between the players, though each player has complete knowledge of the games parameters and the games starting state. Different types of game are defined with a payoff matrix for each player, based on the outcome of the game. Some common games investigated include the Prisoner dilemma, Stag hunt and Chicken games. For the two-player Prisoner dilemma (PD) game we have the payoff matrix for player A

$$G_{ij}^{A} = \begin{bmatrix} 3 & 0 \\ 5 & 1 \end{bmatrix} = \begin{bmatrix} G_{00} & G_{01} \\ G_{10} & G_{11} \end{bmatrix}. \tag{5.1}$$

For symmetric games, such as the well known PD game, we have for player B that $G_{ij}^{B} = G_{ji}^{A}$. Each player has two choices in the PD game, to cooperate or defect. If player A defects and player B cooperates, the payoff for player A will be $G_{10} = 5$ as shown, where the first subscript indicates player A's choice of defection and the second subscript, player B's choice of cooperation. In fact for the second column, where player B defects in both cases, player A is still better off defecting, receiving $G_{11} = 1$ as opposed $G_{01} = 0$ if he cooperates. Hence, we can see that player A will always receive a higher payoff by defecting, irrespective of players' B choice and hence rational self interest will create a NE of $G_{11} = 1$ payoff for both players by symmetry. The game produces a dilemma because if they could somehow cooperate with each other then they could both achieve a payoff of 3 units each. The Prisoner's dilemma has wide applicability in diverse areas of science such as biology, politics, economics and sociology. For example the PD game has applicability to climate change negotiations, in that each country will benefit from a stable climate and so they should cooperate to achieve this, however no country wants to act unilaterally because its extra manufacturing costs for example, will put it in a weaker position economically, hence all countries will tend not to cooperate and hence do nothing (that is defect), as in the PD game.

A well known criticism [vEP02], [ÖSI07] of games incorporating quantum mechanics, questions whether these quantum games should be considered completely new games rather than extended versions of an existing classical game, because the players in quantum games are typically given access to extended strategy sets (such as unitary transformations), relative to what they are allowed to employ in the corresponding classical game. However the approach we adopt to quantum games is based on an EPR type setting [ICA08, Iqb05], developed in Chapter 6, which avoids this criticism because the players' strategy sets in this formulation remain classical, being a choice of two measurement directions, and the classical game is recovered when the quantum entanglement of the shared state goes to zero. Thus this category of quantum games can be genuinely considered to embed the corresponding classical game and hence a genuine extension of the classical game.

As a first step in studying quantum games, we present quantum games from the perspective of a table of non-factorisable joint probabilities, published in [CIA10]. This provides a natural link from classical probabilistic games to quantum games. From this perspective, quantum effects are represented as non-factorisable joint probability distributions. We then look at quantum games from a true quantum mechanical perspective but using the formalism of GA in place of the more conventional bra-ket formalism. We introduce for the first time [CILVS09] the tools of GA to present an improved analysis of Meyer's penny flip game [Mey99]. In this work, we found that GA indeed provided a geometric picture of the quantum mechanical interactions for this two-player game, which allowed a visualization of the solution strategy that emerges in this quantum game. We then extend this approach to two-player, three-player and finally N-player games, which can be used to model more complicated strategic interactions. Multiqubit games are naturally modeled in GA as probabilistic outcomes over multiple qubits and have a very efficient solution shown in Eq. (1.25).

5.1 Constructing quantum games from symmetric non-factorisable joint probabilities

Quantum games constructed from a table of non-factorisable joint classical probabilities avoids the use of the conventional quantum mechanical formalism typically required in quantum game theory. Classical games are described when the joint probabilities are factorisable but games with quantum mechanical features are produced when the joint probabilities become non-factorisable. Incorporating a symmetry constraint, we then give the Nash equilibrium and payoff relations for a general quantum game which still embeds the classical game when the joint probabilities become factorisable. Quantum versions of Prisoner dilemma, Stag Hunt and the Chicken game are then investigated with this scheme. We show that this approach provides a general framework for both classical and quantum games without recourse to the formalism of quantum mechanics, thus making the field more accessible to the non-physicist. A follow up paper linking this approach to a quantum mechanical approach as described in Chapter 6, has been submitted for publication.

Published in Phys. Lett. A, 20010. [CIA10] (attached).

Authors: J. M. Chappell(Adelaide University), A. Iqbal(Adelaide University) and D. Abbott(Adelaide University).

Statement of contributions: Dr. Iqbal had been working on non-factorisable joint probabilities as a way to represent quantum games without using the normal quantum mechanical formalism. J. Chappell suggested that a symmetry constraint on the table, might naturally produce classical and quantum games in this framework. J. Chappell worked through the consequences of this idea, and along with the support of Dr. Iqbal and Prof. D. Abbott produced a paper, accepted for publication in Phys. Lett. A.

Signed:

J. M. Chappell Dr A. Iqbal Prof. D. Abbott

5.2 The penny flip quantum game and geometric algebra

We analyze Meyer's quantum penny flip game using the language of geometric algebra(GA) and so determine all possible unitary transformations which enable the player Q to implement a winning strategy. We find that GA can provide a direct derivation of the winning transformation, which can be parameterized by the two angles θ and ϕ. Our results show that GA facilitates a clear visual picture of the penny flip game, that is helpful in motivating and developing further analysis of this quantum game. The result is significant, because for the first time the mathematical formalism of GA is applied to the field of quantum games and it appears to be superior to conventional approaches. Its specific benefits are the removal of the redundancy of the global phase and a simple visual representation of the problem. The success with a single qubit game naturally leads to an extension to two-player games with two qubits.

Published in Journal of the Physical Society of Japan, Volume 78. [CILVS09] (attached).

Authors: J. M. Chappell(Adelaide University), A. Iqbal(Adelaide University), M. A. Lohe(Adelaide University) and Lorenz von Smekal(Adelaide University).

Statement of contributions: Dr. A. Iqbal initially introduced J. Chappell to Meyer's quantum Penny Flip game. J. Chappell then proceeded to rework the original paper, using GA. It soon became clear that GA provided a clear and concise derivation of a general solution. With Dr Azhar's, Dr Lohe's and Dr Lorenz von Smekal's oversight, J. Chappell then prepared a suitable document for publication.

Signed:

J. M. Chappell Dr A. Iqbal Dr M.A.Lohe Dr Lorenz von Smekal

6

Two-player Quantum Games

The quantum game analyzed in the previous chapter, Meyer's penny flip game (attached), described a two-player game in which players apply unitary transformations on a single common qubit, which is then submitted for measurement to determine the outcome of the game. We now progress to two-player games, in which two qubits are employed, with a separate qubit allocated to each player and, significantly, by utilizing a pair of quantum particles, we now have available the quantum mechanical resource of entanglement. The previous schemes were analyzed using conventional techniques of Bra-ket notation and density matrices, however, we now introduce an analysis based on Geometric Algebra(GA).

6.1 Introduction

Although its origins can be traced to earlier works [Bla80, Wie83, Mer90b, Mer90a], the extension of game theory [Bin07, Ras07] to the quantum regime [Per93] was proposed by Meyer [Mey99] and Eisert et al [EWL99] and has since been investigated by others [Vai99, BH01, vEP02, Joh01, MW00, IT01, DLX$^+$02b, DLX$^+$02a, PS02, FA03, IT02, PS03, SOMI04a, FA05a, IW04, Men05, CT06, Iqb05, NT04, SÖMI04b, IT07, ÖSI07, IC07, RNTK08, FH07, AV08, GZK08, ITC08, ICA08, LHJ09, IA09, CILVS09, CIA10, JMCL11a]. Game theory is a vast subject but many interesting strategic interactions can still be found in simple-to-analyze two-player two-strategy non-cooperative games. The well known games of Prisoners' Dilemma (PD) and Stag Hunt [Bin07, Ras07] are two such examples.

The general idea in the quantization scheme proposed by Eisert et al [EWL99] for such games involves a referee who forwards a two-qubit entangled state to the two players. Players perform their strategic actions on the state that consist of local unitary transformations to their respective qubits. The qubits are subsequently returned to the referee for measurement from which the players' payoffs are determined. The setup ensures that players sharing a product initial state corresponds to the mixed-strategy version of the considered classical game. However, players sharing an entangled state can lead to new Nash equilibria (NE) [Bin07, Ras07] consisting of pairs of unitary transformations [Per93, EWL99]. At these quantum NE the players can have higher payoffs relative to what they obtain at the NE in the mixed-strategy version of the classical game.

This approach to constructing quantum games was subsequently criticized [vEP02] as follows. The players' strategic actions in the quantum game are extended operations relative to their actions in the original mixed-strategy version of the classical game, in which, each player can perform a strategic action consisting of a probabilistic combination of their two pure strategies. The mentioned criticism [vEP02] argued that as the quantum players have expanded strategy sets and can do more than what the classical players can do, it is plausible to represent the quantum game as an extended classical game that also involves new pure strategies. The entries in the extended game matrix can then be suitably chosen so to be representative of the players' payoffs at the obtained quantum NE. This line of reasoning can be extended further in stating that quantum games are in fact 'disguised' classical games and to quantize a game is equivalent to replacing the original game by an extended classical game.

As a way to counter the criticism in [vEP02], two-party Einstein-Podolsky-Rosen (EPR) type experiments [EPR35, Boh51, B$^+$64, Bel87, Bel66, ADR82, CS78, Cer00] are recognized to have genuinely quantum features. One observes that the setting of such experiments can

be fruitfully adapted [IW04, Iqb05, IC07, ICA08, IA09] for playing a quantum version of a two-player two-strategy game, which allows us to avoid the criticism from another perspective. In particular, with the EPR type setting the players' strategies can be defined entirely classically—consisting of a probabilistic combination of a player's choice between two measurement directions. That is, with this setting, the players' strategy sets remain identical to ones they have in a standard arrangement for playing a mixed-strategy version of a classical two-player two-strategy game. As the players' strategy sets in the quantum game are not extended relative to the classical game, for this route to constructing quantum games, the mentioned criticism [vEP02] does not apply.

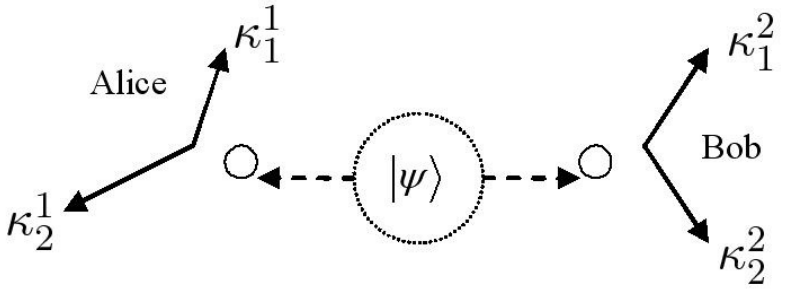

Figure 6.1: The EPR setup.

The usefulness of applying the formalism of geometric algebra (GA) [Hes99, HS84, DL03, DSD07] in the investigation of quantum games has recently been shown [CILVS09] for the well known quantum penny flip game [Mey99]. One may ask about the need of using the formalism of GA when, for instance, the GA based analysis of two-player quantum games developed in the following can also be reproduced with the standard analysis with Pauli matrices. We can argue that the Pauli matrices are not always the preferred representation. Especially, as it is quite often overlooked that the algebra of Pauli matrices is the matrix representation for the Clifford's geometric algebra $\mathcal{R}^3$, which is no more and no less than a system of directed numbers representing the geometrical properties of Euclidean 3-space. As a GA based analysis allows using operations in 3-space with *real coordinates*, it thus permits a visualization that is simply not available in the standard approach using matrices over the field of complex numbers. Pauli matrices are isomorphic to the quaternions, and hence represent rotations of particle states. This fact paves the way to describe general unitary transformations on qubits, in a simplified algebraic form, as *rotors* that bring noticeable simplifications and geometrical clarifications. We apply constraints on the parameters of EPR type arrangements that ensure a faithful embedding of the mixed-strategy version of the original classical game within the corresponding quantum game. In particular, we show how using GA we can determine new NE in quantum games of Stag Hunt and Prisoners' Dilemma played in the EPR type setting.

6.2 EPR setting for playing a quantum game

We have the following payoff matrices

$$\mathcal{A} = \begin{array}{c} \\ \text{Alice} \\ \\ \end{array} \begin{array}{c} \begin{array}{cc} & \text{Bob} \\ S_1' & S_2' \end{array} \\ \begin{array}{c} S_1 \\ S_2 \end{array} \begin{pmatrix} G_{00} & G_{01} \\ G_{10} & G_{11} \end{pmatrix} \end{array}, \quad \mathcal{B} = \begin{array}{c} \\ \text{Alice} \\ \\ \end{array} \begin{array}{c} \begin{array}{cc} & \text{Bob} \\ S_1' & S_2' \end{array} \\ \begin{array}{c} S_1 \\ S_2 \end{array} \begin{pmatrix} H_{00} & H_{01} \\ H_{10} & H_{11} \end{pmatrix} \end{array}, \tag{6.1}$$

giving Alice's and Bob's payoffs, respectively. Here Alice's pure strategies are S_1 and S_2 and Bob's pure strategies are S_1' and S_2'. In a run, Alice chooses her strategy to be either S_1 or S_2 and likewise, in the same run, Bob chooses his strategy to be either S_1' or S_2'. We consider games with symmetrical payoffs for which $\mathcal{B} = \mathcal{A}^T$, where T indicates transpose. This requires $H_{00} = G_{00}$, $H_{01} = G_{10}$, $H_{10} = G_{01}$, and $H_{11} = G_{11}$.

The EPR setting assumes that players Alice and Bob are spatially-separated participants, who are located at the two arms of the EPR system. In a run, each player receives one half of a two-particle system emitted by the same source. We associate Alice's strategies S_1, S_2 to the directions κ_1^1, κ_2^1 respectively and similarly, associate Bob's strategies S_1', S_2' to the directions κ_1^2, κ_2^2, respectively. On receiving a pair of particles, players Alice and Bob together choose a pair of directions from the four possible cases (κ_1^1, κ_1^2), (κ_1^1, κ_2^2), (κ_2^1, κ_1^2), (κ_2^1, κ_2^2) and a quantum measurement is performed along the chosen pair. The outcome of the measurement at either arm is $+1$ or -1. Over a large number of runs, a record is maintained of the players' choices of directions, representing their strategies, and one of the four possible outcomes $(+1, +1)$, $(+1, -1)$, $(-1, +1)$, $(-1, -1)$ emerging out of the measurement. Within each of the brackets, the first entry is reserved for the outcome at Alice's side and the second entry for the outcome at Bob's side. Players' payoff relations are expressed in terms of the outcomes of measurements that are recorded for a large number of runs, as the players sequentially receive, two-particle systems emitted from the source. These payoffs depend on the strategic choices that each player adapts for his/her two directions over many runs, and on the dichotomic outcomes of the measurements performed along those directions.

6.3 Geometric algebra

Geometric algebra (GA) [Hes99, HS84, DL03, DSD07] is an associative non-commutative algebra, that can provide an equivalent description to the conventional Dirac bra-ket and matrix formalisms of quantum mechanics, consisting of solely of algebraic elements over a strictly real field. Recently, Christian [Chr07] has used the formalism of GA in thought provoking investigations of some of the foundational questions in quantum mechanics. In the area of quantum games, GA has been used by Chappell et al [CILVS09] to determine all possible unitary transformations that implement a winning strategy in Meyer's PQ penny flip quantum game [Mey99], and also in analyzing three-player quantum games [JMCL11a].

Using the one-to-one mapping from quantum states to GA defined in Eq. (1.24) it can then be shown using the Schmidt decomposition of a general two qubit state, that a general two-particle state can be represented (see Appendix) in GA as

$$\psi = AB(\cos\frac{\gamma}{2} + \sin\frac{\gamma}{2}\iota\sigma_2^1\iota\sigma_2^2), \tag{6.2}$$

where $\gamma \in [0, \frac{\pi}{2}]$ is a measure of the entanglement and where A, B are single particle rotors applied to the first and second qubit, respectively.

General unitary operations in GA can be represented as

$$\mathbf{R}(\theta_1, \theta_2, \theta_3) = \mathrm{e}^{-\theta_3\iota\sigma_3/2}\mathrm{e}^{-\theta_1\iota\sigma_2/2}\mathrm{e}^{-\theta_2\iota\sigma_3/2}. \tag{6.3}$$

This rotation, in Euler angle form, can completely explore the available space of a single qubit, and is equivalent to a general unitary transformation acting on a spinor. We have the rotors for each qubit defined as

$$\begin{aligned} A &= R(\alpha_1, \alpha_2, \alpha_3) = \mathrm{e}^{-\alpha_3\iota\sigma_3/2}\mathrm{e}^{-\alpha_1\iota\sigma_2/2}\mathrm{e}^{-\alpha_2\iota\sigma_3/2} \\ B &= R(\beta_1, \beta_2, \beta_3) = \mathrm{e}^{-\beta_3\iota\sigma_3/2}\mathrm{e}^{-\beta_1\iota\sigma_2/2}\mathrm{e}^{-\beta_2\iota\sigma_3/2}. \end{aligned} \tag{6.4}$$

We see that with the three degrees of freedom provided in each rotor and with the entanglement angle γ, we have defined a two particle quantum state with 7 degrees of freedom, as required for a two-particle quantum state ignoring the global phase. For example, for $A = B = 1$ and $\gamma = -\frac{\pi}{2}$, we find the Bell state, or with $A = 1$ and $B = \mathbf{R}(\pi, 0, 0)$ and $\gamma = \frac{\pi}{2}$, we produce the singlet state.

To simulate the process of measurement, we form a separable state $\phi = RS$, where R and S are single particle rotors, which allow general measurement directions to be specified. The overlap probability between two states in the N-particle case is given by Eq.(1.25), which for the two particle case becomes

$$P(\psi, \phi) = \left\langle \psi E \psi^\dagger \phi E \phi^\dagger \right\rangle - \left\langle \psi J \psi^\dagger \phi J \phi^\dagger \right\rangle, \tag{6.5}$$

where E and J are defined by Eq.(1.26) and Eq.(1.28).

6.3.1 Calculating observables

Employing Eq. (1.25), we firstly calculate

$$\begin{aligned}
\psi E \psi^\dagger &= \frac{1}{2} AB \left(\cos\frac{\gamma}{2} + \sin\frac{\gamma}{2} \iota\sigma_2^1 \iota\sigma_2^2 \right) \left(1 - \iota\sigma_3^1 \iota\sigma_3^2 \right) \left(\cos\frac{\gamma}{2} + \sin\frac{\gamma}{2} \iota\sigma_2^1 \iota\sigma_2^2 \right) B^\dagger A^\dagger \\
&= \frac{1}{2} AB \left(1 - \iota\sigma_3^1 \iota\sigma_3^2 + \sin\gamma \left(\iota\sigma_2^1 \iota\sigma_2^2 - \iota\sigma_1^1 \iota\sigma_1^2 \right) \right) B^\dagger A^\dagger \\
&= \frac{1}{2} \left(1 - \iota A \sigma_3^1 A^\dagger \iota B \sigma_3^2 B^\dagger + \sin\gamma \left(\iota A \sigma_2^1 A^\dagger \iota B \sigma_2^2 B^\dagger - \iota A \sigma_1^1 A^\dagger \iota B \sigma_1^2 B^\dagger \right) \right)
\end{aligned} \tag{6.6}$$

and

$$\begin{aligned}
\psi J \psi^\dagger &= \frac{1}{2} AB \left(\cos\frac{\gamma}{2} + \sin\frac{\gamma}{2} \iota\sigma_2^1 \iota\sigma_2^2 \right) \left(\iota\sigma_3^1 + \iota\sigma_3^2 \right) \left(\cos\frac{\gamma}{2} + \sin\frac{\gamma}{2} \iota\sigma_2^1 \iota\sigma_2^2 \right) B^\dagger A^\dagger \\
&= \frac{1}{2} AB \left(\cos^2\frac{\gamma}{2} - \sin^2\frac{\gamma}{2} \right) \left(\iota\sigma_3^1 + \iota\sigma_3^2 \right) B^\dagger A^\dagger \\
&= \frac{1}{2} \cos\gamma \left(\iota A \sigma_3^1 A^\dagger + \iota B \sigma_3^2 B^\dagger \right).
\end{aligned} \tag{6.7}$$

To describe the players measurement directions, we have $R = e^{-\iota\kappa^1\sigma_2^1}$ and $S = e^{-\iota\kappa^2\sigma_2^2}$. For the quantum game in the EPR setting, κ^1 can be either of Alice's two directions i.e. κ_1^1 or κ_2^1. Similarly, in the expression for S the κ^2 can be either of Bob's two directions i.e. κ_1^2 or κ_2^2. Hence we obtain

$$\begin{aligned}
\phi J \phi^\dagger &= RSJS^\dagger R^\dagger \\
&= \frac{1}{2} \left(\iota R \sigma_3^1 R^\dagger + \iota S \sigma_3^2 S^\dagger \right) \\
&= \frac{1}{2} \left(\iota\sigma_3^1 e^{\iota\kappa^1\sigma_2^1} + \iota\sigma_3^2 e^{\iota\kappa^2\sigma_2^2} \right),
\end{aligned} \tag{6.8}$$

and

$$\begin{aligned}
\phi E \phi^\dagger &= RSES^\dagger R^\dagger \\
&= \frac{1}{2} \left(1 - \iota R \sigma_3^1 R^\dagger \iota S \sigma_3^2 S^\dagger \right) \\
&= \frac{1}{2} \left(1 - \iota\sigma_3^1 e^{\iota\kappa^1\sigma_2^1} \iota\sigma_3^2 e^{\iota\kappa^2\sigma_2^2} \right).
\end{aligned} \tag{6.9}$$

Now from Eq. (1.25), we calculate

$$\begin{aligned}
-\left\langle \psi J \psi^\dagger \phi J \phi^\dagger \right\rangle_0 &= -\frac{1}{4} \left\langle \cos\gamma \left(\iota A \sigma_3^1 A^\dagger + \iota B \sigma_3^2 B^\dagger \right) \left(\iota\sigma_3^1 e^{\iota\kappa^1\sigma_2^1} + \iota\sigma_3^2 e^{\iota\kappa^2\sigma_2^2} \right) \right\rangle_0 \\
&= \frac{1}{4} \cos\gamma \left[(-)^m X(\kappa^1) + (-)^n Y(\kappa^2) \right],
\end{aligned} \tag{6.10}$$

where $m, n \in \{0, 1\}$ refers to measuring a $|0\rangle$ or a $|1\rangle$ state, respectively, and using the results in Appendix, we have

$$X(\kappa^1) = \cos\alpha_1 \cos\kappa^1 + \cos\alpha_3 \sin\alpha_1 \sin\kappa^1, \tag{6.11}$$
$$Y(\kappa^2) = \cos\beta_1 \cos\kappa^2 + \cos\beta_3 \sin\beta_1 \sin\kappa^2. \tag{6.12}$$

Also, from Eq. (1.25) we obtain

$$\begin{aligned} &\left\langle \psi E \psi^\dagger \phi E \phi^\dagger \right\rangle_0 \qquad (6.13)\\ &= \Big\langle (1 - \iota A \sigma_3^1 A^\dagger \iota B \sigma_3^2 B^\dagger + \sin\gamma(\iota A \sigma_2^1 A^\dagger \iota B \sigma_2^2 B^\dagger - \iota A \sigma_1^1 A^\dagger \iota B \sigma_1^2 B^\dagger)) \\ &\times (1 - \iota\sigma_3^1 \iota\sigma_3^2 e^{\iota\kappa\sigma_2^1} e^{\iota\tau\sigma_2^2}) \Big\rangle_0 \\ &= \frac{1}{4}\left[1 + (-)^{m+n} XY - (-)^{m+n} \sin\gamma\{U(k^1)V(k^2) - F(k^1)G(k^2)\}\right], \qquad (6.14) \end{aligned}$$

where

$$F(\kappa^1) = \cos\alpha_2(\cos\kappa^1 \sin\alpha_1 - \cos\alpha_3 \sin\kappa^1 \cos\alpha_1) + \sin\kappa^1 \sin\alpha_2 \sin\alpha_3, \tag{6.15}$$
$$G(\kappa^2) = \cos\beta_2(\cos\kappa^2 \sin\beta_1 - \cos\beta_3 \sin\kappa^2 \cos\beta_1) + \sin\kappa^2 \sin\beta_2 \sin\beta_3 \tag{6.16}$$

and

$$U(\kappa^1) = -\sin\alpha_2(\cos\kappa^1 \sin\alpha_1 - \cos\alpha_3 \sin\kappa^1 \cos\alpha_1) + \sin\kappa^1 \cos\alpha_2 \sin\alpha_3, \tag{6.17}$$
$$V(\kappa^2) = -\sin\beta_2(\cos\kappa^2 \sin\beta_1 - \cos\beta_3 \sin\kappa^2 \cos\beta_1) + \sin\kappa^2 \cos\beta_2 \sin\beta_3. \tag{6.18}$$

To simplify the equations, we define

$$\begin{aligned} Z(\kappa^1, \kappa^2) &= F(k^1)G(k^2) - U(k^1)V(k^2) \qquad (6.19)\\ &= \cos\phi[\cos\kappa^1 \cos\kappa^2 \sin\beta_1 \sin\alpha_1 - \sin\kappa^1 \cos\kappa^2 \sin\beta_1 \cos\alpha_1 \cos\alpha_3 \\ &+ \sin\kappa^1 \sin\kappa^2(\cos\alpha_1 \cos\alpha_3 \cos\beta_1 \cos\beta_3 - \sin\alpha_3 \sin\beta_3) \\ &- \cos\kappa^1 \sin\kappa^2 \sin\alpha_1 \cos\beta_1 \cos\beta_3] \\ &+ \sin\phi[\sin\kappa^1 \cos\kappa^2 \sin\alpha_3 \sin\beta_1 + \cos\kappa^1 \sin\kappa^2 \sin\alpha_1 \sin\beta_3 \\ &+ \sin\kappa^1 \sin\kappa^2(\cos\beta_1 \cos\beta_3 \sin\alpha_3 + \cos\alpha_1 \cos\alpha_3 \sin\beta_3)]. \qquad (6.20) \end{aligned}$$

Now combining Eq. (6.10) and Eq. (6.14) we have the probability to observe a particular state

$$P_{mn} = \frac{1}{4}\left[1 + \cos\gamma\{(-)^m X_i + (-)^n Y_j\} + (-)^{m+n}(X_i Y_j + \sin\gamma Z_{ij})\right]. \tag{6.21}$$

To simplify notation we have written $Z_{ij} = Z(\kappa_i^1, \kappa_j^2)$, $X_i = X(\kappa_i^1)$ and $Y_j = Y(\kappa_j^2)$, where $i, j \in \{1, 2\}$ represent the two possible measurement directions available to each player. We notice that we were able to make the substitution $\phi = \alpha_2 + \beta_2$ in Eq. (6.20), which as shown in Appendix, is as expected from the known redundancy in the rotors. If we put $\gamma = 0$, that is, for no entanglement, we have the probability

$$\begin{aligned} P_{mn} &= \frac{1}{4}\left(1 + (-)^m X_i + (-)^n Y_j + (-)^{m+n} X_i Y_j\right) \\ &= \frac{(1 + (-)^m X_i)^1}{2} \frac{(1 + (-)^n Y_j)^2}{2}, \qquad (6.22) \end{aligned}$$

which shows a product state incorporating general measurement directions for each qubit.

Writing out the probabilities for the four measurement outcomes we find

$$P_{00}(\kappa_i^1,\kappa_j^2)=\frac{1}{4}\left[1+\cos\gamma(X_i+Y_j)+(X_iY_j+\sin\gamma Z_{ij})\right], \tag{6.23}$$

$$P_{01}(\kappa_i^1,\kappa_j^2)=\frac{1}{4}\left[1+\cos\gamma(X_i-Y_j)-(X_iY_j+\sin\gamma Z_{ij})\right], \tag{6.24}$$

$$P_{10}(\kappa_i^1,\kappa_j^2)=\frac{1}{4}\left[1+\cos\gamma(-X_i+Y_j)-(X_iY_j+\sin\gamma Z_{ij})\right], \tag{6.25}$$

$$P_{11}(\kappa_i^1,\kappa_j^2)=\frac{1}{4}\left[1+\cos\gamma(-X_i-Y_j)+(X_iY_j+\sin\gamma Z_{ij})\right]. \tag{6.26}$$

6.3.2 Finding the payoff relations

We allow each player the classical probabilistic choice between their two chosen measurement directions for their Stern-Gerlach detectors. The two players, Alice and Bob choose their first measurement direction with probability x and y respectively, where $x,y\in[0,1]$. Now, we have the mathematical expectation of Alice's payoff, where she chooses the direction κ_1^1 with probability x and the measurement direction κ_2^1 with probability $1-x$, as

$$\begin{aligned}\Pi_A(x,y)=&\,xy[P_{00}G_{00}+P_{01}G_{01}+P_{10}G_{10}+P_{11}G_{11}]\\&+x(1-y)[P_{00}G_{00}+P_{01}G_{01}+P_{10}G_{10}+P_{11}G_{11}]\\&+y(1-x)[P_{00}G_{00}+P_{01}G_{01}+P_{10}G_{10}+P_{11}G_{11}]\\&+(1-x)(1-y)[P_{00}G_{00}+P_{01}G_{01}+P_{10}G_{10}+P_{11}G_{11}],\end{aligned} \tag{6.27}$$

where we have used the payoff matrix, defined for Alice, in Eq. (6.1) and the subscript A refers to Alice. We also define

$$\Delta_1=G_{10}-G_{00},\ \Delta_2=G_{11}-G_{01},\ \Delta_3=\Delta_2-\Delta_1, \tag{6.28}$$

so that by using Eqs. (6.23-6.26) the payoff for Alice (6.27) is expressed as

$$\begin{aligned}&\Pi_A(x,y)\\&=\frac{1}{4}\Big[G_{00}+G_{10}+G_{01}+G_{11}\\&+\Delta_3\{x((X_1-X_2)Y_2+(Z_{12}-Z_{22})\sin\gamma)+y((Y_1-Y_2)X_2+(Z_{21}-Z_{22})\sin\gamma)\\&+xy\{(X_1-X_2)(Y_1-Y_2)+\sin\gamma(Z_{11}+Z_{22}-Z_{12}-Z_{21})\}+X_2Y_2+Z_{22}\sin\gamma\}\\&-\cos\gamma\{(\Delta_1+\Delta_2)((X_1-X_2)x+X_2)-\Delta_4((Y_1-Y_2)y+Y_2)\}\Big],\end{aligned} \tag{6.29}$$

where $\Delta_4=G_{00}-G_{01}+G_{10}-G_{11}$. Bob's payoff, when Alice plays x and Bob plays y can now be obtained by interchanging x and y in the right hand side of Eq. (6.29).

6.3.3 Solving the general two-player game

We now find the optimal solutions by calculating the Nash equilibrium (NE), that is, the expected response assuming rational self interest. To find the NE we simply require

$$\Pi_A(x^*,y^*)\geq\Pi_A(x,y^*),\quad \Pi_B(x^*,y^*)\geq\Pi_B(x^*,y), \tag{6.30}$$

which is stating that any unilateral movement of a player away from the NE of (x^*,y^*), will result in a lower payoff for that player. We find

$$\begin{aligned}&\Pi_A(x^*,y^*)-\Pi_A(x,y^*)\\&=\frac{1}{4}(x^*-x)\Big[\Delta_3\{y^*((X_1-X_2)(Y_1-Y_2)+\sin\gamma(Z_{11}+Z_{22}-Z_{12}-Z_{21}))\\&+(X_1-X_2)Y_2+(Z_{12}-Z_{22})\sin\gamma\}-\cos\gamma(\Delta_1+\Delta_2)(X_1-X_2)\Big]\end{aligned} \tag{6.31}$$

and for the second player Bob we have similarly

$$\begin{aligned}&\Pi_B(x^*,y^*)-\Pi_B(x^*,y)\\&=\frac{1}{4}(y^*-y)\Big[\Delta_3\big\{x^*((X_1-X_2)(Y_1-Y_2)+\sin\gamma(Z_{11}+Z_{22}-Z_{12}-Z_{21}))\\&+(Y_1-Y_2)X_2+(Z_{21}-Z_{22})\sin\gamma\big\}-\cos\gamma(\Delta_1+\Delta_2)(Y_1-Y_2)\Big].\end{aligned}\tag{6.32}$$

6.3.4 Embedding the classical game

To embed the classical game, we require at zero entanglement, not only the same pair of strategies being a NE but also to have the bilinear structure of the classical payoff relations. At a NE of $(x^*,y^*)=(0,0)$, with zero entanglement, we find the payoff from Eq. (6.29) to be

$$\begin{aligned}\Pi_A(0,0)=\frac{1}{4}\big[&G_{00}(1+X_2)(1+Y_2)+G_{10}(1-X_2)(1+Y_2)\\&+G_{01}(1+X_2)(1-Y_2)+G_{11}(1-X_2)(1-Y_2)\big].\end{aligned}\tag{6.33}$$

This result illustrates how we could select any one of the payoff entries we desire with the appropriate selection of X_2 and Y_2, however in order to achieve the classical payoff of G_{11} for this NE, we can see that we require $X_2=-1$ and $Y_2=-1$. If we have a game which also has a classical NE of $(x^*,y^*)=(1,1)$ then from Eq. (6.29) at zero entanglement we find the payoff

$$\begin{aligned}\Pi_A(1,1)=\frac{1}{4}\big[&G_{00}(1+X_1)(1+Y_1)+G_{10}(1-X_1)(1+Y_1)\\&+G_{01}(1+X_1)(1-Y_1)+G_{11}(1-X_1)(1-Y_1)\big].\end{aligned}\tag{6.34}$$

So, we can see, that we can select the required classical payoff, of G_{00}, by the selection of $X_1=1$ and $Y_1=1$.

Referring to Eq. (6.12), we then have the conditions

$$X(\kappa^1) = \cos\alpha_1\cos\kappa^1+\cos\alpha_3\sin\alpha_1\sin\kappa^1=\pm1,\tag{6.35}$$

$$Y(\kappa^2) = \cos\beta_1\cos\kappa^2+\cos\beta_3\sin\beta_1\sin\kappa^2=\pm1.\tag{6.36}$$

Looking at the equation for Alice, we have two classes of solution: If $\alpha_3\neq0$, then for the equations satisfying $X_2=Y_2=-1$, we have for Alice in the first equation $\alpha_1=0$, $\kappa_2^1=\pi$ or $\alpha_1=\pi$, $\kappa_2^1=0$ and for the equations satisfying $X_1=Y_1=+1$, we have $\alpha_1=\kappa_1^1=0$ or $\alpha_1=\kappa_1^1=\pi$, which can be combined to give either $\alpha_1=0$, $\kappa_1^1=0$ and $\kappa_2^1=\pi$ or $\alpha_1=\pi$, $\kappa_1^1=\pi$ and $\kappa_2^1=0$. For the second class with $\alpha_3=0$, we have the solution $\alpha_1-\kappa_2^1=\pi$ and for $X_1=Y_1=+1$ we have $\alpha_1-\kappa_1^1=0$.

So, in summary, for both cases we have that the two measurement directions are π out of phase with each other, and for the first case ($\alpha_3\neq0$) we can freely vary α_2 and α_3, and for the second case ($\alpha_3=0$), we can freely vary α_1 and α_2 to change the initial quantum quantum state without affecting the game NE or the payoffs. The same arguments hold for the equations for Y. Combining these results and substituting into Eq. (6.20), we see by inspection for the two cases that

$$F(\kappa^1)=G(\kappa^2)=U(\kappa^1)=V(\kappa^2)=0,\tag{6.37}$$

and hence, we find that

$$Z_{22}=Z_{21}=Z_{12}=Z_{11}=0.\tag{6.38}$$

This then reduces the equation governing the NE in Eq. (6.31) to

$$\Pi_A(x^*,y^*)-\Pi_A(x,y^*)=\frac{1}{2}(x^*-x)\big[\Delta_3\{2y^*-1\}-\cos\gamma(\Delta_1+\Delta_2)\big]\geq0,\tag{6.39}$$

which now has the new quantum behavior governed solely by the entanglement angle γ. We have the associated payoffs

$$\Pi_A(x,y) = \frac{1}{2}\big[G_{00} + G_{11} - \cos\gamma(G_{00} - G_{11}) + 2xy\Delta_3 \\ - x\{\Delta_3 + \cos\gamma(\Delta_1 + \Delta_2)\} - y\{\Delta_3 - \cos\gamma(G_{00} - G_{01} + G_{10} - G_{11})\}\big]. \quad (6.40)$$

Setting $\gamma = 0$ in Eq. (8.22) we find

$$\Pi_A(x,y) = G_{11} + x(G_{01} - G_{11}) + y(G_{10} - G_{11}) + xy(G_{00} - G_{01} - G_{10} + G_{11}), \quad (6.41)$$

which has the classical bilinear payoff structure in terms of x and y. Hence we have faithfully embedded the classical game inside a quantum version of the game, when the entanglement goes to zero.

We also have the probabilities for each state $|m\rangle|n\rangle$, after measurement from Eq. (6.21), for this form of the quantum game as

$$(P_{mn})_{ij} = \frac{1}{4}\left[1 + \cos\gamma((-)^{m+i+1} + (-)^{n+j+1}) + (-)^{m+n+i+j}\right], \quad (6.42)$$

for the two measurement directions i and j.

6.4 Examples

Here we explore the above results for the games of Prisoners' Dilemma and Stag Hunt. The quantum versions of these games are discussed in Refs. [EWL99, BH01, FA03, FA05a, IA09].

6.4.1 Prisoners' Dilemma

The game of Prisoners' Dilemma (PD) [Ras07] is widely known to economists, social and political scientists and is one of the earliest games to be investigated in the quantum regime [EWL99]. PD describes the following situation: two suspects are investigated for a crime that authorities believe they have committed together. Each suspect is placed in a separate cell and may choose between not confessing or confessing to have committed the crime. Referring to the matrices (6.1) we take $S_1 \sim S_1'$ and $S_2 \sim S_2'$ and identify S_1 and S_2 to represent the strategies of 'not confessing' and 'confessing', respectively. If neither suspect confesses, i.e. (S_1, S_1), they go free, which is represented by G_{00} units of payoff for each suspect. The situation (S_1, S_2) or (S_2, S_1) represents in which one prisoner confesses while the other does not. In this case, the prisoner who confesses gets G_{10} units of payoff, which represents freedom as well as financial reward as $G_{10} > G_{00}$, while the prisoner who did not confess gets G_{01}, represented by his ending up in the prison. When both prisoners confess, i.e. (S_2, S_2), they both are given a reduced term represented by G_{11} units of payoff, where $G_{11} > G_{01}$, but it is not so good as going free i.e. $G_{00} > G_{11}$.

With reference to Eq. (6.28), we thus have Δ_1, $\Delta_2 > 0$. However, depending on the relative sizes of Δ_1, Δ_2, the quantity $\Delta_3 = \Delta_2 - \Delta_1$ can be positive or negative. At maximum entanglement ($\cos\gamma = 0$), we note from Eq. (6.39), that there are two cases depending on Δ_3. If $\Delta_3 > 0$, we notice that both the NE of $(x^*, y^*) = (0,0)$ and $(x^*, y^*) = (1,1)$ are present, and from Eq. (8.22) we have the payoff in both cases

$$\Pi_A(0,0) = \Pi_B(0,0) = \frac{1}{2}(G_{00} + G_{11}) = \Pi_A(1,1) = \Pi_B(1,1), \quad (6.43)$$

which is a significant improvement over the classical payoff of G_{11}. For $\Delta_3 < 0$, we have the two NE of $(x^*, y^*) = (0,1)$ and $(x^*, y^*) = (1,0)$, and from Eq. (8.22) we have the payoff

$$\Pi_A(0,1) = \Pi_B(0,1) = \frac{1}{2}(G_{01} + G_{10}) = \Pi_A(1,0) = \Pi_B(1,0). \quad (6.44)$$

If we reduce the entanglement of the qubits provided for the game, increasing $\cos\gamma$ towards one, then from Eq. (6.39), we find a phase phase transition to the classical NE of $(x^*, y^*) = (0, 0)$, at $\Delta_3 - \cos\gamma(\Delta_1 + \Delta_2) = 0$ or

$$\cos\gamma = \frac{\Delta_3}{\Delta_1 + \Delta_2} = \frac{\Delta_2 - \Delta_1}{\Delta_2 + \Delta_1}. \tag{6.45}$$

Because we know that Δ_1, $\Delta_2 > 0$, for the PD game, then a phase transition to the classical NE is guaranteed to occur, in the range $[0, 1]$.

Consider a particular example of PD by taking $G_{00} = 3 = H_{00}$, $G_{01} = 0 = H_{10}$, $G_{10} = 4 = H_{01}$, and $G_{11} = 2 = H_{11}$ in matrices (6.1). From (6.28) we find $\Delta_1 = 1$, $\Delta_2 = 2$ and $\Delta_3 = 1$ and we obtain $\gamma \leq \cos^{-1}(1/3)$ for a transition to the classical NE. Thus, for this PD game, to generate a non-classical NE the entanglement parameter γ should be greater than $\cos^{-1}(1/3)$.

6.4.2 Stag Hunt

The game of Stag Hunt (SH) [Ras07] is encountered in the problems of social cooperation. For example, if two hunters are hunting for food, in a situation where they have two choices, either to hunt together and kill a stag, which provides a large meal, or become distracted and hunt rabbits separately instead, which while tasty, make a substantially smaller meal. Hunting a stag of course is quite challenging and the hunters need to cooperate with each other in order to be successful. The game of SH has three classical NE, two of which are pure and one is mixed. The two pure NE correspond to the situation where both hunters hunt the stag as a team or where each hunts rabbits by himself.

The SH game can be defined by the conditions $\Delta_3 > \Delta_2 > 0$ and $\Delta_1 + \Delta_2 > 0$ and $\Delta_3 > \Delta_1 + \Delta_2$. In the classical (mixed-strategy) version of this game three NE (two pure and one mixed) appear consisting of $(x^*, y^*) = (0, 0)$, $(x^*, y^*) = (1, 1)$ and $(x^*, y^*) = (\frac{\Delta_2}{\Delta_3}, \frac{\Delta_2}{\Delta_3})$. From Eq. (6.39) and the defining conditions of SH game we notice that both the strategy pairs $(0, 0)$ and $(1, 1)$ also remain NE in the quantum game for an arbitrary γ. Eq. (8.22) give the players' payoffs at these NE as follows:

$$\Pi_A(0,0) = \frac{1}{2}\left[G_{00} + G_{11} - \cos\gamma(G_{00} - G_{11})\right] = \Pi_B(0,0), \tag{6.46}$$

$$\Pi_A(1,1) = \frac{1}{2}\left[G_{00} + G_{11} + \cos\gamma(G_{00} - G_{11})\right] = \Pi_B(1,1), \tag{6.47}$$

which assume the values G_{11} and G_{00} at $\gamma = 0$, respectively. When $\gamma = \frac{\pi}{2}$ we have $\Pi_A(0,0) = \Pi_A(1,1) = \frac{1}{2}(G_{00} + G_{11}) = \Pi_B(1,1) = \Pi_B(0,0)$. For the mixed NE for the quantum SH game we require from Eq. (6.39), $\Delta_3\{2y^* - 1\} - \cos\gamma(\Delta_1 + \Delta_2) = 0$ or

$$x^* = \frac{\cos\gamma(\Delta_1 + \Delta_2) + \Delta_2 - \Delta_1}{2\Delta_3} = y^*, \tag{6.48}$$

which returns the classical mixed NE of $(\frac{\Delta_2}{\Delta_3}, \frac{\Delta_2}{\Delta_3})$ at zero entanglement. Depending on the amount of entanglement, the pair (x^*, y^*), however, will shift themselves between $\frac{\Delta_2}{\Delta_3}$ and $\frac{\Delta_2 - \Delta_1}{2\Delta_3}$. Players' payoffs at this shifted NE can be obtained from Eq. (8.22). Consider a particular example of SH by taking $G_{00} = 10 = H_{00}$, $G_{01} = 0 = H_{10}$, $G_{10} = 8 = H_{01}$, and $G_{11} = 7 = H_{11}$ in matrices (6.1). From (6.28) we find $\Delta_1 = -2$, $\Delta_2 = 7$ and $\Delta_3 = 9$. At $\gamma = \frac{\pi}{2}$ we have $\Pi_A(0,0) = \Pi_A(1,1) = \frac{17}{2} = \Pi_B(1,1) = \Pi_B(0,0)$. That is, the players' payoffs at the NE strategy pair $(0, 0)$ are increased from 7 to $\frac{17}{2}$ while at the NE strategy pair $(1, 1)$ these are decreased from 10 to $\frac{17}{2}$. The mixed NE in the classical game is at $x^* = \frac{7}{9} = y^*$ whereas it shifts to $\frac{1}{2}$ at $\gamma = \frac{\pi}{2}$.

6.5 Discussion

The EPR type setting for playing a quantum version of a two-player two-strategy game is explored using the formalism of Clifford geometric algebra (GA), used for the representation of the quantum states, and the calculation of observables. We find that analyzing quantum games using GA comes with some clear benefits, for instance, improved perception of the quantum mechanical situation involved and particularly an improved geometrical visualization of quantum operations. To obtain equivalent results using the familiar algebra with Pauli matrices would be possible but obscures intuition. We also find that an improved geometrical visualization becomes helpful in significantly simplifying quantum calculations.

We find that by using an EPR type setting we produce a faithful embedding of symmetric mixed-strategy versions of classical two-player two-strategy games into its quantum version, and that GA provides a simplified formalism over the field of reals for describing quantum states and measurements.

For a general two-player two-strategy game, we find the governing equation for a strategy pair forming a NE and the associated payoff relations. We find that at zero entanglement the quantum game returns the same pair(s) of NE as the classical mixed-strategy game, while the payoff relations in the quantum game reduce themselves to their bilinear form corresponding to a mixed-strategy classical game. We find that, within our GA based analysis, even though the requirement to properly embed a classical game puts constraints on the possible quantum states allowing this, we still have a degree of freedom, available with the entanglement angle γ, with which we can generate new NE. As a specific example the PD was found to have a NE of $(x^*, y^*) = (1, 1)$ at high entanglement.

Analysis of quantum PD game in this paper can be compared with the results developed for this game in Ref. [IC07] also using an EPR type setting, directly from a set of non-factorizable joint probabilities. Although Ref. [IC07] and the present paper both use an EPR type setting, they use non-factorizability and entanglement for obtaining a quantum game, respectively. Our recent work [CIA10] has observed that Ref. [IC07] does not take into consideration a symmetry constraint on joint probabilities that is relevant both when joint probabilities are factorizable or non-factorizable. When this symmetry constraint is taken into consideration, an analysis of quantum PD game played using an EPR setting does generate a non-classical NE in agreement with the results in this paper.

Many other classical games could now be investigated in this setting, however, we proceed instead to demonstrate the use of GA in solving three-player and N-player games using an EPR setting.

7

Three-player Quantum Games in an EPR setting

In the paper attached, we extend the Einstein-Podolsky-Rosen (EPR) framework for two-player quantum games, to three-player quantum games. As already noted, by using an EPR setting, the players' strategy sets remain identical to those available to players in the mixed-strategy version of the classical game, obtained as a proper subset of the corresponding quantum game, thus avoiding a common criticism of quantum games, that they are not genuine extensions of existing classical games. Using general symmetrical three-qubit pure states in this framework, we analyze the three-player quantum game of Prisoners' Dilemma.

The usefulness of achieving this is firstly to establish a sound framework for quantum games for three players which authentically extend classical games, but also in establishing an approach which is immediately extendable to the N-player quantum game.

Published in Public Library of Science, Volume 6(7). [JMCL11a] (attached).

Authors: J. M. Chappell(Adelaide University), A. Iqbal(Adelaide University) and D. Abbott(Adelaide University)

Statement of contributions: J. Chappell extended the mathematics developed in the previous chapter based on two qubits to three qubits. Dr A. Iqbal and Prof D. Abbott consulted on the extra difficulties posed by games played with the three qubit GHZ and W states analyzed. J. Chappell and A. Iqbal then prepared a paper for publication, with further checking by D. Abbott and M.A. Lohe.

Signed:

J. M. Chappell Dr A. Iqbal Prof. D.Abbott Dr M.A. Lohe

8

N-player Quantum Games

We now generalize our analysis of two-player and three-player quantum games to multi-player quantum games which are also analyzed in the context of an Einstein-Podolsky-Rosen (EPR) experiment. As previously noted, in this setting, the players' strategy sets remain identical to the ones in the mixed-strategy version of the classical game, and so we obtain a proper embedding of the classical game. Expressions are found for the probability distribution for N qubit states subject to general measurement directions, from which expressions for the mixed Nash Equilibrium and the payoffs are found, producing a general quantum game environment for $N \geq 2$ players. In order to avoid the cumbersome use of large $N \times N$ matrices defining the payoffs, we define the player payoffs with linear functions, and as a specific example the Prisoner dilemma is solved for all N, finding a new property for the Prisoner dilemma, that for an even number of players the payoffs at the Nash equilibrium are equal, whereas for an odd number of players the cooperating players receive a higher payoff.

8.1 Introduction

Initially, studies in the arena of quantum games focused on two-player, two-strategy non-cooperative games but was extended to multi-player quantum games by Benjamin and Hayden [BH01]. Such games can be used to describe multi-party situations, such as in the analysis of secure quantum communication [NC02]. As multi-player quantum games are usually found significantly harder to analyze, as we are required to define an $N \times N$ payoff matrix, and calculate measurement outcomes over N-qubit states, GA is identified as the most suitable formalism in order to allow ease of analysis. Also, in the case where $N \to \infty$, clearly matrix methods will become unworkable and so an algebraic approach, such as GA, becomes essential.

8.2 EPR setting for playing multi-player quantum games

For a multi-player quantum game in a EPR setting [IW04, IC07, ICA08] we have players P^i who are spatially-separated participants, located at the N arms of an EPR system [Per93], as shown in Fig. 8.1. In one run of the experiment, each player chooses one out of two possible measurement directions. These two directions in space, along which spin or polarization measurements can be made, are the players' strategies.

As Fig. 8.1 shows, we represent the i^{th} players two measurement directions as κ_1^i, κ_2^i, with the measurement outcome being $+1$ or -1.

Over a large number of runs the players are allocated a qubit from an N-particle system emitted from a source upon which measurements are performed and a record is maintained of the players' payoffs. These payoffs depend on the N-tuples of the various players' strategic choices made over a large number of runs and on the dichotomic outcomes (measuring spin-up or spin-down) from the measurements performed along those directions.

8.2.1 Symmetrical N qubit states

For N-player quantum games an entangled state of N qubits is prepared by the supervisor, which for fair games should be symmetric with regard to the interchange of the N players,

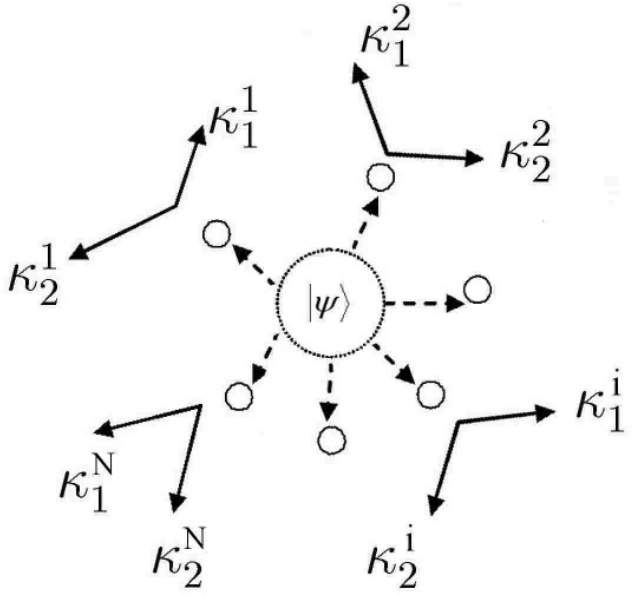

Figure 8.1: The EPR setup for an N-player quantum game. In this setting, each player is given a choice of two measurement directions for their allocated qubit, from a shared N-qubit quantum state.

and we assume that all information about the state once prepared is known by the players. Two types of entangled starting states can readily be identified which are symmetrical with respect to the N players. The GHZ-type state

$$|\mathrm{GHZ}\rangle_N = \cos\frac{\gamma}{2}|00\ldots0\rangle + \sin\frac{\gamma}{2}|11\ldots1\rangle, \tag{8.1}$$

where we include an entanglement angle $\gamma \in [-\frac{\pi}{2}, \frac{\pi}{2}]$ and the W-type state

$$|\mathrm{W}\rangle_N = \frac{1}{\sqrt{N}}\left(|1000\ldots00\rangle + |0100\ldots00\rangle + |0010\ldots00\rangle + \cdots + |0000\ldots01\rangle\right). \tag{8.2}$$

To represent these in geometric algebra, we start with the mapping for a single qubit from Eq. (1.24), so that for the GHZ-type state we have

$$\psi_{\mathrm{GHZ}_N} = \cos\frac{\gamma}{2} + \sin\frac{\gamma}{2}\iota e_2^1 \iota e_2^2 \ldots \iota e_2^N, \tag{8.3}$$

where the superscript indicates which particle space each qubit belongs to, and the negative coefficient on the second term for an odd number of particles can be absorbed into $\sin\gamma$. Also for the W-type state we have in GA

$$\psi_{\mathrm{W}_N} = -\frac{1}{\sqrt{N}}\left(\iota e_2^1 + \iota e_2^2 + \cdots + \iota e_2^N\right). \tag{8.4}$$

8.2.2 Unitary operations and observables in GA

We define $U^i = R(\theta_1^i, \theta_2^i, \theta_3^i)$ for a general unitary transformation acting locally on each qubit i, where R is defined in Eq. (6.3), which the supervisor applies to the individual qubits, which gives the starting state

$$\left(U^1 \otimes U^2 \otimes \cdots \otimes U^N\right)|\psi\rangle, \tag{8.5}$$

upon which the players now decide upon their measurement directions.

The overlap probability between two states ψ and ϕ, in the N-particle case is given in Eq.(1.25). Initially we assume that N is odd, in order to simplify our derivation, but our results are then easily generalized for all N.

The supervisor now submits each qubit for measurement, through N Stern-Gerlach type detectors, with each detector being set at one of the two angles chosen by each player. As mentioned, the players choices, are a classical choice between two possible measurement directions, and hence the players strategy sets remain the same as in the classical game, with the quantum outcomes arising solely from the shared quantum state.

In order to calculate the measurement outcomes, we define a separable state $\phi = A_1 A_2 \dots A_N$, to represent the players directions of measurement, where A_i is a rotor defined in Eq. (6.3), with probabilistic outcomes calculated according to Eq.(1.25). The $|0\rangle$ and $|1\rangle$ outcomes, obtainable from measurement, correspond to the two classical choices 0 and 1, and each player is rewarded according to a payoff matrix, for each player p, given by G^p. The payoff calculated from

$$\Pi_p = \sum_{i^1,\dots,i^N=0}^{1} G^p_{i^1\dots i^N} P_{i^1\dots i^N} = f\left(P_{i^1\dots i^N}\right), \tag{8.6}$$

where $P_{i^1\dots i^N}$ is the probability of recording the state $|i^1\rangle|i^2\rangle\dots|i^N\rangle$ upon measurement, where $i^1,\dots,i^N \in \{0,1\}$, and $G^p_{i^1\dots i^N}$ is the payoff for this measured state. For large N it is preferable to calculate the payoff as some function f of the measured states, to avoid the need for large $N \times N$ payoff matrices.

8.2.3 GHZ-type state

Firstly, we calculate the probability distribution of measurement outcomes from Eq.(1.25), from which we then calculate player payoffs from Eq. (8.6). For the GHZ-type state we have the first part of the observable given by

$$\begin{aligned}
\psi E \psi^\dagger &= \frac{1}{2^{N-1}} \left(\prod_{i=1}^{N} U^i\right) \left(\cos\frac{\gamma}{2} + \sin\frac{\gamma}{2} \iota e_2^1 \iota e_2^2 \dots \iota e_2^N\right) \\
&\quad \left(1 + \sum_{r=1}^{\lfloor \frac{N}{2} \rfloor} (-)^r C_{2r}^N (\iota e_3^i)\right) \left(\cos\frac{\gamma}{2} - \sin\frac{\gamma}{2} \iota e_2^1 \iota e_2^2 \dots \iota e_2^N\right) \left(\prod_{i=1}^{N} U^{i\dagger}\right) \\
&= \frac{1}{2^{N-1}} \left(\prod_{i=1}^{N} U^i\right) \left(1 + \sum_{r=1}^{\lfloor \frac{N}{2} \rfloor} (-)^r C_{2r}^N (\iota e_3^i)\right) \left(\prod_{i=1}^{N} U^{i\dagger}\right) \\
&= \frac{1}{2^{N-1}} \left(1 + \sum_{r=1}^{\lfloor \frac{N}{2} \rfloor} (-)^r C_{2r}^N (V_3^i)\right),
\end{aligned} \tag{8.7}$$

where $V_k^j = \iota U^j e_k U^{j\dagger}$, and

$$\begin{aligned}
\psi J \psi^\dagger &= \frac{1}{2^{N-1}} \left(\prod_{i=1}^{N} U^i \right) \left(\cos\frac{\gamma}{2} + \sin\frac{\gamma}{2} \iota e_2^1 \iota e_2^2 \dots \iota e_2^N \right) \\
&\quad \left(\sum_{r=1}^{\lfloor \frac{N+1}{2} \rfloor} (-)^{r+1} C_{2r-1}^N (\iota e_3^i) \right) \left(\cos\frac{\gamma}{2} - \sin\frac{\gamma}{2} \iota e_2^1 \iota e_2^2 \dots \iota e_2^N \right) \left(\prod U^{i\dagger} \right) \\
&= \frac{1}{2^{N-1}} \left(\prod U^i \right) \left(\cos\gamma + \sin\gamma \iota e_2^1 \iota e_2^2 \dots \iota e_2^N \right) \sum_{r=1}^{\lfloor \frac{N+1}{2} \rfloor} (-)^{r+1} C_{2r-1}^N (\iota e_3^i) \left(\prod U^{i\dagger} \right) \\
&= \frac{1}{2^{N-1}} \cos\gamma \sum_{r=1}^{\lfloor \frac{N+1}{2} \rfloor} (-)^{r+1} C_{2r-1}^N (V_3^i) \\
&\quad - \sin\gamma \left(\sum_{i}^{N} V_2^1 \dots V_1^i \dots V_2^N - \sum_{\substack{i,j,k=1 \\ i \neq j \neq k}}^{N} V_2^1 \dots V_1^i V_1^j V_1^k \dots V_2^N + \dots (-)^{\frac{N-1}{2}} V_1^1 V_1^2 \dots V_1^N \right). \\
&= \frac{1}{2^{N-1}} \cos\gamma \sum_{r=1}^{\lfloor \frac{N+1}{2} \rfloor} (-)^{r+1} C_{2r-1}^N (V_3^i) - \sin\gamma \Big(\sum_{r=0}^{\lfloor N/2 \rfloor} (-)^{r+\frac{N-1}{2}} C_{2r}^N (V_2^i V_2^j) V_1^k \dots V_1^N \Big).
\end{aligned} \tag{8.8}$$

For the measurement settings with a separable wave function $\phi = \prod_i A^i$, we deduce the observables by setting $\gamma = 0$ in Eq. (8.7) and Eq. (8.8) to be

$$\begin{aligned}
\phi J \phi^\dagger &= \frac{1}{2^{N-1}} \sum_{r=1}^{\lfloor \frac{N+1}{2} \rfloor} (-)^{r+1} C_{2r-1}^N (M_3^i) \\
\phi E \phi^\dagger &= \frac{1}{2^{N-1}} \left(1 + \sum_{r=1}^{\lfloor \frac{N}{2} \rfloor} (-)^r C_{2r}^N (M_3^i) \right),
\end{aligned} \tag{8.9}$$

where $M_k^j = \iota A^j e_k A^{j\dagger}$. For $A^j = e^{-\iota\kappa e_2^j/2}$ which allows a rotation of the detectors by an angle κ, we find

$$\begin{aligned}
\phi J \phi^\dagger &= \frac{1}{2^{N-1}} \sum_{r=1}^{\lfloor \frac{N+1}{2} \rfloor} (-)^{r+1} C_{2r-1}^N \left(\iota e_3^i e^{\iota\kappa e_2^i} \right) \\
\phi E \phi^\dagger &= \frac{1}{2^{N-1}} \left(1 + \sum_{r=1}^{\lfloor \frac{N}{2} \rfloor} (-)^r C_{2r}^N \left(\iota e_3^i e^{\iota\kappa e_2^i} \right) \right).
\end{aligned} \tag{8.10}$$

It should be noted in Eq. (8.10), that we have defined the measurement angles with a simplified rotor, $e^{-\iota\kappa e_2^i/2}$, and we assume that this will still provide full generality, which is in accordance with the known result [Per93] that Bell's inequalities can still be maximally violated when the allowed directions of measurement are located in a single plane as opposed to being defined in three dimensions.

So, referring to Eq.(1.25), we find, through combining Eq. (8.7) and Eq. (8.10)

$$\begin{aligned}
2^{N-2} \langle \psi E \psi^\dagger \phi E \phi^\dagger \rangle_0 &= \frac{1}{2^N} \Big\langle \Big(1 + \sum_{r=1}^{\lfloor \frac{N}{2} \rfloor} (-)^r C_{2r}^N \left(V_3^i \right) \Big) \Big(1 + \sum_{r=1}^{\lfloor \frac{N}{2} \rfloor} (-)^r C_{2r}^N \big(\iota e_3^i e^{\iota\kappa e_2^i} \big) \Big) \Big\rangle_0 \\
&= \frac{1}{2^N} \left(1 + \sum_{r=1}^{\lfloor \frac{N}{2} \rfloor} C_{2r}^N \left(K^i \right) \right),
\end{aligned} \tag{8.11}$$

where $K^i = V_3^i \iota e_3^i \mathrm{e}^{\iota\kappa e_2^i} = \cos\kappa^i \cos\alpha_1^i + \sin\kappa^i \sin\alpha_1^i \cos\alpha_3^i$, using the standard results listed in Appendix A.4. We notice that the cross terms in the expansion of the brackets in Eq. (8.11), do not contribute because we only retain the scalar components in this expression.

We also have for the second part of Eq.(1.25), through combining Eq. (8.8) and Eq. (8.10)

$$
\begin{aligned}
- \quad & 2^{N-2}\langle \psi J \psi^\dagger \phi J \phi^\dagger \rangle_0 \qquad (8.12)\\
& = \frac{1}{2^N}\Big\langle \Big(\cos\gamma \sum_{r=1}^{\lfloor \frac{N+1}{2} \rfloor} (-)^{r+1} C_{2r-1}^N (V_3^i) - \sin\gamma \Big(\sum_{r=0}^{\lfloor N/2 \rfloor} (-)^{r+\frac{N-1}{2}} C_{2r}^N (V_2^i V_2^j) V_1^k \dots V_1^N \Big) \\
& \sum_{r=1}^{\lfloor \frac{N+1}{2} \rfloor} (-)^{r+1} C_{2r-1}^N \left(\iota e_3^i e^{\iota\kappa e_2^i} \right) \Big\rangle_0 \\
& = \frac{1}{2^N}\Big(\cos\gamma \sum_{r=1}^{\lfloor \frac{N+1}{2} \rfloor} C_{2r-1}^N \left(K^i \right) + \sin\gamma \Omega \Big),
\end{aligned}
$$

where $\Omega = \sum_{r=0}^{\lfloor N/2 \rfloor} (-)^r C_{2r}^N (X_2^i X_2^j) X_1^k \dots X_1^N$ and

$$
X_1^i = V_1^i \iota e_3^i \mathrm{e}^{\iota\kappa e_2^i} = \left(-\sin\kappa (\cos\alpha_1 \cos\alpha_2 \cos\alpha_3 - \sin\alpha_2 \sin\alpha_3) + \sin\alpha_1 \cos\alpha_2 \cos\kappa \right)^i , \quad (8.13)
$$

and

$$
X_2^i = V_2^i \iota e_3^i \mathrm{e}^{\iota\kappa e_2^i} = \left(\sin\kappa (\cos\alpha_2 \sin\alpha_3 + \sin\alpha_2 \cos\alpha_3 \cos\alpha_1) - \sin\alpha_1 \sin\alpha_2 \cos\kappa \right)^i , \quad (8.14)
$$

see Appendix A.4.

Probability amplitudes for N qubit state, general measurement directions

So combining our last two results using Eq.(1.25), we find the probability to find any state after measurement, valid now for all N

$$
P_{k^1 \dots k^N} = \frac{1}{2^N}\Big(1 + \sum_{r=1}^{\lfloor \frac{N}{2} \rfloor} C_{2r}^N (\epsilon^i K^i) + \cos\gamma \sum_{r=1}^{\lfloor \frac{N+1}{2} \rfloor} C_{2r-1}^N (\epsilon^i K^i) + \epsilon^{1\dots N} \Omega \sin\gamma \Big),
$$

where we have included $\epsilon^i = (-)^{k^i} \in \{+1, -1\}$, to select the probability to measure spin-up or spin-down on a given qubit.

If we take $\gamma = 0$, describing the classical limit, we have from Eq. (8.15)

$$
\begin{aligned}
P_{k^1 \dots k^N} &= \frac{1}{2^N}\left(1 + \sum_{r=1}^{\lfloor N/2 \rfloor} C_{2r}^N (\epsilon^i K^i) + \sum_{r=1}^{\lfloor (N+1)/2 \rfloor} C_{2r-1}^N (\epsilon^i K^i) \right) \qquad (8.15)\\
&= \frac{1}{2^N}\left(1 + \sum_{r=1}^{N} C_r^N (\epsilon^i K^i) \right) \\
&= \frac{1}{2^N}\left(1 + \epsilon^1 K^1 \right)\left(1 + \epsilon^2 K^2 \right) \dots \left(1 + \epsilon^N K^N \right),
\end{aligned}
$$

which shows that for zero entanglement we can form a product state as expected. Alternatively with general entanglement, but only operations on the first two qubits, we have

$$
P_{k^i k^j} = \frac{1}{8}\left(1 + \epsilon^k \cos\gamma \right)\left(1 + \sum_{r=2}^{N} C_r^N (\epsilon^i) \right)\left(1 + \epsilon^{ik} K^i \right)\left(1 + \epsilon^{jk} K^j \right),
$$

which show that for the GHZ-type entanglement that each pair of qubits is mutually unentangled, a well known property of the GHZ state.

Player payoffs

In general to represent the permutation of signs introduced by the measurement operator we can define for the first player, say Alice,

$$a^{i^1\ldots i^N} = \frac{1}{2^N}\sum_{j^1\ldots j^N=0}^{1} \epsilon^{i^1\ldots i^N} G^1_{j^1\ldots j^N}, \tag{8.16}$$

so for example, $a^{0\ldots0} = \frac{1}{2^N}\sum_{j^1\ldots j^N=0}^{1} G^1_{j^1\ldots j^N}$, and we have the relation $a^i a^j = a^{ij}$ etc. that is we write $a^{0\ldots1\ldots0}$ with a 1 in the ith position as a^i.

Using the payoff function we find for the first player, say Alice

$$\Pi_A(\kappa^i_j) = a^{0\ldots0} + \sum_{r=1}^{\lfloor N/2\rfloor} C^N_{2r}(a^i K^i) + \cos\gamma \sum_{r=1}^{\lfloor (N+1)/2\rfloor} C^N_{2r-1}(a^i K^i) + a^{k^1\ldots k^N}\Omega\sin\gamma \tag{8.17}$$

and similarly for the second player, say Bob, where we would use Bob's payoff matrix in place of Alices'.

Mixed-strategy payoff relations

For a mixed strategy game, players choose their first measurement direction κ^i_1, with probabilities x^i, where $x^i \in [0,1]$ and hence choose the direction κ^i_2 with probabilities $(1-x^i)$, respectively. The first player Alice's payoff is now given as

$$\begin{aligned}
&\Pi_A(x^1, x^2, \ldots, x^N) \qquad (8.18)\\
=\;& x^1\ldots x^N \sum_{i,j,k=0}^{1} P_{i^1\ldots i^N}(\kappa^1_1, \kappa^2_1, \ldots, \kappa^3_1) G_{i^1\ldots i^N}\\
+\;& \cdots + x^1(1-x^2)\ldots x^N \sum_{i,j,k=0}^{1} P_{i^1\ldots i^N}(\kappa^1_1, \kappa^2_2, \ldots, \kappa^3_1) G_{i^1\ldots i^N}\\
+\;& \cdots + (1-x^1)(1-x^2)x^3\ldots x^N \sum_{i,j,k=0}^{1} P_{i^1\ldots i^N}(\kappa^1_2, \kappa^2_2, \kappa^3_1, \ldots, \kappa^N_1) G_{i^1\ldots i^N}\\
+\;& \cdots + (1-x^1)(1-x^2)(1-x^3)\ldots(1-x^N) \sum_{i,j,k=0}^{1} P_{i^1\ldots i^N}(\kappa^1_2, \kappa^2_2, \kappa^3_2, \ldots, \kappa^N_2) G_{i^1\ldots i^N}.
\end{aligned}$$

8.2.4 Embedding the classical game

If we consider a strategy N-tuple $(x^1, x^2, x^3, \ldots, x^N) = (0,1,0,\ldots 0)$ for example, at zero entanglement, then the payoff for Alice is obtained from Eq. (8.18) to be

$$\begin{aligned}
\Pi_A(x^1,\ldots,x^N) \;=\; & \frac{1}{2^N}[G_{000\ldots0}(1+K^1_2)(1+K^2_1)(1+K^3_2)\ldots(1+K^N_2) \qquad (8.19)\\
& + G_{100\ldots0}(1-K^1_2)(1+K^2_1)(1+K^3_2)\ldots(1+K^N_2)\\
& + G_{010\ldots0}(1+K^1_2)(1-K^2_1)(1+K^3_2)\ldots(1+K^N_2)\\
& + G_{110\ldots0}(1-K^1_2)(1-K^2_1)(1+K^3_2)\ldots(1+K^N_2)\\
& + \cdots + G_{111\ldots1}(1-K^1_2)(1-K^2_1)(1-K^3_2)\ldots(1-K^N_2)].
\end{aligned}$$

Hence, in order to achieve the classical payoff of $G_{101\ldots1}$, we can see that we require $K^1_2 = -1$, $K^2_1 = +1$ and $K^3_2\ldots K^N_2 = -1$.

This shows that we can select any required classical payoff by the appropriate selection of $K_j^i = \pm 1$. We therefore have the conditions for obtaining the classical mixed-strategy payoff relations as

$$K_j^i = \cos\alpha_1^i \cos\kappa_j^i + \sin\alpha_1^i \cos\alpha_3^i \sin\kappa_j^i = \pm 1. \tag{8.20}$$

We find two classes of solution: If $\alpha_3^i \neq 0$, then for the equations satisfying $K_2^i = -1$ we have for Alice in the first equation $\alpha_1^i = 0$, $\kappa_2^i = \pi$ or $\alpha_1^i = \pi$, $\kappa_2^i = 0$ and for the equations satisfy $K_1^i = +1$ we have $\alpha_1^i = \kappa_1^i = 0$ or $\alpha_1^i = \kappa_1^i = \pi$, which can be combined to give either $\alpha_1^i = 0$, $\kappa_1^i = 0$ and $\kappa_2^i = \pi$ or $\alpha_1^i = \pi$, $\kappa_1^i = \pi$ and $\kappa_2^i = 0$. For the second class with $\alpha_3 = 0$ we have the solution $\alpha_1^i - \kappa_2^i = \pi$ and for $K_1^i = +1$ we have $\alpha_1^i - \kappa_2^i = 0$.

So in summary for both cases we have that the two measurement directions are π out of phase with each other, and for the first case ($\alpha_3^i \neq 0$) we can freely vary α_2^i and α_3^i, and for the second case ($\alpha_3^i = 0$), we can freely vary α_1^i and α_2^i to change the initial quantum quantum state without affecting the game Nash equilibrium (NE) or payoffs [Ras07, Bin07]. These results imply in both cases that $\Omega = 0$.

We then have the associated payoff for Alice

$$\begin{aligned}\Pi_A(x^1, x^2, \ldots x^N) &= a_{00\ldots0} - \cos\gamma \sum_{r=1}^{\lfloor (N+1)/2 \rfloor} C_{2r-1}^N [a^{i0}(1-2x^i) + a^{0i}(1-2x^i)] \\ &\quad + \sum_{r=1}^{\lfloor N/2 \rfloor} C_{2r}^N [a^{1i}(1-2x^1)(1-2x^i) + a^{0ij}(1-2x^i)(1-2x^j)].\end{aligned} \tag{8.21}$$

For example, for three players this will reduce to

$$\begin{aligned}&\Pi_A(x^1, x^2, x^3) \\ =\ & a_{000} + a_{011}(1-2x^2)(1-2x^3) + a_{110}(1-2x^1)((1-2x^2)+(1-2x^3)) \\ -\ & \cos\gamma \left(a_{111}(1-2x^1)(1-2x^2)(1-2x^3) + a_{100}(1-2x^1) + a_{001}(2-2x^2-2x^3) \right).\end{aligned} \tag{8.22}$$

Now, we can write the equations governing the NE for the first player as

$$\begin{aligned}&\Pi_A(x^{i*}, x^{2*}, \ldots x^{N*}) - \Pi_A(x^i, x^{2*}, \ldots, x^{N*}) \\ =\ & (x^{1*} - x^1) \left(- \sum_{r=1}^{\lfloor N/2 \rfloor} C_{2r}^N (a^{1i} I^1 (1-2x^{i*})) + \cos\gamma \sum_{r=1}^{\lfloor (N+1)/2 \rfloor} C_{2r-1}^N (a^{i0} I^1 (1-2x^{i*})) \right) \geq 0.\end{aligned}$$

We are using I^1 as a placeholder, which has a value one, but ensures that the correct number of terms are formed from $C_r^N()$. For example, for three players we find the NE governed by

$$\begin{aligned}&\Pi_A(x^{1*}, x^{2*}, x^{3*}) - \Pi_A(x^1, x^{2*}, x^{3*}) \\ =\ & (x^{1*} - x^1)[a_{110}(2x^{2*}-1) + a_{101}(2x^{3*}-1) + \cos\gamma\{a_{100} + a_{111}(2x^{2*}-1)(2x^{3*}-1)\}] \geq 0.\end{aligned}$$

Symmetric game

For a symmetric game we have $a^{1\ldots1} = b^{1\ldots1} =$ etc, $a^{0\ldots0} = b^{0\ldots0} =$ etc and $a_{11000\ldots0} = a_{10100\ldots0} = a_{10010\ldots0} = \ldots$, and similarly for other symmetries, and using these conditions for a symmetric game, we can find the NE for other players

$$\begin{aligned}&\Pi_A(x^{i*}, x^{2*}, \ldots x^{N*}) - \Pi_A(x^{i*}, x^2, \ldots, x^{N*}) \\ =\ & (x^{2*} - x^2) \left(- \sum_{r=1}^{\lfloor N/2 \rfloor} C_{2r}^N (a^{1i} I^2 (1-2x^{i*})) + \cos\gamma \sum_{r=1}^{\lfloor (N+1)/2 \rfloor} C_{2r-1}^N (a^{i0} I^2 (1-2x^{i*})) \right) \geq 0.\end{aligned}$$

We can see that the new quantum behavior is governed solely by the payoff matrix and by the entanglement angle γ, and not by other properties of the quantum state.

Linear payoff relations

We can see that as $N \to \infty$, that we need to define an infinite number of components of the payoff matrix through a^i. Hence in order to proceed to solve specific games, we need to write the payoff matrix as some functional form of the measurement outcomes, as shown in Eq. (8.6). The simplest approach is to define linear functions over the set of player choices, as developed in [FH07], defining the following general payoff function, for the non-flipping player

$$\$_0 = an + b \tag{8.23}$$

and for the flipping player

$$\$_1 = cn + d \tag{8.24}$$

where n is the number of players not flipping.

This approach enables us to simply define various common games. For example the Prisoner dilemma, which has the essential feature that a defecting player achieves a higher payoff, is represented if we have $c \geq a$,$d > a + b$ and $a > 0$. This result is determined by ensuring that if a non-flipping player decides to flip, then his payoff rises as determined by Eq. (8.23) and Eq. (8.24). For example for $a = 3, b = -3, c = 4, d = 1$ we have defined an N player Prisoner dilemma, and for $N = 2$ we find

$$G_{ij}^A = \begin{bmatrix} 3 & 0 \\ 5 & 1 \end{bmatrix}, \tag{8.25}$$

which gives us the typical payoff matrix for two-player Prisoner dilemma.

For the Chicken game we require $c \geq a$, $d < a + b$ and $a > 0$ and for the minority game, assuming a symmetry between payoffs for the $|0\rangle$ and $|1\rangle$ states we require $c = -a$, $d = b - aN$ and $a < 0$. Hence it is natural to define

$$p_1 = d - (a + b), \quad p_2 = c - a, \tag{8.26}$$

as two key determinants of various games.

It should be noted that while this definition in Eq. (8.23) and Eq. (8.24) can generally define an infinite set of Prisoner dilemma games through simply putting conditions on a, b, c, d, it is still only a subset of the space of all possible Prisoner dilemma games defined over $N \times N$ payoff matrices.

Using the linear functions defined in Eq.(8.23) and Eq.(8.24) we find

$$\begin{aligned} a^{0\ldots0} &= \frac{1}{4}(N(c+a) - p_2 + 2(b+d)) \\ a^{10\ldots0} &= -\frac{1}{4}((N-1)(c-a) + 2(d-(a+b))) = -\frac{1}{4}\left((N-1)p_2 + 2p_1\right) \\ a^{110\ldots0} &= -\frac{c-a}{4} = -\frac{p_2}{4} \\ a^{1110\ldots0}, a^{11110\ldots0} \ldots &= 0 \end{aligned} \tag{8.27}$$

and

$$\begin{aligned} a^{010\ldots0} &= \frac{c+a}{4} \\ a^{011\ldots0}, a^{0111\ldots0}, \ldots &= 0. \end{aligned} \tag{8.28}$$

If required, Eq. (8.23) and Eq. (8.24) can be extended with quadratic terms in n, in order to allow a greater variety of Prisoner dilemma games to be defined.

NE and payoff for linear payoff relations

We can see that the series above terminates, which thus allows us to simplify the NE conditions, for the first player to

$$(x^{1*} - x^1)\left(p_2 \sum_{i=2}^{N}(1-2x^{i*}) - \cos\gamma\left((N-1)p_2 + 2p_1\right)\right) \geq 0 \tag{8.29}$$

and similarly for the other $N-1$ players.

The payoff can then also be simplified to

$$\begin{aligned}
\Pi_A &= a^{0\ldots0} + (1-2x^1)(-\cos\gamma a^{10\ldots0} + a^{110\ldots0}\sum_{i=2}^{N}(1-2x^i)) - \cos\gamma a^{010\ldots0}\sum_{i=2}^{N}(1-2x^i) \\
&= \frac{1}{4}(2(b+d) - p_2 + (c+a)(N - \cos\gamma\sum_{i=2}^{N}(1-2x^i)) \\
&+ (1-2x^1)(\cos\gamma((N-1)p_2 + 2p_1)) - p_2\sum_{i=2}^{N}(1-2x^i))).
\end{aligned} \tag{8.30}$$

Prisoner dilemma

For the Prisoner dilemma, having $p_2 \geq 0$ and $p_1 > 0$ as defined in Eq. (8.26), we find from the equation for Nash equilibrium Eq.(8.29) to produce the classical outcome $\cos\gamma > \frac{N-1}{N-1+\delta}$ and more generally

$$\frac{N-1-2n}{N-1+\delta} < \cos\gamma < \frac{N+1-2n}{N-1+\delta} = \lambda_n, \tag{8.31}$$

where $\delta = \frac{2p_1}{p_2} = \frac{2(d-(a+b))}{c-a}$, so we find for the Prisoner dilemma $\delta \in (0,\infty)$, hence the above inequality will hold for $N \geq 2$. So in summary, at the classical limit we have all players flipping, and then we have the transition to the non-classical region at λ_1 and we then have equally spaced transitions as entanglement increases down to maximum entanglement where we have the number of players not flipping $n = \lfloor N/2 \rfloor$. So we always have the same number of transitions for a given number of players, but they concertina closer together as the first transition λ_1, moves to wards zero, through changing the game parameters, p_1 and p_2.

The maximum payoff, close to maximum entanglement is

$$\begin{aligned}
\Pi_A^n &= \frac{1}{4}(2(b+d) + (c+a)N + (c-a)_{N\in Odd}) \\
\Pi_A^f &= \frac{1}{4}(2(b+d) + (c+a)N - (c-a)_{N\in Odd}),
\end{aligned} \tag{8.32}$$

where the final $(c-a)$ term only occurs for N odd. So for N even the payoffs are equal, but for N odd, the non-flipping player receives a higher or equal payoff to the flipping player. The payoff rises linearly with N, whereas without entanglement, we have the payoff fixed at d units from Eq.(8.24).

The conventional Prisoner dilemma game for all N

For the Prisoner dilemma settings shown in Eq. (8.25), which gives the conventional Prisoner dilemma game for two players, then we find from Eq. (8.26), $p_1 = 1$ and $p_2 = 1$, and so we can then simplify the general NE conditions in Eq. (8.29), for the first player, to

$$(x^{1*} - x^1)\left(\sum_{i=2}^{N}(1-2x^{i*}) - (N+1)\cos\gamma\right) \geq 0 \tag{8.33}$$

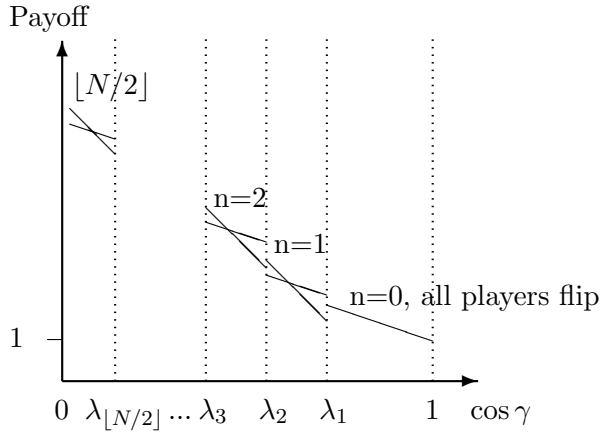

Figure 8.2: Phase structure for N-player Prisoner dilemma. For $\cos\gamma > \lambda_1$ we have the classical regime, where all players flip, and as entanglement increases we find an increasing number of players flipping, up to $\lfloor N/2 \rfloor$ near maximum entanglement.

and similarly for the other $N-1$ players. The left and right edges of each NE zone, shown in Fig. 8.2, can now be written from Eq. (8.31) as

$$\frac{N-1-2n}{N+1} < \cos\gamma < \frac{N+1-2n}{N+1}. \tag{8.34}$$

In each zone we find the payoff for the flipping and non-flipping player, from Eq. (8.30), now given by

$$\begin{aligned} \Pi^f &= \frac{1}{2}\left(3N-2+n+(4-3N+7n)\cos\gamma\right) \\ \Pi^n &= \frac{1}{2}\left(4N-2-n+(4+4N-7n)\cos\gamma\right), \end{aligned} \tag{8.35}$$

which defines the payoff diagram for an N player PD, and which produces the classical PD at $N=2$ at zero entanglement.

At each LH boundary, for the flipping player, we have from Eq. (8.34), $\frac{N-1-2n}{N+1} = \cos\gamma$ or $n = N-1-(N+1)\cos\gamma$. Substituting this into the flipping player payoff in Eq. (8.35), we find

$$\Pi^f = -3 + \frac{7}{4}(N+1)(1-\cos^2\gamma) = -3 + \frac{7}{4}(N+1)\sin^2\gamma, \tag{8.36}$$

for the flipping players' payoff. We thus see that the payoff at each boundary follows a downwards parabolic shape in $\cos\gamma$, if drawn on Fig. 8.2. If we allow N to increase without limit, then the boundaries would concertina infinitesimally close together, and in the limit as $N\to\infty$, the payoff's would form a continuous parabolic curve in $\cos\gamma$, given by Eq. (8.36).

8.2.5 W entangled state

Following the same procedure as used for the GHZ-type state, we find the probability distribution for the W-type state

$$P_{k^1\ldots k^N} = \frac{1}{N2^N}\left(N + \sum_{r=1}^{N}(N-2r)\,C_r^N\left(\epsilon^i K^i\right) + 2\sum_{r=2}^{N} C_r^N\left(\epsilon^i\epsilon^j\epsilon^k\left(X_2^iX_2^j + X_1^iX_1^j\right)K^k\right)\right),$$

see Appendix B for derivation. We can then find the payoff function for the first player, Alice

$$\Pi_A(\kappa^1,\ldots,\kappa^N) = Na^{0\ldots0} + \sum_{r=1}^{N}(N-2r)C_r^N(a^iK^i) + 2\sum_{r=2}^{N}C_r^N(a^{ijk}(X_2^iX_2^j + X_1^iX_1^j)K^k) \quad (8.37)$$

and similarly for other players.

However with the W-type state it is impossible to turn off the entanglement, and so it will not be possible to embed the classical game, as we have done with the GHZ-type state. Hence we will not proceed any further except to show the result of maximizing the payoff function in Eq. (8.37) for the Prisoner dilemma.

Prisoner Dilemma

For the Prisoner dilemma we can maximize the payoff function, and we find that we require all players to flip, for all N and the resultant payoff for the first player Alice and hence all players is

$$\Pi_A = c + d - \frac{c+d-(a+b)}{N}. \quad (8.38)$$

So as $N \to \infty$, then the payoff approaches $c + d$ from below.

8.3 Conclusion

Using geometric algebra, the probability distribution is found after applying general measurement directions on a general N qubit entangled state, for the GHZ type Eq.(8.15) and W states Eq.(8.37).

Linear functions parameterized by the number of non-flipping players for an N player game are then defined , from which games can then be defined in a general way. The linear functions are solved for N players and the Nash equilibrium and payoff relations then determined.

As a specific example the Prisoner dilemma is solved for a general N and we find an interesting feature, that the payoffs at the Nash equilibrium are equal for the flipping and non-flipping player only for even N and also in the limit of large N the payoff rises linearly with N given by $(c + a)N/4$ for the GHZ type state.

At maximum entanglement the payoff for the GHZ type and W type states for the Prisoner dilemma become equal at $N = 2$, producing the formula

$$\Pi_{GHZ} = \Pi_W = \frac{a+b+c+d}{2}. \quad (8.39)$$

This equality is to be expected at $N = 2$, because these two states are equivalent up to local operations.

So in summary we have produced a general quantum game environment, for any number of players $N \geq 2$, which will embed the classical game at zero entanglement, and using linear functions for player payoffs we can produce game outcomes for all N. Hence, the results previously obtained for two-player and three-player games, are now subsumed by these results.

The linear functions could be generalized to second order to increase the range of games represented. For example, a quadratic term could be added to Eq. (8.24) to expand the variety of games.

9 Conclusions

The research began with a general overview of the field of quantum computing, with the key elements and principles being outlined in chapter one. We then described the basic construction of quantum computers from qubits using the circuit model framework for quantum computing, describing one qubit and two qubit gates, and some simple algorithms. We also introduced the formalism of Clifford geometric algebra which we proceeded to show in subsequent chapters can be used as an alternative to the conventional bra-ket notation, and is particularly suited to represent and describe rotations on qubits.

In chapter two we investigated the first of the two key algorithms of the field, Shor's factorization algorithm, followed by Grover's search algorithm in chapter three.

Shor's algorithm, is based on the operation of the phase estimation procedure, which entails an associated probability of error. Several different estimates of this error have been produced in the literature, all requiring simplifying assumptions and approximations in order to obtain a concise formula. A careful review of these derivations was carried out which noted an asymmetry in the definition of the error, which once corrected allowed an analytic solution to be found [JMCL11b]. This formula will more easily allow the optimal design of quantum computers using the phase estimation procedure in the future.

The work on the error formula also motivated the development of a quantum computing simulator, written in the Java programming language, to allow visual modeling of the key algorithms, which was extended over time to model most aspects of quantum computing. Using a graphical user interface, the program allowed the dragging of basic gates onto a circuit board type layout, which allowed the sequential analysis of the wave function after each set of gates to be displayed. The software allowed a very clear visual picture of the operation of basic algorithms, and the software simulator could perhaps be utilized by students in the future to improve understanding of the basic operations of quantum computers.

In chapter three Grover's search algorithm was investigated, and because it is known that the search process is an SU(2) rotation, we found a set of SU(2) generators for this space, based on the two non-orthogonal basis vectors $|m\rangle$ and $|\sigma\rangle$. This allowed us to identify the Grover search process as equivalent to the precession of the polarization axis of a spin-$\frac{1}{2}$ particle in a magnetic field. These results were presented on a poster at Quantum Information and Control in Queensland (QICIQ) and the 4th Asia Pacific Conference in Quantum Information Science (4APCQIS) in 2008.

In chapter four The Grover search algorithm was then recast in the mathematical formalism of GA (geometric algebra). This was done for two reasons, firstly because, as noted previously in chapter three, the Grover search process is an SU(2) rotation, and GA is known to be a natural language in which to describe rotations, and secondly, because it provides a clear geometric picture within a real three dimensional space. We were then, for the first time, able to concisely reproduce the known results of the Grover search algorithm in this formalism. We also found an efficient algebraic solution to the exact Grover search, and also using the visual picture provided by GA in three space, the more general search situations could easily be understood in terms of different precession axes, or different locations in the space of the starting and final states.

In chapter five we extended the use of qubits to the field of quantum game theory. Quantum games like quantum computers are based on application of unitary operations to qubits, and we apply the formalism of GA, successfully used for the Grover search, to describe Meyer's penny flip game. This game is based on two players applying unitary operations to a single

common spin $\frac{1}{2}$ particle. An analysis was completed, which enabled a general solution to be found, along with a clear geometric picture describing the solution space [CILVS09](attached).

We then investigated quantum games from a more general perspective, representing games as a table of non-factorizable joint probabilities [CIA10]. This provides a natural link from classical probabilistic games to quantum games without recourse to the conventional quantum mechanical formalisms, thus making the field of quantum games more accessible to the non-physicist. This approach provides a general framework within which both classical and quantum games can be located.

In chapter six and seven following the analysis of quantum games based on a single qubit, it was then natural to extend this analysis to two-player and three-player and finally N-player quantum games, which differ from the Penny flip game in that each player is allocated a separate qubit from an entangled quantum state. Several different approaches, in fact, have been proposed in order to describe quantum games, but we chose a more recent approach, basing the quantum game on a physical EPR experiment. This approach has the advantage of avoiding a common criticism of quantum games, which states that quantum games are simply different enhanced classical games. With the EPR approach, players choices remain completely classical, being simply the choice of two possible measurement directions, thus avoiding this criticism. We then investigated two-player and three-player games, with the three-player game analysis being published in PLoS [JMCL11a], which was then extended to N-player games. The two-player and three-player games were both conducted in the same pattern in order to allow a straightforward generalization to the much more difficult N-player games.

In chapter eight we extended the analysis of quantum games to the general N-player case. For N players, clearly the use of matrices becomes unwieldy, but through describing unitary operations in GA and through writing the $N \times N$ payoff matrices in a functional form, we found that we could achieve general results as $N \to \infty$. We found for the Prisoner dilemma game a new result could be found, that the payoffs at the Nash equilibrium are equal to each other for the flipping and non-flipping player only for even N.

9.0.1 Original contributions

Several new results were obtained during the different investigations undertaken as part of my thesis, including four major results which were successfully published [JMCL11b, CILVS09, CIA10, JMCL11a].

The first new result achieved was the analytic solution to the problem of finding the error limits for the phase estimation procedure [JMCL11b], its significance being that this procedure is the basis for Shor's factorization algorithm. Further investigations of the phase estimation procedure then resulted in its novel application to performing the Grover search process in Chapter 3.

The Grover search algorithm was then analyzed more generally, finding the three generators of the SU(2) Grover search space, and finding an analogy of the search process with the precession of a spin-$\frac{1}{2}$ particle in a magnetic field, which was presented on a poster at an international conference. The formalism of geometric algebra(GA) was then applied for the first time to the analysis of the Grover search algorithm, which showed a very efficient description of this important algorithm, and due to its clarity may provide further insights.

The use of GA was then applied to an analogous situation involving the quantum penny flip game, a game based on manipulating a single qubit, for which a general solution was found [CILVS09] and we showed that the use of GA also allowed a clear visual picture of the general solution. Investigations in the field of quantum game theory continued which led to the development of a probabilistic framework for quantum games, which interprets entanglement as a classical non-factorizable joint probability distribution, and using a symmetric distribution we found a very general framework within which to describe two-player games [CIA10].

As a special type of quantum game we then developed a quantum game framework based on an EPR experiment, with general results for two-player, three-player and finally N-player games achieved in Chapters $6-8$, with three-player games being successfully published [JMCL11a] and two-player games currently submitted for peer review and N-player games in preparation. This approach is significant as it has the advantage of avoiding a common criticism of other quantum game frameworks of not properly embedding the underlying classical game.

As a more general product of the research we also showed how GA provides a suitable formalism for the whole field of quantum computing, and we found for example an efficient representation for the Grover search in Chapter 4, and Shor's factorization algorithm in Chapter 2 as well as the common gate operations shown in Chapter 1. Also, during this research a quantum circuit simulation program was developed in the Java programming language, which allowed easy graphical analysis of the wavefunction for simple circuits, and which could continue to be developed as an analysis tool.

9.0.2 Further work

We have presented the general equation for the Grover search in GA, but perhaps some specific cases could now be solved, such as more general starting states, and also the partial search process could also perhaps be now placed within this framework.

The N-player formula could now be applied to specific game scenarios and perhaps many specific results could be forthcoming, such as investigating the common games of Stag hunt or Minority game, along with the optimal use of coalitions between players when more than two players are involved. We have also defined N-player game payoffs using linear functions as opposed to a general $N \times N$ payoff matrix, so that to achieve more generality, quadratic functions could now be employed to allow more general game definitions. Clearly these relations could be expanded to arbitrary powers of n, in order to create more general games.

The use of a non-factorizable joint distribution in order to represent entanglement is in fact a very generic approach, and if it could be extended to N participants it could be applied in a general way to optimizing network performance, for example.

The Java simulator, which we developed, was a useful tool to test various ideas and to visually see the resultant wave functions. This program could now be developed further as a useful learning tool for students wishing to gain a better understanding of the basic principles of quantum computing algorithms.

Appendix

A.1 Actions of SU(2) generators on basis vectors

$$
\begin{aligned}
J_1|\sigma\rangle &= \frac{-\alpha^*}{2|\alpha|}|m\rangle = \frac{-\mathrm{e}^{-\mathrm{i}\delta}}{2}|m\rangle \\
J_1|m\rangle &= \frac{-\alpha}{2|\alpha|}|\sigma\rangle = \frac{-\mathrm{e}^{\mathrm{i}\delta}}{2}|\sigma\rangle \\
J_2|\sigma\rangle &= \frac{-\mathrm{i}\alpha^*}{2|\alpha|\beta}|m\rangle + \frac{\mathrm{i}|\alpha|}{2\beta}|\sigma\rangle = \frac{-\mathrm{i}\mathrm{e}^{-\mathrm{i}\delta}}{2\beta}|m\rangle + \frac{\mathrm{i}|\alpha|}{2\beta}|\sigma\rangle \\
J_2|m\rangle &= \frac{-\mathrm{i}|\alpha|}{2\beta}|m\rangle + \frac{\mathrm{i}\alpha}{2|\alpha|\beta}|\sigma\rangle = \frac{-\mathrm{i}|\alpha|}{2\beta}|m\rangle + \frac{\mathrm{i}\mathrm{e}^{\mathrm{i}\delta}}{2\beta}|\sigma\rangle \\
J_3|\sigma\rangle &= \frac{1}{2\beta}(|\sigma\rangle - \alpha^*|m\rangle) \\
J_3|m\rangle &= \frac{1}{2\beta}(\alpha|\sigma\rangle - |m\rangle) \\
J_+|\sigma\rangle &= \frac{\mathrm{e}^{-\mathrm{i}\delta}(1-\beta)}{2\beta}|m\rangle - \frac{|\alpha|}{2\beta}|\sigma\rangle \\
J_+|m\rangle &= \frac{-\mathrm{e}^{\mathrm{i}\delta}(1+\beta)}{2\beta}|\sigma\rangle + \frac{|\alpha|}{2\beta}|m\rangle \\
J_-|\sigma\rangle &= \frac{-\mathrm{e}^{-\mathrm{i}\delta}(1+\beta)}{2\beta}|m\rangle + \frac{|\alpha|}{2\beta}|\sigma\rangle \\
J_-|m\rangle &= \frac{\mathrm{e}^{\mathrm{i}\delta}(1-\beta)}{2\beta}|\sigma\rangle - \frac{|\alpha|}{2\beta}|m\rangle.
\end{aligned}
\tag{A.1}
$$

A.2 Euler angles in geometric algebra

Expanding a general rotor in the Euler angle form in terms of trigonometric functions, we have

$$
\begin{aligned}
R &= \mathrm{e}^{-\iota\sigma_3\frac{\alpha}{2}}\mathrm{e}^{-\iota\sigma_2\frac{\beta}{2}}\mathrm{e}^{-\iota\sigma_3\frac{\chi}{2}} \\
&= \cos\frac{\beta}{2}\cos\frac{\alpha+\chi}{2} + \sin\frac{\beta}{2}\sin\frac{\alpha-\chi}{2}\iota\sigma_1 - \sin\frac{\beta}{2}\cos\frac{\alpha-\chi}{2}\iota\sigma_2 - \cos\frac{\beta}{2}\sin\frac{\alpha+\chi}{2}\iota\sigma_3.
\end{aligned}
\tag{A.2}
$$

We can now derive a few special cases:

Case 1: $\chi = -\alpha$:

$$
\begin{aligned}
R &= \mathrm{e}^{-\iota\sigma_3\frac{\alpha}{2}}\mathrm{e}^{-\iota\sigma_2\frac{\beta}{2}}\mathrm{e}^{\iota\sigma_3\frac{\alpha}{2}} \\
&= \cos\frac{\beta}{2} + \sin\frac{\beta}{2}\sin\alpha\iota\sigma_1 - \sin\frac{\beta}{2}\cos\alpha\iota\sigma_2 \\
&= \mathrm{e}^{\iota\frac{\beta}{2}(\sin\alpha\sigma_1 - \cos\alpha\sigma_2)}.
\end{aligned}
\tag{A.3}
$$

Case 2: $\chi = \alpha - \pi$:

$$\begin{aligned} R &= \mathrm{e}^{-\iota\sigma_3\frac{\alpha}{2}}\mathrm{e}^{-\iota\sigma_2\frac{\beta}{2}}\mathrm{e}^{-\iota\sigma_3\frac{(\alpha-\pi)}{2}} && \text{(A.4)}\\ &= \cos\frac{\beta}{2}\sin\alpha + \sin\frac{\beta}{2}\iota\sigma_1 + \cos\frac{\beta}{2}\cos\alpha\iota\sigma_3 \\ &= \mathrm{e}^{\iota\frac{b}{2}(\sin a\sigma_1 + \cos a\sigma_3)}, \end{aligned}$$

where

$$\begin{aligned} \tan a &= \tan\frac{\beta}{2}\sec\alpha && \text{(A.5)}\\ \cos\frac{b}{2} &= \cos\frac{\beta}{2}\sin\alpha, && \text{(A.6)} \end{aligned}$$

or inverting the formulas we have

$$\begin{aligned} \sin\frac{\beta}{2} &= \sin a\sin\frac{b}{2} && \text{(A.7)}\\ \cot\alpha &= \cos a\tan\frac{b}{2}. && \text{(A.8)} \end{aligned}$$

Case 3:

$$\begin{aligned} R &= \mathrm{e}^{\iota\sigma_3\frac{\alpha}{2}}\mathrm{e}^{\iota\sigma_2\frac{\beta}{2}}\mathrm{e}^{\iota\sigma_3\frac{\alpha-\pi}{2}} && \text{(A.9)}\\ &= \cos\frac{\beta}{2}\sin\alpha + \sin\frac{\beta}{2}\iota\sigma_1 - \cos\frac{\beta}{2}\cos\alpha\iota\sigma_3 \\ &= \mathrm{e}^{\iota\frac{b}{2}(\sin a\sigma_1 - \cos a\sigma_3)}. \end{aligned}$$

Case 4:

$$\begin{aligned} R &= \mathrm{e}^{-\iota\sigma_3\frac{\alpha}{2}}\mathrm{e}^{\iota\sigma_2\frac{\beta}{2}}\mathrm{e}^{\iota\sigma_3\frac{-\alpha+\pi}{2}} && \text{(A.10)}\\ &= \cos\frac{\beta}{2}\sin\alpha - \sin\frac{\beta}{2}\iota\sigma_1 + \cos\frac{\beta}{2}\cos\alpha I\sigma_3 \\ &= \mathrm{e}^{\iota\frac{b}{2}(-\sin a\sigma_1 + \cos a\sigma_3)}. \end{aligned}$$

A.3 Demonstration that the Grover oracle is a reflection about m using GA

In the $|\uparrow\rangle, |\downarrow\rangle$ basis, a general state can be written

$$|\psi\rangle = \begin{bmatrix} -\cos\frac{\chi}{4} \\ \sin\frac{\chi}{4} \end{bmatrix} = -\cos\frac{\chi}{4}|\uparrow\rangle + \sin\frac{\chi}{4}|\downarrow\rangle. \quad \text{(A.11)}$$

Writing the Grover oracle in this space, we have

$$G_m = I - 2|m\rangle\langle m| = I - 2\sin^2\frac{\theta}{4}|\uparrow\rangle\langle\uparrow| - 2\cos^2\frac{\theta}{4}|\downarrow\rangle\langle\downarrow| + \sin\frac{\theta}{2}|\uparrow\rangle\langle\downarrow| + \sin\frac{\theta}{2}|\downarrow\rangle\langle\uparrow|. \quad \text{(A.12)}$$

We find

$$\begin{aligned} G_m|\psi\rangle &= \left(-\cos\frac{\chi}{4} + 2\sin^2\frac{\theta}{4}\cos\frac{\chi}{4} + \sin\frac{\theta}{2}\sin\frac{\chi}{4}\right)|\uparrow\rangle && \text{(A.13)}\\ &+ \left(\sin\frac{\chi}{4} - 2\cos^2\frac{\theta}{4}\sin\frac{\chi}{4} - \sin\frac{\theta}{2}\cos\frac{\chi}{4}\right)|\downarrow\rangle && \text{(A.14)}\\ &= -\cos\left(\frac{\theta}{2} + \frac{\chi}{4}\right)|\uparrow\rangle - \sin\left(\frac{\theta}{2} + \frac{\chi}{4}\right)|\downarrow\rangle && \text{(A.15)}\\ &\leftrightarrow -\cos\left(\frac{\theta}{2} + \frac{\chi}{4}\right) + \sin\left(\frac{\theta}{2} + \frac{\chi}{4}\right)\iota\sigma_2. && \text{(A.16)} \end{aligned}$$

Using Eq.(4.6), we find

$$\langle S\rangle = \sin\left(\theta+\frac{\chi}{2}\right)\sigma_1 + \cos\left(\theta+\frac{\chi}{2}\right)\sigma_3. \tag{A.17}$$

We see this new vector is then a reflection about the vector m.

A similar result holds for G_σ, that is

$$G_\sigma|\psi\rangle \leftrightarrow -\cos\left(\frac{\theta}{2}-\frac{\chi}{4}\right) + \sin\left(\frac{\theta}{2}-\frac{\chi}{4}\right)\iota\sigma_2, \tag{A.18}$$

which gives us

$$\langle S\rangle = \sin\left(\theta-\frac{\chi}{2}\right)\sigma_1 + \cos\left(\theta-\frac{\chi}{2}\right)\sigma_3, \tag{A.19}$$

which once again is a simple reflection, but this time about σ.

A.4 Standard results when calculating observables

These results, particularly those shown in Eq. (A.25), are used when calculating the observables in GA. We have also calculated the general case with general measurement directions in Eq. (A.23). If we have a rotor defined as

$$A = \mathrm{e}^{-\alpha_3\iota\sigma_3/2}\mathrm{e}^{-\alpha_1\iota\sigma_2/2}\mathrm{e}^{-\alpha_2\iota\sigma_3/2} \tag{A.20}$$

and for measurement, we use

$$R = \mathrm{e}^{-\lambda\iota\sigma_3/2}\mathrm{e}^{-\kappa\iota\sigma_2/2}\mathrm{e}^{-\eta\iota\sigma_3/2}. \tag{A.21}$$

We find, firstly

$$\begin{aligned}
\iota A\sigma_1 A^\dagger &= \iota\mathrm{e}^{-\alpha_3\iota\sigma_3/2}\mathrm{e}^{-\alpha_1\iota\sigma_2/2}\mathrm{e}^{-\alpha_2\iota\sigma_3/2}\sigma_1\mathrm{e}^{\alpha_2\iota\sigma_3/2}\mathrm{e}^{\alpha_1\iota\sigma_2/2}\mathrm{e}^{\alpha_3\iota\sigma_3/2} \\
&= \mathrm{e}^{-\alpha_3\iota\sigma_3/2}\mathrm{e}^{-\alpha_1\iota\sigma_2/2}(\cos\alpha_2 - \sin\alpha_2\iota\sigma_3)\mathrm{e}^{-\alpha_1\iota\sigma_2/2}\mathrm{e}^{-\alpha_3\iota\sigma_3/2}\iota\sigma_1 \\
&= \mathrm{e}^{-\alpha_3\iota\sigma_3/2}(\cos\alpha_2\mathrm{e}^{-\alpha_1\iota\sigma_2} - \sin\alpha_2\iota\sigma_3)\mathrm{e}^{-\alpha_3\iota\sigma_3/2}\iota\sigma_1 \\
&= \mathrm{e}^{-\alpha_3\iota\sigma_3/2}(\cos\alpha_2\cos\alpha_1 - \cos\alpha_2\sin\alpha_1\iota\sigma_2 - \sin\alpha_2\iota\sigma_3)\mathrm{e}^{-\alpha_3\iota\sigma_3/2}\iota\sigma_1 \\
&= (\cos\alpha_1\cos\alpha_2\mathrm{e}^{-\alpha_3\iota\sigma_3} - \sin\alpha_1\cos\alpha_2\iota\sigma_2 - \sin\alpha_2\iota\sigma_3\mathrm{e}^{-\alpha_3\iota\sigma_3})\iota\sigma_1 \\
&= (\cos\alpha_1\cos\alpha_2\cos\alpha_3 - \cos\alpha_1\cos\alpha_2\sin\alpha_3\iota\sigma_3 - \sin\alpha_1\cos\alpha_2\iota\sigma_2 \\
&- \sin\alpha_2\cos\alpha_3\iota\sigma_3 - \sin\alpha_2\sin\alpha_3)\iota\sigma_1 \\
&= (\cos\alpha_1\cos\alpha_2\cos\alpha_3 - \sin\alpha_2\sin\alpha_3)\iota\sigma_1 - \sin\alpha_1\cos\alpha_2\iota\sigma_3 \\
&\quad +(\cos\alpha_1\cos\alpha_2\sin\alpha_3 + \sin\alpha_2\cos\alpha_3)\iota\sigma_2 \\
\iota A\sigma_2 A^\dagger &= \iota\mathrm{e}^{-\alpha_3\iota\sigma_3/2}\mathrm{e}^{-\alpha_1\iota\sigma_2/2}\mathrm{e}^{-\alpha_2\iota\sigma_3/2}\sigma_2\mathrm{e}^{\alpha_2\iota\sigma_3/2}\mathrm{e}^{\alpha_1\iota\sigma_2/2}\mathrm{e}^{\alpha_3\iota\sigma_3/2} \\
&= \mathrm{e}^{-\alpha_3\iota\sigma_3/2}\mathrm{e}^{-\alpha_1\iota\sigma_2/2}(\cos\alpha_2 - \sin\alpha_2\iota\sigma_3)\mathrm{e}^{\alpha_1\iota\sigma_2/2}\mathrm{e}^{-\alpha_3\iota\sigma_3/2}\iota\sigma_2 \\
&= \mathrm{e}^{-\alpha_3\iota\sigma_3/2}(\cos\alpha_2 - \sin\alpha_2\iota\sigma_3\mathrm{e}^{\alpha_1\iota\sigma_2})\mathrm{e}^{-\alpha_3\iota\sigma_3/2}\iota\sigma_2 \\
&= \mathrm{e}^{-\alpha_3\iota\sigma_3/2}(\cos\alpha_2 - \cos\alpha_1\sin\alpha_2\iota\sigma_3 - \sin\alpha_1\sin\alpha_2\iota\sigma_1)\mathrm{e}^{-\alpha_3\iota\sigma_3/2}\iota\sigma_2 \\
&= (\cos\alpha_2\mathrm{e}^{-\alpha_3\iota\sigma_3} - \cos\alpha_1\sin\alpha_2\iota\sigma_3\mathrm{e}^{-\alpha_3\iota\sigma_3} - \sin\alpha_1\sin\alpha_2\iota\sigma_1)\iota\sigma_2 \\
&= (\cos\alpha_2\cos\alpha_3 - \cos\alpha_1\sin\alpha_2\sin\alpha_3)\iota\sigma_2 - (\cos\alpha_2\sin\alpha_3 + \cos\alpha_1\sin\alpha_2\cos\alpha_3)\iota\sigma_1 \\
&\quad + \sin\alpha_1\sin\alpha_2\iota\sigma_3 \\
\iota A\sigma_3 A^\dagger &= \cos\alpha_1\iota\sigma_3 + \sin\alpha_1\cos\alpha_3\iota\sigma_1 + \sin\alpha_1\sin\alpha_3\iota\sigma_2,
\end{aligned} \tag{A.22}$$

then we find the following results

$$\begin{aligned}
\langle \iota A\sigma_3 A^\dagger \iota R\sigma_3 R^\dagger\rangle_0 &= -\cos\alpha_1\cos\kappa - \sin\alpha_1\cos\alpha_3\sin\kappa\cos\lambda \\
&\quad -\sin\alpha_1\sin\alpha_3\sin\kappa\sin\lambda \\
&= -\cos\alpha_1\cos\kappa - \cos(\alpha_3-\lambda)\sin\alpha_1\sin\kappa \\
\langle \iota A\sigma_2 A^\dagger \iota R\sigma_3 R^\dagger\rangle_0 &= \sin\kappa\cos\lambda(\cos\alpha_2\sin\alpha_3+\sin\alpha_2\cos\alpha_3\cos\alpha_1) - \sin\alpha_1\sin\alpha_2\cos\kappa \\
&\quad -\sin\kappa\sin\lambda(\cos\alpha_2\cos\alpha_3-\cos\alpha_1\sin\alpha_2\sin\alpha_3) \\
&= -\cos\kappa\sin\alpha_1\sin\alpha_2+\sin\kappa(\cos\alpha_1\cos(\alpha_3-\lambda)\sin\alpha_2 \\
&\quad +\cos\alpha_2\sin(\alpha_3-\lambda)) \\
\langle \iota A\sigma_1 A^\dagger \iota R\sigma_3 R^\dagger\rangle_0 &= -\sin\kappa\cos\lambda(\cos\alpha_1\cos\alpha_2\cos\alpha_3-\sin\alpha_2\sin\alpha_3)+\sin\alpha_1\cos\alpha_2\cos\kappa \\
&\quad -\sin\kappa\sin\lambda(\cos\alpha_1\cos\alpha_2\sin\alpha_3+\sin\alpha_2\cos\alpha_3) \\
&= \cos\alpha_2(\cos\kappa\sin\alpha_1-\cos\alpha_1\cos(\alpha_3-\lambda)\sin\kappa^1) \\
&\quad +\sin\alpha_2\sin\kappa\sin(\alpha_3-\lambda)
\end{aligned} \tag{A.23}$$

and also, we find

$$\begin{aligned}
\langle \iota A\sigma_1 A^\dagger \iota R\sigma_1 R^\dagger\rangle_0 &= -\sin\alpha_1\cos\alpha_2\sin\kappa\cos\eta \\
&- (\cos\alpha_1\cos\alpha_2\sin\alpha_3+\sin\alpha_2\cos\alpha_3)(\cos\kappa\cos\eta\sin\lambda+\sin\eta\cos\lambda) \\
&- (\cos\alpha_1\cos\alpha_2\cos\alpha_3-\sin\alpha_2\sin\alpha_3)(\cos\kappa\cos\eta\cos\lambda-\sin\eta\sin\lambda) \\
&= \sin(\alpha_3-\lambda^1)(\cos\eta^1\cos\kappa^1\sin\alpha_2-\cos\alpha_1\cos\alpha_2\sin\eta^1) \\
&- \cos(\alpha_3-\lambda^1)(\cos\alpha_1\cos\alpha_2\cos\eta^1\cos\kappa^1+\sin\alpha_2\sin\eta^1) \\
&\quad -\cos\alpha_2\cos\eta^1\sin\alpha_1\sin\kappa^1 \\
\langle \iota A\sigma_2 A^\dagger \iota R\sigma_2 R^\dagger\rangle_0 &= -\sin\alpha_1\sin\alpha_2\sin\kappa\sin\eta \\
&- (\cos\alpha_2\sin\alpha_3+\cos\alpha_1\sin\alpha_2\cos\alpha_3)(\cos\eta\sin\lambda+\cos\kappa\sin\eta\cos\lambda) \\
&- (\cos\alpha_2\cos\alpha_3-\cos\alpha_1\sin\alpha_2\sin\alpha_3)(\cos\eta\cos\lambda-\cos\kappa\sin\eta\sin\lambda) \\
&= \sin(\alpha_3-\lambda^1)(\cos\alpha_1\cos\eta^1\sin\alpha_2-\cos\alpha_2\cos\kappa^1\sin\eta^1) \\
&- \cos(\alpha_3-\lambda^1)(\cos\alpha_1\cos\kappa^1\sin\alpha_2\sin\eta^1+\cos\alpha_2\cos\eta^1) \\
&\quad -\sin\alpha_1\sin\alpha_2\sin\eta^1\sin\kappa^1.
\end{aligned} \tag{A.24}$$

We have the special cases for just a single measurement direction κ

$$\begin{aligned}
\langle \iota A\sigma_3 A^\dagger \iota\sigma_3 \mathrm{e}^{\kappa\iota\sigma_2}\rangle_0 &= -\cos\alpha_1\cos\kappa-\sin\alpha_1\cos\alpha_3\sin\kappa \\
\langle \iota A\sigma_2 A^\dagger \iota\sigma_3 \mathrm{e}^{\kappa\iota\sigma_2}\rangle_0 &= \sin\kappa(\cos\alpha_2\sin\alpha_3+\sin\alpha_2\cos\alpha_3\cos\alpha_1)-\sin\alpha_1\sin\alpha_2\cos\kappa \\
\langle \iota A\sigma_1 A^\dagger \iota\sigma_3 \mathrm{e}^{\kappa\iota\sigma_2}\rangle_0 &= -\sin\kappa(\cos\alpha_1\cos\alpha_2\cos\alpha_3-\sin\alpha_2\sin\alpha_3)+\sin\alpha_1\cos\alpha_2\cos\kappa.
\end{aligned} \tag{A.25}$$

A.5 Deriving the general two qubit state representation in GA

The Schmidt decomposition of a general two particle state can be written [DL03]

$$\begin{aligned}
|\psi\rangle = \rho^{\frac{1}{2}}\mathrm{e}^{\mathrm{i}\chi}\Big[&\cos\frac{\gamma}{2}\mathrm{e}^{\frac{-\mathrm{i}\phi}{2}}\left(\cos\frac{\alpha_1}{2}\mathrm{e}^{\frac{-\mathrm{i}\alpha_3}{2}}|0\rangle+\sin\frac{\alpha_1}{2}\mathrm{e}^{\frac{\mathrm{i}\alpha_3}{2}}|1\rangle\right) \\
&\otimes\left(\cos\frac{\beta_1}{2}\mathrm{e}^{\frac{-\mathrm{i}\beta_3}{2}}|0\rangle+\sin\frac{\beta_1}{2}\mathrm{e}^{\frac{\mathrm{i}\beta_3}{2}}|1\rangle\right) \\
&+\sin\frac{\gamma}{2}\mathrm{e}^{\frac{\mathrm{i}\phi}{2}}\left(\sin\frac{\alpha_1}{2}\mathrm{e}^{\frac{-\mathrm{i}\alpha_3}{2}}|0\rangle-\cos\frac{\alpha_1}{2}\mathrm{e}^{\frac{\mathrm{i}\alpha_3}{2}}|1\rangle\right) \\
&\otimes\left(\sin\frac{\beta_1}{2}\mathrm{e}^{\frac{-\mathrm{i}\beta_3}{2}}|0\rangle-\cos\frac{\beta_1}{2}\mathrm{e}^{\frac{\mathrm{i}\beta_3}{2}}|1\rangle\right)\Big].
\end{aligned} \tag{A.26}$$

We note that the Schmidt decomposition assumes that $\cos\gamma \geq \sin\gamma$, hence we need to enforce the condition $\gamma \in [0, \frac{\pi}{2}]$. Using the mapping defined in Eq. (1.24), we find that

$$\begin{aligned}
&\mathrm{e}^{\frac{-\mathrm{i}\phi}{2}}\left(\cos\frac{\alpha_1}{2}\mathrm{e}^{\frac{-\mathrm{i}\alpha_3}{2}}|0\rangle + \sin\frac{\alpha_1}{2}\mathrm{e}^{\frac{\mathrm{i}\alpha_3}{2}}|1\rangle\right)\\
&= \cos\frac{\alpha_1}{2}\mathrm{e}^{\frac{-\mathrm{i}(\phi+\alpha_3)}{2}}|0\rangle + \sin\frac{\alpha_1}{2}\mathrm{e}^{\frac{\mathrm{i}(\alpha_3-\phi}{2}}|1\rangle\\
&= \left(\cos\frac{\alpha_1}{2}\cos\frac{\phi+\alpha_3}{2} - \mathrm{i}\cos\frac{\alpha_1}{2}\sin\frac{\phi+\alpha_3}{2}\right)|0\rangle\\
&+ \left(\sin\frac{\alpha_1}{2}\cos\frac{\alpha_3-\phi}{2} + \mathrm{i}\sin\frac{\alpha_1}{2}\sin\frac{\alpha_3-\phi}{2}\right)|1\rangle\\
&\to \cos\frac{\alpha_1}{2}\cos\frac{\phi+\alpha_3}{2} - \cos\frac{\alpha_1}{2}\sin\frac{\phi+\alpha_3}{2}\iota\sigma_3\\
&- \sin\frac{\alpha_1}{2}\cos\frac{\alpha_3-\phi}{2}\iota\sigma_2 + \sin\frac{\alpha_1}{2}\sin\frac{\alpha_3-\phi}{2}\iota\sigma_1\\
&= \mathrm{e}^{-\iota\alpha_3\sigma_3/2}\mathrm{e}^{-\iota\alpha_1\sigma_2/2}\mathrm{e}^{-\iota\phi\sigma_3/2}.
\end{aligned} \tag{A.27}$$

We can then also deduce that

$$\mathrm{e}^{\mathrm{i}\chi}\left(\cos\frac{\beta_1}{2}\mathrm{e}^{\frac{-\mathrm{i}\beta_3}{2}}|0\rangle + \sin\frac{\beta_1}{2}\mathrm{e}^{\frac{\mathrm{i}\beta_3}{2}}|1\rangle\right) \to \mathrm{e}^{-\iota\beta_3\sigma_3/2}\mathrm{e}^{-\iota\beta_1\sigma_2/2}\mathrm{e}^{\iota\chi\sigma_3}. \tag{A.28}$$

If we then make the substitution $\frac{\alpha_1}{2} \to -(\frac{\pi}{2} - \frac{\alpha_1}{2})$ we find

$$\begin{aligned}
\mathrm{e}^{\frac{\mathrm{i}\phi}{2}}\left(\sin\frac{\alpha_1}{2}\mathrm{e}^{\frac{-\mathrm{i}\alpha_3}{2}}|0\rangle - \cos\frac{\alpha_1}{2}\mathrm{e}^{\frac{\mathrm{i}\alpha_3}{2}}|1\rangle\right) &\to -\mathrm{e}^{-\frac{\iota\alpha_3\sigma_3}{2}}\mathrm{e}^{\iota(\frac{\pi}{2}-\frac{\alpha_1}{2})\sigma_2}\mathrm{e}^{\frac{\iota\phi\sigma_3}{2}}\\
&= -\mathrm{e}^{-\frac{\iota\alpha_3\sigma_3}{2}}\mathrm{e}^{-\frac{\iota\alpha_1\sigma_2}{2}}\mathrm{e}^{-\frac{\iota\phi\sigma_3}{2}}\iota\sigma_2^1,
\end{aligned} \tag{A.29}$$

and

$$\mathrm{e}^{\mathrm{i}\chi}\left(\sin\frac{\beta_1}{2}\mathrm{e}^{\frac{-\mathrm{i}\beta_3}{2}}|0\rangle - \cos\frac{\beta_1}{2}\mathrm{e}^{\frac{\mathrm{i}\beta_3}{2}}|1\rangle\right) \to -\mathrm{e}^{-\frac{\iota\beta_3\sigma_3}{2}}\mathrm{e}^{-\frac{\iota\beta_1\sigma_2}{2}}\iota\sigma_2^2\mathrm{e}^{\iota\chi\sigma_3}. \tag{A.30}$$

The general state is then represented as

$$\psi = \rho^{\frac{1}{2}}\mathrm{e}^{-\iota\alpha_3\sigma_3/2}\mathrm{e}^{-\iota\alpha_1\sigma_2/2}\mathrm{e}^{-\iota\phi\sigma_3/2}\mathrm{e}^{-\iota\beta_3\sigma_3/2}\mathrm{e}^{-\iota\beta_1\sigma_2/2}(\cos\frac{\gamma}{2} + \sin\frac{\gamma}{2}\iota\sigma_2^1\iota\sigma_2^2)\mathrm{e}^{\iota\chi\sigma_3}. \tag{A.31}$$

We notice the first qubit has an extra degree of freedom available in the applied rotor as compared to the second qubit, namely, the parameter ϕ. However, we had a choice where we associated the complex phase during the derivation. So if we split the phase $\mathrm{e}^{\mathrm{i}\phi\sigma_3/2}$ between the two qubits as $\mathrm{e}^{\mathrm{i}\alpha_2\sigma_3/2}$ and $\mathrm{e}^{\mathrm{i}\beta_2\sigma_3/2}$, we can have symmetrical rotors on each qubit with

$$A = \mathrm{e}^{-\iota\alpha_3\sigma_3/2}\mathrm{e}^{-\iota\alpha_1\sigma_2/2}\mathrm{e}^{-\iota\alpha_2\sigma_3/2},\ B = \mathrm{e}^{-\iota\beta_3\sigma_3/2}\mathrm{e}^{-\iota\beta_1\sigma_2/2}\mathrm{e}^{-\iota\beta_2\sigma_3/2}, \tag{A.32}$$

where $\phi = \alpha_2 + \beta_2$. The general two qubit state can now be written as

$$\psi = \rho^{\frac{1}{2}}AB\left(\cos\frac{\gamma}{2} + \sin\frac{\gamma}{2}\iota\sigma_2^1\iota\sigma_2^2\right)\mathrm{e}^{\iota\chi\sigma_3}E. \tag{A.33}$$

The extra E term on the end of the wave function is included because we have introduced a second copy of ι for the second particle space, whereas normally the complex number i is common across all particle spaces. We can remove this redundancy with a projection operator, $E = \frac{1}{2}(1 - \iota\sigma_3^1\iota\sigma_3^2)$. However, when we come to form the observables $\psi E\psi^\dagger$ and $\psi J\psi^\dagger$, we notice that because $E^2 = E$ and $EJ = JE = J$, we see that the inclusion of E, as well as the global phase term $\mathrm{e}^{\iota\chi\sigma_3}$, will cancel out in both cases and hence is superfluous. Also for a pure state we have $\rho = 1$ and so without loss of generality, in regard to the observables, we can write a general two-particle state in GA, compactly as

$$\psi = AB\left(\cos\frac{\gamma}{2} + \sin\frac{\gamma}{2}\iota\sigma_2^1\iota\sigma_2^2\right). \tag{A.34}$$

We see that with the five degrees of freedom provided with the rotors and also the entanglement angle γ, we have defined a two particle quantum state with six degrees of freedom, as required for a normalized two-particle quantum state ignoring the global phase.

A.6 Two-player games: SO6 geometric algebra

This approach is the most general method for two particles because it also allows a disentangling operation but, unfortunately, it cannot be generalized beyond two particles, because the isomorphism does not continue beyond $SU(4)$.

We define two separate SO3 spaces e_1, e_2, e_3 and f_1, f_2, f_3 where $e_1^2 = f_i^2 = 1$ and all six orthonormal vectors anti-commute with each other, and where we define

$$\begin{aligned} \sigma_i^1 &= e_i f_1 f_2 f_3 = e_i \iota^2 \\ \sigma_i^2 &= e_1 e_2 e_3 f_i = \iota^1 f_i, \end{aligned} \tag{A.35}$$

where the superscripts indicate which particle space the vector belongs to and let $\iota = \iota^1 \iota^2$, where we find ι^1 and ι^2 anti-commute, and so using this new combined ι, we find $(\iota)^2 = \iota\iota = -1$. From now on ι will always refer to $\iota = e_1 e_2 e_3 f_1 f_2 f_3$, combined from both particle spaces. Then we find

$$\sigma_i \sigma_j = \delta_{ij} + \iota \epsilon_{ijk} \sigma_k, \tag{A.36}$$

which mimics the Pauli algebra and

$$\sigma_i^1 \sigma_j^2 = \sigma_j^2 \sigma_i^1 \tag{A.37}$$

with its commuting property allows us to use the geometric product in the same way as the tensor product. We can identify a basis for two-particle spinor space as

$$\begin{aligned} |0\rangle|0\rangle &\longleftrightarrow 1 \\ |0\rangle|1\rangle &\longleftrightarrow \iota\sigma_2^2 \\ |1\rangle|0\rangle &\longleftrightarrow \iota\sigma_2^1 \\ |1\rangle|1\rangle &\longleftrightarrow \iota\sigma_2^1\sigma_2^2. \end{aligned} \tag{A.38}$$

In fact, for a general entangled two-particle state, we can write

$$\psi = A^1 B^2 (\cos\frac{\gamma}{2} + \sin\frac{\gamma}{2} \iota\sigma_2^1\sigma_2^2), \tag{A.39}$$

where γ is a measure of the entanglement, and A^1 and B^2 are general single particle rotors(unitary rotations) on each qubit.

General unitary operations in GA can be represented as

$$R(\alpha_1, \alpha_2, \alpha_3) = \mathrm{e}^{-\alpha_3 \iota\sigma_3/2} \mathrm{e}^{-\alpha_1 \iota\sigma_2/2} \mathrm{e}^{-\alpha_2 \iota\sigma_3/2}. \tag{A.40}$$

This rotation, represented in geometric algebra, is in Euler angle form and can completely explore the available space of a single qubit, and is equivalent to the general unitary transformation denoted by the matrix

$$\begin{bmatrix} \mathrm{e}^{\mathrm{i}\theta_3/2}\cos\frac{\theta_1}{2} & -\mathrm{e}^{-\mathrm{i}\theta_2/2}\sin\frac{\theta_1}{2} \\ \mathrm{e}^{\mathrm{i}\theta_2/2}\sin\frac{\theta_1}{2} & \mathrm{e}^{-\mathrm{i}\theta_3/2}\cos\frac{\theta_1}{2} \end{bmatrix} \tag{A.41}$$

acting on a spinor. We see that with the 3 degrees of freedom provided in each rotor and the entanglement angle γ, we have defined a two particle quantum state with 7 degrees of freedom as required for a two-particle quantum state ignoring the global phase.

The observables are found in geometric algebra from a density operator(which mimic density matrices) [PD01]

$$\rho = \psi P_3^1 P_3^2 \psi^\dagger \tag{A.42}$$

where $P_3^k = 1 + \sigma_3^k$. So, we find

$$P_3^1 P_3^2 = (1+\sigma_3^1)(1+\sigma_3^2) = (1+\sigma_3^1\sigma_3^2) + (\sigma_3^1 + \sigma_3^2). \tag{A.43}$$

So, we have

$$\begin{aligned} \rho &= \psi P_3^1 P_3^2 \psi^\dagger \\ &= \psi(1+\sigma_3^1+\sigma_3^2+\sigma_3^1\sigma_3^2)\psi^\dagger \\ &= 1 + \psi\sigma_3^1\sigma_3^2\psi^\dagger + \psi\sigma_3^1\psi^\dagger + \psi\sigma_3^2\psi^\dagger. \end{aligned} \tag{A.44}$$

Taking each term from Eq.(A.44) in turn, starting with σ_3^1, we find $\psi\sigma_3^1\psi^\dagger$

$$\begin{aligned} &= AB(\cos\frac{\gamma}{2} + \sin\frac{\gamma}{2}\iota\sigma_2^1\sigma_2^2)\sigma_3^1(\cos\frac{\gamma}{2} - \sin\frac{\gamma}{2}\iota\sigma_2^1\sigma_2^2)B^\dagger A^\dagger \\ &= AB(\cos\frac{\gamma}{2} + \sin\frac{\gamma}{2}\iota\sigma_2^1\sigma_2^2)(\cos\frac{\gamma}{2} + \sin\frac{\gamma}{2}\iota\sigma_2^1\sigma_2^2)\sigma_3^1 B^\dagger A^\dagger \\ &= AB(\cos\gamma + \sin\gamma\iota\sigma_2^1\sigma_2^2)\sigma_3^1 B^\dagger A^\dagger \\ &= \cos\gamma A\sigma_3^1 A^\dagger - \sin\gamma A\sigma_1^1 A^\dagger B\sigma_2^2 B^\dagger, \end{aligned} \tag{A.45}$$

where we used the results $\sigma_3^1\sigma_2^1 = -\sigma_2^1\sigma_3^1$, $\iota\sigma_2^1\sigma_2^2\iota\sigma_2^1\sigma_2^2 = \iota^2 = -1$ and $\iota\sigma_2^1\sigma_2^2\sigma_3^1 = -\sigma_1^1\sigma_2^2$. By symmetry of the first and second particle, we can immediately write

$$\psi\sigma_3^2\psi^\dagger = \cos\gamma B\sigma_3^2 B^\dagger - \sin\gamma A\sigma_2^1 A^\dagger B\sigma_1^2 B^\dagger. \tag{A.46}$$

Finally, we have $\psi\sigma_3^1\sigma_3^2\psi^\dagger$

$$\begin{aligned} &= AB(\cos\frac{\gamma}{2} + \sin\frac{\gamma}{2}\iota\sigma_2^1\sigma_2^2)\sigma_3^1\sigma_3^2(\cos\frac{\gamma}{2} - \sin\frac{\gamma}{2}\iota\sigma_2^1\sigma_2^2)B^\dagger A^\dagger \\ &= AB(\cos\frac{\gamma}{2} + \sin\frac{\gamma}{2}\iota\sigma_2^1\sigma_2^2)(\cos\frac{\gamma}{2} - \sin\frac{\gamma}{2}\iota\sigma_2^1\sigma_2^2)\sigma_3^1\sigma_3^2 B^\dagger A^\dagger \\ &= AB\sigma_3^1\sigma_3^2 B^\dagger A^\dagger \\ &= A\sigma_3^1 A^\dagger B\sigma_3^2 B^\dagger. \end{aligned} \tag{A.47}$$

So, the full density operator is

$$\begin{aligned} \rho &= 1 + \cos\gamma A\sigma_3^1 A^\dagger - \sin\gamma A\sigma_1^1 A^\dagger B\sigma_2^2 B^\dagger \\ &+ \cos\gamma B\sigma_3^2 B^\dagger - \sin\gamma A\sigma_2^1 A^\dagger B\sigma_1^2 B^\dagger + A\sigma_3^1 A^\dagger B\sigma_3^2 B^\dagger \\ &= 1 + \cos\gamma(A\sigma_3^1 A^\dagger + B\sigma_3^2 B^\dagger) \\ &+ A\sigma_3^1 A^\dagger B\sigma_3^2 B^\dagger - \sin\gamma(A\sigma_1^1 A^\dagger B\sigma_2^2 B^\dagger + A\sigma_2^1 A^\dagger B\sigma_1^2 B^\dagger). \end{aligned} \tag{A.48}$$

For measurement, we employ the density operator

$$\rho_M = R^1 R^2(1+\sigma_3^1+\sigma_3^2+\sigma_3^1\sigma_3^2)R^1 R^2 \tag{A.49}$$

and we have $R^1 = \mathrm{e}^{\iota\kappa^1\sigma_2^1}$ and $R^2 = \mathrm{e}^{\iota\kappa^2\sigma_2^2}$ where κ^1 and κ^2 are measurement directions for players 1 and 2 respectively, so that we have

$$\begin{aligned} \rho_M &= \mathrm{e}^{\iota\kappa\sigma_2^1/2}\mathrm{e}^{\iota\kappa\sigma_2^2/2}(1+\sigma_3^1+\sigma_3^2+\sigma_3^1\sigma_3^2)\mathrm{e}^{-\iota\kappa\sigma_2^2/2}\mathrm{e}^{-\iota\kappa\sigma_2^1/2} \\ &= 1 + \sigma_3^1\mathrm{e}^{-\iota\kappa\sigma_2^1} + \sigma_3^2\mathrm{e}^{-\iota\kappa\sigma_2^1} + \sigma_3^1\sigma_3^2\mathrm{e}^{-\iota\kappa\sigma_2^2}\mathrm{e}^{-\iota\kappa_2\sigma_2}. \end{aligned} \tag{A.50}$$

Retaining the scalar part of the product $\rho_M\rho$, written as $\langle\rho_M\rho\rangle_0$, we find the probability of measuring each wave state as

$$\begin{aligned}
4P_{mn} &= \langle\rho_M\rho\rangle_0 \\
&= \langle[1+\cos\gamma(A\sigma_3^1A^\dagger + B\sigma_3^2B^\dagger) \\
&+ A\sigma_3^1A^\dagger B\sigma_3^2B^\dagger - \sin\gamma(A\sigma_1^1A^\dagger B\sigma_2^2B^\dagger + A\sigma_2^1A^\dagger B\sigma_1^2B^\dagger)] \\
&\times [1+\sigma_3^1\mathrm{e}^{-\iota\kappa^1\sigma_2^1} + \sigma_3^2\mathrm{e}^{-\iota\kappa^2\sigma_2^2} + \sigma_3^1\sigma_3^2\mathrm{e}^{-\iota\kappa^1\sigma_2^1}\mathrm{e}^{-\iota\kappa^2\sigma_2^2}]\rangle_0 \\
&= \langle 1+\cos\gamma(A\sigma_3^1A^\dagger\sigma_3^1\mathrm{e}^{-\iota\kappa^1\sigma_2^1} + B\sigma_3^2B^\dagger\sigma_3^2)\mathrm{e}^{-\iota\kappa^2\sigma_2^2} \\
&+ A\sigma_3^1A^\dagger\sigma_3^1B\sigma_3^2B^\dagger\sigma_3^2\mathrm{e}^{-\iota\kappa^1\sigma_2^1}\mathrm{e}^{-\iota\kappa^2\sigma_2^2} \\
&- \sin\gamma(A\sigma_1^1A^\dagger\sigma_3^1B\sigma_2^2B^\dagger\sigma_3^2 + A\sigma_2^1A^\dagger\sigma_3^1B\sigma_1^2B^\dagger\sigma_3^2)\mathrm{e}^{-\iota\kappa^1\sigma_2^1}\mathrm{e}^{-\iota\kappa^2\sigma_2^2}\rangle_0 \\
&= 1+\cos\gamma((-)^mA + (-)^nB + (-)^{m+n}AB + (-)^{m+n}\sin\gamma Z,
\end{aligned} \tag{A.51}$$

where

$$\begin{aligned}
A(\kappa^1) &= \cos\alpha_1\cos\kappa^1 - \sin\alpha_1\cos\alpha_3\sin\kappa^1 \\
B(\kappa^2) &= \cos\beta_1\cos\kappa^2 - \sin\beta_1\cos\beta_3\sin\kappa^2
\end{aligned} \tag{A.52}$$

and

$$\begin{aligned}
Z(\kappa^1,\kappa^2) &= (\cos k^1\sin\alpha_1 + \cos\alpha_1\cos\alpha_3\sin\kappa^1) \\
&\quad\times(\cos\kappa^2\sin\beta_1\sin\phi + \sin\kappa^2\sin\beta_3\cos\phi + \sin\kappa^2\cos\beta_1\cos\beta_3\sin\phi) \\
&- \sin\kappa^1\sin\kappa^2\sin\beta_3\sin\alpha_3\sin\phi + \cos\kappa^2\sin\beta_1\cos\phi\sin\alpha_3\sin\kappa^1 \\
&+ \sin\kappa^2\cos\beta_1\cos\beta_3\cos\phi\sin\alpha_3\sin\kappa^1.
\end{aligned} \tag{A.53}$$

To simplify notation, we will write $Z_{ij} = Z(\kappa_i^1,\kappa_j^2)$, $A_i = A(\kappa_i^1)$ and $B_j = B(\kappa_j^2)$, where $i,j\in\{1,2\}$ represent the two possible measurement directions available to each player. We notice that we still have some symmetry in our result because we have made the substitution $\phi = \alpha_2+\beta_2$, so that we have six degrees of freedom out of a possible seven. This final symmetry would probably be lost if we allow variations of measurement directions out of the plane perpendicular to the line of sight.

If we try $\gamma = 0$ for no entanglement, we have the probability

$$\begin{aligned}
P_{mn} &= \frac{1}{4}(1+(-)^mA + (-)^nB \\
&\quad +(-)^{m+n}AB) \\
&= \frac{(1+(-)^mA)^1}{2}\frac{(1+(-)^nB)^2}{2},
\end{aligned} \tag{A.54}$$

which shows a product state incorporating general measurement directions for each qubit.

Writing out the probabilities for the four measurement outcomes with general measurement directions, we find

$$\begin{aligned}
P_{00}(\kappa^1,\kappa^2) &= \frac{1}{4}[1+\cos\gamma(A(\kappa^1)+B(\kappa^2)) + (A(\kappa^1)B(\kappa^2)+\sin\gamma Z(\kappa^1,\kappa^2))] \\
P_{01}(\kappa^1,\kappa^2) &= \frac{1}{4}[1+\cos\gamma(A(\kappa^1)-B(\kappa^2)) - (A(\kappa^1)B(\kappa^2)+\sin\gamma Z(\kappa^1,\kappa^2))] \\
P_{10}(\kappa^1,\kappa^2) &= \frac{1}{4}[1+\cos\gamma(-A(\kappa^1)+B(\kappa^2)) - (A(\kappa^1)B(\kappa^2)+\sin\gamma Z(\kappa^1,\kappa^2))] \\
P_{11}(\kappa^1,\kappa^2) &= \frac{1}{4}[1+\cos\gamma(-A(\kappa^1)-B(\kappa^2)) + (A(\kappa^1)B(\kappa^2)+\sin\gamma Z(\kappa^1,\kappa^2))].
\end{aligned} \tag{A.55}$$

We allow each player the classical probabilistic choice between the two allocated measurement directions for their Stern-Gerlach detectors. The two players choose their first measurement

direction with probability x and y respectively, where $x, y \in [0, 1]$. We will assume the general case where players can choose different measurement directions to each other.

Now, we have the mathematical expectation of Alices' payoff where she chooses the direction κ_1^1 with probability x and the measurement direction κ_2^1 with probability $1 - x$ as

$$\begin{aligned}\Pi_A(x,y) &= xy(P_{00}(\kappa_1^1,\kappa_1^2)G_{00} + P_{01}(\kappa_1^1,\kappa_1^2)G_{01} + P_{10}(\kappa_1^1,\kappa_1^2)G_{10} + P_{11}(\kappa_1^1,\kappa_1^2)G_{11}) \\ &+ x(1-y)(P_{00}(\kappa_1^1,\kappa_2^2)G_{00} + P_{01}(\kappa_1^1,\kappa_2^2)G_{01} + P_{10}(\kappa_1^1,\kappa_2^2)G_{10} + P_{11}(\kappa_1^1,\kappa_2^2)G_{11}) \\ &+ y(1-x)(P_{00}(\kappa_2^1,\kappa_1^2)G_{00} + P_{01}(\kappa_2^1,\kappa_1^2)G_{01} + P_{10}(\kappa_2^1,\kappa_1^2)G_{10} + P_{11}(\kappa_2^1,\kappa_1^2)G_{11}) \\ &+ (1-x)(1-y)(P_{00}(\kappa_2^1,\kappa_2^2)G_{00} + P_{01}(\kappa_2^1,\kappa_2^2)G_{01} + P_{10}(\kappa_2^1,\kappa_2^2)G_{10} + P_{11}(\kappa_2^1,\kappa_2^2)G_{11}),\end{aligned} \tag{A.56}$$

where, for the Prisoner dilemma, we have

$$G_{ij}^A = \begin{bmatrix}3 & 0\\ 5 & 1\end{bmatrix} = \begin{bmatrix}G_{00} & G_{01}\\ G_{10} & G_{11}\end{bmatrix} = \begin{bmatrix}K & L\\ M & N\end{bmatrix}. \tag{A.57}$$

For symmetric games, such as the Prisoner dilemma game, we have $G_{ij}^B = G_{ji}^A$. Generally speaking, any payoff matrix satisfying $G_{10} > G_{00} > G_{11} > G_{01}$ is in the form of a Prisoner dilemma.

In the classical Prisoner dilemma game, we have two prisoners Alice and Bob being held in separate cells ready to be interviewed. To encourage confessions, the interrogator sets out a reward scheme, where if the players qubit is measured as the $|0\rangle$ state, then this corresponds to exonerating the other prisoner(co-operating with the other prisoner) and $|1\rangle$ corresponds to accusing the other prisoner(defection), which allows four possible payoff results, as shown in the payoff matrix. So, if Alice co-operates but Bob defects against her, for example, Alice receives a reward of 0, and Bob receives a payoff of 5 units. This game forms a dilemma for both players because there is a conflict between the maximum payout received by two rational responses based on satisfying self interest(called the Nash equilibrium), and the Pareto optimum, which is the best overall payoff available to both players. The Nash equilibrium will be both players defecting and receiving 1 unit in this case, because we can see that if either player decides to change their choice from this position they will receive a smaller payoff of 0. If both players though could trust each other and co-operate they would both receive a greater payout of 3 units, however there is a great temptation for either player to break the agreement and defect and improve his payoff to 5. We find that this impasse appears to be partially solved through the use of entanglement in the quantum form of the game.

We also define $\Delta_1 = G_{10} - G_{00}$, $\Delta_2 = G_{11} - G_{01}$ and $\Delta_3 = \Delta_2 - \Delta_1$. We have $\Delta_1, \Delta_2 > 0$ for the Prisoner dilemma game in general. We define

$$p = \frac{1}{4}[(A_1 - A_2)(B_1 - B_2) + \sin\gamma(Z_{11} + Z_{22} - Z_{12} - Z_{21})] \tag{A.58}$$

so that we find the payoff for Alice

$$\begin{aligned}\Pi_A(x,y) &= \frac{1}{4}[G_{00} + G_{10} + G_{01} + G_{11} \\ &+ \Delta_3\{4pxy + x((A_1 - A_2)B_2 + (Z_{12} - Z_{22})\sin\gamma) + y((B_1 - B_2)A_2 + (Z_{21} - Z_{22})\sin\gamma) \\ &+ A_2B_2 + Z_{22}\sin\gamma\} - \cos\gamma(\Delta_1 + \Delta_2)((A_1 - A_2)x + A_2) \\ &+ \cos\gamma(G_{00} - G_{01} + G_{10} - G_{11})((B_1 - B_2)y + B_2)].\end{aligned} \tag{A.59}$$

A.6.1 Solving the two-player game

To find the Nash equilibrium, we require

$$\begin{aligned}\Pi_A(x^*, y^*) &\geq \Pi_A(x, y^*) \\ \Pi_B(x^*, y^*) &\geq \Pi_B(x^*, y)\end{aligned} \tag{A.60}$$

which is stating that any movement of a player away from the Nash equilibrium (x^*, y^*), will result in a lower payoff for that player. We find

$$\begin{aligned} & \Pi_A(x^*, y^*) - \Pi_A(x, y^*) \qquad (A.61) \\ = \; & \frac{1}{4}(x^* - x)[\Delta_3\{4py^* + (A_1 - A_2)B_2 + (Z_{12} - Z_{22})\sin\gamma\} - \cos\gamma(\Delta_1 + \Delta_2)(A_1 - A_2)] \\ = \; & \frac{1}{4}(x^* - x)(A_1 - A_2)[\Delta_3\{y^*(B_1 + \frac{\sin\gamma(Z_{11} - Z_{21})}{A_1 - A_2}) + (1 - y^*)(B_2 + \frac{\sin\gamma(Z_{12} - Z_{22})}{A_1 - A_2})\} \\ & - \cos\gamma(\Delta_1 + \Delta_2)] \end{aligned}$$

and for the second player Bob we have similarly

$$\begin{aligned} & \Pi_B(x^*, y^*) - \Pi_B(x^*, y) \qquad (A.62) \\ = \; & \frac{1}{4}(y^* - y)[\Delta_3\{4px^* + (B_1 - B_2)A_2 + (Z_{21} - Z_{22})\sin\gamma\} - \cos\gamma(\Delta_1 + \Delta_2)(B_1 - B_2)]. \end{aligned}$$

A.6.2 Embedding the classical game

We would like the classical game embedded in the quantum game at zero entanglement($\gamma = 0$), and so the requirement for a N.E. becomes

$$\begin{aligned} & \Pi_A(x^*, y^*) - \Pi_A(x, y^*) \qquad (A.63) \\ = \; & \frac{1}{4}(x^* - x)(A_1 - A_2)[\Delta_3\{y^*B_1 + (1 - y^*)B_2\} - (\Delta_1 + \Delta_2)] \geq 0. \end{aligned}$$

Because $|\Delta_3| \leq |\Delta_1 + \Delta_2|$, the term in square brackets is always negative and if $A_1 - A_2 > 0$, then we have the classical NE ($x^* = 0$). By symmetry, Bob also has the NE $y^* = 0$, provided $B_1 - B_2 > 0$. At this NE of $(x^*, y^*) = (0, 0)$ and at zero entanglement we find the payoff from Eq. (A.59) to be

$$\begin{aligned} \Pi_A(x, y) \; = \; & \frac{1}{4}[G_{00}(1 + A_2)(1 + B_2) + G_{10}(1 - A_2)(1 + B_2) \qquad (A.64) \\ & + G_{01}(1 + A_2)(1 - B_2) + G_{11}(1 - A_2)(1 - B_2)]. \end{aligned}$$

In order to achieve the classical payoff of G_{11}, we can see that we require $A_2 = -1$ and $B_2 = -1$, that is

$$\begin{aligned} A(\kappa_2^1) &= \cos\alpha_1\cos\kappa_2^1 - \sin\alpha_1\cos\alpha_3\sin\kappa_2^1 = -1 \qquad (A.65) \\ B(\kappa_2^2) &= \cos\beta_1\cos\kappa_2^2 - \sin\beta_1\cos\beta_3\sin\kappa_2^2 = -1. \end{aligned}$$

These equations have two classes of solution: if $\alpha_3, \beta_3 \neq 0$, then we have for the first equation $\alpha_1 = 0$, $\kappa_2^1 = \pi$ or $\alpha_1 = \pi$, $\kappa_2^1 = 0$ and similarly for the second equation. For the second class with $\alpha_3, \beta_3 = 0$, we have the solution $\alpha_1 + \kappa_2^1 = \pi$ and $\beta_1 + \kappa_2^2 = \pi$.

For the first class, we find $Z_{22} = Z_{21} = Z_{12} = 0$ and $Z_{11} = \sin\kappa_1^1\sin\kappa_1^2\sin(\alpha_3+\beta_3+\alpha_2+\beta_2)$ and for the second class, we find $Z_{22} = Z_{21} = Z_{12} = 0$ and $Z_{11} = \sin(\alpha_1 + \kappa_1^1)\sin(\beta_1 + \kappa_1^2)\sin(\alpha_2 + \beta_2)$.

These two classes gives the NE, governed in both cases

$$\begin{aligned} & \Pi_A(x^*, y^*) - \Pi_A(x, y^*) \qquad (A.66) \\ = \; & \frac{1}{4}(x^* - x)(\cos\kappa_1^1 + 1)[\Delta_3\{y^*(\cos\kappa_1^2 + \frac{\sin\gamma Z_{11}}{\cos\kappa_1^1 + 1}) - (1 - y^*)\} - \cos\gamma(\Delta_1 + \Delta_2)] \geq 0 \end{aligned}$$

with a corresponding payoff of

$$\begin{aligned} \Pi_A(x, y) \; = \; & \frac{1}{4}[2(G_{00} + G_{11}) - 2\cos\gamma(G_{00} - G_{11}) \qquad (A.67) \\ + \; & xy\Delta_3\{(A_1 + 1)(B_1 + 1) + \sin\gamma Z_{11}\} - x(A_1 + 1)\{\Delta_3 + \cos\gamma(\Delta_1 + \Delta_2)\} \\ & - y(B_1 + 1)\{\Delta_3 - \cos\gamma(G_{00} - G_{01} + G_{10} - G_{11})\}]. \end{aligned}$$

Thus Eq. (A.66) governs the possible NE and Eq. (A.67) the associated payoffs for a quantum Prisoner dilemma game which will embed the classical game at zero entanglement.

A.7 Two-player games: entangled measurement model

In this approach we have a local realist model consisting of two unentangled qubits upon which Alice and Bob act with their local unitary transformations. We then measure using a Bell type measurement operator, placing all non-local correlations in the final measurement operator. The advantage is, that we can easily visualize the state of the two separate qubits as two separate Bloch sphere vectors.

We use the same basis as Alternative Method 1 two-particle spinor space as

$$\begin{aligned} |0\rangle|0\rangle &\longleftrightarrow 1 \\ |0\rangle|1\rangle &\longleftrightarrow -\iota\sigma_2^2 \\ |1\rangle|0\rangle &\longleftrightarrow -\iota\sigma_2^1 \\ |1\rangle|1\rangle &\longleftrightarrow \iota\sigma_2^1\iota\sigma_2^2. \end{aligned} \tag{A.68}$$

We assume a separable state is prepared for Alice and Bob upon which they act producing,

$$\psi = AB \tag{A.69}$$

where

$$\begin{aligned} A &= R(\alpha_1, \alpha_2, \alpha_3) \\ B &= R(\beta_1, \beta_2, \beta_3). \end{aligned} \tag{A.70}$$

We have the two observables $\psi J\psi^\dagger$ and $\psi E\psi^\dagger$, where

$$\begin{aligned} J &= \iota\sigma_3^1 + \iota\sigma_3^2 \\ E &= 1 - \iota\sigma_3^1\iota\sigma_3^2. \end{aligned} \tag{A.71}$$

Given a measurement operator

$$\phi = \mathrm{e}^{\iota\kappa\sigma_2^1/2}\mathrm{e}^{\iota\kappa\sigma_2^2/2}(\cos\gamma + \sin\gamma\iota\sigma_2^1\iota\sigma_2^2) \tag{A.72}$$

to represent the measurement, where $\gamma \in [-\frac{\pi}{2}, \frac{\pi}{2}]$, and $\kappa = 0, \pi$ for the measurement direction. We are using the notation $\kappa\sigma_2^2 = \kappa^2\sigma_2^2$, so we can have separate κ for each particle space. So forming the observables we have

$$\begin{aligned} \psi J\psi^\dagger &= AB(\iota\sigma_3^1 + \iota\sigma_3^2)A^\dagger B^\dagger \\ &= \frac{1}{2}(\iota A\sigma_3^1 A^\dagger + \iota B\sigma_3^2 B^\dagger) \end{aligned} \tag{A.73}$$

and for the joint observable

$$\begin{aligned} \psi E\psi^\dagger &= AB(1 - \iota\sigma_3^1\iota\sigma_3^2)A^\dagger B^\dagger \\ &= \frac{1}{2}\left(1 - \iota A\sigma_3^1 A^\dagger \iota B\sigma_3^2 B^\dagger\right) \end{aligned} \tag{A.74}$$

and for the measurement settings

$$\begin{aligned} \phi J\phi^\dagger &= \mathrm{e}^{\iota\kappa\sigma_2^1/2}\mathrm{e}^{\iota\kappa\sigma_2^2/2}(\cos\frac{\gamma}{2} + \sin\frac{\gamma}{2}\iota\sigma_2^1\iota\sigma_2^2)(\iota\sigma_3^1 + \iota\sigma_3^2) \\ &\times (\cos\frac{\gamma}{2} + \sin\frac{\gamma}{2}\iota\sigma_2^1\iota\sigma_2^2)\mathrm{e}^{-\iota\kappa\sigma_2^2/2}\mathrm{e}^{-\iota\kappa\sigma_2^2/2} \\ &= \frac{1}{2}\mathrm{e}^{\iota\kappa\sigma_2^1/2}\mathrm{e}^{\iota\kappa\sigma_2^2/2}(\cos^2\frac{\gamma}{2} - \sin^2\frac{\gamma}{2}) \\ &\times (\iota\sigma_3^1 + \iota\sigma_3^2)\mathrm{e}^{\iota\kappa\sigma_2^2/2}\mathrm{e}^{-\iota\kappa\sigma_2^1/2} \\ &= \frac{1}{2}\cos\gamma(\mathrm{e}^{\iota\kappa\sigma_2^1}\iota\sigma_3^1 + \mathrm{e}^{\iota\kappa\sigma_2^2}\iota\sigma_3^2) \end{aligned} \tag{A.75}$$

$$\begin{aligned}\phi E\phi^\dagger &= \mathrm{e}^{\iota\kappa\sigma_2^1/2}\mathrm{e}^{\iota\kappa\sigma_2^2/2}(\cos\frac{\gamma}{2}+\sin\frac{\gamma}{2}\iota\sigma_2^1\iota\sigma_2^2)(1-\iota\sigma_3^1\iota\sigma_3^2) \\ &\times (\cos\frac{\gamma}{2}+\sin\frac{\gamma}{2}\iota\sigma_2^1\iota\sigma_2^2)\mathrm{e}^{-\kappa\sigma_2^2/2}\mathrm{e}^{-\kappa\sigma_2^1/2} \\ &= \frac{1}{2}(1-\iota\mathrm{e}^{\iota\kappa\sigma_2^1}\mathrm{e}^{\iota\kappa\sigma_2^2}\sigma_3^1\iota\sigma_3^2+\sin\gamma(\iota\sigma_2^1\iota\sigma_2^2-\iota\mathrm{e}^{\iota\kappa\sigma_2^1}\mathrm{e}^{\iota\kappa\sigma_2^2}\sigma_1^1\iota\sigma_1^2)),\end{aligned} \tag{A.76}$$

from which we can calculate the probabilities to measure different states. For the special cases $\kappa = 0, \pi$, which defines the standard measurement basis, we have

$$\phi J\phi^\dagger = \frac{1}{2}\cos\gamma((-)^x\iota\sigma_3^1+(-)^y\iota\sigma_3^2),$$

where each $x, y \in \{0,1\}$ refers to measuring a $|0\rangle$ or a $|1\rangle$ state, respectively and

$$\phi E\phi^\dagger = -\frac{1}{2}\left(1+(-)^{x+y}\iota\sigma_3^1\iota\sigma_3^2+\sin\gamma(\iota\sigma_2^1\iota\sigma_2^2+(-)^{x+y}\iota\sigma_1^1\iota\sigma_1^2)\right).$$

So, the separable part of the measurement is

$$\begin{aligned}&= -\langle\psi J\psi^\dagger\phi J\phi^\dagger\rangle \\ &= -\frac{1}{2}(\iota A\sigma_3^1A^\dagger+\iota B\sigma_3^2B^\dagger)\frac{1}{2}\cos\gamma((-)^x\iota\sigma_3^1+(-)^y\iota\sigma_3^2) \\ &= \frac{1}{4}\cos\gamma((-)^x\cos\alpha_1+(-)^y\cos\beta_1).\end{aligned} \tag{A.77}$$

For the joint measurement

$$\begin{aligned}&= \langle\psi E\psi^\dagger\phi E\phi^\dagger\rangle \\ &= -\frac{1}{4}(1-\iota A\sigma_3^1A^\dagger\iota B\sigma_3^2B^\dagger) \\ &\times \left(1+(-)^{x+y}\iota\sigma_3^1\iota\sigma_3^2+\sin\gamma(\iota\sigma_2^1\iota\sigma_2^2+(-)^{x+y}\iota\sigma_1^1\iota\sigma_1^2)\right) \\ &= \frac{1}{4}(1+(-)^{x+y}\cos\alpha_1\cos\beta_1-\sin\gamma\sin\alpha_1\sin\alpha_2\sin\beta_1\sin\beta_2 \\ &+ (-)^{x+y}\sin\gamma\sin\alpha_1\cos\alpha_2\sin\beta_1\cos\beta_2) \\ &= \frac{1}{4}(1+(-)^{x+y}\cos\alpha_1\cos\beta_1+(-)^{x+y}\sin\gamma\sin\alpha_1\sin\beta_1\cos(\alpha_2-(-)^{x+y}\beta_2).\end{aligned} \tag{A.78}$$

So, the final density operator is

$$\begin{aligned}\rho &= \frac{1}{4}(1+\cos\gamma((-)^x\cos\alpha_1+(-)^y\cos\beta_1) \\ &+ (-)^{x+y}\cos\alpha_1\cos\beta_1+(-)^{x+y}\sin\gamma\sin\alpha_1\sin\beta_1\cos(\alpha_2-(-)^{x+y}\beta_2)).\end{aligned} \tag{A.79}$$

So, we can generate the four probabilities

$$\begin{aligned}P_{00} &= \frac{1}{4}(1+\cos\alpha_1\cos\beta_1+\cos\gamma(\cos\alpha_1+\cos\beta_1) \\ &+ \sin\gamma\sin\alpha_1\sin\beta_1\cos(\alpha_2-\beta_2)) \\ P_{01} &= \frac{1}{4}(1-\cos\alpha_1\cos\beta_1+\cos\gamma(\cos\alpha_1-\cos\beta_1) \\ &- \sin\gamma\sin\alpha_1\sin\beta_1\cos(\alpha_2+\beta_2)) \\ P_{10} &= \frac{1}{4}(1-\cos\alpha_1\cos\beta_1+\cos\gamma(-\cos\alpha_1+\cos\beta_1) \\ &- \sin\gamma\sin\alpha_1\sin\beta_1\cos(\alpha_2+\beta_2)) \\ P_{11} &= \frac{1}{4}(1+\cos\alpha_1\cos\beta_1-\cos\gamma(\cos\alpha_1+\cos\beta_1) \\ &+ \sin\gamma\sin\alpha_1\sin\beta_1\cos(\alpha_2-\beta_2)).\end{aligned} \tag{A.80}$$

We have the payoff functions for Alice and Bob,

$$\begin{aligned}
\Pi_A &= 3P_{00} + 5P_{10} + P_{11} \\
&= \frac{1}{4}(9 - 3\cos\gamma\cos\alpha_1 + 7\cos\gamma\cos\beta_1 \\
&- \cos\alpha_1\cos\beta_1 + \sin\gamma\sin\alpha_1\sin\beta_1\cos\alpha_2\cos\beta_2 \\
&+ 9\sin\gamma\sin\alpha_1\sin\beta_1\sin\alpha_2\sin\beta_2) \\
\Pi_B &= 3P_{00} + 5P_{01} + P_{11} \\
&= \frac{1}{4}(9 + 7\cos\gamma\cos\alpha_1 - 3\cos\gamma\cos\beta_1 \\
&- \cos\alpha_1\cos\beta_1 + \sin\gamma\sin\alpha_1\sin\beta_1\cos\alpha_2\cos\beta_2 \\
&+ 9\sin\gamma\sin\alpha_1\sin\beta_1\sin\alpha_2\sin\beta_2),
\end{aligned} \tag{A.81}$$

which confirm the relations from the previous method with $\kappa^1 = \kappa^2 = 0$.

A.8 Three-player quantum game examples

A.8.1 Prisoner dilemma, W-state

Given the following payoff matrix, which is in the form of a Prisoner dilemma

State	Payoff
$\|000\rangle$	(3,3,3)
$\|001\rangle$	(0,0,5)
$\|010\rangle$	(0,5,0)
$\|100\rangle$	(5,0,0)
$\|011\rangle$	(0,4,4)
$\|101\rangle$	(4,0,4)
$\|110\rangle$	(4,4,0)
$\|111\rangle$	(1,1,1)

we then have

$$\begin{aligned}
c1 &= \frac{1}{6}(3 - 0 + 0 - 5 + 4 - 1) = \frac{1}{6} \\
c2 &= \frac{1}{6}(-3 + 0 + 5 - 8) = 1 \\
c3 &= \frac{1}{6}(0 - 0 - 8 + 1) = \frac{7}{6}.
\end{aligned} \tag{A.82}$$

Thus, we have satisfied all conditions for one and three flips, giving us four NE. This gives us the payoffs

Choices	Player1,Player2,Player3
(d,c,c)	(11/3,7/3,7/3)
(c,d,c)	(7/3,11/3,7/3)
(c,c,d)	(7/3,7/3,11/3)
(d,d,d)	(8/3,8/3,8/3)

A.8.2 Prisoner dilemma with GHZ state at Pareto optimum

This example shows that a three player quantum Prisoner dilemma game carefully chosen can in fact reach the Pareto optimum. We have $l = d : dc - c : cd > 0$ for the Prisoner dilemma game and also we find $a > 0$ and $b < 0$ and therefore, we can refer to [JMCL11a]. Also, we have $b - a\cos\gamma < 0$ and so we do not have the no-flip case.

So to satisfy the condition for a NE we could pick

State	Payoff
$\|000\rangle$	(6,6,6)
$\|001\rangle$	(3,3,12)
$\|010\rangle$	(3,12,3)
$\|100\rangle$	(12,3,3)
$\|011\rangle$	(0,9,9)
$\|101\rangle$	(9,0,9)
$\|110\rangle$	(9,9,0)
$\|111\rangle$	(1,1,1)

We have $\mathrm{c:cc}=6, \mathrm{c:cd}=3, \mathrm{d:cc}=12, \mathrm{c:dd}=0, \mathrm{d:dc}=9, \mathrm{d:dd}=1$, giving us $m = d:cc - c:cc = 12-6 = 6$ and $n = d:dd - c:dd = 1-0 = 1$, giving us $a = n+m = 7$ and $b = n-m = -5$, and so $b/a < 0$, so we have the first case. Also, we have $l = \mathrm{d:dc} - \mathrm{c:cd} = 9-3 > 0$ and so no single flip NE exist. We have a transition at $\cos\gamma = 5/7$ from a quantum to a classical region and the maximum payoff at $\cos\gamma = 0$ for not flipping

$$\begin{aligned} \Pi^f &= \frac{1}{2}(0+12) = 6 \\ \Pi^n &= \frac{1}{2}(3+9) = 6, \end{aligned} \tag{A.83}$$

so that, at maximum entanglement, we reach the Pareto optimum as a Nash equilibrium. Classically, the NE is at 1.

A.9 W entangled state

We have the state before measurement from Eq.(8.4) as

$$\psi = -\frac{1}{\sqrt{N}}\left(\prod U^i\right)\sum_i^N \iota e_2^i. \tag{A.84}$$

So forming the observables from Eq.(1.25) we have

$$\begin{aligned} & \psi J \psi^\dagger \qquad\qquad (A.85) \\ = & -\frac{1}{N2^{N-1}}\left(\prod U^i\right)\sum_i^N \iota e_2^i \left(\sum_{r=1}^{\frac{N+1}{2}}(-)^{r+1}C_{2r-1}^N(\iota e_3^i)\right)\sum_i^N \iota e_2^i\left(\prod U^{i^\dagger}\right) \\ = & \frac{1}{N2^{N-1}}\left(\prod U^i\right)\Big(\sum_{r=1}^{(N+1)/2}(N-4r+2)C_{2r-1}^N(\iota e_3^i) - 2\sum_{r=1}^{(N-1)/2} C_{2r+1}^N(\iota e_2^i \iota e_2^j \iota e_3^k) \\ - & 2\sum_{r=1}^{(N-1)/2} C_{2r+1}^N(\iota e_1^i \iota e_1^j \iota e_3^k)\Big)\left(\prod U^{i^\dagger}\right) \\ = & \frac{1}{N2^{N-1}}\Big(\sum_{r=1}^{(N+1)/2}(-)^{r+1}(N-4r+2)C_{2r-1}^N(V_3^i) + 2\sum_{r=1}^{(N-1)/2}(-)^r C_{2r+1}^N(V_2^i V_2^j V_3^k) \\ + & 2\sum_{r=1}^{(N-1)/2}(-)^r C_{2r+1}^N(V_1^i V_1^j V_3^k)\Big), \end{aligned}$$

where $V_k^i = \iota U^i e_k U^{i^\dagger}$. Also from Eq.(1.25) we have

$$\begin{aligned}
& \psi E \psi^\dagger \qquad (A.86)\\
= & -\frac{1}{N2^{N-1}}\left(\prod U^i\right)\sum_i^N \iota e_2^i \left(1+\sum_{r=1}^{N/2}(-)^r C_{2r}^N(\iota e_3^i)\right)\sum_i^N \iota e_2^i \left(\prod U^{i^\dagger}\right)\\
= & \frac{1}{N2^{N-1}}\prod U^i\Big(N-2\sum_{r=1}^{N/2} C_{2r}^N(\iota e_2^i \iota e_2^j \iota e_3^k)+\sum_{r=1}^{N/2}(4r-N)C_{2r}^N(\iota e_3^i)\\
- & 2\sum_{r=1}^{N/2} C_{2r}^N(\iota e_1^i \iota e_1^j \iota e_3^k)\Big)\prod U^{i\dagger}\\
= & \frac{1}{N2^{N-1}}\Big(N+2\sum_{r=1}^{N/2}(-)^r C_{2r}^N(V_2^i V_2^j V_3^k)+\sum_{n=1}^{N/2}(-)^r(N-4r)C_{2r}^N(V_3^i)\\
+ & 2\sum_{r=1}^{N/2}(-)^r C_{2r}^N(V_1^i V_1^j V_3^k)\Big).
\end{aligned}$$

So, referring to Eq.(1.25), we find

$$\begin{aligned}
& -2^{N-2}\langle \psi J \psi^\dagger \phi J \phi^\dagger\rangle_0 \qquad (A.87)\\
= & -\frac{1}{N2^N}\Big\langle\Big(\sum_{r=1}^{(N+1)/2}(-)^{r+1}(N-4r+2)C_{2r-1}^N(V_3^i)+2\sum_{r=1}^{(N-1)/2}(-)^r C_{2r+1}^N(V_2^iV_2^jV_3^k)\\
+ & 2\sum_{r=1}^{(N-1)/2}(-)^r C_{2r+1}^N(V_1^iV_1^jV_3^k)\Big)\Big(\sum_{r=1}^{\frac{N+1}{2}}(-)^{r+1}C_{2r-1}^N(\iota e_3^i e^{\iota\kappa e_2^i})\Big)\Big\rangle_0\\
= & \frac{1}{N2^N}\left(\sum_{r=1}^{\frac{N+1}{2}}(N-4r+2)C_{2r-1}^N(K^i)+2\sum_{r=1}^{\frac{N-1}{2}}C_{2r+1}^N(X_2^iX_2^jK^k)+2\sum_{r=1}^{\frac{N-1}{2}}C_{2r+1}^N(X_1^iX_1^jK^k)\right)\\
= & \frac{1}{N2^N}\left(\sum_{r=1}^{\frac{N+1}{2}}(N-4r+2)C_{2r-1}^N(K^i)+2\sum_{r=1}^{\frac{N-1}{2}}C_{2r+1}^N\left((X_2^iX_2^j+X_1^iX_1^j)X_3^k\right)\right).
\end{aligned}$$

Also from Eq.(1.25), we find

$$\begin{aligned}
& 2^{N-2}\langle \psi E \psi^\dagger \phi E \phi^\dagger\rangle_0 \qquad (A.88)\\
= & \frac{1}{N2^N}\Big\langle\Big(N+2\sum_{r=1}^{N/2}(-)^r C_{2r}^N(V_2^iV_2^jV_3^k)+\sum_{r=1}^{N/2}(-)^r(N-4r)C_{2r}^N(V_3^i)\\
+ & 2\sum_{r=1}^{N/2}(-)^r C_{2r}^N(V_1^iV_1^jV_3^k)\Big)\Big(1+\sum_{r=1}^{N/2}(-)^r C_{2r}^N(\iota e_3^i e^{\iota\kappa e_2^i})\Big)\Big\rangle_0\\
= & \frac{1}{N2^N}(N+2\sum_{r=1}^{N/2}C_{2r}^N(\epsilon^i\epsilon^jX_2^iX_2^jX_3^k)+\sum_{r=1}^{N/2}(N-4r)C_{2r}^N(K^i)\\
& +2\sum_{r=1}^{N/2}C_{2r}^N(\epsilon^i\epsilon^j\epsilon^kX_1^iX_1^jX_3^k))\\
= & \frac{1}{N2^N}\left(N+\sum_{r=1}^{N/2}(N-4r)C_{2r}^N(K^i)+2\sum_{r=1}^{N/2}C_{2r}^N\big((X_2^iX_2^j+X_1^iX_1^j)K^k\big)\right).
\end{aligned}$$

So the probabilities that a measurement will return a given state will be

$$\begin{aligned} P_{k^1\ldots k^N} &= \frac{1}{N2^N}\Big(\sum_{r=1}^{(N+1)/2}(N-4r+2)C_{2r-1}^N(K^i)+2\sum_{r=1}^{(N-1)/2}C_{2r+1}^N\big((X_2^iX_2^j+X_1^iX_1^j)K^k\big)\\ &+ N+\sum_{r=1}^{N/2}(N-4r)C_{2r}^N\big(K^i\big)+2\sum_{r=1}^{N/2}C_{2r}^N\big((X_2^iX_2^j+X_1^iX_1^j)K^k\big)\Big) \end{aligned}$$

and combining the summation terms we find the probability distribution, for the W-type state subject to general measurement directions

$$P_{k^1\ldots k^N} = \frac{1}{N2^N}\left(N+\sum_{r=1}^{N}(N-2r)C_r^N\big(\epsilon^iK^i\big)+2\sum_{r=2}^{N}C_r^N\big(\epsilon^i\epsilon^j\epsilon^k(X_2^iX_2^j+X_1^iX_1^j)K^k\big)\right).$$

Bibliography

[ADR82] A. Aspect, J. Dalibard, and G. Roger. Experimental test of Bell's inequalities using time-varying analyzers. *Physical Review Letters*, 49(25):1804–1807, 1982.

[AR10] H. Anton and C. Rorres. *Elementary linear algebra: applications version*. Wiley, 2010.

[AS64] M. Abramowitz and I.A. Stegun. *Handbook of mathematical functions with formulas, graphs, and mathematical tables*. Dover publications, New York, 1964.

[AV08] N. Aharon and L. Vaidman. Quantum advantages in classically defined tasks. *Physical Review A*, 77(5):052310, 2008.

[B+64] J.S. Bell et al. On the Einstein-Podolsky-Rosen paradox. *Physics*, 1(3):195–200, 1964.

[BBB+99a] E. Biham, O. Biham, D. Biron, M. Grassl, and D.A. Lidar. Grovers quantum search algorithm for an arbitrary initial amplitude distribution. *Physical Review A*, 60(4):2742, 1999.

[BBB+99b] D. Biron, O. Biham, E. Biham, M. Grassl, and D. Lidar. Generalized Grover search algorithm for arbitrary initial amplitude distribution. *Quantum Computing and Quantum Communications*, pages 140–147, 1999.

[BBB+00] E. Biham, O. Biham, D. Biron, M. Grassl, D.A. Lidar, and D. Shapira. Analysis of generalized Grover quantum search algorithms using recursion equations. *Physical Review A*, 63(1):012310, 2000.

[BBBV97] E. Bernstein, C. Bennett, G. Brassard, and U. Vazirani. Strengths and weaknesses of quantum computing. *SIAM J. Computing*, 26:1510–1523, 1997.

[BBHT98] M. Boyer, G. Brassard, P. Høyer, and A. Tappa. Tight bounds on quantum searching. *Fortschritte der Physik*, 46:493–506, 1998.

[Bel66] J.S. Bell. On the problem of hidden variables in quantum mechanics. *Reviews of Modern Physics*, 38(3):447–452, 1966.

[Bel87] JS Bell. *Speakable and Unspeakable in Quantum Mechanics*. Cambridge Univ. Press, 1987.

[BH01] S.C. Benjamin and P.M. Hayden. Multiplayer quantum games. *Physical Review A*, 64(3):030301, 2001.

[Bin07] K.G. Binmore. *Game theory: a very short introduction*, volume 173. Oxford University Press, USA, 2007.

[BJ] P. Blanchard and A. Jadczyk. *Quantum future*. Springer-Verlag.

[BK02a] J. Bae and Y. Kwon. Generalized quantum search hamiltonian. *Physical Review A*, 66(1):012314, 2002.

[BK02b] E. Biham and D. Kenigsberg. Grovers quantum search algorithm for an arbitrary initial mixed state. *Physical Review A*, 66(6):062301, 2002.

[Bla80] A. Blaquiere. Wave mechanics as a two-player game. *Dynamical Systems and Microphysics*, 33, 1980.

[Boh51] D. Bohm. *Quantum theory*. Dover Publications, 1951.

[CEMM98] R. Cleve, A. Ekert, C. Macchiavello, and M. Mosca. Quantum algorithms revisited. *Proceedings of the Royal Society of London. Series A: Mathematical, Physical and Engineering Sciences*, 454(1969):339, 1998.

[Cer00] J.L. Cereceda. Quantum mechanical probabilities and general probabilistic constraints for Einstein–Podolsky–Rosen–Bohm experiments. *Foundations of Physics Letters*, 13(5):427–442, 2000.

[CH01] A. Carlini and A. Hosoya. Quantum computers and unstructured search: finding and counting items with an arbitrarily entangled initial state. *Physics Letters A*, 280(3):114–120, 2001.

[Chr07] J. Christian. Disproof of Bell's theorem by Clifford algebra valued local variables. *Arxiv preprint quant-ph/0703179*, 2007.

[CIA10] J.M. Chappell, A. Iqbal, and D. Abbott. Constructing quantum games from symmetric non-factorizable joint probabilities. *Physics Letters A*, 374, 2010.

[CILVS09] J.M. Chappell, A. Iqbal, M.A. Lohe, and L. Von Smekal. An analysis of the quantum penny flip game using geometric algebra. *Journal of the Physical Society of Japan*, 78(5):4801, 2009.

[Cli78] W.K. Clifford. Applications of grassmann's extensive algebra. *American Journal of Mathematics*, 1(4):350–358, 1878.

[CS78] J.F. Clauser and A. Shimony. Bell's theorem. experimental tests and implications. *Reports on Progress in Physics*, 41:1881, 1978.

[CT06] T. Cheon and I. Tsutsui. Classical and quantum contents of solvable game theory on hilbert space. *Physics Letters A*, 348(3-6):147–152, 2006.

[CvD10] A.M. Childs and W. van Dam. Quantum algorithms for algebraic problems. *Reviews of Modern Physics*, 82(1):1, 2010.

[CZ95] J.I. Cirac and P. Zoller. Quantum computations with cold trapped ions. *Physical Review Letters*, 74(20):4091–4094, 1995.

[Daw76] R. Dawkins. *The selfish gene*. Oxford University Press, USA, 1976.

[DDL02] L. Dorst, C.J.L. Doran, and J. Lasenby. *Applications of geometric algebra in computer science and engineering*. Birkhauser, Boston, 2002.

[Deu85] D. Deutsch. Quantum theory, the Church-Turing principle and the universal quantum computer. *Proceedings of the Royal Society of London. A. Mathematical and Physical Sciences*, 400(1818):97, 1985.

[DKK03] S. Das, R. Kobes, and G. Kunstatter. Energy and efficiency of adiabatic quantum search algorithms. *Journal of Physics A: Mathematical and General*, 36:2839, 2003.

[DL03] C.J.L. Doran and A.N. Lasenby. *Geometric algebra for physicists*. Cambridge Univ Pr, 2003.

[DLX+02a] J. Du, H. Li, X. Xu, M. Shi, J. Wu, X. Zhou, and R. Han. Experimental realization of quantum games on a quantum computer. *Physical Review Letters*, 88(13):137902, 2002.

[DLX+02b] J. Du, H. Li, X. Xu, X. Zhou, and R. Han. Entanglement enhanced multiplayer quantum games. *Physics Letters A*, 302(5-6):229–233, 2002.

[DSD07] V. De Sabbata and B.K. Datta. *Geometric algebra and applications to physics*. Taylor & Francis Group, 2007.

[dSR08] P.B.M. de Sousa and R.V. Ramos. Multiplayer quantum games and its application as access controller in architecture of quantum computers. *Quantum Information Processing*, 7(2):125–135, 2008.

[EF02] V.L. Ermakov and BM Fung. Experimental realization of a continuous version of the Grover algorithm. *Physical Review A*, 66(4):042310, 2002.

[Eke91] A.K. Ekert. Quantum cryptography based on Bells theorem. *Physical Review Letters*, 67(6):661–663, 1991.

[EPR35] A. Einstein, B. Podolsky, and N. Rosen. Can quantum-mechanical description of physical reality be considered complete? *Physical review*, 47(10):777, 1935.

[EWL99] J. Eisert, M. Wilkens, and M. Lewenstein. Quantum games and quantum strategies. *Physical Review Letters*, 83(15):3077–3080, 1999.

[F.98] Werner R. F. Optimal cloning of pure states. *Phys. Rev. A*, 58:1827, 1998.

[FA03] A.P. Flitney and D. Abbott. Advantage of a quantum player over a classical one in 2 &# 50 2 quantum games. *Royal Society of London Proceedings Series A*, 459:2463–2474, 2003.

[FA05a] A.P. Flitney and D. Abbott. Quantum games with decoherence. *Journal of Physics A: Mathematical and General*, 38:449, 2005.

[FA05b] A.P. Flitney and D. Abbott. A semi-quantum version of the game of life. *Advances in Dynamic Games*, pages 667–679, 2005.

[FB00] B.R. Frieden and P.M. Binder. Physics from Fisher information: a unification. *American Journal of Physics*, 68:1064, 2000.

[Fen00] S.A. Fenner. An intuitive hamiltonian for quantum search. *Arxiv preprint quant-ph/0004091*, 2000.

[Fey82] R.P. Feynman. Simulating physics with computers. *International journal of theoretical physics*, 21(6):467–488, 1982.

[Fey86] R.P. Feynman. Quantum mechanical computers. *Foundations of physics*, 16(6):507–531, 1986.

[FG98a] E. Farhi and S. Gutmann. Analog analogue of a digital quantum computation. *Physical Review A*, 57(4):2403, 1998.

[FG98b] E. Farhi and S. Gutmann. Quantum computation and decision trees. *Physical Review A*, 58(2):915, 1998.

[FGGS00] E. Farhi, J. Goldstone, S. Gutmann, and M. Sipser. Quantum computation by adiabatic evolution. *Arxiv preprint quant-ph/0001106*, 2000.

[FH07] A.P. Flitney and L.C.L. Hollenberg. Nash equilibria in quantum games with generalized two-parameter strategies. *Physics Letters A*, 363(5-6):381–388, 2007.

[Fli05] A.P. Flitney. *Aspects of quantum game theory*. PhD thesis, The University of Adelaide, Australia, PhD thesis, University of Adelaide, URL: http://thesis.library.adelaide.edu.au/public/adt-SUA20050429.143949, 2005.

[FNA02] A.P. Flitney, J. Ng, and D. Abbott. Quantum parrondo's games. *Physica A: Statistical Mechanics and its Applications*, 314(1-4):35–42, 2002.

[Fri89] B.R. Frieden. Fisher information as the basis for the schrödinger wave equation. *American Journal of Physics*, 57:1004, 1989.

[FS95] B.R. Frieden and B.H. Soffer. Lagrangians of physics and the game of Fisher-information transfer. *Physical Review E*, 52(3):2274, 1995.

[GH97] N. Gisin and B. Huttner. Quantum cloning, eavesdropping and Bell's inequality. *Physics Letters A*, 228(1-2):13–21, 1997.

[GR05] L.K. Grover and J. Radhakrishnan. Is partial quantum search of a database any easier? In *Proceedings of the seventeenth annual ACM symposium on Parallelism in algorithms and architectures*, pages 186–194. ACM, 2005.

[Gro97] L.K. Grover. Quantum mechanics helps in searching for a needle in a haystack. *Physical review letters*, 79(2):325–328, 1997.

[Gro98a] L.K. Grover. A framework for fast quantum mechanical algorithms. In *Proceedings of the thirtieth annual ACM symposium on Theory of computing*, pages 53–62. ACM, 1998.

[Gro98b] L.K. Grover. Quantum computers can search rapidly by using almost any transformation. *Physical Review Letters*, 80(19):4329–4332, 1998.

[Gru99] J. Gruska. Quantum computing. advanced topics in computer science series, 1999.

[Gud88] S. Gudder. *Quantum probability*. Academic Press, 1988.

[GZK08] H. Guo, J. Zhang, and G.J. Koehler. A survey of quantum games. *Decision Support Systems*, 46(1):318–332, 2008.

[HD02a] T.F. Havel and C.J.L. Doran. Geometric algebra in quantum information processing. *Quantum computation and information: AMS Special Session Quantum Computation and Information, January 19-21, 2000, Washington*, 305:81, 2002.

[HD02b] T.F. Havel and C.J.L. Doran. Geometric algebra in quantum information processing. *Quantum computation and information: AMS Special Session Quantum Computation and Information, January 19-21, 2000, Washington*, 305:81, 2002.

[Hes99] D. Hestenes. *New foundations for classical mechanics: Fundamental Theories of Physics*. Kluwer Academic Pub, 1999.

[Hes03] D. Hestenes. Oersted medal lecture 2002: Reforming the mathematical language of physics. *American Journal of Physics*, 71:104, 2003.

[Hir01] M. Hirvensalo. Quantum computing. *Natural Computing Series*, page 190, 2001.

[HL02] J.Y. Hsieh and C.M. Li. General su (2) formulation for quantum searching with certainty. *Physical Review A*, 65(5):052322, 2002.

[HMN+97] E. Hagley, X. Maitre, G. Nogues, C. Wunderlich, M. Brune, JM Raimond, and S. Haroche. Generation of Einstein-Podolsky-Rosen pairs of atoms. *Physical Review Letters*, 79(1):1–5, 1997.

[Høy00] P. Høyer. Arbitrary phases in quantum amplitude amplification. *Physical Review A*, 62(5):052304, 2000.

[HS84] D. Hestenes and G. Sobczyk. *Clifford Algebra to Geometric Calculus: A unified language for mathematics and physics*, volume 5. Springer, 1984.

[IA09] A. Iqbal and D. Abbott. Non-factorizable joint probabilities and evolutionarily stable strategies in the quantum prisoner's dilemma game. *Physics Letters A*, 373(30):2537–2541, 2009.

[IB02] S. Imre and F. Balázs. A tight bound for probability of error for quantum counting based multiuser detection. *Arxiv preprint quant-ph/0205138*, 2002.

[IC07] A. Iqbal and T. Cheon. Constructing quantum games from nonfactorizable joint probabilities. *Physical Review E*, 76(6):061122, 2007.

[ICA08] A. Iqbal, T. Cheon, and D. Abbott. Probabilistic analysis of three-player symmetric quantum games played using the Einstein-Podolsky-Rosen-Bohm setting. *Physics Letters A*, 372(44):6564–6577, 2008.

[Iqb05] A. Iqbal. Playing games with EPR-type experiments. *Journal of Physics A: Mathematical and General*, 38:9551, 2005.

[IT01] A. Iqbal and AH Toor. Evolutionarily stable strategies in quantum games. *Physics Letters A*, 280(5-6):249–256, 2001.

[IT02] A. Iqbal and AH Toor. Backwards-induction outcome in a quantum game. *Physical Review A*, 65(5):052328, 2002.

[IT07] T. Ichikawa and I. Tsutsui. Duality, phase structures, and dilemmas in symmetric quantum games. *Annals of Physics*, 322(3):531–551, 2007.

[ITC08] T. Ichikawa, I. Tsutsui, and T. Cheon. Quantum game theory based on the Schmidt decomposition. *Journal of Physics A: Mathematical and Theoretical*, 41:135303, 2008.

[IW04] A. Iqbal and S. Weigert. Quantum correlation games. *Journal of Physics A: Mathematical and General*, 37:5873, 2004.

[JMCL11a] A. Iqbal J. M. Chappell and M. A. Lohe. Analyzing three-player quantum games in an EPR type setup. *Public Library of Science(PLoS) ONE*, 6(7), 2011.

[JMCL11b] L. von Smekal A. Iqbal J. M. Chappell, M. A. Lohe and M. A. Lohe. A precise error bound for quantum phase estimation. *PLoS ONE*, 6(5), 2011.

[Joh01] N.F Johnson. Playing a quantum game with a corrupted source. *Phys. Rev. A*, 63(020302):1–4, 2001.

[Joz99] R. Jozsa. Searching in Grover's algorithm. *Arxiv preprint quant-ph/9901021*, 1999.

[KG06] V.E. Korepin and L.K. Grover. Simple algorithm for partial quantum search. *Quantum Information Processing*, 5(1):5–10, 2006.

[KL06] V.E. Korepin and J. Liao. Quest for fast partial search algorithm. *Quantum Information Processing*, 5(3):209–226, 2006.

[KX07] VE Korepin and Y. Xu. Binary quantum search. In *PROCEEDINGS-SPIE THE INTERNATIONAL SOCIETY FOR OPTICAL ENGINEERING*, volume 6573, page 65730. International Society for Optical Engineering; 1999, 2007.

[LHJ09] Q. Li, Y. He, and J. Jiang. A novel clustering algorithm based on quantum games. *Journal of Physics A: Mathematical and Theoretical*, 42:445303, 2009.

[LJ02] C.F. Lee and N. Johnson. Let the quantum games begin. *Physics world*, 15(10):25–29, 2002.

[LL01] D. Li and X. Li. More general quantum search algorithm $q = -I_\gamma V I_\tau U$ and the precise formula for the amplitude and the non-symmetric effects of different rotating angles. *Physics Letters A*, 287(5-6):304–316, 2001.

[LLH05] D.F. Li, X.X. Li, and H.T. Huang. Phase condition for the Grover algorithm. *Theoretical and mathematical physics*, 144(3):1279–1287, 2005.

[LLHL02] D. Li, X. Li, H. Huang, and X. Li. Invariants of Grovers algorithm and the rotation in space. *Physical Review A*, 66(4):044304, 2002.

[LLZN99] G.L. Long, Y.S. Li, W.L. Zhang, and L. Niu. Phase matching in quantum searching. *Physics Letters A*, 262(1):27–34, 1999.

[LSP98] H.K. Lo, T. Spiller, and S. Popescu. *Introduction to quantum computation and information*. World Scientific Pub Co Inc, 1998.

[LTL+01] G.L. Long, C.C. Tu, Y.S. Li, W.L. Zhang, and H.Y. Yan. An so (3) picture for quantum searching. *Journal of Physics A: Mathematical and General*, 34:861, 2001.

[LXS01] G.L. Long, L. Xiao, and Y. Sun. General phase matching condition for quantum searching. *Arxiv preprint quant-ph/0107013*, 2001.

[Mac83] AR Mackintosh. The stern-gerlach experiment, electron spin and intermediate quantum mechanics. *European Journal of Physics*, 4:97, 1983.

[Men05] R.V. Mendes. The quantum ultimatum game. *Quantum Information Processing*, 4(1):1–12, 2005.

[Mer90a] N.D. Mermin. Extreme quantum entanglement in a superposition of macroscopically distinct states. *Physical Review Letters*, 65(15):1838–1840, 1990.

[Mer90b] N.D. Mermin. Quantum mysteries revisited. *American Journal of Physics*, 58(8):731–734, 1990.

[Mey99] D.A. Meyer. Quantum strategies. *Physical Review Letters*, 82(5):1052–1055, 1999.

[Mey02] D.A. Meyer. Quantum games and quantum algorithms. *Quantum computation and information: AMS Special Session Quantum Computation and Information, January 19-21, 2000, Washington*, 305:213, 2002.

[MHT05] D. Mc Hugh and J. Twamley. Quantum computer using a trapped-ion spin molecule and microwave radiation. *Physical Review A*, 71(1):012315, 2005.

[Mil51] J.W. Milnor. Games against nature. 1951.

[Mos99] M. Mosca. Quantum computer algorithms. 1999.

[MW00] L. Marinatto and T. Weber. A quantum approach to games of static information. *Phys. Lett. A*, 272:291–303, 2000.

[NC02] M.A. Nielsen and I.L. Chuang. *Quantum Computation and Quantum Information*. Addison-Wesley, Cambridge UK, first edition, 2002.

[NT04] A. Nawaz and AH Toor. Generalized quantization scheme for two-person non-zero sum games. *Journal of Physics A: Mathematical and General*, 37:11457, 2004.

[ÖSI07] SK Özdemir, J. Shimamura, and N. Imoto. A necessary and sufficient condition to play games in quantum mechanical settings. *New Journal of Physics*, 9:43, 2007.

[Pat98] A.K. Pati. Fast quantum search algorithm and bounds on it. *Arxiv preprint quant-ph/9807067*, 1998.

[PD01] R. Parker and C. Doran. Analysis of 1 and 2 particle quantum systems using geometric algebra. *Arxiv preprint quant-ph/0106055*, 2001.

[Per93] A. Peres. *Quantum theory: concepts and methods*, volume 57. Kluwer Academic Publishers, 1993.

[Pie02] A. Pietarinen. Quantum logic and quantum theory in a game-theoretic perspective. *Open Systems & Information Dynamics*, 9(3):273–290, 2002.

[Pir05] S. Pirandola. A quantum teleportation game. *International Journal of Quantum Information*, 3(1):239–243, 2005.

[PS02] E.W. Piotrowski and J. Sadkowski. Quantum market games. *Physica A: Statistical Mechanics and its Applications*, 312(1-2):208–216, 2002.

[PS03] E.W. Piotrowski and J. Sładkowski. An invitation to quantum game theory. *International Journal of Theoretical Physics*, 42(5):1089–1099, 2003.

[PS08] E.W. Piotrowski and J. Sladkowski. Quantum auctions: Facts and myths. *Physica A: Statistical Mechanics and its Applications*, 387(15):3949–3953, 2008.

[PZ93] J.P. Paz and W.H. Zurek. Environment-induced decoherence, classicality, and consistency of quantum histories. *Physical Review D*, 48(6):2728, 1993.

[Ras07] E. Rasmusen. *Games and information: An introduction to game theory*. Wiley-blackwell, 2007.

[RC02] J. Roland and N.J. Cerf. Quantum search by local adiabatic evolution. *Physical Review A*, 65(4):042308, 2002.

[RC08] J. Roland and N. Cerf. Quantum circuit implementation of the hamiltonian versions of Grover's algorithm. 2008.

[RHA96] R.P. Richard, A.J.G. Hey, and R.W. Allen. *Feynman lectures on computation*. Addison-Wesley, Reading, Mass.; Tokyo, 1996.

[RNTK08] M. Ramzan, A. Nawaz, AH Toor, and MK Khan. The effect of quantum memory on quantum games. *Journal of Physics A: Mathematical and Theoretical*, 41:055307, 2008.

[Sho] PW Shor. Fault-tolerant quantum computation. In *Foundations of Computer Science, 1996. Proceedings., 37th Annual Symposium on*, pages 56–65. IEEE.

[Sho94] P.W. Shor. Algorithms for quantum computation: discrete logarithms and factoring. In *Foundations of Computer Science, 1994 Proceedings., 35th Annual Symposium on*, pages 124–134. IEEE, 1994.

[Sho95] P.W. Shor. Scheme for reducing decoherence in quantum computer memory. *Physical review A*, 52(4):2493–2496, 1995.

[Sho97] P.W. Shor. Polynomial-time algorithms for prime factorization and discrete logarithms on a quantum computer. *SIAM J. Comp.*, 26(5):1484–1509, 1997.

[SOMI04a] J. Shimamura, S.K. Ozdemir, F. Morikoshi, and N. Imoto. Entangled states that cannot reproduce original classical games in their quantum version. *Physics Letters A*, 328(1):20–25, 2004.

[SÖMI04b] J. Shimamura, S.K. Özdemir, F. Morikoshi, and N. Imoto. Quantum and classical correlations between players in game theory. *International Journal of Quantum Information*, 2(1):79–89, 2004.

[SSB05] D. Shapira, Y. Shimoni, and O. Biham. Algebraic analysis of quantum search with pure and mixed states. *Physical Review A*, 71(4):042320, 2005.

[Ste96] A.M. Steane. Error correcting codes in quantum theory. *Physical Review Letters*, 77(5):793–797, 1996.

[Sze04] P. Szekeres. *A course in modern mathematical physics: groups, Hilbert space, and differential geometry*. Cambridge Univ Pr, 2004.

[THL+95] Q.A. Turchette, CJ Hood, W. Lange, H. Mabuchi, and H.J. Kimble. Measurement of conditional phase shifts for quantum logic. *Physical Review Letters*, 75(25):4710–4713, 1995.

[Tur36] A.M. Turing. On computable numbers, with an application to the Entscheidungs problem. *Proc. London Math. Soc*, 2(42):230–265, 1936.

[Vai99] L. Vaidman. Time-symmetrized counterfactuals in quantum theory. *Foundations of physics*, 29(5):755–765, 1999.

[VDMV01] W. Van Dam, M. Mosca, and U. Vazirani. How powerful is adiabatic quantum computation? In *Foundations of Computer Science, 2001. Proceedings. 42nd IEEE Symposium on*, pages 279–287. IEEE, 2001.

[VE00] SJ Van Enk. Quantum and classical game strategies. *Physical Review Letters*, 84(4):789–789, 2000.

[vEP02] S. J. van Enk and R. Pike. Classical rules and quantum games. *Phys Rev A*, 66:024306, 2002.

[VSB+01] L.M.K. Vandersypen, M. Steffen, G. Breyta, C.S. Yannoni, M.H. Sherwood, and I.L. Chuang. Experimental realization of Shor's quantum factoring algorithm using nuclear magnetic resonance. *Nature*, 414(6866):883–887, 2001.

[VSS+00] L.M.K. Vandersypen, M. Steffen, M.H. Sherwood, C.S. Yannoni, G. Breyta, and I.L. Chuang. Implementation of a three-quantum-bit search algorithm. *Applied Physics Letters*, 76:646, 2000.

[Wie83] S. Wiesner. Conjugate coding. *ACM Sigact News*, 15(1):78–88, 1983.

[WY04] Z. Wei and M. Ying. Quantum search algorithm by adiabatic evolution under a priori probability. *Arxiv preprint quant-ph/0412117*, 2004.

[WZ82] W.K. Wootters and W.H. Zurek. A single quantum cannot be cloned. *Nature*, 299(5886):802–803, 1982.

[YS99] S. Yu and C.P. Sun. Quantum searching's underlying su (2) structure and its quantum decoherence effects. *Arxiv preprint quant-ph/9903075*, 1999.

[YSÖ+05] T. Yamamoto, J. Shimamura, ŞK Özdemir, M. Koashi, and N. Imoto. Faithful qubit distribution assisted by one additional qubit against collective noise. *Physical review letters*, 95(4):40503, 2005.

[Zal99] C. Zalka. Grovers quantum searching algorithm is optimal. *Physical Review A*, 60(4):2746, 1999.

Chappell, J.M., Iqbal, A., Lohe, M.A. and von Smekal, L. (2009) An analysis of the Quantum Penny Flip game using geometric algebra.
Journal of the Physical Society of Japan, v.78 (5), pp. 054801-1 - 054801-4, May 2009

Chappell, J.M., Iqbal, A. and Abbott, D. (2010) Constructing quantum games from symmetric non-factorizable joint probabilities.
Physics Letters A, v.374 (40), pp. 4104-4111, September 2010

OPEN ACCESS Freely available online

PLoS one

A Precise Error Bound for Quantum Phase Estimation

James M. Chappell[1]*, Max A. Lohe[1], Lorenz von Smekal[2], Azhar Iqbal[3], Derek Abbott[3]

1 School of Chemistry and Physics, University of Adelaide, Adelaide, South Australia, Australia, **2** Institut für Kernphysik, Technische Universität Darmstadt, Darmstadt, Germany, **3** School of Electrical and Electronic Engineering, University of Adelaide, Adelaide, South Australia, Australia

Abstract

Quantum phase estimation is one of the key algorithms in the field of quantum computing, but up until now, only approximate expressions have been derived for the probability of error. We revisit these derivations, and find that by ensuring symmetry in the error definitions, an exact formula can be found. This new approach may also have value in solving other related problems in quantum computing, where an expected error is calculated. Expressions for two special cases of the formula are also developed, in the limit as the number of qubits in the quantum computer approaches infinity and in the limit as the extra added qubits to improve reliability goes to infinity. It is found that this formula is useful in validating computer simulations of the phase estimation procedure and in avoiding the overestimation of the number of qubits required in order to achieve a given reliability. This formula thus brings improved precision in the design of quantum computers.

Citation: Chappell JM, Lohe MA, von Smekal L, Iqbal A, Abbott D (2011) A Precise Error Bound for Quantum Phase Estimation. PLoS ONE 6(5): e19663. doi:10.1371/journal.pone.0019663

Editor: Jürgen Kurths, Humboldt University, Germany

Received January 10, 2011; **Accepted** April 2, 2011; **Published** May 10, 2011

Funding: The authors have no support or funding to report.

Competing Interests: The authors have declared that no competing interests exist.

* E-mail: james.m.chappell@adelaide.edu.au

Introduction

Phase estimation is an integral part of Shor's algorithm [1] as well as many other quantum algorithms [2], designed to run on a quantum computer, and so an exact expression for the maximum probability of error is valuable, in order to efficiently achieve a predetermined accuracy. Suppose we wish to determine a phase angle ϕ to an accuracy of s bits, which hence could be in error, with regard to the true value of ϕ, by up to 2^{-s}, then due to the probabilistic nature of quantum computers, to achieve this we will need to add p extra qubits to the quantum register in order to succeed with a probability of $1-\varepsilon$. Quantum registers behave like classical registers upon measurement, returning a one or a zero from each qubit. Previously, Cleve et al. [3] determined the following upper bound:

$$p_C = \lceil \log_2\left(\frac{1}{2\varepsilon}+\frac{1}{2}\right)\rceil. \tag{1}$$

Thus the more confident we wish to be (a small ε), for the output to achieve a given precision s, the more qubits, p, will need to be added to the quantum register. Formulas of essentially the same functional form as Eq. (1), are produced by two other authors, in [2] and [4], due to the use of similar approximations in their derivation. For example, we have $p=\lceil \log_2\left(\frac{1}{2\varepsilon}+2\right)+\log_2\pi\rceil$, given in [4]. As we show in the following, these approximate error formulas are unsatisfactory in that they overestimate the number of qubits required in order to achieve a given reliability.

The phase angle is defined as follows, given a unitary operator U, we produce the eigenvalue equation $U|u\rangle = e^{2\pi i\phi}|u\rangle$, for some eigenvector $|u\rangle$, and we seek to determine the phase $\phi\in[0,1)$ using the quantum phase estimation procedure [5]. The first stage in phase estimation produces, in the measurement register with a t qubit basis $\{|k\rangle\}$, the state [2]

$$|\tilde{\phi}\rangle_{\text{Stage1}} = \frac{1}{2^{t/2}}\sum_{k=0}^{2^t-1} e^{2\pi i\phi k}|k\rangle. \tag{2}$$

If $\phi = b/2^t$ for some integer $b=0,1,\ldots 2^t-1$, then

$$|\tilde{\phi}\rangle_{\text{Stage1}} = \sum_{k=0}^{2^t-1} y_k|k\rangle\ ,\quad with\quad y_k = \frac{e^{2\pi ibk/2^t}}{2^{t/2}}, \tag{3}$$

is the discrete Fourier transform of the basis state $|b\rangle$, that is, the state with amplitudes $x_k=\delta_{kb}$. We then read off the exact phase $\phi=b/2^t$ from the inverse Fourier transform as $|b\rangle = \mathcal{F}^\dagger|\tilde{\phi}\rangle$.

In general however, when ϕ cannot be written in an exact t bit binary expansion, the inverse Fourier transform in the final stage of the phase estimation procedure yields a state

$$|\phi\rangle \equiv F^\dagger|\tilde{\phi}\rangle_{\text{Stage1}}\ , \tag{4}$$

from which we only obtain an estimate for ϕ. That is, the coefficients x_k of the state $|\phi\rangle$ in the t qubit basis $\{|k\rangle\}$ will yield probabilities which peak at the values of k closest to ϕ.

Our goal now is to derive an upper bound which avoids the approximations used in the above formulas and hence obtain a precise result.

Results

In order to derive an improved accuracy formula for phase estimation, we initially follow the procedure given in [3], where it

is noted, that because of the limited resolution provided by the quantum register of t qubits, the phase ϕ must be approximated by the fraction $\frac{b}{2^t}$, where b is an integer in the range 0 to 2^t-1 such that $b/2^t=0.b_1\ldots b_t$ is the best t bit approximation to ϕ, which is less than ϕ. We then define

$$\delta=\phi-b/2^t,$$

which is the difference between ϕ and $b/2^t$ and where clearly $0\le\delta<2^{-t}$. The first stage of the phase estimation procedure produces the state given by Eq. (2). Applying the inverse quantum Fourier transform to this state produces

$$|\phi\rangle=\sum_{k=0}^{2^t-1}x_k|k\rangle\,, \tag{5}$$

where

$$x_k=\frac{1}{2^t}\sum_{\ell=0}^{2^t-1}e^{2\pi i(\phi-k/2^t)\ell}=\frac{1}{2^t}\,\frac{1-e^{2\pi i 2^t\delta}}{1-e^{2\pi i(\delta-\frac{k-b}{2^t})}}\,. \tag{6}$$

Assuming the outcome of the final measurement is m, we can bound the probability of obtaining a value of m such that $|m-b|\le e$, where e is a positive integer characterizing our desired tolerance to error, where m and b are integers such that $0\le m<2^t$ and $0\le b<2^t$. The probability of observing such an m is given by

$$pr(|m-b|\le e)=\sum_{\ell=-e}^{e}|x_{b+\ell}|^2. \tag{7}$$

This is simply the sum of the probabilities of the states within e of b, where

$$x_{b+\ell}=\frac{1}{2^t}\,\frac{1-e^{2\pi i 2^t\delta}}{1-e^{2\pi i(\delta-\ell/2^t)}}, \tag{8}$$

which is the standard result obtained from Eq. (6), in particular see equation 5.26 in [2]. Typically at this point approximations are now made to simplify x_ℓ, however we proceed without approximations. We have

$$|x_{b+\ell}|^2=\frac{1}{2^{2t}}\,\frac{1-\cos(2\pi 2^t\delta)}{1-\cos(2\pi(\delta-\ell/2^t))}\,. \tag{9}$$

Suppose we wish to approximate ϕ to an accuracy of 2^{-s}, that is, we choose $e=2^{t-s-1}=2^{p-1}$, using $t=s+p$, which can be compared with Eq. 5.35 in [2], and if we denote the probability of failure

$$\epsilon=p(|m-b|>e), \tag{10}$$

then we have

$$\epsilon=1-\frac{1-\cos2\pi 2^t\delta}{2^{2t}}\sum_{\ell=-2^{p-1}}^{2^{p-1}}\frac{1}{1-\cos2\pi(\delta-\ell/2^t)}. \tag{11}$$

This formula assumes that for a measurement m, we have a successful result if we measure a state either side of b within a distance of e, which is the conventional assumption.

This definition of error however is asymmetric because there will be unequal numbers of states summed about the phase angle ϕ to give the probability of a successful result, because an odd number of states is being summed. We now present a definition of the error which is symmetric about ϕ.

Modified definition of error

Given an actual angle ϕ that we are seeking to approximate in the phase estimation procedure, a measurement is called successful if it lies within a certain tolerance e of the true value ϕ. That is, for a measurement of state m out of a possible 2^t states, the probability of failure will be

$$\epsilon=p\left(|2\pi\frac{m}{2^t}-\phi|>\frac{1}{2}\frac{2\pi}{2^s}\right). \tag{12}$$

Thus we consider the angle to be successfully measured accurate to s bits, if the estimated ϕ lies in the range $\phi\pm\frac{1}{2}\frac{2\pi}{2^s}$. Considering our previous definition Eq. (10), due to the fact that b is defined to be always less than ϕ, then compared to the previous definition of ϵ, we lose the outermost state at the lower end of the summation in Eq. (11) as shown in Fig. (1). For example for $p=1$, the upper bracket in Fig. (1) (representing the error bound) can only cover two states instead of three, and so the sum in Eq. (11) will now sum from 0 to 1, instead of -1 to 1, for this case.

An optimal bound

Based on this new definition then for all cases we need to add 1 to the lower end of the summation giving

$$\epsilon=1-\frac{1-\cos2\pi 2^t\delta}{2^{2t}}\sum_{\ell=-2^{p-1}+1}^{2^{p-1}}\frac{1}{1-\cos2\pi(\delta-\ell/2^t)} \tag{13}$$

and if we define $a=2^t\delta$ and rearrange the cosine term in the summation we find

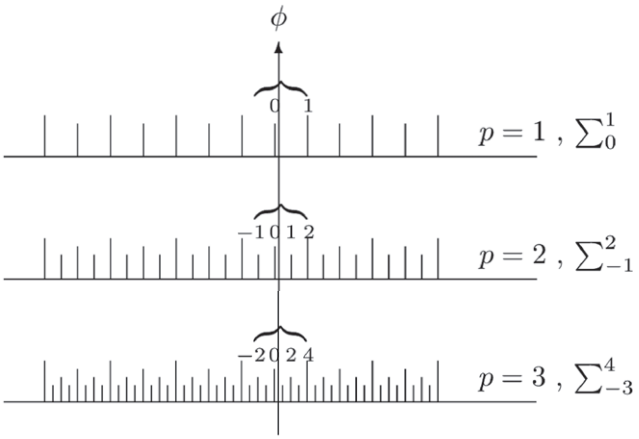

Figure 1. Defining the limits of summation for the phase estimation error. For the cases $p=1,2,3$, we show the measurements which are accepted as lying within the required distance of ϕ, shown by the vertical arrow, which define the limits of summation used in Eq. (13).
doi:10.1371/journal.pone.0019663.g001

$$\epsilon = 1 - \frac{1-\cos 2\pi a}{2^{2t+1}} \sum_{\ell=-2^{p-1}+1}^{2^{p-1}} \csc^2 \frac{\pi}{2^t}(a-\ell). \qquad (14)$$

Next, we demonstrate that the right hand side of Eq. (14) takes its maximum value at $a=\frac{1}{2}$. Since we know $0 \le a < 1$, and since we expect the maximum value of $\epsilon = \epsilon(a,t,p)$ to lie about midway between the two nearest states to generate the largest error, that is at $a = 1/2$, we will substitute $a = \frac{1}{2} + \Delta$, where $\Delta \ll \frac{1}{2}$. To maximize ϵ we need to minimize

$$\cos 2\pi\left(\frac{1}{2}+\Delta\right) \sum_{\ell=-2^{p-1}+1}^{2^{p-1}} \csc^2 \frac{\pi}{2^t}\left(\frac{1}{2}-\ell+\Delta\right), \qquad (15)$$

as a function of Δ. Expanding to quadratic order with a Taylor series, we seek to minimize

$$\left(1-\pi^2\Delta^2+O(\Delta^4)\right)\left(c_0+c_1\Delta+c_2\Delta^2+c_3\Delta^3+O(\Delta^4)\right), \qquad (16)$$

where c_i are the coefficients of the Taylor expansion of cosecant^2 in Δ. We find by the odd symmetry of the cotangent about $\ell = \frac{1}{2}$ that

$$c_1 = \frac{2\pi}{2^t} \sum_{\ell=-2^{p-1}+1}^{2^{p-1}} \cot\frac{\pi}{2^t}(\tfrac{1}{2}-\ell)\csc^2\frac{\pi}{2^t}(\tfrac{1}{2}-\ell) = 0, \qquad (17)$$

and so we just need to minimize

$$c_0 + (c_2 - c_0\pi^2)\Delta^2 + O(\Delta^3). \qquad (18)$$

Differentiating, we see we have an extremum at $\Delta = 0$, and therefore $\epsilon(a,t,p)$ has a maximum at $a = 1/2$.

Substituting $a = \frac{1}{2}$ we obtain

$$\epsilon \le 1 - \frac{2}{2^{2t}} \sum_{\ell=-2^{p-1}+1}^{2^{p-1}} \frac{1}{1-\cos\frac{2\pi}{2^t}(\frac{1}{2}-\ell)}. \qquad (19)$$

We note that the summation is symmetrical about $\ell = 1/2$, and substituting $t = p+s$, we obtain for our final result

$$\epsilon(s,p) = 1 - \frac{1}{2^{2(p+s)-2}} \sum_{\ell=1}^{2^{p-1}} \frac{1}{1-\cos\frac{\pi(2\ell-1)}{2^{(p+s)}}}. \qquad (20)$$

That is, given a desired accuracy of s bits, then if we add p more bits, we have a probability of success given by $1-\epsilon$, of obtaining a measurement to at least s bits of accuracy. Thus we have succeeded in deriving a best possible bound for the failure rate $\epsilon = \epsilon(s,p)$.

Special Cases

Numerical calculations show that $\epsilon(t,p)$ quickly approaches its asymptotic value as $t \to \infty$, and this limit gives a fairly accurate upper bound for ϵ, for t greater than about 10 qubits. Using $\cos x \ge 1 - \frac{x^2}{2}$ which is valid for all x, and is accurate for $x = O(1/2^t)$ as $t \to \infty$,

$$\begin{aligned} \epsilon &\le 1 - \frac{4}{2^{2t}} \sum_{\ell=1}^{2^{p-1}} \frac{1}{1-(1-\frac{1}{2}(\frac{\pi}{2^t}(2\ell-1))^2)} \\ &= 1 - \frac{8}{\pi^2} \sum_{\ell=1}^{2^{p-1}} \frac{1}{(2\ell-1)^2} \end{aligned} \qquad (21)$$

An exact form for this can be found in terms of the trigamma function, being a special case of the polygamma function as shown in Abramowitz and Stegun [6], Eq. 6.4.5:

$$\epsilon \le \frac{2}{\pi^2}\psi'\left(\frac{1+2^p}{2}\right) \qquad (22)$$

where $\psi'(z) = \frac{d\psi}{dz}$ is the trigamma function, $\psi(z) = \frac{\Gamma'(z)}{\Gamma(z)}$ is the digamma function, and $\Gamma(z) = \int_0^\infty t^{z-1}\mathrm{e}^{-t}dt$ is the standard gamma function.

Now considering the $p \to \infty$ limit, which also includes the $t \to \infty$ limit because $t = p+s$, we can find an asymptotic form in the limit of large p also from [6], Eq. 6.4.12, namely

$$\epsilon = \frac{4}{\pi^2} 2^{-p}, \qquad (23)$$

which shows that the error rate drops off exponentially with p extra qubits. The formula Eq. (23) can be re-arranged to give

$$p_\infty = \left\lceil \log_2 \frac{2\sqrt{2}}{\pi^2\epsilon} \right\rceil \qquad (24)$$

which can be compared with the previous approximate formula shown in Eq. (1).

We have checked the new error formula through simulations, by running the phase estimation algorithm on a 2-dimensional rotation matrix, and undertaking a numerical search for the rotation angle that maximizes the error ϵ, which has confirmed Eq. (20) to six decimal places.

Discussion

An exact formula is derived for the probability of error in the quantum phase estimation procedure, as shown in Eq. (20). That is, to calculate ϕ accurate to a required s bits with a given probability of success $1-\epsilon$ we add p extra qubits, where p is given by Eq. (20). If we have a large number of qubits then we can use Eq. (22) valid at the $t \to \infty$ limit. In the $p \to \infty$ limit the asymptote is found as a simple exponential form Eq. (23).

The exact formula avoids overestimating the number of qubits actually required in order to achieve a given reliability for phase estimation and we have also found this formula to be useful in confirming the operation of classical simulators of the phase estimation procedure.

Acknowledgments

Discussions with Anthony G. Williams and Sanjeev Naguleswaran during the early stages of this work are gratefully acknowledged.

References

1. Shor PW (1997) Polynomial-time algorithms for prime factorization and discrete logarithms on a quantum computer. SIAM, J Comp 26(5): 1484–1509.
2. Nielsen MA, Chuang IL (2002) Quantum Computation and Quantum Information. Cambridge UK: Addison-Wesley, first edition.
3. Cleve R, Ekert A (1998) Quantum algorithms revisited. Proc R Soc London A 454(1969): 339–354.
4. Imre S, Balazs F (2002) A tight bound for probability of error for quantum counting based multiuser detection. Proc ISIT 2002: 43.
5. Mosca M (1999) Quantum Computer Algorithms. Ph.D. thesis, University of Oxford.
6. Abramowitz M, Stegun IA (1964) Handbook of Mathematical Functions with Formulas, Graphs, and Mathematical Tables. New York: Dover.

Author Contributions

Analyzed the data: MAL LvS JMC AI DA. Contributed reagents/materials/analysis tools: DA. Wrote the paper: JMC AI. Proofreading: MAL AI DA.

OPEN ACCESS Freely available online

PLoS one

Analyzing Three-Player Quantum Games in an EPR Type Setup

James M. Chappell[1,2]*, Azhar Iqbal[2], Derek Abbott[2]

1 School of Chemistry and Physics, University of Adelaide, Adelaide, South Australia, Australia, **2** School of Electrical and Electronic Engineering, University of Adelaide, Adelaide, South Australia, Australia

Abstract

We use the formalism of Clifford Geometric Algebra (GA) to develop an analysis of quantum versions of three-player non-cooperative games. The quantum games we explore are played in an Einstein-Podolsky-Rosen (EPR) type setting. In this setting, the players' strategy sets remain identical to the ones in the mixed-strategy version of the classical game that is obtained as a proper subset of the corresponding quantum game. Using GA we investigate the outcome of a realization of the game by players sharing GHZ state, W state, and a mixture of GHZ and W states. As a specific example, we study the game of three-player Prisoners' Dilemma.

Citation: Chappell JM, Iqbal A, Abbott D (2011) Analyzing Three-Player Quantum Games in an EPR Type Setup. PLoS ONE 6(7): e21623. doi:10.1371/journal.pone.0021623

Editor: Attila Szolnoki, Hungarian Academy of Sciences, Hungary

Received April 13, 2011; **Accepted** June 3, 2011; **Published** July 27, 2011

Funding: The authors have no support or funding to report.

Competing Interests: The authors have declared that no competing interests exist.

* E-mail: james.m.chappell@adelaide.edu.au

Introduction

The field of game theory [1,2] has a long history [3], but was first formalized in 1944 with the work of von Neumann and Morgenstern [4], aiming to develop rational analysis of situations that involve strategic interdependence.

Classical game theory has found increasing expression in the field of physics [3] and its extension to the quantum regime [5] was proposed by Meyer [6] and Eisert et al [7], though its origins can be traced to earlier works [8–11]. Early studies in the area of quantum games focused on the two-player two-strategy non-cooperative games, with the proposal for a quantum Prisoners' Dilemma (PD) being well known [7]. A natural further development of this work was its extension to multiplayer quantum games that was explored by Benjamin and Hayden [12]. Du et al. [13,14] explored the phase transitions in quantum games for the first time that are central in the present article.

The usual approach in three-player quantum games considers players sharing a three-qubit quantum state with each player accessing their respective qubit in order to perform local unitary transformation. Quantum games have been reported [15] in which players share Greenberger-Horne-Zeilinger (GHZ) states and the W states [5], while other works have, for instance, investigated the effects of noise [16,17] and the benefits of players forming coalitions [18,19].

A suggested approach [20–23] in constructing quantum games uses an Einstein-Podolsky-Rosen (EPR) type setting [24–31]. In this approach, quantum games are setup with an EPR type apparatus, with the players' strategies being local actions related to their qubit, consisting of a linear combination (with real coefficients) of (spin or polarization) measurements performed in two selected directions.

Note that in a standard arrangement for playing a mixed-strategy game, players are faced with the identical situation, in that in each run, a player has to choose one out of two pure strategies. As the players' strategy sets remain classical, the EPR type setting avoids a well known criticism [32] of quantum games. This criticism refers to quantization procedures in which players are given access to extended strategy sets, relative to what they are allowed to have in the classical game. Quantum games constructed with an EPR type setting have been studied in situations involving two players [22] and also three players [23]. The applications of three-player quantum games include describing three-party situations, involving strategic interaction in quantum communication [33].

In recent works, the formalism of Clifford's geometric algebra (GA) [34–38] has been applied to the analysis of two-player quantum games with significant benefits [39,40], and so is also adopted here in the analysis of three-player quantum games. The use of GA is justified on the grounds that the Pauli spin algebra is a matrix representation of Clifford's geometric algebra in $\mathcal{R}^3$, and hence we are choosing to work directly with the underlying Clifford algebra. There are also several other documented benefits of GA such as:

a) The unification of the dot and cross product into a single product, has the significant advantage of possessing an inverse. This results in increased mathematical compactness, thereby aiding physical intuition and insight [41].

b) The use of the Pauli and Dirac matrices also unnecessarily introduces the imaginary scalars, in contrast to GA, which uses exclusively real elements [42]. This fact was also pointed out by Sommerfield in 1931, who commented that '*Dirac's use of matrices simply rediscovered Clifford algebra*' [43].

c) In the density matrix formalism of quantum mechanics, the expectation for an operator Q is given by $\mathrm{Tr}(\rho Q) = \langle\psi|Q|\psi\rangle$, from which we find the isomorphism to GA, $\mathrm{Tr}(\rho Q) \leftrightarrow \langle \rho Q \rangle_0$, the subscript zero, indicating to take the scalar part of the algebraic product ρQ, where ρ and Q are

now constructed from real Clifford elements. This leads to a uniquely compact expression for the overlap probability between two states in the N-particle case, given by Eq. (13), which allows straightforward calculations that normally require 8×8 complex matrices representing operations on three qubits.

d) Pauli wave functions are isomorphic to the quaternions, and hence represent rotations of particle states [44]. This fact paves the way to describe general unitary transformations on qubits, in a simplified algebraic form, as *rotors*. In regard to Hestenes' analysis of the Dirac equation using GA, Boudet [41] notes that, 'the use of the pure real formalism of Hestenes brings noticeable simplifications and above all the entire geometrical clarification of the theory of the electron. '

e) Recent works [6,39,40] show that GA provides a better intuitive understanding of Meyer's quantum penny flip game [6], using operations in 3-space with *real coordinates*, permitting helpful visualizations in determining the quantum player's winning strategy. Also, Christian [45,46] has recently used GA to produce thought provoking investigations into some of the foundational questions in quantum mechanics.

Our quantum games use an EPR type setting and players have access to general pure quantum states. We determine constraints that ensure a faithful embedding of the mixed-strategy version of the original classical game within the corresponding quantum game. We find how a Pareto-optimal quantum outcome emerges in three-player quantum PD game at high entanglement. We also report phase transitions taking place with increasing entanglement when players share a mixture of GHZ and W type states in superposition.

In an earlier paper [23], two of the three authors contributed to developing an entirely probabilistic framework for the analysis of three-player quantum games that are also played using an EPR type setting, whereas the present paper, though using an EPR type setting, provides an analysis from the perspective of quantum mechanics, with the mathematical formalism of GA. The previous work analyzed quantum games from the non-factorizable property of a joint probability distribution relevant to a physical system that the players shared in order to implement the game. For the game of three-player Prisoners' Dilemma, our probabilistic analysis showed that non-factorizability of a joint probability distribution indeed can lead to a new equilibrium in the game. The three-player quantum Prisoners' Dilemma, in the present analysis, however, moves to the next step and explores the phase structure relating players' payoffs with shared entanglement and also the impact of players sharing GHZ and W states and their mixture. We believe that without using the powerful formalism of GA, a similar analysis will nearly be impossible to perform using an entirely probabilistic approach as developed in [22].

EPR setting for playing quantum games

The EPR setting [20,22,23] two player quantum games involves a large number of runs when, in a run, two halves of an EPR pair originate from the same source and move in the opposite directions. Player Alice receives one half whereas player Bob receives the other half. To keep the non-cooperative feature of the game, it is assumed that players Alice and Bob are located at some distance from each other and are not unable to communicate between themselves. The players, however, can communicate about their actions, which they perform on their received halves, to a *referee* who organizes the game and ensures that the rules of the game are followed. The referee makes available two directions to each player. In a run, each player has to choose one of two available directions. The referee rotates Stern-Gerlach type detectors [5] along the two chosen directions and performs quantum measurement. The outcome of the quantum measurement, on Alice's side, and on Bob's side of the Stern-Gerlach detectors, is either $+1$ or -1. Runs are repeated as the players receive a large number of halves in pairs, when each pair comes from the same source and the measurement outcomes are recorded for all runs. A player's strategy, defined over a large number of runs, is a linear combination (with normalized and real coefficients) of the two directions along which the measurement is performed. The referee makes public the payoff relations at the start of the game and announces rewards to the players after the completion of runs. The payoff relations are constructed in view of a) the matrix of the game, b) the list of players' choices of directions over a large number of runs, and c) the list of measurement outcomes that the referee prepares using his/her Stern-Gerlach apparatus.

For a three-player quantum game, this setting is extended to consider three players Alice, Bob and Chris who are located at the three arms of an EPR system [5]. In the following they will be denoted by A, B and C, respectively. As it is the case with two-player EPR setting, in a run of the experiment, each player chooses one out of two directions.

We have used the EPR setting in view of the well known Enk and Pike's criticism [32] of quantum games that are played using Eisert et al's setting [7]. Essentially this criticism attempts to equate a quantum game to a classical game in which the players are given access to an extended set of classical strategies. The present paper uses an EPR setting in which each player has two classical strategies consisting of the two choices he/she can make between two directions along which a quantum measurement can be performed. That is, the player's pure strategy, in a run, consists of choosing one direction out of the two. As the sets of strategies remain exactly identical in both the classical and the quantum forms of the game, it is difficult to construct an Enk and Pike type argument for a quantum game that is played with an EPR setting.

As Fig. 1 shows, we represent Alice's two directions as κ_1^1,κ_2^1. Similarly, Bob's directions are κ_1^2,κ_2^2 and Chris' are κ_1^3,κ_2^3. The players measurement directions form a triplet out of eight possible cases $(\kappa_1^1,\kappa_1^2,\kappa_1^3)$, $(\kappa_1^1,\kappa_2^2,\kappa_1^3)$, $(\kappa_2^1,\kappa_1^2,\kappa_1^3)$, $(\kappa_2^1,\kappa_2^2,\kappa_1^3)$, $(\kappa_1^1,\kappa_1^2,\kappa_2^3)$, $(\kappa_1^1,\kappa_2^2,\kappa_2^3)$, $(\kappa_2^1,\kappa_1^2,\kappa_2^3)$, $(\kappa_2^1,\kappa_2^2,\kappa_2^3)$ and measurement is performed along the chosen directional triplet. The measurement outcome for each player along their chosen direction is $+1$ or -1.

Over a large number of runs the players sequentially receive three-particle systems emitted from a source and a record is maintained of the players' choices of directions over all runs. One of the eight possible outcomes $(+1,+1,+1)$, $(+1,-1,+1)$, $(-1,+1,+1)$, $(-1,-1,+1)$, $(+1,+1,-1)$, $(+1,-1,-1)$, $(-1,+1,-1)$, $(-1,-1,-1)$ emerges out of the measurement in an individual run, with the first entry for Alice's outcome, the second entry for Bob's outcome and the third entry for Chris' outcome.

In the following we express the players' payoff relations in terms of the outcomes of these measurements. These payoffs depend on the triplets of the players' strategic choices made over a large number of runs and on the dichotomic outcomes of the measurements performed along those directions.

Players' sharing a symmetric initial state

We consider the situation in which an initial quantum state of three qubits is shared among three players. To obtain a fair game, we assume this state is symmetric with regard to the interchange of the three players. The GHZ state is a natural candidate given by

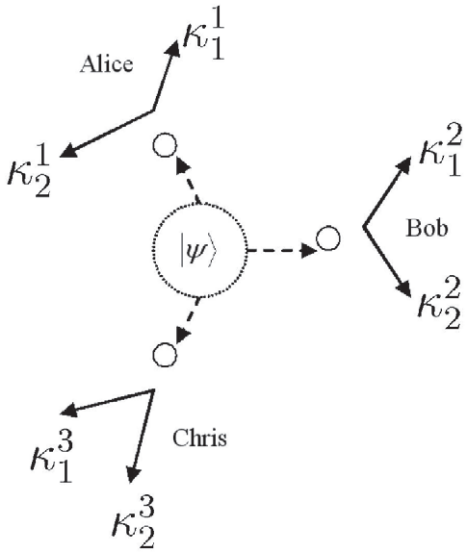

Figure 1. The EPR setup for three-player quantum game. A three-qubit entangled quantum state is distributed to the three players, who each choose between two possible measurement directions.
doi:10.1371/journal.pone.0021623.g001

$$|\mathrm{GHZ}\rangle = \cos\frac{\gamma}{2}|000\rangle + \sin\frac{\gamma}{2}|111\rangle, \tag{1}$$

where we have an entanglement angle $\gamma \in \Re$, which has been shown [5] to be capable of producing the maximally entangled three qubit state. Alternatively we could start with the W entangled state

$$|\mathrm{W}\rangle = \frac{1}{\sqrt{3}}(|100\rangle + |010\rangle + |001\rangle). \tag{2}$$

The other symmetric state would be an inverted W state

$$|\bar{\mathrm{W}}\rangle = \frac{1}{\sqrt{3}}(|110\rangle + |011\rangle + |101\rangle). \tag{3}$$

After the measurement along three directions selected by the players, each player is rewarded according to a payoff matrix $G^{\mathcal{P}}$, for each player $\mathcal{P} \in \{A,B,C\}$. Thus the expected payoffs for a player is given by

$$\Pi_{\mathcal{P}}(\kappa^1,\kappa^2,\kappa^3) = \sum_{i,j,k=0}^{1} G^{\mathcal{P}}_{ijk} P_{ijk}, \tag{4}$$

where P_{ijk} is the probability the state $|i\rangle|j\rangle|k\rangle$ is obtained after measurement, with $i,j,k \in \{0,1\}$, along the three directions $\kappa^1,\kappa^2,\kappa^3$ chosen by Alice, Bob and Chris respectively. In the EPR setting, κ^1 can be either of Alice's two directions i.e. κ_1^1 or κ_2^1 and similarly for Bob and Chris.

Clifford's geometric algebra

The formalism of GA [34–38] has been shown to provide an equivalent description to the conventional tensor product formalism of quantum mechanics.

To set up the GA framework for representing quantum states, we begin by defining $\sigma_1,\sigma_2,\sigma_3$ as a right-handed set of orthonormal basis vectors, with

$$\sigma_i.\sigma_j = \delta_{ij}, \tag{5}$$

where δ_{ij} is Kronecker delta. Multiplication between algebraic elements is defined to be the geometric product, which for two vectors u and v is given by

$$uv = u.v + u \wedge v, \tag{6}$$

where $u.v$ is the conventional symmetric dot product and $u \wedge v$ is the anti-symmetric outer product related to the Gibb's cross product by $u \times v = -\imath u \wedge v$, where $\imath = \sigma_1\sigma_2\sigma_3$. For distinct basis vectors we find

$$\sigma_i\sigma_j = \sigma_i.\sigma_j + \sigma_i \wedge \sigma_j = \sigma_i \wedge \sigma_j = -\sigma_j \wedge \sigma_i = -\sigma_j\sigma_i. \tag{7}$$

This can be summarized by

$$\sigma_i\sigma_j = \delta_{ij} + \imath\varepsilon_{ijk}\sigma_k, \tag{8}$$

where ε_{ijk} is the Levi-Civita symbol. We can therefore see that $\imath$ squares to minus one, that is $\imath^2 = \sigma_1\sigma_2\sigma_3\sigma_1\sigma_2\sigma_3 = \sigma_1\sigma_2\sigma_1\sigma_2 = -1$ and commutes with all other elements and so has identical properties to the unit imaginary i. Thus we have an isomorphism between the basis vectors $\sigma_1,\sigma_2,\sigma_3$ and the Pauli matrices through the use of the geometric product.

In order to express quantum states in GA we use the one-to-one mapping [36,38] defined as follows

$$\begin{aligned} |\psi\rangle = \alpha|0\rangle + \beta|1\rangle = \begin{bmatrix} a_0 + \mathrm{i}a_3 \\ -a_2 + \mathrm{i}a_1 \end{bmatrix} \leftrightarrow \psi \\ = a_0 + a_1\imath\sigma_1 + a_2\imath\sigma_2 + a_3\imath\sigma_3, \end{aligned} \tag{9}$$

where a_i are real scalars.

For a single particle we then have the basis vectors

$$|0\rangle \leftrightarrow 1, \ \ |1\rangle \leftrightarrow -\imath\sigma_2 \tag{10}$$

and so for three particles we can use as a basis

$$|0\rangle|0\rangle|0\rangle \leftrightarrow 1 \tag{11a}$$

$$|0\rangle|0\rangle|1\rangle \leftrightarrow -\imath\sigma_2^3 \tag{11b}$$

$$|0\rangle|1\rangle|0\rangle \leftrightarrow -\imath\sigma_2^2 \tag{11c}$$

$$|0\rangle|1\rangle|1\rangle \leftrightarrow \imath\sigma_2^2\imath\sigma_2^3, \tag{11d}$$

$$|1\rangle|0\rangle|0\rangle \leftrightarrow -\imath\sigma_2^1 \tag{11e}$$

$$|1\rangle|0\rangle|1\rangle \leftrightarrow \imath\sigma_2^1\imath\sigma_2^3 \tag{11f}$$

$$|1\rangle|1\rangle|0\rangle \leftrightarrow \imath\sigma_2^1\imath\sigma_2^2 \tag{11g}$$

$$|1\rangle|1\rangle|1\rangle \leftrightarrow -\imath\sigma_2^1\imath\sigma_2^2\imath\sigma_2^3, \tag{11h}$$

where to reduce the number of superscripts representing particle number we write $\imath^1\sigma_2^1$ as $\imath\sigma_2^1$. General unitary operations are equivalent to rotors in GA [36], represented as

$$R(\theta_1,\theta_2,\theta_3) = \mathrm{e}^{-\theta_3\imath\sigma_3/2}\mathrm{e}^{-\theta_1\imath\sigma_2/2}\mathrm{e}^{-\theta_2\imath\sigma_3/2}, \tag{12}$$

which is in Euler angle form and can completely explore the available space of a single qubit. Using the definition of unitary operations given by Eq. (12) we define $A=R(\alpha_1,\alpha_2,\alpha_3)$, $B=R(\beta_1,\beta_2,\beta_3)$, $C=R(\chi_1,\chi_2,\chi_3)$ for general unitary transformations acting locally on each of the three players qubit in order to generalize the starting state, that is the GHZ or W states, as far as possible.

We define a separable state $\phi=KLM$, where K, L and M are single particle rotors, which allow the players' measurement directions to be specified on the first, second and third qubit respectively. The state to be measured is now projected onto this separable state ϕ. The overlap probability between two states ψ and ϕ in the N-particle case is given in Ref. [36] as

$$P(\psi,\phi) = 2^{N-2}\left[\langle\psi E\psi^\dagger\phi E\phi^\dagger\rangle_0 - \langle\psi J\psi^\dagger\phi J\phi^\dagger\rangle_0\right], \tag{13}$$

where the angle brackets $\langle\rangle_0$ mean to retain only the scalar part of the expression and E and J are defined for 3 particles in Ref. [36] as

$$E = \prod_{i=2}^{N}\frac{1}{2}\left(1-\imath\sigma_3^1\imath\sigma_3^i\right) = \frac{1}{4}\left(1-\imath\sigma_3^1\imath\sigma_3^2-\imath\sigma_3^1\imath\sigma_3^3-\imath\sigma_3^2\imath\sigma_3^3\right) \tag{14a}$$

$$J = E\imath\sigma_3^1 = \frac{1}{4}\left(\imath\sigma_3^1+\imath\sigma_3^2+\imath\sigma_3^3-\imath\sigma_3^1\imath\sigma_3^2\imath\sigma_3^3\right). \tag{14b}$$

The † operator acts the same as complex conjugation: flipping the sign of $\imath$ and inverting the order of the terms.

Results

We now, firstly, calculate the observables from Eq. (11) for the GHZ state in GA, which from Eq. (11) gives

$$\psi = ABC\left(\cos\frac{\gamma}{2}-\sin\frac{\gamma}{2}\imath\sigma_2^1\imath\sigma_2^2\imath\sigma_2^3\right), \tag{15}$$

where A, B, and C represent the referee's local unitary actions, written as rotors A, B, and C in GA, on the respective player's qubits, in order to generalize the starting state. Referring to Eq. (13), we firstly calculate

$$\begin{aligned}
\psi J\psi^\dagger &= \frac{1}{4}ABC\left(\cos\frac{\gamma}{2}-\sin\frac{\gamma}{2}\imath\sigma_2^1\imath\sigma_2^2\imath\sigma_2^3\right)\left(\imath\sigma_3^1+\imath\sigma_3^2+\imath\sigma_3^3-\imath\sigma_3^1\imath\sigma_3^2\imath\sigma_3^3\right)\\
&\times\left(\cos\frac{\gamma}{2}+\sin\frac{\gamma}{2}\imath\sigma_2^1\imath\sigma_2^2\imath\sigma_2^3\right)C^\dagger B^\dagger A^\dagger\\
&= \frac{1}{4}ABC\left(\cos\gamma-\sin\gamma\imath\sigma_2^1\imath\sigma_2^2\imath\sigma_2^3\right)\\
&\left(\imath\sigma_3^1+\imath\sigma_3^2+\imath\sigma_3^3-\imath\sigma_3^1\imath\sigma_3^2\imath\sigma_3^3\right)C^\dagger B^\dagger A^\dagger\\
&= \frac{1}{4}\cos\gamma(R_3+S_3+T_3-R_3S_3T_3)\\
&+\sin\gamma(R_1S_2T_2+R_2S_1T_2+R_2S_2T_1-R_1S_1T_1)
\end{aligned} \tag{16}$$

where $R_k=\imath A\sigma_k A^\dagger$, $S_k=\imath B\sigma_k B^\dagger$, $T_k=\imath C\sigma_k C^\dagger$.
We also calculate

$$\begin{aligned}
\psi E\psi^\dagger &= \frac{1}{4}ABC\left(\cos\frac{\gamma}{2}-\sin\frac{\gamma}{2}\imath\sigma_2^1\imath\sigma_2^2\imath\sigma_2^3\right)\\
&\left(1-\imath\sigma_3^1\imath\sigma_3^2-\imath\sigma_3^1\imath\sigma_3^3-\imath\sigma_3^2\imath\sigma_3^3\right)\\
&\times\left(\cos\frac{\gamma}{2}+\sin\frac{\gamma}{2}\imath\sigma_2^1\imath\sigma_2^2\imath\sigma_2^3\right)C^\dagger B^\dagger A^\dagger\\
&= \frac{1}{4}ABC\left(1-\imath\sigma_3^1\imath\sigma_3^2-\imath\sigma_3^1\imath\sigma_3^3-\imath\sigma_3^2\imath\sigma_3^3\right)C^\dagger B^\dagger A^\dagger\\
&= \frac{1}{4}(1-R_3S_3-R_3T_3-S_3T_3).
\end{aligned} \tag{17}$$

For measurement defined with $K=e^{-\imath\kappa\sigma_2^1/2}$, $L=e^{-\imath\kappa\sigma_2^2/2}$ and $M=e^{-\imath\kappa\sigma_2^3/2}$ allowing a rotation of the detectors by an angle κ, where we have written $\kappa^1\sigma_2^1$ as $\kappa\sigma_2^1$, we find

$$\begin{aligned}
&\phi J\phi^\dagger =\\
&\frac{1}{4}\left(\imath\sigma_3^1e^{\imath\kappa\sigma_2^1}+\imath\sigma_3^2e^{\imath\kappa\sigma_2^2}+\imath\sigma_3^3e^{\imath\kappa\sigma_2^3}-\imath\sigma_3^1\imath\sigma_3^2\imath\sigma_3^3e^{\imath\kappa\sigma_2^1}e^{\imath\kappa\sigma_2^2}e^{\imath\kappa\sigma_2^3}\right)
\end{aligned} \tag{18a}$$

$$\begin{aligned}
&\phi E\phi^\dagger =\\
&\frac{1}{4}\left(1-\imath\sigma_3^1\imath\sigma_3^2e^{\imath\kappa\sigma_2^1}e^{\imath\kappa\sigma_2^2}-\imath\sigma_3^1\imath\sigma_3^3e^{\imath\kappa\sigma_2^1}e^{\imath\kappa\sigma_2^3}-\imath\sigma_3^2\imath\sigma_3^3e^{\imath\kappa\sigma_2^2}e^{\imath\kappa\sigma_2^3}\right).
\end{aligned} \tag{18b}$$

From Eq. (13) we find

$$\begin{aligned}
2\langle\psi E\psi^\dagger\phi E\phi^\dagger\rangle &= \frac{1}{8}(1-R_3S_3-R_3T_3-S_3T_3)\\
&\times(1-\imath\sigma_3^1\imath\sigma_3^2e^{\imath\kappa\sigma_2^1}e^{\imath\kappa\sigma_2^2}-\imath\sigma_3^1\imath\sigma_3^3e^{\imath\kappa\sigma_2^1}e^{\imath\kappa\sigma_2^3}-\imath\sigma_3^2\imath\sigma_3^3e^{\imath\kappa\sigma_2^2}e^{\imath\kappa\sigma_2^3})\\
&= \frac{1}{8}\left[1+(-)^{l+m}X(\kappa^1)Y(\kappa^2)+(-)^{l+n}X(\kappa^1)Z(\kappa^3)\right.\\
&\left.+(-)^{m+n}Y(\kappa^2)Z(\kappa^3)\right]\\
&= \frac{1}{8}\left[1+(-)^{l+m}X_iY_j+(-)^{l+n}X_iZ_k+(-)^{m+n}Y_jZ_k\right],
\end{aligned} \tag{19}$$

where $l,m,n\in\{0,1\}$ refers to measuring a $|0\rangle$ or $|1\rangle$ state, respectively, and using the standard results listed in the Appendix S1, we have

$$X_i = X\left(\kappa_i^1\right) = \cos\alpha_1\cos\kappa_i^1+\cos\alpha_3\sin\alpha_1\sin\kappa_i^1, \tag{20a}$$

$$Y_j = Y\left(\kappa_j^2\right) = \cos\beta_1\cos\kappa_j^2+\cos\beta_3\sin\beta_1\sin\kappa_j^2, \tag{20b}$$

$$Z_k = Z\left(\kappa_k^3\right) = \cos\chi_1\cos\kappa_k^3+\cos\chi_3\sin\chi_1\sin\kappa_k^3, \tag{20c}$$

with $i,j,k\in\{1,2\}$, representing the two measurement directions

available to each player. Also from Eq. (13) we have

$$
\begin{aligned}
&-2\langle\psi J\psi^{\dagger}\phi J\phi^{\dagger}\rangle = -\frac{1}{8}\langle(\cos\gamma(R_3+S_3+T_3-R_3S_3T_3)\\
&+\sin\gamma(R_1S_2T_2+R_2S_1T_2+R_2S_2T_1-R_1S_1T_1))\\
&\times(\imath\sigma_3^1 e^{\imath\kappa\sigma_2^1}+\imath\sigma_3^2 e^{\imath\kappa\sigma_2^2}+\imath\sigma_3^3 e^{\imath\kappa\sigma_2^3}-\imath\sigma_3^1\imath\sigma_3^2\imath\sigma_3^3 e^{\imath\kappa\sigma_2^1}e^{\imath\kappa\sigma_2^2}e^{\imath\kappa\sigma_2^3})\rangle_0\\
&=\frac{1}{8}(\cos\gamma((-)^l X_i+(-)^m Y_j+(-)^n Z_k+(-)^{lmn}X_iY_jZ_k)\\
&+(-)^{lmn}\sin\gamma(F_iV_jW_k+U_iG_jW_k+U_iV_jH_k-F_iG_jH_k))\\
&=\frac{1}{8}[\cos\gamma\{(-)^l X_i+(-)^m Y_j+(-)^n Z_k+(-)^{lmn}X_iY_jZ_k\}\\
&+(-)^{lmn}\sin\gamma\,\Theta_{ijk}],
\end{aligned}
\tag{21}
$$

where

$$
\begin{aligned}
F_i=F(\kappa^1)=&-\sin\kappa_i^1(\cos\alpha_1\cos\alpha_2\cos\alpha_3-\sin\alpha_2\sin\alpha_3)\\
&+\sin\alpha_1\cos\alpha_2\cos\kappa_i^1,
\end{aligned}
\tag{22a}
$$

$$
\begin{aligned}
G_j=G(\kappa^2)=&-\sin\kappa_j^2(\cos\beta_1\cos\beta_2\cos\beta_3-\sin\beta_2\sin\beta_3)\\
&+\sin\beta_1\cos\beta_2\cos\kappa_j^2,
\end{aligned}
\tag{22b}
$$

$$
\begin{aligned}
H_k=H(\kappa^3)=&-\sin\kappa_k^3(\cos\chi_1\cos\chi_2\cos\chi_3-\sin\chi_2\sin\chi_3)\\
&+\sin\chi_1\cos\chi_2\cos\kappa_k^3
\end{aligned}
\tag{22c}
$$

and

$$
\begin{aligned}
U_i=U(\kappa^1)=&\sin\kappa_i^1(\cos\alpha_2\sin\alpha_3+\sin\alpha_2\cos\alpha_3\cos\alpha_1)\\
&-\sin\alpha_1\sin\alpha_2\cos\kappa_i^1,
\end{aligned}
\tag{23a}
$$

$$
\begin{aligned}
V_j=V(\kappa^2)=&\sin\kappa_j^2(\cos\beta_2\sin\beta_3+\sin\beta_2\cos\beta_3\cos\beta_1)\\
&-\sin\beta_1\sin\beta_2\cos\kappa_j^2,
\end{aligned}
\tag{23b}
$$

$$
\begin{aligned}
W_k=W(\kappa^3)=&\sin\kappa_k^3(\cos\chi_2\sin\chi_3+\sin\chi_2\cos\chi_3\cos\chi_1)\\
&-\sin\chi_1\sin\chi_2\cos\kappa_k^3
\end{aligned}
\tag{23c}
$$

and

$$
\Theta_{ijk}=F_iV_jW_k+U_iG_jW_k+U_iV_jH_k-F_iG_jH_k. \tag{24}
$$

So we find from Eq. (13) the probability to observe a particular state after measurement as

$$
\begin{aligned}
P_{lmn}=&\frac{1}{8}[1+\cos\gamma\{(-)^l X_i+(-)^m Y_j+(-)^n Z_k\}\\
&+(-)^{lm}X_iY_j+(-)^{ln}X_iZ_k+(-)^{mn}Y_jZ_k\\
&+(-)^{lmn}\{\cos\gamma X_iY_jZ_k+\sin\gamma\Theta_{ijk}\}].
\end{aligned}
\tag{25}
$$

For instance, at $\gamma=0$ we obtain

$$
P_{lmn}=\frac{1}{8}\left(1+(-)^l X_i\right)\left(1+(-)^m Y_j\right)(1+(-)^n Z_k), \tag{26}
$$

which shows a product state, as expected. Alternatively with general entanglement, but no operation on the third qubit, that is $\chi_i=0$, we have

$$
\begin{aligned}
P_{lm}=&\frac{1}{8}[1+\cos\gamma\{(-)^l X_i+(-)^m Y_j+1+(-)^{lmn}X_iY_j\}\\
&+(-)^{lm}X_iY_j+(-)^l X_i+(-)^m Y_j].\\
=&\frac{1}{8}[(1+\cos\gamma)\left(1+(-)^l X_i\right)\left(1+(-)^m Y_j\right)],
\end{aligned}
\tag{27}
$$

which shows that for the GHZ type entanglement each pair of qubits is mutually unentangled.

Obtaining the payoff relations

We extend the approach of Ichikawa and Tsutsui [47] to three qubits and represent the permutation of signs introduced by the measurement process. For Alice we define

$$
a_{000}=\frac{1}{8}\sum_{ijk}G_{ijk}^A,\ a_{100}=\frac{1}{8}\sum_{ijk}(-)^i G_{ijk}^A, \tag{28a}
$$

$$
a_{010}=\frac{1}{8}\sum_{ijk}(-)^j G_{ijk}^A,\ a_{001}=\frac{1}{8}\sum_{ijk}(-)^k G_{ijk}^A, \tag{28b}
$$

$$
a_{110}=\frac{1}{8}\sum_{ijk}(-)^{i+j} G_{ijk}^A,\ a_{011}=\frac{1}{8}\sum_{ijk}(-)^{j+k} G_{ijk}^A, \tag{28c}
$$

$$
a_{101}=\frac{1}{8}\sum_{ijk}(-)^{i+k} G_{ijk}^A,\ a_{111}=\frac{1}{8}\sum_{ijk}(-)^{i+j+k} G_{ijk}^A. \tag{28d}
$$

Using Eq. (4), we then can find the payoff for each player

$$
\begin{aligned}
\Pi_A\left(\kappa_i^1,\kappa_j^2,\kappa_k^3\right)=&a_{000}+\cos\gamma\{a_{100}X_i+a_{010}Y_j+a_{001}Z_k\}\\
&+a_{110}X_iY_j+a_{101}X_iZ_k+a_{011}Y_jZ_k\\
&+a_{111}\{\cos\gamma X_iY_jZ_k+\sin\gamma\Theta_{ijk}\},
\end{aligned}
\tag{29a}
$$

$$
\begin{aligned}
\Pi_B\left(\kappa_i^1,\kappa_j^2,\kappa_k^3\right)=&b_{000}+\cos\gamma\{b_{100}X_i+b_{010}Y_j+b_{001}Z_k\}\\
&+b_{110}X_iY_j+b_{101}X_iZ_k+b_{011}Y_jZ_k\\
&+b_{111}\{\cos\gamma X_iY_jZ_k+\sin\gamma\Theta_{ijk}\},
\end{aligned}
\tag{29b}
$$

$$
\begin{aligned}
\Pi_C\left(\kappa_i^1,\kappa_j^2,\kappa_k^3\right)=&c_{000}+\cos\gamma\{c_{100}X_i+c_{010}Y_j+c_{001}Z_k\}\\
&+c_{110}X_iY_j+c_{101}X_iZ_k+c_{011}Y_jZ_k\\
&+c_{111}\{\cos\gamma X_iY_jZ_k+\sin\gamma\Theta_{ijk}\},
\end{aligned}
\tag{29c}
$$

where, as Eqs. (20) show, the three measurement directions

$\kappa_i^1,\kappa_j^2,\kappa_k^3$ are held in X_i,Y_i,Z_i. Alternatively, in order to produce other quantum game frameworks [7,48], we can interpret the rotors A,B,C, held in X_i,Y_i,Z_i, as the unitary operations which can be applied by each player to their qubit, where in this case, the measurement directions will be set by the referee.

Mixed-strategy payoff relations. For a mixed strategy game, Alice, Bob and Chris choose their first measurement directions κ_1^1, κ_1^2, κ_1^3 with probabilities x, y and z respectively, where $x,y,z\in[0,1]$ and hence choose the directions κ_2^1, κ_2^2, κ_2^3 with probabilities $(1-x)$, $(1-y)$, $(1-z)$, respectively. Alice's payoff is now given as

$$\begin{aligned}
&\Pi_A(x,y,z)\\
&=xyz\sum_{i,j,k=0}^{1}P_{ijk}\left(\kappa_1^1,\kappa_1^2,\kappa_1^3\right)G_{ijk}+x(1-y)z\sum_{i,j,k=0}^{1}P_{ijk}\left(\kappa_1^1,\kappa_2^2,\kappa_1^3\right)G_{ijk}\\
&+(1-x)yz\sum_{i,j,k=0}^{1}P_{ijk}\left(\kappa_2^1,\kappa_1^2,\kappa_1^3\right)G_{ijk}+(1-x)(1-y)z\\
&\sum_{i,j,k=0}^{1}P_{ijk}\left(\kappa_2^1,\kappa_2^2,\kappa_1^3\right)G_{ijk}\\
&+xy(1-z)\sum_{i,j,k=0}^{1}P_{ijk}\left(\kappa_1^1,\kappa_1^2,\kappa_2^3\right)G_{ijk}+x(1-y)(1-z)\\
&\sum_{i,j,k=0}^{1}P_{ijk}\left(\kappa_1^1,\kappa_2^2,\kappa_2^3\right)G_{ijk}\\
&+(1-x)y(1-z)\sum_{i,j,k=0}^{1}P_{ijk}\left(\kappa_2^1,\kappa_1^2,\kappa_2^3\right)G_{ijk}\\
&+(1-x)(1-y)(1-z)\sum_{i,j,k=0}^{1}P_{ijk}\left(\kappa_2^1,\kappa_2^2,\kappa_2^3\right)G_{ijk}.
\end{aligned}\tag{30}$$

Payoff relations for a symmetric game. For a symmetric game we have $\Pi_A(x,y,z)=\Pi_A(x,z,y)=\Pi_B(y,x,z)=\Pi_B(z,x,y)=\Pi_C(y,z,x)=\Pi_C(z,y,x)$. This requires $a_{111}=b_{111}=c_{111}$, $a_{000}=b_{000}=c_{000}$, $a_{110}=b_{110}=a_{101}=c_{101}=b_{011}=c_{011}$, $b_{100}=c_{100}=a_{010}=c_{010}=a_{001}=b_{001}$, $a_{100}=b_{010}=c_{001}$ and $a_{011}=b_{101}=c_{110}$. The payoff relations (0) are then reduced to

$$\begin{aligned}
&\Pi_A\left(\kappa_i^1,\kappa_j^2,\kappa_k^3\right)=a_{000}+\cos\gamma\{a_{100}X_i+a_{001}Y_j+a_{001}Z_k\}\\
&+a_{110}X_i\{Y_j+Z_k\}+a_{011}Y_jZ_k+a_{111}\{\cos\gamma X_iY_jZ_k+\sin\gamma\Theta_{ijk}\},
\end{aligned}\tag{31a}$$

$$\begin{aligned}
&\Pi_B\left(\kappa_i^1,\kappa_j^2,\kappa_k^3\right)=a_{000}+\cos\gamma\{a_{001}X_i+a_{100}Y_j+a_{001}Z_k\}\\
&+a_{110}Y_j\{X_i+Z_k\}+a_{011}X_iZ_k+a_{111}\{\cos\gamma X_iY_jZ_k+\sin\gamma\Theta_{ijk}\},
\end{aligned}\tag{31b}$$

$$\begin{aligned}
&\Pi_C\left(\kappa_i^1,\kappa_j^2,\kappa_k^3\right)=a_{000}+\cos\gamma\{a_{001}X_i+a_{001}Y_j+a_{100}Z_k\}\\
&+a_{110}Z_k\{X_i+Y_j\}+a_{011}X_iY_j+a_{111}\{\cos\gamma X_iY_jZ_k+\sin\gamma\Theta_{ijk}\}.
\end{aligned}\tag{31c}$$

Embedding the classical game

If we consider a strategy triplet $(x,y,z)=(0,1,0)$ for example, at zero entanglement, then the payoff to Alice is obtained from Eq. (30) to be

$$\begin{aligned}
&\Pi_A(x,y,z)=\\
&\frac{1}{8}[G_{000}(1+X_2)(1+Y_1)(1+Z_2)+G_{100}(1-X_2)(1+Y_1)(1+Z_2)\\
&+G_{010}(1+X_2)(1-Y_1)(1+Z_2)+G_{110}(1-X_2)(1-Y_1)(1+Z_2)\\
&+G_{001}(1+X_2)(1+Y_1)(1-Z_2)+G_{101}(1-X_2)(1+Y_1)(1-Z_2)\\
&+G_{011}(1+X_2)(1-Y_1)(1-Z_2)+G_{111}(1-X_2)(1-Y_1)(1-Z_2)].
\end{aligned}\tag{32}$$

Hence, in order to achieve the classical payoff of G_{101} for this triplet, we can see that we require $X_2=-1$, $Y_1=+1$ and $Z_2=-1$.

This shows that we can select any required classical payoff by the appropriate selection of X_i, Y_i, $Z_i=\pm1$. Referring to Eq. (20), we therefore have the conditions for obtaining classical mixed-strategy payoff relations as

$$X_i=\cos\alpha_1\cos\kappa_i^1+\cos\alpha_3\sin\alpha_1\sin\kappa_i^1=\pm1,\tag{33a}$$

$$Y_j=\cos\beta_1\cos\kappa_j^2+\cos\beta_3\sin\beta_1\sin\kappa_j^2=\pm1,\tag{33b}$$

$$Z_k=\cos\chi_1\cos\kappa_k^3+\cos\chi_3\sin\chi_1\sin\kappa_k^3=\pm1.\tag{33c}$$

For the equation for Alice, we have two classes of solution: If $\alpha_3\neq0$, then for the equations satisfying $X_2=Y_2=Z_2=-1$ we have for Alice in the first equation $\alpha_1=0$, $\kappa_2^1=\pi$ or $\alpha_1=\pi$, $\kappa_2^1=0$ and for the equations satisfy $X_1=Y_1=Z_1=+1$ we have $\alpha_1=\kappa_1^1=0$ or $\alpha_1=\kappa_1^1=\pi$, which can be combined to give either $\alpha_1=0$, $\kappa_1^1=0$ and $\kappa_2^1=\pi$ or $\alpha_1=\pi$, $\kappa_1^1=\pi$ and $\kappa_2^1=0$. For the second class with $\alpha_3=0$ we have the solution $\alpha_1-\kappa_2^1=\pi$ and for $X_1=Y_1=Z_1=+1$ we have $\alpha_1-\kappa_2^1=0$.

So in summary for both cases we have that the two measurement directions are π out of phase with each other, and for the first case ($\alpha_3\neq0$) we can freely vary α_2 and α_3, and for the second case ($\alpha_3=0$), we can freely vary α_1 and α_2 to change the initial quantum quantum state without affecting the game Nash equilibrium (NE) or payoffs [1,2]. The same arguments hold for the equations for Y and Z. Using these results in Eq. (24) we find that $\Theta_{ijk}=0$.

We have the associated payoff for Alice

$$\begin{aligned}
&\Pi_A(x,y,z)=\frac{1}{2}[G_{000}+G_{111}-\cos\gamma(G_{000}-G_{111})\\
&-4(y+z)(a_{110}+a_{011})+\cos\gamma\{4x(a_{111}+a_{100})\\
&+4(a_{111}+a_{001})(y+z)\}+8xa_{110}(y+z-1)+8yza_{011}\\
&-8a_{111}\cos\gamma\{xy+xz+yz-2xyz\}].
\end{aligned}\tag{34}$$

Setting $\gamma=0$ in Eq. (34) we find Alice's payoff as

$$\begin{aligned}
&\Pi_A(x,y,z)=G_{111}+x(G_{011}-G_{111})+y(G_{110}-G_{111})\\
&+z(G_{110}-G_{111})+4xy(a_{110}-a_{111})+4xz(a_{110}-a_{111})\\
&+4yz(a_{011}-a_{111})+8xyza_{111},
\end{aligned}\tag{35}$$

which has the same payoff structure as the mixed-strategy version of the classical game.

Now, we can also write the equations governing the NE as

$$\begin{aligned}
&\Pi_A(x^*,y^*,z^*)-\Pi_A(x,y^*,z^*)\\
&=(x^*-x)[a_{110}(2y^*-1)+a_{101}(2z^*-1)\\
&+\cos\gamma\{a_{100}+a_{111}(2y^*-1)(2z^*-1)\}]\geq 0\\
&\Pi_B(x^*,y^*,z^*)-\Pi_B(x^*,y,z^*)\\
&=(y^*-y)[b_{110}(2x^*-1)+b_{011}(2z^*-1)\\
&+\cos\gamma\{b_{010}+b_{111}(2x^*-1)(2z^*-1)\}]\geq 0\\
&\Pi_C(x^*,y^*,z^*)-\Pi_C(x^*,y^*,z)\\
&=(z^*-z)[c_{101}(2x^*-1)+c_{011}(2y^*-1)\\
&+\cos\gamma\{c_{001}+c_{111}(2x^*-1)(2y^*-1)\}]\geq 0,
\end{aligned}\tag{36}$$

where the strategy triple (x^*,y^*,z^*) is a NE. Using the conditions defined earlier for a symmetric game, we can reduce our equations governing the NE for the three players to

$$\begin{aligned}
&(x^*-x)[2a_{110}(y^*+z^*-1)\\
&+\cos\gamma\{a_{100}+a_{111}(2y^*-1)(2z^*-1)\}]\geq 0,
\end{aligned}\tag{37a}$$

$$\begin{aligned}
&(y^*-y)[2a_{110}(x^*+z^*-1)\\
&+\cos\gamma\{a_{100}+a_{111}(2x^*-1)(2z^*-1)\}]\geq 0,
\end{aligned}\tag{37b}$$

$$\begin{aligned}
&(z^*-z)[2a_{110}(x^*+y^*-1)\\
&+\cos\gamma\{a_{100}+a_{111}(2x^*-1)(2y^*-1)\}]\geq 0
\end{aligned}\tag{37c}$$

We can see that the new quantum behavior is governed solely by the payoff matrix through a_{100}, a_{110} and a_{111} and by the entanglement angle γ, and not by other properties of the quantum state.

For completeness, we have Bob's payoff, in the symmetric case, as

$$\begin{aligned}
\Pi_B(x,y,z)=&\frac{1}{2}[G_{000}+G_{111}-\cos\gamma(G_{000}-G_{111})\\
&-4(x+z)(a_{110}+a_{011})+\cos\gamma 4y(a_{111}+a_{100})\\
&+4(x+z)(a_{111}+a_{001})]+8ya_{110}(x+z-1)+8xza_{011}\\
&-8a_{111}\cos\gamma\{xy+xz+yz-2xyz\}].
\end{aligned}\tag{38}$$

The mixed NE for all players is

$$x^*=y^*=z^*=\frac{-a_{110}+\cos\gamma a_{111}\pm\sqrt{a_{110}^2-\cos\gamma a_{100}a_{111}}}{2\cos\gamma a_{111}}.\tag{39}$$

Maximally entangled case. For $\gamma=\pi/2$ at maximum entanglement for both NE of $(x^*,y^*,z^*)=(0,0,0)$ and $(x^*,y^*,z^*)=(1,1,1)$ we have the payoff

$$\Pi_A(x^*,y^*,z^*)=\Pi_B(x^*,y^*,z^*)=\Pi_C(x^*,y^*,z^*)=\frac{1}{2}(G_{000}+G_{111})\tag{40}$$

which gives the average of the two corners of the payoff matrix, which is as expected.

Prisoners' Dilemma. An example of a three-player PD game is shown in Table 1. For this game, from Eq. (28), we have $a_{000}=32/8, a_{001}=14/8$, $a_{010}=14/8, a_{011}=0, a_{100}=-8/8, a_{101}=-2/8, a_{110}=-2/8, a_{111}=0$, with the NE from Eqs. (37) given by

$$(x^*-x)[-(y^*+z^*-1)-2\cos\gamma]\geq 0,\tag{41a}$$

$$(y^*-y)[-(x^*+z^*-1)-2\cos\gamma]\geq 0,\tag{41b}$$

$$(z^*-z)[-(x^*+y^*-1)-2\cos\gamma]\geq 0.\tag{41c}$$

We have the classical NE of $(x^*,y^*,z^*)=(0,0,0)$ for $\cos\gamma=1$, but we have a phase transition, as the entanglement increases, at $\cos\gamma=\frac{1}{2}$ where we find the new NE $(x^*,y^*,z^*)=(1,0,0)$, $(x^*,y^*,z^*)=(0,1,0)$ and $(x^*,y^*,z^*)=(0,0,1)$. The payoff for Alice from Eq. (34) is given by

$$\begin{aligned}
\Pi_A(x,y,z)=&\frac{1}{2}[7+2x+(y+z)(1-2x)\\
&-\cos\gamma\{5+4x-7(y+z)\}].
\end{aligned}\tag{42}$$

For the classical region we have $\Pi_A(0,0,0)=\Pi_B(0,0,0)=\Pi_C(0,0,0)=\frac{7}{2}-\frac{5}{2}\cos\gamma$, which is graphed in Fig. 2 along with other parts of the phase diagram. It should be noted that $\cos\gamma$ can go negative, which will produce a mirror image about the vertical axis of the current graph. That is for $\cos\gamma$ decreasing from $-\frac{1}{2}$ to -1, we have a NE of $(x^*,y^*,z^*)=(1,1,1)$, falling from 2.25 down to 1. We will also have the NE of $(x^*,y^*,z^*)=(1,1,0)$ and $(x^*,y^*,z^*)=(0,1,1)$ for $-\frac{1}{2}\cos\gamma<0$.

This graph also illustrates the value of coalitions, because if Bob and Chris both agree to implement the same strategy, then the only NE available for $0<\cos\gamma<\frac{1}{2}$ for example, is $(x^*,y^*,z^*)=(1,0,0)$. However, for a NE in the region of $\cos\gamma$ just less than one half, both Bob and Chris receive a significantly greater payoff, of around 4.5 units, as opposed to 2.5 for Alice, so the coalition will receive nearly twice the payoff.

Table 1. An example of three-player Prisoners' Dilemma.

State	$\|000\rangle$	$\|001\rangle$	$\|010\rangle$	$\|100\rangle$	$\|011\rangle$	$\|101\rangle$	$\|110\rangle$	$\|111\rangle$
Payoff	(6,6,6)	(3,3,9)	(3,9,3)	(9,3,3)	(0,5,5)	(5,0,5)	(5,5,0)	(1,1,1)

The payoff for each player (one,two,three), for each measurement outcome.
doi:10.1371/journal.pone.0021623.t001

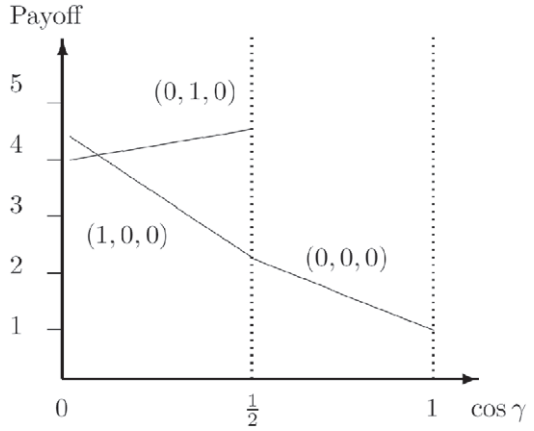

Figure 2. Phase structure for Alice in quantum PD game using EPR setting. For the PD example given in Table 1, the classical outcome of (0,0,0), is still returned for low entanglement, $\cos\gamma > \frac{1}{2}$, but with new NE arising at higher entanglement. As the game is symmetric, we have $\Pi_A(0,1,0) = \Pi_A(0,0,1)$ and the NE (0,0,1) is not shown.
doi:10.1371/journal.pone.0021623.g002

Players sharing the W state

The second type of three particle entangled state [49] is the W state

$$\psi = -ABC\frac{1}{\sqrt{3}}\left(\imath\sigma_2^1 + \imath\sigma_2^2 + \imath\sigma_2^3\right), \tag{43}$$

where once again we have used the three rotors A, B and C in order to generalize the state as far as possible. So proceeding as for the GHZ state, the probability that a particular state will be observed after measurement can be found to be

$$\begin{aligned} P_{lmn} = \frac{1}{24}[3 &+ (-)^l X_i + (-)^m Y_j + (-)^n Z_k \\ &+ (-)^{l+m+n}(2(X_i G_j H_k + F_i Y_j H_k + F_i G_j Z_k + X_i V_j W_k \\ &+ U_i Y_j W_k + U_i V_j Z_k) - 3X_i Y_j Z_k) \\ &+ (-)^{l+m}(2F_i G_j + 2U_i V_j - X_i Y_j) \\ &+ (-)^{l+n}(2F_i H_k + 2U_i W_k - X_i Z_k) \\ &+ (-)^{m+n}(2G_j H_k + 2V_j W_k - Y_j Z_k)]. \end{aligned} \tag{44}$$

Clearly the same probability distribution would be found for the second type of W state, shown in Eq. (3), because it is simply an inverse of this state.

Obtaining the pure-strategy payoff relations. With players sharing a W state, referring to Eq. (28), we introduce the following notation for Alice

$$a'_{xyz} = \frac{1}{3}a_{xyz}. \tag{45}$$

Using the payoff function given by Eq. (4), we then find for Alice

$$\begin{aligned} &\Pi_A(\kappa_i^1, \kappa_j^2, \kappa_k^3) \\ &= 3a'_{000} + a'_{100}X_i + a'_{010}Y_j + a'_{001}Z_k + a'_{011}(2G_jH_k + 2V_jW_k - Y_jZ_k) \\ &+ a'_{110}(2F_iG_j + 2U_iV_j - X_iY_j) + a'_{101}(2F_iH_k + 2U_iW_k - X_iZ_k) \\ &+ a'_{111}\left[2\{X_iG_jH_k + F_iY_jH_k + F_iG_jZ_k + X_iV_jW_k + U_iY_jW_k + U_iV_jZ_k\}\right. \\ &\left. - 3X_iY_jZ_k\right]. \end{aligned} \tag{46}$$

Similarly for other players, simply by switching to their payoff matrix in place of Alices'.

Obviously for the W state there is no way to turn off the entanglement and so it is not possible to embed a classical game, hence we now turn to a more general state which is in a superposition of the GHZ and W type states.

Games with general three-qubit state

It is noted in Ref. [49] that there are two inequivalent classes of tripartite entanglement, represented by the GHZ and W states. More specifically, Ref. [50] finds a general three qubit pure state

$$|\psi\rangle_3 = \lambda_0|000\rangle + \lambda_1 e^{i\phi}|100\rangle + \lambda_2|101\rangle + \lambda_3|110\rangle + \lambda_4|111\rangle \tag{47}$$

where $\lambda_1, \phi \in \Re$, with $\lambda_1 \geq 0$, $0 \leq \phi \leq \pi$ and $\sum_{j=0}^{4}\lambda_j^2 = 1$.

We have a $1:1$ mapping from complex spinors to GA given in Eq. (9), so we will have a general three qubit state represented in GA as

$$\begin{aligned} \psi = ABC[&\lambda_0 - \lambda_1\cos x\imath\sigma_2^1 + \lambda_1\sin x\imath\sigma_1^1 \\ &+ \lambda_2\imath\sigma_2^1\imath\sigma_2^3 + \lambda_3\imath\sigma_2^1\imath\sigma_2^2 - \lambda_4\imath\sigma_2^1\imath\sigma_2^2\imath\sigma_2^3], \end{aligned} \tag{48}$$

which with the rotors gives us 15 degrees of freedom.

We desire though, a symmetrical three-qubit state in order to guarantee a fair game and so we construct

$$\begin{aligned} |\psi\rangle_3 = \rho_0|000\rangle &+ \rho_1(|001\rangle + |010\rangle + |100\rangle) \\ &+ \rho_2(|011\rangle + |101\rangle + |110\rangle) + \rho_3|111\rangle \end{aligned} \tag{49}$$

as the most general symmetrical three qubit quantum state, with ρ_i subject to the conventional normalization conditions. We might think to add complex phases to the four terms, however we find that this addition has no effect on the payoff or the NE and so can be neglected. This symmetrical state can be represented in GA, by referring to Eq. (11), as

$$\begin{aligned} \psi = ABC[&\cos\frac{\gamma}{2}\cos\frac{\phi}{2} + \sin\frac{\phi}{2}\sin\frac{\delta}{2}(\imath\sigma_2^1 + \imath\sigma_2^2 + \imath\sigma_2^3)/\sqrt{3} \\ &+ \sin\frac{\phi}{2}\cos\frac{\delta}{2}(\imath\sigma_2^1\imath\sigma_2^2 + \imath\sigma_2^2\imath\sigma_2^3 + \imath\sigma_2^1\imath\sigma_2^3) \\ &/\sqrt{3} + \sin\frac{\gamma}{2}\cos\frac{\phi}{2}\imath\sigma_2^1\imath\sigma_2^2\imath\sigma_2^3]. \end{aligned} \tag{50}$$

If we set $\gamma = 0$ and $\phi = 0$ we find the product state $|000\rangle$, which we will constrain to return the classical game as for the GHZ state. For $\gamma = \pi/2$ and $\phi = 0$ we produce the maximally entangled GHZ state and for $\phi = \pi$ we have the W type states in a superposition controlled by δ. Using Eq. (50) and following the same calculation path used for the GHZ state, we can arrive at the NE, using the same condition for classical embedding as for the GHZ state, finding for Alice

$$\begin{aligned} &\Pi_A(x^*, y^*, z^*) - \Pi_A(x, y^*, z^*) \\ &= (x^* - x)[3(a_{100} + U_2)\cos\gamma(1 + \cos\phi) \\ &+ 2U_1(1 + 2\cos\phi) - (a_{100} - 3U_2)(1 - \cos\phi)\cos\delta], \end{aligned} \tag{51}$$

where

$$U_1 = a_{110}(2y^* - 1) + a_{101}(2z^* - 1) = 2a_{110}(y^* + z^* - 1) \quad (52a)$$

$$U_2 = a_{111}(1 - 2y^*)(1 - 2z^*). \quad (52b)$$

We can see the effect of the W type states in the $\cos\delta$ term and so it illustrates how both types of W states contribute. The reason they can both appear is because by demanding the classical embedding we have severely restricted the available unitary transformations available to transform the starting state.

The payoff relations. The payoff function for Alice given by

$$\Pi_A = a_{000} - \frac{1}{2}(V_1 + V_3)\cos\gamma(1 + \cos\phi) + \frac{1}{3}V_2(1 + 2\cos\phi) + \frac{1}{6}(V_1 - 3V_3)(1 - \cos\phi)\cos\delta, \quad (53)$$

where

$$V_1 = a_{100}(1 - 2x) + a_{010}(1 - 2y) + a_{001}(1 - 2z) \quad (54a)$$

$$V_2 = a_{110}(1 - 2x)(1 - 2y) + a_{101}(1 - 2x)(1 - 2z) + a_{011}(1 - 2y)(1 - 2z) \quad (54b)$$

$$V_3 = a_{111}(1 - 2x)(1 - 2y)(1 - 2z). \quad (54c)$$

The payoff for Bob and Chris found by simply replacing a_{ijk} with b_{ijk} and c_{ijk} from their respective payoff matrices. When comparing with the payoff formula above with the classical result at $(x,y,z) = (0,0,0)$, it is helpful to note that $a_{000} + a_{001} + a_{010} + a_{011} + a_{100} + a_{101} + a_{110} + a_{111} = G_{000}$ and generally $a_{000} + (-1)^n a_{001} + (-1)^m a_{010} + (-1)^{m+n} a_{011} + (-1)^l a_{100} + (-1)^{l+n} a_{101} + (-1)^{l+m} a_{110} + (-1)^{l+m+n} a_{111} = G_{lmn}$.

Uniform superposition state. If we select a uniform superposition state, with $\rho_0 = \rho_1 = \rho_2 = \rho_3 = \frac{1}{2}$, that is, substituting $\gamma = \frac{\pi}{2}$, $\phi = \frac{2\pi}{3}$ and $\delta = \frac{\pi}{2}$, giving a product state $H^{\otimes 3}|000\rangle$, with H being the Hadamard operator, then we find that $\Pi_A(x^*,y^*,z^*) - \Pi_A(x,y^*,z^*) = 0$ for Alice, and similarly for the other players. That is the payoff will be independent of the player choices and Eq. (53) gives $\Pi_A = \Pi_B = \Pi_C = a_{000}$. Where a_{000} represents the average of all the entries in the payoff matrix, as expected for a uniform superposition state.

Prisoners' Dilemma. For the PD game from the previous section with the GHZ state, we found $a_{100} = -8/8, a_{110} = -2/8, a_{111} = 0$, so $U_2 = 0$, with the NE from Eq. (79) for the three players given by

$$(x^* - x)[(1 - y^* - z^*)(1 + 2\cos\phi) - 3\cos\gamma(1 + \cos\phi) + (1 - \cos\phi)\cos\delta] \geq 0, \quad (55a)$$

$$(y^* - y)[(1 - x^* - z^*)(1 + 2\cos\phi) - 3\cos\gamma(1 + \cos\phi) + (1 - \cos\phi)\cos\delta] \geq 0, \quad (55b)$$

$$(z^* - z)[(1 - x^* - y^*)(1 + 2\cos\phi) - 3\cos\gamma(1 + \cos\phi) + (1 - \cos\phi)\cos\delta] \geq 0, \quad (55c)$$

with the payoff for Alice given by

$$\Pi_A = 4 - \frac{1}{6}(1 - 2x)(1 - y - z)(1 + 2\cos\phi) - \frac{1}{4}(5 + 4x - 7y - 7z)[\cos\gamma(1 + \cos\phi) - \frac{1}{3}(1 - \cos\phi)\cos\delta]. \quad (56)$$

We can see with $\phi = 0$ we recover the NE for the GHZ state, in Eq. (37).

Shifting of the NE compared to the GHZ state. We have the classical NE of $(x^*,y^*,z^*) = (0,0,0)$ for $\cos\gamma = 1$ and $\cos\phi = 1$, but we can see, that once again, we have a phase transition, as the entanglement increases, to a new NE of $(x^*,y^*,z^*) = (1,0,0)$, $(x^*,y^*,z^*) = (0,1,0)$ and $(x^*,y^*,z^*) = (0,0,1)$.

The phase transition will be at $\cos\gamma = \frac{1}{3}(2 - \cos\delta) + \frac{2\cos\delta - 1}{3(1 + \cos\phi)}$. We notice that as we increase the weighting towards the W state, by increasing ϕ, that it becomes easier to make the phase transition in comparison to the pure GHZ state, that is, we improve access to the phase transition as we introduce the weight of the $|011\rangle + |101\rangle + |110\rangle$ state. In fact, even at $\cos\gamma = 1$, we can achieve the NE of $(x^*,y^*,z^*) = (1,1,1)$, with $\phi = \pi$, giving a payoff of $3\frac{1}{3}$ units.

Maximizing the payoff. Looking at the payoff function for Alice in Eq. (56), we can seek to maximize this function. The maximum achievable payoff is found to be 4.5, which is equal to the maximum payoff found for the GHZ state, see Fig. 2. Thus incorporating W type states into a superposition with the GHZ state, cannot improve the maximum payoff.

Observing Fig. 3, we can see that as we mix in the W state, that the phase transitions move to the right, with an extra offset available by changing δ, and the maximum payoff obtainable, will drop below the maximum achievable of 4.5 with the pure GHZ state. Fig. 3, shows the shifted NE from 0.5 to 2/3 and payoffs for the case $\phi = \frac{\pi}{2}$ and $\delta = 0$.

Discussion

A quantum version of a three-player two-strategy game is explored, where the player strategy sets remain classical but their payoffs are obtained from the outcome of quantum measurement performed, as in a typical EPR experiment. If players share a product state, then the quantum games reduces itself to the classical game, thus ensuring a faithful embedding of a mixed-strategy version of a classical three-player two-strategy game within the more general quantum version of the game.

For a general three-player two-strategy game, we find the governing equation for a strategy triplet forming a NE is given by Eq. (51) with the associated payoff relations obtained in Eq. (53). At zero entanglement the quantum game returns the same triplet(s) of NE as the classical mixed-strategy game and the payoff relations in the quantum game reduce to the trilinear form given in Eq. (35), equivalent to the classical game involving mixed-strategies. We find that even though the requirement to properly embed a classical game puts significant restrictions on the initial quantum states, we still have a degree of freedom, available with the entanglement angle γ, with which we can generate a new NE.

As a specific example the PD was found to have a NE of $(x^*,y^*,z^*) = (1,1,1)$ at high entanglement. For the GHZ state, the phase diagram is shown in Fig. 2, which is modulated with the inclusion of the W type states, by reducing the payoffs and sliding the NE closer to the classical region.

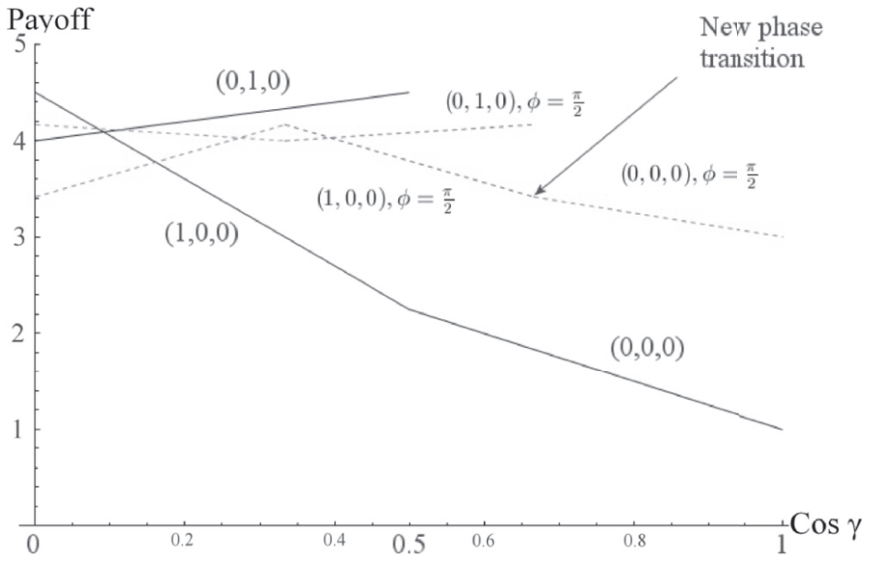

Figure 3. Phase transition in three-player quantum Prisoners' Dilemma with a general three qubit state. The solid lines indicate the phase transitions from Table 1, and shown in Fig. 1, with the dashed lines indicating the shifted transitions when the W-state is mixed in. We observe that new NE now arise at lower entanglement, at $\cos\gamma=\frac{2}{3}$, as indicated by the arrow pointer.
doi:10.1371/journal.pone.0021623.g003

As our setup for a three-player quantum game involves players performing classical strategies, our conclusions are restricted by not only players sharing GHZ or W states but also by the EPR setting that we use. The most general form of the GHZ state permits a description in terms of a single entanglement parameter γ. However, as the general W state involves three kets, the entanglement in such a state cannot be described by a single parameter. It appears that as for symmetric W states with equal superposition it is not possible to remove entanglement, therefore, embedding a classical game within the quantum game (while players share such states) is not possible in the EPR-type setup in which players can perform only classical strategies. Our results in this regard are general in that although they rely on the EPR setting, but not on a particular game as these use the parameters introduced in Eqs. (28a–28d) that can be evaluated for any game. Also, this is discussed in the Section 5, where games with general three-qubit symmetric states are considered, that include combination of GHZ and W states. However, the situation with sharing non-equally weighted superposition states can be entirely different, not considered in the present paper, but represents a useful extension for future work.

Our analysis shows that, with a quantization based on the EPR setting, a faithful embedding of a classical game can be achieved that also avoids an Enk-Pike type argument [32] because players' strategy sets are not extended relative to the classical game. However, with players sharing entangled states, while their strategy sets remain classical, our quantum games lead to new game-theoretic outcomes.

We also find that an analysis of three-player quantum games using Clifford's geometric algebra (GA) comes with some clear benefits, for instance, a better perception of the quantum mechanical situation involved and particularly an improved geometrical visualization of quantum mechanical operations. The same results using the familiar algebra with Pauli matrices may possibly be tractable but would certainly obscure intuition. Also, the simple expression given in (13) for the overlap probability between two quantum states in the N-particle case is another benefit of the GA approach.

The results reported in the paper can be useful in a game-theoretic analysis of the EPR paradox. Bell's consideration of the EPR paradox usually implies the inconsistency between locality and completeness of quantum mechanics, or in more broader terms, simply the surprising nonlocal effects invoked by entanglement. However, one notices that these conclusions are merely sufficient but not necessary for the violation of Bell's inequality and that other interpretations are also reported [45,51–54], especially, the interpretation based on the non-existence of a single probability space for incompatible experimental contexts [55]. This non-existence also presents a new route in constructing quantum games and the first step in this direction was taken in Ref [56]. Because such quantum games originate directly from the violation of Bell's inequality, they allow a discussion of the EPR paradox in the context of game theory. This is also supported by the fact that for quantum games with players sharing entanglement, a game-theoretic analysis that involves Bell's settings [26–28] has been reported in Refs [57,58].

A variety of other classical games could now be adapted and applied to this three-player framework, with new NE being expected. The present study of three-player quantum games can also be naturally extended to analyze the N-player quantum games. We believe that the mathematical formalism of GA permits this in a way not possible using the usual complex matrices. Also, this extension could be fruitfully exploited in developing a game-theoretic perspective on quantum search algorithms and quantum walks. We find that our analysis can be helpful in providing an alternative viewpoint (with emphasis on underlying geometry) on multi-party entanglement shared by a group of individuals (players), while they have conflicting interests and can perform only classical actions on the quantum state. That is, a viewpoint that is motivated by the geometrical perspective that Clifford's geometric algebra provides. Such situations take place in the area of quantum communication and particularly in quantum cryptography [59–61].

Supporting Information

Appendix S1
(PDF)

Author Contributions

Conceived and designed the experiments: JC. Wrote the paper: JC AI DA. Conceived idea and worked on manuscript: JC AI. Analysis of results and design of paper: JC DA AI. Checking results: DA AI JC.

References

1. Binmore K (2007) Game theory: a very short introduction, volume 173 Oxford University Press, USA.
2. Rasmusen E (2007) Games and information: An introduction to game theory Wiley-blackwell.
3. Abbott D, Davies P, Shalizi C (2002) Order from disorder: the role of noise in creative processes: a special issue on game theory and evolutionary processes-overview. Fluct Noise Lett 2: C1–C12.
4. von Neumann J, Morgenstern O (1944) Theory of Games and Economic Behavior Princeton University Press.
5. Peres A (1993) Quantum theory: concepts and methods, volume 57 Kluwer Academic Publishers.
6. Meyer D (1999) Quantum strategies. Physical Review Letters 82: 1052–1055.
7. Eisert J, Wilkens M, Lewenstein M (1999) Quantum games and quantum strategies. Physical Review Letters 83: 3077–3080.
8. Blaquiere A (1980) Wave mechanics as a two-player game. Dynamical Systems and Microphysics 33.
9. Wiesner S (1983) Conjugate coding. ACM Sigact News 15: 78–88.
10. Mermin N (1990) Quantum mysteries revisited. American Journal of Physics 58: 731–734.
11. Mermin N (1990) Extreme quantum entanglement in a superposition of macroscopically distinct states. Physical Review Letters 65: 1838–1840.
12. Benjamin S, Hayden P (2001) Multiplayer quantum games. Physical Review A 64: 030301.
13. Du J, Xu X, Li H, Zhou X, Han R (2001) Entanglement playing a dominating role in quantum games. Physics Letters A 289: 9–15.
14. Du J, Li H, Xu X, Zhou X, Han R (2003) Phase-transition-like behaviour of quantum games. Journal of Physics A: Mathematical and General 36: 6551.
15. Han Y, Zhang Y, Guo G (2002) W state and Greenberger-Horne-Zeilinger state in quantum threeperson prisoner's dilemma. Physics Letters A 295: 61–64.
16. Flitney A, Abbott D (2005) Quantum games with decoherence. Journal of Physics A: Mathematical and General 38: 449.
17. Ramzan M, Nawaz A, Toor A, Khan M (2008) The effect of quantum memory on quantum games. Journal of Physics A: Mathematical and Theoretical 41: 055307.
18. Iqbal A, Toor A (2002) Quantum cooperative games. Physics Letters A 293: 103–108.
19. Flitney A, Greentree A (2007) Coalitions in the quantum minority game: classical cheats and quantum bullies. Physics Letters A 362: 132–137.
20. Iqbal A, Weigert S (2004) Quantum correlation games. Journal of Physics A: Mathematical and General 37: 5873.
21. Iqbal A (2005) Playing games with EPR-type experiments. Journal of Physics A: Mathematical and General 38: 9551.
22. Iqbal A, Cheon T (2007) Constructing quantum games from nonfactorizable joint probabilities. Physical Review E 76: 061122.
23. Iqbal A, Cheon T, Abbott D (2008) Probabilistic analysis of three-player symmetric quantum gamesplayed using the Einstein-Podolsky-Rosen-Bohm setting. Physics Letters A 372: 6564–6577.
24. Einstein A, Podolsky B, Rosen N (1935) Can quantum-mechanical description of physical reality be considered complete? Physical review 47: 777.
25. Bohm D (1951) Quantum theory Dover Publications.
26. Bell J (1964) On the Einstein-Podolsky-Rosen paradox. Physics 1: 195–200.
27. Bell J (1987) Speakable and Unspeakable in Quantum Mechanics Cambridge University Press.
28. Bell J (1966) On the problem of hidden variables in quantum mechanics. Reviews of Modern Physics 38: 447–452.
29. Aspect A, Dalibard J, Roger G (1982) Experimental test of Bell's inequalities using time-varying analyzers. Physical Review Letters 49: 1804–1807.
30. Clauser J, Shimony A (1978) Bell's theorem. experimental tests and implications. Reports on Progress in Physics 41: 1881.
31. Cereceda J (2000) Quantum mechanical probabilities and general probabilistic constraints for Einstein–Podolsky–Rosen–Bohm experiments. Foundations of Physics Letters 13: 427–442.
32. van Enk SJ, Pike R (2002) Classical rules and quantum games. Phys Rev A 66: 024306.
33. Nielsen M, Chuang I (2002) Quantum Computation and Quantum Information. Cambridge, UK: Addison-Wesley, first edition.
34. Hestenes D, Sobczyk G (1984) Clifford Algebra to Geometric Calculus: A unified language for mathematics and physics, volume 5 Springer.
35. Hestenes D (1999) New foundations for classical mechanics: Fundamental Theories of Physics Kluwer Academic Pub.
36. Doran C, Lasenby A (2003) Geometric algebra for physicists Cambridge University Press.
37. De Sabbata V, Datta B (2007) Geometric algebra and applications to physics Taylor & Francis Group.
38. Dorst L, Doran C, Lasenby J (2002) Applications of geometric algebra in computer science and engineering. Boston: Birkhauser.
39. Chappell J, Iqbal A, Lohe M, Von Smekal L (2009) An analysis of the quantum penny flip game using geometric algebra. Journal of the Physical Society of Japan 78: 4801.
40. Chappell J, Iqbal A, Abbott D (2010) Analysis of two-player quantum games using geometric algebra. Arxiv preprint arXiv: 10071332.
41. Boudet R (2008) Relativistic Transitions in the Hydrogenic atoms: Elementary Theory, volume 52 Springer Verlag.
42. Hestenes D (1986) Clifford Algebras and their Applications in Mathematical Physics. Dordrecht/Boston: Reidel, chapter Clifford Algebra and the interpretation of quantum mechanics.
43. Schmeikal B (2005) Algebra of matter. Advances in Applied Clifford Algebras 15: 271–290.
44. Horn ME (2006) Tagungs-CD des Fachverbandes Didaktik der Physik der DPG in Kassel, Berlin: Lehmanns Media, chapter Quaternions and Geometric Algebra (Quaternionen und Geometrische Algebra). Arxiv: 0709.2238.
45. Christian J (2007) Disproof of Bell's theorem by Clifford algebra valued local variables. Arxiv preprint quant-ph/0703179.
46. Christian J (2011) Restoring local causality and objective reality to the entangled photons. Arxiv preprint arXiv: 11060748.
47. Ichikawa T, Tsutsui I (2007) Duality, phase structures, and dilemmas in symmetric quantum games. Annals of Physics 322: 531–551.
48. Marinatto L, Weber T (2000) A quantum approach to games of static information. Phys Lett A 272: 291–303.
49. Dür W, Vidal G, Cirac J (2000) Three qubits can be entangled in two inequivalent ways. Physical Review A 62: 062314.
50. Acin A, Andrianov A, Costa L, Jane E, Latorre J, et al. (2000) Generalized Schmidt decomposition and classification of three-quantum-bit states. Physical Review Letters 85: 1560–1563.
51. Pitowsky I (1982) Resolution of the Einstein-Podolsky-Rosen and Bell paradoxes. Physical Review Letters 48: 1299–1302.
52. Pitowsky I (1983) Deterministic model of spin and statistics. Physical Review D 27: 2316.
53. Rastall P (1983) The Bell inequalities. Foundations of Physics 13: 555–570.
54. De Baere W, Mann A, Revzen M (1999) Locality and Bell's theorem. Foundations of physics 29: 67–77.
55. Khrennikov A (2008) Bell-Boole inequality: nonlocality or probabilistic incompatibility of random variables? Entropy 10: 19–32.
56. Iqbal A, Abbott D (2010) Constructing quantum games from a system of Bell's inequalities. Physics Letters A 374: 3155–3163.
57. Cheon T (2006) Quantum computing: Back action. AIP Conf Proc 864: 254–260.
58. Cleve R, Hoyer P, Toner B, Watrous J (2004) Consequences and limits of nonlocal strategies. In: Proceedings of the 19th IEEE Annual Conference on Computational Complexity IEEE Computer Society. pp 236–249.
59. Lee C, Johnson N (2003) Game-theoretic discussion of quantum state estimation and cloning. Physics Letters A 319: 429–433.
60. Pirandola S (2005) A quantum teleportation game. International Journal of Quantum Information 3: 239–243.
61. Houshmand M, Houshmand M, Mashhadi H (2010) Game theory based view to the quantum key distribution BB84 protocol. In: Third International Symposium on Intelligent Information Technology and Security Informatics IEEE. pp 332–336.